

University of South Wales



2053157

ANALYSIS OF SHALLOW AND DEEP FOUNDATIONS
USING SOIL-STRUCTURE INTERACTION TECHNIQUES

by

ANTHONY JAMES JONES

A thesis submitted in partial fulfilment of the
requirements of the Council for National Academic Awards
for the degree of Doctor of Philosophy

September 1991

The Polytechnic of Wales
in collaboration with
South Glamorgan County Council

FOR ALL THOSE WHO HAVE SUFFERED.

LIST OF CONTENTS

	PAGE No.
INDEX	i
LIST OF TABLES	vi
LIST OF FIGURES	viii
ACKNOWLEDGEMENTS	xii
DECLARATION	xiii
CERTIFICATION OF RESEARCH	xiv
ABSTRACT	xv
LIST OF SYMBOLS	xvii

INDEX.

CHAPTER 1: APPRAISAL OF THE PROBLEM.

1.1. INTRODUCTION.	1.1
1.2. PILED RAFT DESIGN.	1.1
1.3. CONTACT PRESSURES.	1.3
1.3.1. Plain rafts.	1.3
1.3.2. Piled raft.	1.7
1.4. SOIL-STRUCTURE INTERACTION.	1.7
1.5. SUMMARY.	1.9
1.6. OBJECT OF THE RESEARCH.	1.11
1.7. LIMITATIONS.	1.12

CHAPTER 2: REVIEW OF THE RELATED LITERATURE.

2.1. INTRODUCTION.	2.1
2.2. SOIL IDEALIZATION.	2.2
2.3. SOLUTION OF PROBLEMS OF ELASTICITY.	2.3
2.3.1. General.	2.3
2.3.2. The Finite Element Method.	2.4
2.3.3. The Boundary Element Method.	2.5
2.3.4. The Subgrade Reaction Theory.	2.6

2.4.	APPLICATIONS OF ANALYTICAL METHODS.	2.7
2.4.1.	Raft Foundations.	2.7
2.4.2.	Axially Loaded Single Piles.	2.11
2.4.3.	Laterally Loaded Single Piles.	2.15
2.4.4.	Pile Groups.	2.19
2.5.	SOIL-STRUCTURE INTERACTION.	2.38
2.6.	DISCUSSION.	2.42
2.7.	CONCLUSIONS.	2.45

CHAPTER 3: PROPOSED METHOD.

3.1.	INTRODUCTION.	3.1
3.2.	CONCEPTUAL MODEL.	3.3
3.3.	CONSTRUCTION OF THE MATHEMATICAL MODEL.	3.4
3.4.	INTERPRETATION OF OUTPUT.	3.5
3.5.	LOADING.	3.7
3.6.	METHOD OF ANALYSIS.	3.8
3.7.	RESULTS.	3.8
3.7.1.	General.	3.8
3.7.2.	Discussion Of Results.	3.9
3.7.3.	PGROUP Parametric Studies.	3.13
3.8.	INVESTIGATION OF RELATIONSHIP BETWEEN Kv, Kh AND Es.	3.16
3.8.1.	General.	3.16
3.8.2.	Background To The Work.	3.17
3.8.3.	Method Of Approach.	3.19
3.8.4.	Results.	3.19
3.9.	DISCUSSION AND CONCLUSIONS.	3.24

CHAPTER 4: ANALYSIS OF PILES WITH NO GROUP INTERACTION.

4.1.	INTRODUCTION.	4.1
4.2.	COMPARISON OF RESULTS.	4.1

4.2.1. General.	4.1
4.2.2. Field Results Of Reese and Cox.	4.2
4.2.3. Field Results Of Alizadeh.	4.4
4.2.4. Field Results Of McClelland and Focht.	4.5
4.2.5. Field Results Of Alizadeh and Davisson.	4.8
4.2.6. Test Results Of Davisson and Salley.	4.10
4.2.7. Test Results Of Mansur and Hunter.	4.11
4.3. INSTRUMENTED BRIDGE ABUTMENT.	4.12
4.3.1. General.	4.12
4.3.2. Pile Load Tests.	4.13
4.3.3. S.S.R.T. Results Of Pile Load Tests.	4.15
4.3.4. Load Distribution Within The Pile Cap.	4.18
4.4. DISCUSSION AND CONCLUSIONS.	4.21
CHAPTER 5: ANALYSIS OF PILES WITH GROUP INTERACTION.	
5.1. GENERAL.	5.1
5.2. SIMPLIFIED ANALYSIS OF AXIALLY LOADED PILES.	5.1
5.2.1. General.	5.1
5.2.2. Procedure.	5.2
5.3. FULL ANALYSIS OF AXIALLY LOADED PILES.	5.5
5.4. SIMPLIFIED ANALYSIS OF Laterally LOADED PILES.	5.6
5.4.1. Procedure.	5.6
5.5. FULL ANALYSIS OF Laterally LOADED PILES.	5.8
5.6. PILED RAFTS.	5.8
5.6.1. General.	5.8
5.6.2. Procedure.	5.9
5.7. COMPARISON WITH THEORETICAL RESULTS.	5.12
5.7.1. General.	5.12
5.7.2. Discussion Of Results.	5.13
5.8. COMPARISON WITH EXPERIMENTAL RESULTS.	5.19
5.8.1. General.	5.19

5.8.2. Comparison With Davisson And Salley.	5.20
5.8.3. Comparison With Ghosh.	5.22
5.8.4. Comparison With Whitaker.	5.24
5.8.5. Comparison With Berezantzev et al.	5.25
5.8.6. Comparison With Whitaker And Sowers et al.	5.25
5.8.7. Comparison With Ghosh For Cap Contact.	5.27
5.8.8. Comparison With Feagin.	5.29
5.9. CASE HISTORIES.	5.31
5.9.1. Hyde Park Cavalry Barracks.	5.31
5.9.2. Piled Raft Foundation At Basildon.	5.36
5.10. DISCUSSION AND CONCLUSIONS.	5.42
5.11. RECOMMENDATIONS FOR INCLUSION OF INTERACTION IN THE ANALYSIS.	5.46
CHAPTER 6: DEVELOPMENT OF A CONSISTENT SOIL MATRIX	
6.1. INTRODUCTION.	6.1
6.2. PROPOSED METHOD OF ANALYSIS.	6.1
6.3. RESULTS.	6.4
6.3.1. Laterally Loaded Pile.	6.5
6.3.2. Axially Loaded Pile.	6.8
6.4. CONCLUSIONS.	6.10
CHAPTER 7: RAFT FOUNDATIONS.	
7.1. INTRODUCTION.	7.1
7.2. AXISYMMETRICALLY LOADED CIRCULAR RAFT.	7.2
7.2.1. Convergence Of S.S.R.T. Results With Mesh Refinement.	7.2
7.2.2. Comparative Results Of Different Ground Models.	7.4
7.2.3. Influence Of Wall Superstructure.	7.10
7.2.4. Cylindrical Core For Building Structure.	7.14
7.2.5. Discussion And Conclusions.	7.17

7.3.	DEVELOPMENT OF PROGRAM FOR SURFACE ELEMENT ANALYSIS.	7.19
7.3.1.	General.	7.19
7.3.2.	The Surface Element Method.	7.20
7.4.	CORRELATION OF RESULTS.	7.24
7.4.1.	General.	7.24
7.4.2.	Ebenezer House.	7.24
7.4.3.	Consideration Of Superstructure.	7.30
7.5.	CONCLUSIONS.	7.34

CHAPTER 8: NON-LINEAR PILE-SOIL BEHAVIOUR.

8.1.	GENERAL.	8.1
8.2.	COMPARISON WITH O'NEILL ET AL.	8.2
8.2.1.	The Method Of O'Neill et al.	8.2
8.2.2.	The Proposed Method.	8.4
8.3.	COMPARISON WITH COYLE AND REESE.	8.6
8.3.1.	The Method Of Coyle And Reese.	8.6
8.3.2.	The Proposed Method.	8.8
8.4.	COMPARISON WITH MATLOCK.	8.11
8.4.1.	The Method Of Matlock.	8.11
8.4.2.	The Proposed Method.	8.16
8.5.	DISCUSSION AND CONCLUSIONS.	8.18

CHAPTER 9: DISCUSSION AND CONCLUSIONS.

REFERENCES.

APPENDIX A: THE SURFACE ELEMENT METHOD APPLIED TO RAFT ANALYSIS.

APPENDIX B: THE INTERACTION FACTOR METHOD.

APPENDIX C: DERIVATION OF THE STIFFNESS MATRIX FOR A ROD SUPPORTED BY AN ELASTIC SUBGRADE.

APPENDIX D: SEM USER MANUAL AND PROGRAM DETAILS.

LIST OF TABLES.

Table 3.1.:	PGROUP pile head forces.	3.26
Table 3.2.(a):	S.S.R.T. pile head forces for vertical loading.	3.26
Table 3.2.(b):	S.S.R.T. pile head forces for horizontal loading.	3.26
Table 4.1.(a):	PGROUP analysis of Alizadeh's test data.	4.23
Table 4.1.(b):	S.S.R.T. analysis of Alizadeh's test data.	4.23
Table 4.2.(a):	PGROUP analysis of McClelland and Focht's test data.	4.24
Table 4.2.(b):	S.S.R.T. analysis of McClelland and Focht's test data.	4.25
Table 4.3.(a):	PGROUP analysis of Alizadeh and Davisson's test data.	4.26
Table 4.3.(b):	S.S.R.T. analysis of Alizadeh and Davisson's test data.	4.26
Table 4.4.:	Adhesion calculated from short term pile load tests.	4.27
Table 4.5.:	Pile 121 - Variation of displacement with soil modulus.	4.27
Table 4.6.:	Pile 122 - Variation of displacement with soil modulus.	4.28
Table 4.7.(a):	Calculated and observed distribution of pile loads.	4.28
Table 4.7.(b):	S.S.R.T. results for the distribution of pile loads.	4.29
Table 5.1.:	Interaction Factors α for various S/d values.	5.48
Table 5.2.(a):	Results for axial loading of Case I.	5.49
Table 5.2.(b):	Results for lateral loading of Case I.	5.49
Table 5.3.(a):	Results for axial loading of Case II.	5.50
Table 5.3.(b):	Results for lateral loading of Case II.	5.50
Table 5.4.(a):	Results for axial loading of Case III.	5.51
Table 5.4.(b):	Results for lateral loading of Case III.	5.51

Table 5.5.:	Comparison of displacements.	5.52
Table 5.6.:	Comparison with Davisson and Salley.	5.52/53
Table 7.1.:	Comparison with Wardle and Fraser.	7.39
Table 8.1.:	Soil strata described by O'Neill et al (1982a).	8.21
Table 8.2.:	f_{\max} and z_c values used for S.S.R.T. analysis.	8.21
Table 8.3.:	Soil strata and average shear strengths from Plate 308 Terzaghi and Peck (1961).	8.21
Table 8.4.:	Relevant data extrapolated from Figure 8.7.	8.22
Table 8.5.:	Relevant data extrapolated from Figure 8.9.	8.22

LIST OF FIGURES.

Figure 1.1.:	Flexible raft foundations.	1.15
Figure 1.2.:	Rigid raft foundations.	1.15
Figure 3.1.:	Idealization of the model.	3.27
Figure 3.2.:	Typical distributions of (a) Axial load (b) Shear force and (c) Bending moment.	3.27
Figure 3.3.:	Effect of K_v on accuracy for vertical loading.	3.28
Figure 3.4.:	Effect of K_h on accuracy for vertical loading.	3.29
Figure 3.5.:	Effect of K_h on accuracy for horizontal loading.	3.30
Figure 3.6.:	Effect of K_v on accuracy for horizontal loading.	3.31
Figure 3.7.:	Distribution of loads against E_s for vertical loading.	3.32
Figure 3.8.:	Distribution of loads against E_s for horizontal loading.	3.33
Figure 3.9.:	Displacement against E_s .	3.34
Figure 3.10.:	Displacement against K_v and K_h .	3.35
Figure 3.11.:	Sensitivity of PGROUP axial load distribution to number of elements for horizontal loading.	3.36
Figure 3.12.:	Sensitivity of PGROUP shear force distribution to number of elements for horizontal loading.	3.37
Figure 3.13.:	Modification Factor M_v against K .	3.38
Figure 3.14.:	Modification Factor M_h against K_R .	3.39
Figure 4.1.:	Comparison with Reese and Cox.	4.30
Figure 4.2.:	Comparison with Alizadeh.	4.31
Figure 4.3.:	Comparison with McClelland and Focht.	4.32
Figure 4.4.:	Comparison with Alizadeh and Davisson.	4.33
Figure 4.5.:	Comparison with Davisson and Salley.	4.34

Figure 4.6.:	Comparison with Mansur and Hunter.	4.34
Figure 4.7.:	Details of piled abutment.	4.35
Figure 4.8.:	Results of load test on Pile 121 (uncoated).	4.36
Figure 4.9.:	Results of load test on Pile 122 (slip-coated).	4.37
Figure 5.1.:	Pile arrangement for axial loading.	5.54
Figure 5.2.:	Pile arrangement for lateral loading.	5.54
Figure 5.3.:	Comparison with Davisson and Salley.	5.55
Figure 5.4.:	Comparison with Ghosh.	5.56
Figure 5.5.:	Comparison with Whitaker. 5x5 pile groups.	5.57
Figure 5.6.:	Comparison with Whitaker. 3x3 pile groups.	5.57
Figure 5.7.:	Comparison with Berezantzev et al.	5.58
Figure 5.8.:	Comparison with Whitaker and Sowers et al. Load sharing between piles.	5.58
Figure 5.9.:	Comparison with Ghosh.	5.59
Figure 5.10.:	Comparison with Feagin.	5.60
Figure 5.11.:	Plan of raft-pile foundation and idealized grillage mesh.	5.61
Figure 5.12.:	Idealized applied loading.	5.61
Figure 5.13.:	Comparison of measured and computed pile loads.	5.62
Figure 5.14.:	Comparison of measured and computed settlements.	5.62
Figure 5.15.:	Plan and section of building at Basildon.	5.63
Figure 5.16.:	Soil characteristics.	5.64
Figure 5.17.:	Grillage, Short term computed settlement (mm) and Pile load as % of column load.	5.65
Figure 5.18.:	Pile design loads.	5.66
Figure 5.19.:	Observed settlements (mm) and Slab/soil effective stresses (KN/m^2)	5.67

Figure 6.1.(a):	Beam resting on an elastic subgrade.	6.13
Figure 6.1.(b):	Pile embedded in an elastic subgrade.	6.13
Figure 6.2.(a):	Pile system subjected to a lateral load.	6.14
Figure 6.2.(b):	Pile system subjected to an axial load.	6.14
Figure 6.3.:	Results for free pile head.	6.15
Figure 6.4.:	Results for restrained pile head.	6.16
Figure 6.5.:	Convergence results for a free pile head.	6.17
Figure 6.6.:	Convergence results for a restrained pile head.	6.18
Figure 6.7.:	Convergence of axial displacement.	6.19/20
Figure 6.8.:	Axial load distribution.	6.21/22
Figure 6.9.:	PGROUP Convergence tests.	6.23/24
Figure 7.1.:	Grillage idealizations.	7.40
Figure 7.2.:	Convergence of displacement for edge loaded raft.	7.41
Figure 7.3.:	Convergence of bending moment for edge loaded raft.	7.42
Figure 7.4.:	Results for edge loaded raft.	7.43
Figure 7.5.:	Results for edge loaded raft.	7.44
Figure 7.6.:	Results for uniformly loaded raft.	7.45
Figure 7.7.:	Results for uniformly loaded raft.	7.46
Figure 7.8.:	Results for combined loading on raft.	7.47
Figure 7.9.:	Results for combined loading on raft.	7.48
Figure 7.10.:	Storage tank configuration.	7.49
Figure 7.11.:	Idealized frame for S.S.R.T. analysis.	7.49
Figure 7.12.:	Raft and wall moments in storage tank.	7.50
Figure 7.13.:	Further results for full storage tank.	7.51/52
Figure 7.14.:	Data for core base analysis.	7.53
Figure 7.15.:	Results for core base analysis.	7.54

Figure 7.16.:	Boussinesq's idealization.	7.55
Figure 7.17.:	Holl's idealization.	7.55
Figure 7.18.:	Drained raft settlements of Ebenezer House.	7.56
Figure 7.19.:	Components of model.	7.57
Figure 7.20.:	Details of model.	7.57
Figure 7.21.:	Details of superstructure.	7.58
Figure 7.22.:	Superstructure idealizations.	7.59
Figure 7.23.:	Coarse grillage.	7.60
Figure 7.24.:	Refined grillage.	7.60
Figure 8.1.:	Comparison with the load-settlement curves of O'Neill et al.	8.23
Figure 8.2.:	Comparison with pile load and soil stress distribution curves of O'Neill et al.	8.24
Figure 8.3.:	S.S.R.T. pile idealization for comparison with O'Neill et al.	8.25
Figure 8.4.:	Shear strength coefficients.	8.25
Figure 8.5.:	Comparison with load-settlement curves of Coyle and Reese.	8.26
Figure 8.6.:	S.S.R.T. pile idealization for comparison with Coyle and Reese.	8.26
Figure 8.7.:	Adjusted field curves. [after Coyle and Reese.]	8.27
Figure 8.8.:	p-y curve for short term static loading.	8.27
Figure 8.9.:	Predicted family of p-y curves for Sabine clay for short term static loading.	8.28
Figure 8.10(a):	Comparison of bending moments for Sabine free head static loadings.	8.29
Figure 8.10(b):	Load-deflection curves for Sabine free head static loadings using proposed method.	8.30

ACKNOWLEDGEMENTS

The candidate is greatly indebted to Mr D.K. Pugh, Director of Studies and former tutor, for the personal attention and guidance he has afforded throughout the course of this work.

The contribution and advice of Dr R. Delpak, the candidate's Supervisor is appreciated.

The candidate is grateful to Mr G.O. Rowlands, former Reader at the Polytechnic, for securing the SERC research grant and for initiating the work. Thanks are also extended to Dr S. Wild the candidate's Shepherd.

He is appreciative of Prof. P.S. Coupe, his Head of Department, for allowing the use of departmental facilities. The assistance of the Department technical and administrative staff and Mr H. Davies is gratefully acknowledged.

Finally, he is grateful for the support given by his mother and family.

DECLARATION

This is to certify that neither this thesis, nor any part of it, has been presented, or is being currently submitted, in candidature for any other university.

A. J. Jones

(Candidate)

CERTIFICATION OF RESEARCH

This is to certify that, except when specific reference to other investigations is made, the work described in this Dissertation is the result of the investigation of the candidate.

A. J. Jones

(Candidate)

10-01-92

(Date)

D. H. H.

(Director of Studies)

10/01/92

(Date)

A. D. D.

(Supervisor)

January 10th 1992

(Date)

ABSTRACT

Methods of analysis are presented which enable the performance of both piled and plain raft foundations to be predicted. Throughout the work the substructure is modelled using a beam-column idealization. This allows the superstructure configuration to be readily incorporated into the model enabling the soil-structure interaction of the complete system to be investigated.

The supporting soil is modelled using a discrete spring representation as in the simplified subgrade reaction theory (S.S.R.T.). The idealized model is analysed using a standard structural program. Relationships are developed between spring stiffness values and soil moduli for a range of axially and laterally loaded pile-soil configurations. The results are verified by comparison with more rigorous solutions and the measured performance of single piles.

The work is extended to consider the interaction of axially and laterally loaded pile groups and piled raft foundations. A simplified treatment of interaction is proposed for approximately uniformly loaded piles. For piles which carry substantially different loads due to interaction effects, a more rigorous procedure is presented.

Consistent matrices are presented to idealize the uniform distribution of soil stiffness along both axially and laterally loaded pile elements. Parametric studies demonstrate that very few elements are required to model laterally loaded piles. The S.S.R.T. method indicates that

the results are very sensitive to the number of pile elements used.

The limitations of the proposed method for the analysis of plain raft foundations is investigated. It is demonstrated that soil-structure interaction generally cannot be modelled by varying the soil stiffness across the raft. Consequently, a method of analysis is developed which combines the grillage idealization with the Surface Element Method. A program is developed for the analysis which incorporates the superstructure configuration. The proposed method is verified by comparison with results from the measured performance of existing buildings and other rigorous solutions.

Finally, the combined S.S.R.T./stiffness approach is successfully developed to predict the non-linear performance of single piles. This is achieved using established non-linear load-displacement curves. The solution process involves less iterations than traditional non-linear methods. The computed results are correlated with the measured performance and other solutions of both axially and laterally loaded piles.

LIST OF SYMBOLS.

A	Cross-sectional area
b	Breadth
Ca	Soil adhesion
Cu	Undrained shear strength
d	Outer pile diameter
dc	Pile cap diameter
di	Inner pile diameter
E	Young's modulus
E'	Drained soil modulus
Ec	Young's modulus of concrete
Eh	Horizontal soil modulus
Ep	Pile modulus
Es	Soil modulus
Eu	Undrained soil modulus
Ev	Vertical soil modulus
E(z)	Soil modulus at depth z
E ₀	Soil modulus at ground surface
E ₁	Soil modulus of bottom layer in 2 layer model
f	Soil shear load on pile
f _{max}	Maximum unit load transfer at a given depth
[F _S]	Soil flexibility matrix
G	Shear modulus
I	Second moment of area
Ih	Interaction factor for lateral behaviour
Ip	Second moment of area of pile
Ir	Interaction factor for axially loaded piled raft
Iv	Interaction factor for axial behaviour

J	Torsional constant
K	Relative stiffness pile to soil (axial behaviour)
[K]	Stiffness matrix
K _{eb}	Subgrade modulus for end bearing reaction (N/m)
K _h	Subgrade modulus for lateral behaviour (N/m)
K _h '	Subgrade modulus for lateral behaviour (N/m ²)
K _{pr}	Soil stiffness at nodal point of pile cap
[K _{p_h}]	Matrix for lateral stiffness of pile
K _R	Relative stiffness pile to soil (lateral behaviour)
K _s	Coefficient of subgrade reaction beneath raft
K _{s1} '	Coefficient of subgrade reaction for a 1ft.squ. plate
[K _{s_h}]	Matrix for lateral stiffness of soil
K _v	Subgrade modulus for axial behaviour (N/m)
K _v '	Subgrade modulus for axial behaviour (N/m ²)
L	Pile embedded length
L'	Pile element length
m	Rate of increase of soil modulus with depth z
M _h	Modification factor for lateral behaviour
M _r	Radial bending moment
M _t	Tangential bending moment
M _v	Modification factor for axial behaviour
p	Lateral load transfer to soil
P	Pile axial load at the head
{P}	Load vector
P _g	Pile axial load from PGROUP
P _u	Ultimate lateral resistance of pile per unit length
q	Tip stress
q _{max}	Maximum tip stress
Q ₀	Axial load at the pile head
R _A	Relative area of hollow pile

R_S	Settlement ratio
S	Pile centre to centre spacing
t	Axial load transfer to soil
T	Pile shear force at the head
T_g	Pile shear force at the head from PGROUP
U_o	Pile head lateral displacement
X_r	Depth of reduced lateral resistance
y	Lateral displacement
z	Depth, vertical displacement
Z	Modification factor for axially loaded pile group
z_c	Pile displacement corresponding to maximum stress
Z_H	Modification factor for laterally loaded pile group
Z_R	Modification factor for axially loaded piled raft
α	Interaction factor for axially loaded pile group
α_R	Interaction factor for axially loaded piled raft
δ	Displacement
$\{\delta\}$	Displacement vector
δ_h	Horizontal displacement
δ_v	Vertical displacement
δ_z	Vertical displacement
ϵ_z	Vertical strain
θ	Rotation
σ_r	Radial stress
σ_θ	Tangential stress
σ_x	Stress in horizontal x direction
σ_y	Stress in horizontal y direction
σ_z	Stress in vertical z direction
μ	Poisson's ratio
μ_s	Poisson's ratio of soil

Other symbols are defined in the text where they occur.
Some symbols are redefined for consistency with the
original reference.

CHAPTER 1.

APPRAISAL OF THE PROBLEM.

1.1. INTRODUCTION.

Engineers have been faced with the problem of transferring load from the structure to the ground for thousands of years. Whereas a plain raft foundation was generally adequate for structures founded on firm ground, the settlement tended to be excessive on softer soils. This was overcome by providing end bearing piles to transfer the load to stronger strata underlying the softer soils, e.g. bedrock. Where the stronger strata was at a depth to which it was impracticable to pile, it was established that a group of piles founded in the softer soils was adequate in supporting the structure. These are referred to as friction piles since they depend on the skin friction, or adhesion, developed at the pile-soil interface to transfer load to the ground. Where a series of individual pile caps were almost contacting each other, a raft provided above the piles was desirable to support the structure. The piled raft foundation distributed the load to the ground more evenly and assisted in reducing differential settlements.

1.2. PILED RAFT DESIGN.

Piles are frequently provided to control the settlement of raft foundations which satisfactorily transfer the structural load to the ground without causing shear failure of the soil. Until recently, the design philosophy for the piled raft was to assume that the piles carried the total load. Because no allowance was made of

the load carried by the raft, the substructure design tended to be conservative in providing support to the overlying superstructure.

Nowadays, the soil-structure interaction of the piled raft foundation is better understood. It is a complex mechanism which the most powerful methods of analysis can only estimate. A method of analysis is only applicable when the solutions have been justified by correlation with the observed behaviour of practical problems. At present the actual behaviour of piled raft foundations can only be conjectured because of field monitoring difficulties. For example, load cells can be provided at certain points beneath the raft and within the piles, and the surface settlement profile can be determined. However, the stress distribution within the bulk of the soil mass is generally unknown, as is the load transfer mechanism within the ground as the soil material deforms.

Development work into the behaviour of piled raft foundations in the London Clay has resulted in savings being made on the substructure costs of prestigious buildings, such as the Queen Elizabeth II Conference Centre as reported by Burland and Karla (1986). This was achieved by considering the proportion of load carried by the raft and using the concept of settlement reducing piles. However, the design philosophy remains obscure. In this case, each pile was assumed to carry the total column load immediately above it. Not all proposed structures lend themselves to this approximation. Hence, a general approach to the design is required.

Cooke (1986) carried out extensive model tests on various piled rafts and free standing groups. Due to the complexity of the problem, the magnitude of stiffening that the addition of a raft provided could not be determined by subtracting one stiffness from another. This is because pile groups transmit shear stresses more effectively when there is no load transferred from the raft. He observed that the raft carries about 45% of the load at the early stages of construction, decreasing to about 25% at the time of occupation. The transfer of load from the raft to the piles is due to settlement mobilizing the skin resistance of the pile shafts.

It can be concluded that there is no adequate design philosophy to determine the load carried by the raft of a piled foundation. Thus each piled raft configuration needs to be analysed using a method of analysis which accommodates load sharing between the piles and raft.

1.3. CONTACT PRESSURES

1.3.1. Plain Rafts

To design a raft foundation the contact pressure distribution at the raft-soil interface is required. This enables the magnitude of the bending moments and shear forces within the raft and the resulting settlement profile to be determined. The contact pressure beneath a foundation is dependent on several factors, the principal ones being:

- the degree of rigidity of the foundation.
- the soil type.
- the loading distribution.
- the form, or shape, of the foundation.

The load distribution and rigidity of the foundation are factors which the designer controls. This is because they depend upon the size and function of the supported structure. However, the soil type governs the general behaviour of the foundation. There are basically two soil types, namely cohesive and cohesionless. Cohesive soils, such as clays and saturated silts, tend to act elastically when loaded, ie. there is a change of shape but no volume change. Hence a foundation on a cohesive soil can be analysed using elasticity if time and consolidation effects are ignored. Smith and Pole (1980) reported that cohesionless soils such as sands and gravels, either dry or submerged, tend not to behave elastically when supporting a surface foundation. Tomlinson (1986) stated that the assumption of the loaded ground being elastic, homogeneous and isotropic was not "strictly true for natural soils, but the assumptions are justifiable for practical design". Tomlinson also reported that the settlement of cohesionless soils is estimated using semi-empirical methods based on the Standard Penetration Test (SPT).

Another difference in the behaviour of cohesive and cohesionless soils is the manner in which the soil strength is mobilized. This behaviour is described by the Coulomb-Mohr equation shown below:

$$s = c + p \tan \phi \dots\dots\dots 1.1$$

where (s) is the shear strength, (c) the cohesion, (ϕ) the angle of shearing resistance of the soil and (p) is the pressure on the soil.

There is no overburden pressure at the edges of a surface foundation on a cohesionless soil to give the soil

any shear strength. However, the soil beneath the centre of the foundation gains strength as it is compressed. For cohesive soils, more shear strength around the periphery of the foundation is mobilized than at the centre as the foundation settles.

The rigidity of the raft significantly influences the contact pressure distribution. The two limiting cases are full rigidity and perfect flexibility. These are considered in turn.

Uniformly loaded flexible foundations impose an approximately uniform contact pressure irrespective of soil type, as shown in Figure 1.1.(a). The settlement profiles of foundations on cohesive and cohesionless soils tend to be of opposite shape as shown in Figure 1.1.(b). This is due to the manner in which the shear strength is mobilized within the different soils.

Uniformly loaded rigid foundations impose a uniform settlement profile. The contact pressure distributions for cohesive and cohesionless soils tend to be dissimilar. For cohesive soils, the contact pressure at the edges is greater than at the centre. Elastic theories predict that the contact pressures tend to increase parabolically to infinity at the edges. However, due to local plastic yielding of the soil, the maximum contact pressure cannot exceed the soil shear strength. This results in a contact pressure distribution similar to that shown in Figure 1.2.(a). For cohesionless soils, large contact pressures develop at the centre which reduce at the edges as shown in Figure 1.2.(b).

The effect of the size of the foundation on the contact pressure distribution is also shown in Figure 1.2(b). For a given applied pressure, the contact pressure distribution becomes less peaked at the centre as the foundation width is increased.

For most practical cases, the shape of the foundation is of minor importance. The work of Hooper and Wood (1977) indicates that the settlement of an axisymmetrically loaded non-circular raft foundation, with a length to breadth ratio (L/B) less than about 4, supported by an elastic continuum can be determined with reasonable accuracy by treating it as a circular raft of the same plan area.

The various contact pressure distributions described above are for limiting cases, ie. either wholly rigid or flexible foundations, and, cohesive or cohesionless soils. In practice, foundations have some degree of flexibility and most soils are a mixture. Hence, the actual contact pressure distribution tends to be intermediate of the limiting cases. As reported by Tomlinson (1986) and Smith and Pole (1980), for practical purposes it is common to assume that the contact pressure will tend to a uniformly distributed profile. Also, wherever possible, designers will attempt to obtain a uniform contact pressure distribution in order to keep differential settlements to a minimum.

The assumption of a uniform contact pressure distribution, may be satisfactory in most straightforward cases. However, as Smith and Pole (1980) recommended, there may be occasions when the loading or the subgrade conditions are such that the calculated values should be

modified to allow for some of the contact pressure characteristics discussed above.

1.3.2. Piled Rafts

The non-uniform contact pressure distributions described above will also occur beneath the raft of a piled foundation. In this case, the stress distribution is further complicated by the presence of piles. The raft contact pressures are difficult to assess as they have peak values between piles, and zero, if not negative values, at the pile head surfaces, as reported by Cooke (1981). Cooke assumed the pressure distribution between piles to vary parabolically.

The raft generally carries less load than elastic equations predict. This is mainly due to the pile shafts transferring load to the soil which causes it to compress. Hence, the contact pressure at the raft-soil interface is reduced. Further complications arise with end bearing piles, which require relatively large settlements to occur before the full base resistance can be developed. Also, the superstructure configuration has a significant influence on the distribution of load and moment in the raft and consequently the contact pressure distribution.

1.4. SOIL-STRUCTURE INTERACTION

Soil-structure interaction is a process which inevitably occurs where a structure is founded on deformable ground. Generally, the two main effects for a piled raft are: (i) the interaction of piles on each other tends to reduce the load in the central piles which is

transferred to the peripheral piles, and (ii), the load is redistributed from the soil to the superstructure via the foundation. The additional stiffness of the superstructure assists the substructure in resisting differential settlements. Thus consideration of the superstructure stiffness in the foundation analysis may enable a more flexible raft to be designed. This would allow the designer to use a thinner and more economical raft. However, the load redistributed into the superstructure needs to be catered for, during the design process, to avoid damage to, or failure of, the superstructure. Considerable loads and moments may also be redistributed into the superstructure from a relatively rigid raft.

It is difficult to accurately determine the superstructure stiffness of a complex high rise building without modelling it fully. In such cases an equivalent raft is commonly used with a stiffness related to the second moment of areas for the upper floors. Because structures in practice are tolerant to reasonable amounts of redistribution and distortion, the most economical solution often consists of a relatively flexible substructure. However, an optimized pile group beneath a flexible raft may produce "hard-spots", resulting in distress in the raft. In this case, care needs to be taken to avoid shear failure of the raft.

King and Chandrasekan (1974) showed that the difference in contact pressure distributions of plain rafts determined from interactive analyses of a relatively flexible and rigid raft was small. This was due to the superstructure contributing additional stiffness to the

raft. Their work demonstrated the necessity to consider the influence of the superstructure in such analyses.

Hain and Lee (1974) stated:

"The complete system which should be analysed consists of a structure-raft-supporting soil-pile group"

Failure to analyse the "complete system" may result in differential settlements being overestimated. This leads to a conservative substructure design, with possibly a poor superstructure design. Consequently, many structures are now "thoroughly" analysed using complex mathematical idealizations. These assess the response of the proposed structure to ground movement and load and moment redistribution. A document produced by the Institution of Structural Engineers (1977) warned against relying on the results obtained from such methods of analysis, because of the simplifying assumptions which have to be made. In the same report it was stated:

"If the definition of the ground conditions is vague then complex structural analyses are irrelevant, and simplified design may be more appropriate".

The site investigation should therefore adequately establish the variation in ground material properties and these should be considered in the mathematical ground model. Thus, the adopted method of analysis should be sufficiently versatile to facilitate numerous variations in ground conditions.

1.5. SUMMARY

Developments in the design philosophy of piled raft foundations in the London Clay have resulted in designs where savings have been made in the substructure costs.

This has been achieved by considering the proportion of load carried by the raft. A further development of this design approach is the increased popularity in the use of settlement reducing piles. These limit the settlement of rafts which are satisfactory against Bearing Capacity failure.

It is difficult to ascertain the load carried by the raft because of the complex contact pressure distribution beneath it. This is further complicated by the presence of piles in the soil mass. For plain raft foundations, the contact pressure distribution varies depending principally on the rigidity of the structure, soil type and load distribution. The assumption of a uniform contact pressure distribution, may be satisfactory in most straightforward cases. However, there may be occasions where the loading or the subgrade conditions are such that the calculated contact pressures should be modified to more realistically model raft-soil interaction. Alternatively, a rigorous method of analysis may be required to determine the contact pressure distribution.

Incorporation of the superstructure details into the structural model has enabled more economical and thinner rafts to be designed. This is because the additional stiffness of the superstructure assists the substructure in resisting differential settlements. However, the load redistributed into the superstructure needs to be catered for during the design process.

It was noted that one of the most important aspects of a method of analysis was the ability to satisfactorily define the ground conditions. This is especially so for

highly variable soil conditions. In which case a simplified method of analysis which can readily idealize such conditions may be more appropriate.

1.6. OBJECT OF THE RESEARCH

The object of the research is to develop suitable methods of analysis which accommodate soil-structure interaction. The successful development of piled raft analysis in the consistent material properties of London Clay will be applied to ground of variable properties. The proposed method will enable soil stiffness parameters to be varied in both the vertical and horizontal direction.

The soil modulus, E_s , is a common property used to define the deformation characteristics of a soil. Consequently, an attempt will be made to relate the soil spring stiffness, used in simplified analyses, to the soil modulus, E_s . This will enable the proposed method to be readily applied to many foundation problems.

The contribution the raft makes to the total load carrying capacity of the substructure system will be examined. In addition, it is proposed that the superstructure configuration and its stiffness shall also be considered in the analysis. This is necessary in order to consider the soil-structure interaction of the complete system.

Bridge foundations are frequently subjected to lateral loads. The method should therefore accommodate laterally loaded piles raked in any direction. Furthermore, provision for pile-raft-soil interaction will be made where

it is anticipated that this will be an important consideration in the design.

It is intended that this work be of practical use. The methods of piled foundation analysis developed must therefore be capable of using standard structural engineering space frame programs which operate on microcomputers. In this way, design engineers can gain easy access to a versatile tool which is capable of solving complex soil-structure interaction problems to a definable degree of accuracy. Other features such as the non-linear nature of the subgrade shall be incorporated in an approximate manner. It is proposed to extend the work to the analysis of plain raft foundations and three dimensional (3-D) superstructures supported on raft foundations with non-uniform contact pressure distributions.

It is not the intention of developing programs similar to PGROUP for the analysis of substructures. It is proposed to develop modelling procedures which allow standard programs to be used in the analysis of such structures. However, a program was written to analyse plain rafts and 3-D superstructures founded on an elastic continuum. This was necessary because of the limitations of the proposed simplified method of analysis in modelling raft-soil interaction.

1.7. LIMITATIONS

The principal factors affecting the performance of a piled foundation include the residual forces caused by the installation of the piles; the effect of swelling or

shrinking of the soil on the foundation and negative friction on piles, especially end bearing piles. These influences lie beyond the scope of the present research. The effect of these factors on the performance of the substructure can be inferred from other work; such as Poulos and Davis (1980).

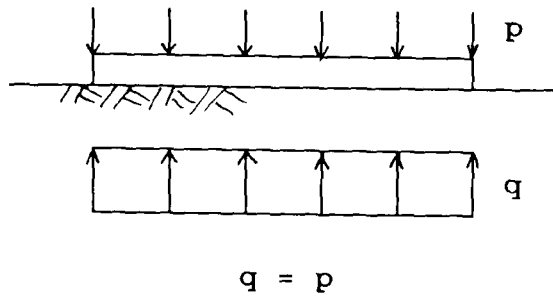
Another primary factor which influences the behaviour of a piled foundation is the depth to a rigid stratum underlying the softer soils in which the substructure lies. For the behaviour of a pile to be completely unaffected by a rigid stratum, the depth from the ground surface to the rigid stratum should be at least 2.5 times the pile length. For instance, in the case of incompressible single piles, with a soil Poisson's ratio of 0.2, the soil below a depth of 2.5 times the pile length is not stressed significantly. The work of Poulos and Davis (1974) indicated that the percentage decrease in the pile-head settlement was about 12% and 10% for L/d ratios of 25 and 100 respectively, as the thickness of the soil layer was reduced from infinity to 2.5 times the pile length.

Consequently, soil layers less than 2.5 times the pile length in depth, are effectively beyond the scope of the present work. The exception is an end bearing pile on a rigid stratum which can be treated as a column. For soil layers less than this thickness modifications can be inferred from the work of Poulos and Davis (1974).

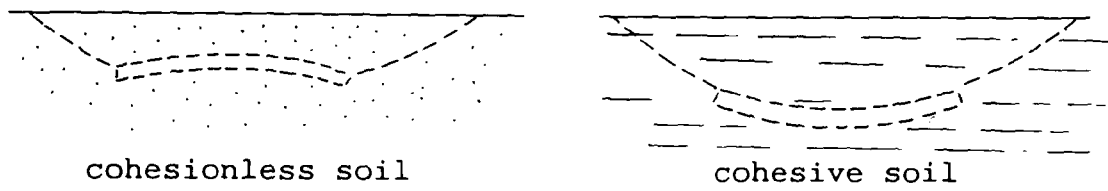
It is intended to apply the proposed method of analysis to variable ground conditions. Although a softer soil overlying a rigid stratum represents a variable ground condition, the behaviour of the two layers are completely

dissimilar. Consequently, results should be treated with caution where the bulb of pressure penetrates a rigid stratum. The behaviour of a multilayered system is theoretically complex. In the proposed simplified method it is necessary to assume the behaviour of the various layers to be approximately similar. This is the assumption Steinbrenner (1934) employed in his method; ie. the stress distribution within the layered system is identical with the Boussinesq distribution for a homogeneous semi-infinite mass. This assumption is only valid where the soil moduli of the various layers are of the same order.

For piled foundations, the stress distribution in the soil is completely altered by the action of the piles transferring load to a greater depth. The resulting stress distribution in the various layers tends to be more uniform than that of a plain raft. Hence, the assumption that the behaviour of the various layers are similar is more applicable for piled foundations. The advantage of the proposed simplified method of analysis over other methods lies in its ability to readily represent the deformation characteristics of variable ground conditions, without recourse to complex numerical techniques.

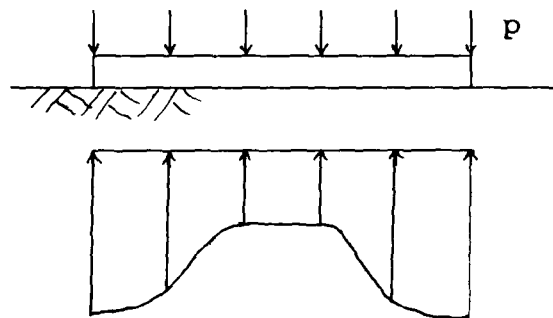


(a) Contact pressure.

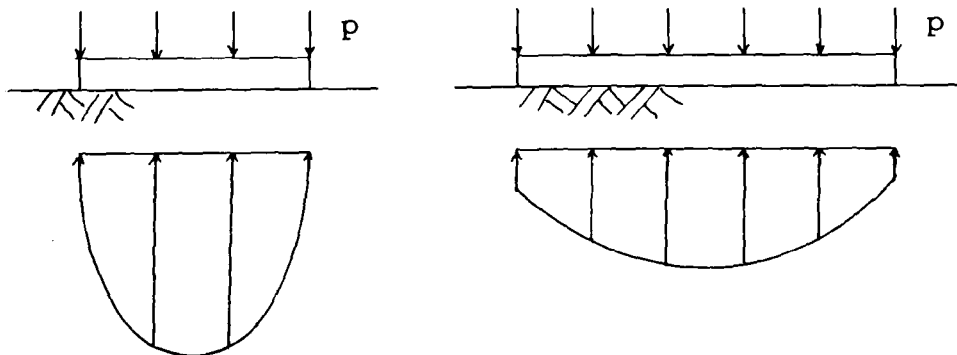


(b) Deflected form.

Figure 1.1.: Flexible raft foundations.



(a) Contact pressure for cohesive soil.



(b) Contact pressure for cohesionless soil.

Figure 1.2.: Rigid raft foundations.

CHAPTER 2

REVIEW OF THE RELATED LITERATURE.

2.1. INTRODUCTION.

McClelland (1972) identified two criteria by which the performance of a substructure is traditionally judged: (i) it must carry the superstructure and imposed loads without causing bearing failure of the soil, (ii) the deformation must be of a magnitude which does not impair the use of the complete structure.

The design of the structural elements is adequately controlled by Codes of Practice and British Standard Institution documents. Bearing capacity and shear strength of the soil are satisfactorily determined from accepted methods of soil mechanics. Consequently these subjects are not addressed in this work. Attention is given to the determination of the load distribution within the substructure and its load-displacement characteristics.

Long term consolidation is usually the most significant component of settlement. Because of the complexities of soil-structure interaction, consolidation effects do not lend themselves readily to theoretical analysis. Consideration of consolidation in the design process is usually confined to approximate solutions, empirical rules and from the behaviour of previously monitored "similar" structures. It may also be accommodated by specifying drained soil parameters in an elastic analysis.

McCelland (1972) proposed that short term settlement of the soil rarely affects design decisions. However, he stated:

"some understanding of short term load deformation behaviour is necessary to correctly anticipate or interpret load transfer from the pile and stress distribution in the soil, both of which are closely related to pile performance."

Elastic theory generally provides satisfactory results for the substructure behaviour up to working loads. Hence, this review focuses on methods of analysis to determine the linear load-deformation behaviour of substructures. The methods are described and the limitations and advantages of each discussed. The Surface Element Method of raft analysis and the Interaction Factor Method of piled foundation analysis are described in Appendices A and B respectively. These methods are presented since they are further developed in this research work.

2.2. SOIL IDEALIZATION.

The behaviour of a substructure is complex in practice and elasticity is not strictly a valid assumption. Barkan (1962) contended that the stress-strain relationships of elastic soil deformations are more complicated than those stipulated by Hooke's Law (1675). However, if Hooke's Law is not used, it is necessary to employ a theory of elasticity which operates with non-linear differential equations. The solution of these equations, even for the simplest problems, presents difficulties. It is therefore usually necessary to assume that the soil strictly obeys Hooke's Law. As a precaution,

Barkan suggested that the numerical values of elastic soil constants should be selected with due consideration to the influence of the simplifying assumptions.

2.3. SOLUTION OF PROBLEMS OF ELASTICITY.

2.3.1. General.

The basic elastic solutions pertinent to a loaded substructure include:

- (i) the Kelvin solution, after Thomson (1848), for a point load acting within an infinite elastic mass,
- (ii) Boussinesq (1885) for a point load acting on the surface of a semi-infinite mass,
- (iii) Mindlin (1936) for a point load acting beneath the surface of a semi-infinite mass,
- (iv) Burmeister (1943, 1945) for a vertical point load acting at the surface of a layer underlain by a rough rigid base.

These solutions require a considerable effort in the manipulation of the resulting equations. Hence, standard results are often presented in the form of charts, which are more easily used. Where the substructure shape, loading or soil profile is irregular, then numerical techniques are necessary to solve the equations. The principal techniques include the Finite Element Method (F.E.M.) and the Boundary Element Method (B.E.M.). The Subgrade Reaction Theory (S.R.T.) has been used extensively in the past for the analysis of substructures supported by an elastic subgrade. However, it does not model an elastic continuum because only the material in contact with the load is deformed.

2.3.2. The Finite Element Method.

The F.E.M. is presently the most powerful numerical tool available for the solution of complex problems of elasticity. The method is fully described by Zienkiewicz (1977) and its geotechnical applications by Smith (1982). For the analysis of geotechnical problems, the superstructure, substructure and soil domain are discretized by finite elements. Each finite element is assigned a specific material stiffness. Adjacent elements are connected at nodal points. Element type depends on the shape and loading of the problem and whether it is a one, two or three dimensional idealization. A stiffness matrix for the complete system is constructed and solved to give the nodal displacements. This enables the stresses and strains within each element to be computed.

The method has also been used to obtain solutions to problems involving non-linear behaviour of materials. Such features as pile slippage, pore water pressure dissipation and installation effects of piles etc. can be considered in the solution process.

Because of the versatility of the method, it is frequently used to obtain the most "accurate" theoretical solution. Although it is widely used for research, its application to general geotechnical problems is limited. This is due to the difficulty encountered and time taken in creating a realistic mesh for the soil, especially for a piled foundation. A further complication is the boundary representation of the soil. This is necessary to create a finite mathematical model for the continuum.

2.3.3. The Boundary Element Method.

The B.E.M. is a popular numerical technique for solving problems of elasticity. Only the boundary surfaces of the problem are defined. The development of the B.E.M. has continued for several years and a breakthrough was achieved by Banerjee (1978), when he simplified the method and combined it with a three dimensional frame analysis routine. This forms the basis of the Department of Transport (D.o.T.) program PGROUP (1981) for the analysis of pile groups. Banerjee (1978) explained that the idealization differs from the behaviour of a real soil, but that it was a more satisfactory approximation than the Winkler (1867) medium. PGROUP has been extended to accommodate soil non-homogeneity to some extent ie. a homogeneous, a linearly varying modulus with depth and a two layer soil can be idealized. The method directly employs the use of Mindlin's (1936) equations, which strictly apply to a homogeneous isotropic half-space. Hence, solutions for soil non-homogeneity can only be approximate.

The program is easy to use and enables pile configurations to be selected with consideration of pile-soil-pile interaction. Its application to practical geotechnical problems is limited. This is because it cannot accommodate multi-layered heterogeneous soils, piles raked in two planes, finite raft stiffness and variable loading over the plan area of the raft. Hence the interaction between the superstructure, substructure and soil cannot be studied. Furthermore, it has a tendency to

exaggerate the interaction between piles. This arises because linear elastic formulations tend not to be applicable to real soils.

2.3.4. The Subgrade Reaction Theory.

The S.R.T. is one of the simplest methods available for the idealization of an elastic subgrade. The method has often been used as a preliminary design tool, enabling a substructure configuration to be selected prior to analysis using a more rigorous method. Because it does not represent a continuum, it should only be used where the soil deformation is localized in the immediate vicinity of the substructure.

The idealization of an elastic beam and simplified elastic subgrade makes use of the coefficient of subgrade reaction, K_s . This is defined as the ratio of the subgrade reaction pressure, p , and the settlement, y , of a particular point. The analogy of springs is used after Winkler (1867). It is assumed that a spring not stressed beyond its elastic limit will have a constant stiffness equal to the load divided by its extension.

A disadvantage of the method is the difficulty in selecting appropriate spring stiffness values to idealize the soil. Terzaghi (1955) presented a method to calculate the spring stiffness values for a raft and a laterally loaded pile from plate loading tests. He discussed the assumptions and limitations of the method and suggested ways in which errors can be reduced.

Smith and Pole (1980) indicated that the method predicts realistic contact pressures. However, it should

only be used where the order of settlement is required. They reported that an error of 100% in the estimation of K_s may change the bending moment and shear force distribution of the substructure by up to 15% only.

2.4. APPLICATIONS OF ANALYTICAL METHODS.

2.4.1. Raft Foundations.

(a) Standard elastic solutions.

Boussinesq's (1885) method is appropriate for the analysis of flexible raft foundations and is frequently used for preliminary analysis. The method enables both pressures and displacements to be determined at various depths within the soil mass. Newmark (1942) presented Boussinesq's solutions in the form of Influence Charts. Recognizing the need to model rafts of finite stiffness and various loading distributions, Boussinesq's solutions were adapted accordingly by several researchers. Poulos and Davis (1974) presented a number of such solutions which include contact pressure, bending moment and shear force distributions, and deformation profiles.

The presented standard solutions enable the behaviour of general raft foundations with a finite stiffness to be inferred. The solutions indicate that contact pressures at the edges of the rafts tend to infinity, whereas in practice the soil reaction is governed by its shear strength.

(b) The Finite Element Method.

The F.E.M. lends itself to the analysis of rafts on multi-layered soils, with or without a superstructure.

Because three dimensional analyses tend to be prohibitively expensive, two dimensional idealizations are more common. These are restricted to axisymmetric cases such as circular rafts under axisymmetric loading and plane strain cases such as continuous strip footings.

(c) The Boundary Element Method.

A B.E.M. solution is obtained by idealizing the raft as a mesh of two-dimensional plate bending elements. The surface of the soil beneath the raft is also defined by an equivalent mesh. Since the adopted techniques rarely involve an integral equation formulation, Tomlinson (1986) suggested it is more appropriate to term this the Surface Element Method (S.E.M.).

The Boundary/Surface Element Methods have been developed to consider soil layering and the variation of soil stiffness with depth within layers. The methods usually employ the Steinbrenner (1934) approximation i.e. the stress distribution within the heterogeneous soil mass due to the applied surface loads is the same as that within an elastic half-space. The vertical strain is then governed by the material properties of the soil at that point. Tomlinson (1986) reported that the method "will give very satisfactory results over a wide range of circumstances". Wood (1977) applied the method to an asymmetrical structure and found that the results compared favourably with the measured settlements. The results also agreed satisfactorily with the plane strain finite element analysis of Moore and Jones (1975). Wood (1978) developed the program RAFTS for general raft analysis.

The method has been extended to include local yielding of the soil where the contact pressures reach a limiting value. Wood (1982) applied the method to circular raft foundations of four grain silos on chalk. The results obtained were again favourable. Hooper and West (1983) reported that in most cases the method of analysis for the simplified layered continuum gave good results.

Hooper (1983) modified the method to include rafts on strata whose thickness, or material properties, varied in the horizontal direction as well as with depth. In the few cases where the Steinbrenner approximation is inappropriate, Hooper and West (1983) developed a more rigorous method based on the integral transform method. In the analysis of a basement raft on a multi-layered soil, solutions were obtained for settlement, contact pressure and bending moments. Good agreement was obtained between Hooper and West's simplified and rigorous layer solutions. The Winkler foundation solution also agreed favourably in this instance. This may have been due to the depth of the deformable material beneath the raft being relatively shallow compared to the raft dimensions. The elastic half-space model considerably overestimated the settlements.

(d) The Subgrade Reaction Theory

With the advent of computers for engineering analysis in the 1960's, it became popular to model the raft foundation as an equivalent grillage of rigidly connected beams. This is supported by discrete vertical springs, representing the soil at the nodal points. A later development was the use of plate bending finite elements

supported by springs to accommodate such effects as openings and variation in raft thickness. Both the grillage and plate bending elements are considered acceptable for representing the behaviour of the raft. The main criticism of the method is the inability of the Winkler (1867) springs to interact with one another.

The Institution of Structural Engineers (1977) reported that the Winkler idealization could not be recommended for the analysis of rafts. This is because it is a poor physical model which may give rise to erroneous results. This recommendation was reinforced by the Institution of Structural Engineers et al (1989). Hooper (1984) commented that the performance of the method is problem dependent and can give good results in certain cases, but, can lead to grossly inaccurate results on the unsafe side. Mawditt (1982) reported that the Winkler foundation gives satisfactory results where, among other requirements, the loading can be approximated by a single point load. Tomlinson (1986) concluded, that since the limits of safe applicability of the Winkler foundation may not be recognized by many design engineers, it cannot be recommended as general practice.

The behaviour of the Winkler foundation is qualified by Heteyni (1946), one of its original advocates, who stated:

"Though [the Winkler foundation] is mathematically simpler, one should not regard it, as some investigators do, as an approximation or an 'elementary' solution for the elastic solid foundation, because it has its own physical characteristics and significance."

Heteyni deduced that some subsoils were of such a character that the deformation is localized mainly in the

loaded region. He cited Foppl's (1934) experiments as the basis of this observation. In such cases, the Winkler assumption is a satisfactory representation of soil structure behaviour.

2.4.2. Axially Loaded Single Piles.

(a) Elastic methods.

These methods are based on Mindlin's (1936) solutions for the effects of subsurface loading in a semi-infinite elastic half-space.

Thurman and D'Appolonia (1965) presented an approach for the analysis of a compressible pile. The pile is divided into a number of elements and the shear stresses on the pile shaft are represented by point loads at the nodal points. Solutions are obtained using Mindlin's equations.

Poulos and Davis (1968) considered a rigid pile embedded in an elastic continuum. They developed the method to consider uniform shear stresses acting around the periphery of each element.

Mattes (1969) and Butterfield and Banerjee (1970) demonstrated that the added complexity of consideration of radial compatibility influences the shear stress and settlement by less than 1% for an incompressible pile. Hence, only compatibility of vertical displacements and vertical equilibrium need to be considered in the solution process.

Mattes and Poulos (1969) and Poulos and Mattes (1969) developed the technique to consider pile compressibility. Poulos and Davis (1968) studied the effect of an elastic layer underlain by a rigid base. An extensive set of

solutions are presented by Poulos and Davis (1974) which enables the settlement of a single pile to be manually computed. Poulos (1979) developed the method to consider soil non-homogeneity in an approximate manner.

(b) The t-z Method.

It is difficult to assess material parameters to model load transfer in general pile-soil systems. Hence, the t-z method is probably the most widely adopted method where the non-linear soil behaviour has to be considered or where the soil stratification is complex.

Seed and Reese (1957) proposed the method, from which analytical procedures were developed to determine load-settlement curves. Examples of these procedures include Reese (1964), Thurman and D'Appolonia (1964) and Coyle and Reese (1966).

The pile is modelled as a member supported by discrete springs which represent the resistance of the soil in skin friction and end bearing. The soil springs are non-linear representations of soil force, t , and axial displacement, z . This provides an unique relationship between load transfer and displacement at each element. The theory implicitly assumes that the displacements along any element are not affected by the load transferred by other elements into the soil. As Vesic (1970a) reported "the concept of a unique transfer function is in obvious contradiction with reality".

Finite difference techniques, such as those adopted by Meyer et al (1975) are often employed to solve the governing equations. An alternative approach is to use a

finite element representation of the pile. This enables a pile with varying cross-section or heterogeneous material properties to be more readily analysed. The use of a computer is required for solution of all but the simplest representations.

A difficulty of the method is the selection of appropriate t-z curves for the soil. This tends to be empirical and based on back-analysis of a limited range of pile load tests. The t-z curves proposed by Coyle and Reese (1966) were determined from relatively small piles, less than 80ft. in length and 18ins. in diameter. Vijayvergiya (1977) proposed t-z curves based on test results of piles having a diameter generally less than 0.6m. For pile diameters of 1m or more, Toolan and Horsenell (1979) considered that modifications need to be made in defining soil springs for the piles. They recommended the use of a combined t-z curve/Mindlin approach.

In the absence of suitable t-z curves, fully instrumented pile load tests can be back-analysed. There are also several published documents available. For bored piles these include Burland et al (1966), O'Neill and Reese (1972) and Whitaker and Cooke (1966). Cooke et al (1979) reported tests on jacked piles. T-z curves for driven piles are generally determined from dynamic formulae.

Kraft et al (1981a) developed theoretical t-z curves by employing a concentric cylinder approach, as described by Randolph and Wroth (1978). It is assumed that the deformation of the soil around the pile can be considered as the shearing of concentric cylinders. Cooke (1974),

Frank (1974) and Baguelin et al (1975) confirmed the validity of this assumption. It is a simplified approach to pile analysis which does not yield exact solutions. However, the closed form equations enable the calculations to be carried out "on the back of an envelope".

Kraft (1991) recently suggested that the unit shaft and toe resistance of piles in sand do not generally reach limiting values. Thus previously reported t - z curves may require appropriate modifications.

(c) The Finite Element Method.

The F.E.M. of analysis for a single axially loaded pile involves idealizing not only the pile, but also the soil domain in which it is embedded. The soil domain that has to be idealized is extensive; typically 50 to 100 times the pile radius in the horizontal direction and at least 2.5 times the pile length in depth. It is assumed that these outer boundaries are fixed in appropriate directions.

Ellison (1968) formulated and programmed a general analysis of load transfer for an arbitrary pile in a soil mass. The method permits the soil mass to be idealized with a non-linear stress-strain response. The general mathematical model contains 377 elements. The analysis accommodates the stresses and displacement conditions imposed by the method of pile installation. The effect of the pile presence on the stress distribution in the soil is also considered.

Developments in the F.E.M. have shown the need to use "interface elements" between the pile and soil in order to model relative slippage. Goodman et al (1968), Zienkiewicz

et al (1970) and Ghaboussi et al (1973) proposed such elements.

2.4.3. Laterally Loaded Single Piles.

(a) Elastic methods.

Spillers and Stoll (1964) idealized the pile as an elastic line inclusion in a homogeneous elastic half space. It is assumed that the normal force distribution along the pile can be represented by a series of concentrated forces. Mindlin's (1936) equations are used to determine the displacement profile along the shaft. For other than low lateral loads, this solution gives large stresses near the surface. To overcome this problem they suggested the use of an approximate yield criterion.

Douglas and Davis (1964) proposed an elastic solution for a pile which is idealized by a rigid vertical plate. The lateral stresses are considered to be uniformly distributed along the length of the pile, rather than concentrated at the nodal points.

Poulos (1971a) extended the approach to a pile of finite stiffness. The pile is idealized as a thin strip and the lateral shear stresses on the sides of the pile are neglected. Finite difference techniques are used to solve the differential equations. A number of solutions based on this approach are presented by Poulos (1971a) and Poulos and Davis (1974). The solutions enable the analysis of a laterally loaded pile in an elastic continuum to be carried out manually.

Banerjee and Driscoll (1976) developed the method to consider a uniform distribution of shear stress around a

circular pile. Solutions are obtained using the B.E.M. as employed by the PGROUP (1981) program. The agreement between their results and those of Poulos (1971a) is generally good.

Randolph (1980,81) carried out several finite element analyses of laterally loaded piles embedded in homogeneous and non-homogeneous soils. Approximate general equations for the deflection and rotation at the pile head were determined from these analyses. He also produced generalized curves giving the deflected shape and bending moment distribution along the pile. Randolph compared his solutions with those of Poulos (1971a) and concluded that Poulos' analysis consistently overestimates the deflection and induced moment by up to 25%. Better agreement was achieved on comparing his results with those from the more realistic idealization of Banerjee and Driscoll (1976).

Elson (1984) reported that Poulos (1975a,b) extended the elastic analysis to accommodate plastic yielding of the soil near the ground surface. This was accomplished with the introduction of yield stresses as presented by Broms (1964a,b). The method represents a simple workable approximation to the non-linear deformation behaviour of the soil. However, Elson cautioned that care should be exercised in using the approach as the model employed is rather crude.

(b) The Equivalent Bent Method.

The "equivalent bent method" is a simple method of analysis for piles subject to small lateral loads. The method is fully described by Tomlinson (1977) and Poulos

and Davis (1980). It is assumed that the pile can be fixed at an arbitrary depth below the ground surface. This enables the deflection to be calculated by treating the pile as a simple cantilever, either free or fixed at the head but with freedom to translate. However, deflections are subjective to the arbitrary depth assumed for fixity.

(c) The Subgrade Reaction Theory.

The S.R.T. idealization of a vertical pile comprises a beam supported by a series of discrete horizontal springs representing the soil mass. The horizontal coefficient of subgrade reaction, K_h , is not a material constant, but varies with the stiffness, breadth of the pile, loading conditions and also generally varies with depth.

The pile-soil system can be analysed by integration of a fourth order linear differential equation. A closed form solution to the differential equation is only available where K_h is constant and for simple loading conditions.

Elson (1984) presented non-dimensional solutions, determined from finite difference techniques, where K_h varies linearly. Davisson and Gill (1963) and Matlock and Reese (1960) also developed solutions for particular profiles of K_h with depth. Elson commented that the use of these solutions are not generally justified. This is due to the uncertainties of assigning realistic values of K_h throughout the soil profile.

The main shortcoming of the method is the difficulty of establishing satisfactory values for the modulus of subgrade reaction K_h . Since K_h is not a fundamental

material soil constant, it cannot be reliably evaluated by back-analysis of pile loading tests and then applied to prototype piles with different stiffness characteristics. It would therefore be useful if K_h could be related to a constant material property, such as the soil modulus, for various pile configurations. This would provide a straightforward approach to determine an appropriate value for K_h .

(d) The p-y method.

This is a variation on the Winkler model. It is also known as the "arbitrary variation of subgrade reaction".

The p-y curves represent the deformation of the soil, y , at any given depth below the soil surface for a range of laterally applied pressures, p , from zero to the stage of yielding of the soil in ultimate shear.

The curves are initially assigned a linear relationship to idealize an elastic soil under a low load. The analysis is extended into the non-linear range using established p-y curves. Secants to the curves are determined at appropriate load increments. These are generally used in fourth order linear differential equations which are solved iteratively.

Finite differences techniques may be used to solve the differential equations. Computer programs for general application have been developed such as those of Reese (1977) and Smith (1982). Matlock and Reese (1961) outlined an iterative desk solution which could be adopted using available solutions for simple profiles of soil stiffness with depth.

Reliable p-y curves can be determined from lateral load tests on piles. Reese and Cox (1969) suggested a simplified approach for determining p-y curves from lateral load tests where only the pile head deflection and rotation were recorded. However, in order to establish p-y curves with confidence, the measured distribution of bending stress in the pile with depth is required.

Matlock (1970) proposed rules relating the stress-strain curve determined from triaxial tests on soft clays to the p-y curve for a pile. Similar rules were proposed by Reese et al (1974) and O'Neill and Murchinson (1983) for laterally loaded piles in sand. Reese et al (1975) established similar relationships for stiff clays. In the absence of more definitive criteria, the American Petroleum Institute (1987) recommended procedures for constructing p-y curves using stress-strain data from soil samples. Reese et al (1975) made recommendations for the establishment of p-y curves to accommodate cyclic loading. However, without field test data, Parry (1976) suggested that establishment of realistic curves tends to be subjective.

2.4.4. Pile Groups

(a) General

Pile group analytical techniques range from simple structural procedures which ignore the restraint afforded by the soil, to those which consider the piles to be embedded in an elastic continuum. Simplified methods of analysis, as suggested by Hooper (1979), are categorized as those in which either the piles or the soil are treated in a crude manner. Conversely, rigorous methods of analysis

treat the piles as discrete structural members embedded in a continuum.

(b) Simplified methods.

(i) Pile group idealized as a frame. These analyses are usually restricted to simple cases of identical piles and minor structures, where lateral loads are small ie. less than 10% of the vertical load. Despite the lack of realism of the conceptual model, a straightforward resolution of forces may give a practical design. The most common method is known as Culmann's method, after Lohmeyer (1930). This was suggested by Terzaghi (1943) for the analysis of a mixed pile group ie. comprising raked and vertical piles.

In Culmann's method, the piles are assumed to be pin jointed at the pile cap and behave as axially loaded columns. The lateral restraint of the soil is ignored, except insofar as the piles are presumed not to buckle. The forces in individual piles are determined by resolving forces or by constructing a polygon of forces. The method is inapplicable to a group of piles containing more than three different directions of rake, because it then becomes statically indeterminate.

Methods based on the Centre of Rotation or Elastic Centre method also ignore the restraint afforded by the soil. However, these do consider the finite stiffness of the piles. The approach is attributed to Westergaard by Anderson (1956). Turzynski (1960) and Sawko (1968) developed the method further. Computer programs have been made available for the structural analysis of pile groups. These include Minipoint and SW Pile based on Sawko's

analysis. Because the stiffness methods may lead to impractical and complicated geometries, Elson (1984) does not recommend their use. Furthermore, they are no more realistic than a simple static analysis, but require considerable more computational effort.

Developments of the above method accommodate the restraining effect of the soil in an approximate manner. Hrennikoff (1950) proposed a method of analysis for a single row of piles. This method became popular after work by Francis (1964a,b) and Gray et al (1964). Aschenbrenner (1967) extended the approach to consider three dimensional pile groups. Lateral displacement of the pile group is computed by assuming a constant value of subgrade lateral modulus. Because the piles are pinned at their tips, vertical displacement is ignored. The solution process generally requires the use of a computer.

Dixon and Berry (1970) proposed a similar approach for the analysis of a single row of piles whereby the piles are pinned to a rigid pile cap with their bases fixed at an arbitrary depth. The lateral restraint of the soil is modelled using the concept of a coefficient of lateral soil displacement which is approximately correlated with the stiffness of the soil.

The methods of pile analysis described above do not accommodate pile-soil-pile interaction. Because the piles are assumed to be restrained at a particular depth, the methods cannot be applied to cases where the vertical settlement of the group is significant. It is implicitly assumed that provided the settlement of a single pile considered in isolation at working load is satisfactory,

then the settlement of the group is also acceptable. This assumption is widely recognized as being incorrect due to the pressure bulb beneath a pile group reaching greater depths than that of a single pile.

A development of the above approach is the Equivalent-Bent Method. The technique assumes that the pile group can be modelled as a pile cap rigidly connected to fixed-end free standing columns or cantilevers of equivalent lengths and cross sectional areas. The equivalent members are selected to accommodate the restraint afforded by the soil in an approximate manner. The equivalent lengths are usually determined from subgrade reaction analyses as proposed by Francis (1964a), Kocsis (1968) and Nair et al (1969). Poulos and Davis (1980) proposed an improvement for calculating the equivalent lengths and areas by comparison of results with elastic solutions for axially and laterally loaded piles. They suggested that the method could be extended to consider group effects by modifying the equivalent members. This is at best an approximation because interaction effects result in some piles being more heavily loaded than others.

Having defined equivalent members for the model, solutions are generally obtained using standard structural analysis techniques. Saul (1968) and Reese et al (1970) presented simpler structural analyses in which the pile cap is assumed to be rigid and the piles assumed to behave elastically. Nair et al (1969) presented a method suitable for manual calculations. A program STRAP II based on this approach is also available.

The Equivalent Bent Method is criticized for not considering a pile cap bearing on the soil surface. Also, by altering the pile geometry, the load and bending moment distribution within the group cannot be determined. Pile-soil-pile interaction is not generally considered.

Reddaway and Elson (1982) reported the use of a structural frame with the piles laterally restrained by a Winkler medium. Because the piles were assumed to be pinned at their bases, it was not possible to predict the vertical displacement of the group.

The Winkler medium cannot accurately model the interaction of piles in groups. Prakash and Saran (1967) proposed empirical group reduction factors to be applied to the moduli of subgrade reaction. These factors are not based on extensive field correlations. Elson (1984) reported that the procedure outlined by the NAVFAC DM7 Manual (1971) may be employed for straightforward groups of widely spaced, identical, vertical piles. Influence values are used to predict the behaviour of single piles in an elastic soil. Approximations are then made to extend this to the group performance.

None of the methods outlined above adequately treat the soil as a continuum, consider the contribution of the raft to the load carrying capacity of the substructure, and interaction between piles. Such considerations require a more rigorous method of solution.

(ii) Soil idealized as a continuum. This analytical technique ignores the presence of the piles and assumes that the structural load is applied at an arbitrary depth below the ground surface. Although the idealization is

crude, it does model the essential feature of a pile group by transferring the structural load to a depth where the soil is generally stronger and less compressible.

Tomlinson (1977) recommended that the designer should exercise caution in evaluating soil parameters for the analysis. Whereas the method of installation of a single pile has a significant effect on the selection of design parameters, it is of less importance when considering group behaviour. This is due to the zone of disturbance of the soil being confined to the immediate vicinity of the individual pile, whereas the soil is significantly stressed to a depth beyond the width of the group.

Terzaghi's (1943) conventional one dimensional method is frequently used to manually calculate the settlement of the sub-surface load. The approach permits several layers of varying strength to be considered. Scott (1974), Tomlinson (1980), Lambe and Whitman (1969), Taylor (1974) and Bolton (1979) also described procedures for the computation of settlement by the conventional method. Padfield and Sharrock (1983) advised that the method is only applicable where the lateral deformation of the soil is insignificant.

One difficulty of the method is the determination of the appropriate depth for the equivalent mat. A common approximation is that suggested by Terzaghi and Peck (1967). The mat is placed at a depth of two-thirds the pile length, and consolidation of the soil below that level is computed as if the piles are absent. Ireland (1964) demonstrated that the settlement obtained by this method correlated well with the observed settlements of an

existing structure. Sowers and Sowers (1970) recommended that only the soil below the pile tips should be included in the settlement calculations. Using a similar approach, Yu et al (1965) established that the agreement achieved with the observed behaviour of several groups was within $\pm 20\%$ to $\pm 50\%$.

McClelland (1972) suggested that the equivalent mat can be placed at the surface, where it is anticipated that load transfer from the piles occurs at a high level. Whitaker (1976) and Tomlinson (1977) proposed alternative variations for the depth of the equivalent mat. They also recommended considering the load spread effect. The angle of load spread is arbitrary and depends on the soil type.

Having defined the depth of the equivalent mat, the settlement can be determined by consideration of a uniformly loaded area within an elastic homogeneous half-space. Hooper (1979) presented graphical solutions for such cases, to which Fox's (1948) correction is applied to account for the effect of depth. These solutions enable an estimate of the reduction in mean and differential settlement to be made, whereas manual methods generally only provide an estimate of the total settlement. Hooper (1979) reported that his solutions of mean settlement are similar to those reported by Butterfield and Banerjee (1971a) for a rigid rectangular disc. Hooper's solutions for a rectangle with a length to breadth ratio (L/B) of 1 agree with those of Nishida (1966) for a uniformly loaded circular area.

Simplified solutions of an equivalent mat within the soil mass represent uniformly loaded flexible areas.

Consequently, differential settlements may be overestimated. Hooper (1979) suggested this could be remedied by applying the load to an "equivalent plain raft" with a bending stiffness based on that of the piled raft and the superstructure.

Poulos (1968a) and Hooper and Wood (1977) idealized the substructure as an equivalent raft located at pile head level supported by a block of reinforced soil. Hooper and Wood compared their results with field measurements and solutions from a conventional pile group analysis where the plain raft was located at a depth of two-thirds the pile length. They observed that the conventional drained settlement was almost double the field value. Drained and undrained analyses of the reinforced soil model provided a satisfactory envelope to the measured time settlement curve.

Hooper (1979) suggested an improvement on this approach by assuming that the pile reinforced soil is a transversely isotropic material. The elastic properties of which are dependent on the soil modulus, pile modulus and the relative area of piles to soil. He demonstrated that very few piles are required to establish a pile reinforced soil mass of appreciable vertical stiffness. Any further increase in the number of piles has a minimal effect in reducing maximum and differential settlement. This agrees with the current design philosophy of settlement reducing piles and the observations of Cooke (1986).

Hongladaromp et al (1973) idealized a piled raft as a raft of finite stiffness resting upon a homogeneous elastic half-space. The piles are replaced by elastic springs. A

similar approach was reported by Hight and Green (1976). Hooper (1979) reported that this method of pile modelling may lead to unsatisfactory results, especially for stiff rafts. The solutions imply that all piles within a group having a rigid pile cap are equally loaded. Rickard et al (1985) described an improvement on this method. The springs idealizing the piles are modified according to Mindlin's equations to accommodate group effects. Appropriate initial spring stiffness values to represent the pile-soil stiffness were determined based on their experience and they offered no guidance.

Unlike piles in cohesive soils, the group capacity of piles embedded in cohesionless soils may be higher than the sum of the capacities of the isolated piles. However, the group settlement in either soil type is generally greater than that of a single pile subject to the average pile load of the group. McClelland (1972) reported the primary method of predicting the settlement of pile groups in a cohesionless soil is by extrapolation of individual test pile results. Skempton (1953) suggested a relationship between the settlement ratio and the number of pile rows in a group. Vesic (1969) related the settlement ratio to the relative width of the pile group. Each of these correlations are approximate at best. Except for the severe case of sand liquefaction, under cyclic or shock loading, the settlement of pile groups in cohesionless soils tends to be moderately low. Hence, approximate solutions are generally satisfactory.

(c) Rigorous Methods.

(i) Free standing pile groups. Poulos and Davis (1968) developed the Interaction Factor Method (I.F.M.) for the analysis of axially loaded pile groups. They considered the displacement of two equally loaded identical rigid piles which interacted with one another through the soil. By application of Mindlin's (1936) equations, Poulos (1968a) expressed the solutions in terms of an interaction factor α , where:

$$\alpha = \frac{\text{additional displacement resulting from adjacent pile}}{\text{displacement of pile under its own load}}$$

The method is extended to the analysis of general pile groups by employing the principle of superposition and making use of compatibility and equilibrium. For large groups the solution process is laborious. Hence, Poulos (1968a) expressed the pile group settlement in terms of a settlement ratio, R_s . This is defined as the ratio of the group settlement to the settlement of a single pile subject to the average load per pile in the group. It is assumed that all piles are equally loaded. The group settlements are strongly dependent on the breadth of the group rather than the number of piles within the group. This is in agreement with Hooper (1979) and Cooke (1986).

Poulos and Mattes (1971a,b) and (1974) developed the I.F.M. to accommodate free standing groups of axially loaded compressible piles embedded in an elastic half-space. They also considered end bearing piles on either a rigid base or a stratum of much greater stiffness than the upper layer. It was demonstrated that pile compressibility generally has a small effect on vertical displacements.

The method was extended to three dimensional raked pile groups subject to horizontal and moment loading by Poulos and Madhav (1971) and Poulos (1974). However, these analyses are limited to either fully flexible or rigid pile caps.

Butterfield and Banerjee (1971b) presented a more rigorous approach based on the B.E.M.. Agreement was generally good between results obtained using this method with those from the I.F.M..

Poulos and Mattes (1971a) developed the I.F.M. for the analysis of general pile groups subject to lateral loads. The method is parallel to that of axially loaded pile groups. However, the interaction factor between any two piles is also dependent on the direction of lateral loading. Interactive effects are greatest where the loading is along the line of the two piles and least where the loading is at right angles to the line of the two piles. Elson (1984) considered that the I.F.M. may overestimate the lateral displacement of a pile group by up to 20%.

Poulos (1971b) and (1975b) developed Group Reduction factors which enable the group lateral displacement to be determined manually. These depend on the loading conditions, layout and fixity of the piles. Poulos (1971b) suggested that there is a common curve expressing the relationship between the reduction factors and B/D for all groups greater than 3×3 . The method assumes all piles carry equal shear forces which may be unrealistic in practice.

Banerjee and Driscoll (1976) extended the B.E.M. to include both vertical and raked pile groups under eccentric inclined loading. The program PGROUP (1981) was developed from this work for general use.

Randolph and Wroth (1979) developed an equation for the interaction between two piles. The developed interaction factors, α_v , are applied in the manner of Poulos (1968a) to analyse symmetrical groups of equally axially loaded piles. The results obtained from the semi-analytical model tend to underestimate the interaction between piles compared to the B.E.M.. They contended:

"in a real soil, the non-linear nature of soil deformation will lead to less interaction than predicted from a linear elastic analysis, since the deformation will be confined more to the immediate vicinity of the pile."

The authors reported that the interaction factors computed by elastic analyses tend to be higher than those observed experimentally. This is because the factors are calculated for homogeneous soils, but in practice the soil stiffness generally increases with depth. Banerjee and Davies (1977) observed that the interaction between piles decreases as the degree of homogeneity decreases. For a homogeneous soil, the interaction factors fail to allow for a higher proportion of load being transferred to the pile base in a pile group than for a single pile as shown by Ghosh (1975). To account for this feature, Randolph and Wroth concluded that a more sophisticated analysis is required for general pile groups.

Randolph (1980) developed the program PIGLET for the analysis of three dimensional groups comprising long flexible piles. The program is based on the normalization

of a large number of finite element analyses. The piles are assumed to be of equal length and can be raked in any direction and subject to vertical, lateral, moment or torsional loading. The soil mass is assumed to have a stiffness which increases linearly with depth. However, no provision is made for a ground contacting cap. Since the program does not involve the solution of large matrices, resulting from the discretisation of surfaces embedded in an elastic continuum, it is simple and quick to operate. Elson (1984) reported that the estimated computer time is about 10% of that used by PGROUP with a subsequent saving in cost.

Based on the results of a non-linear three dimensional analysis, Trochanis et al (1991a,b) proposed a simplified model for analysis of single and pairs of piles. The piles are modelled as elastic beams and the soil as a Winkler-type foundation. To accommodate interaction the pair of piles are connected by various springs. It is unlikely that this approach could be successfully applied to general pile groups because the conceptual model would involve a complex network of springs.

(ii) Piled raft foundations. Poulos (1968b) extended the I.F.M. to determine approximate solutions for a unit comprising a single rigid pile with a rigid circular pile cap in contact with the surface of a homogeneous elastic half-space. Davis and Poulos (1972) extended this work to the application of rigid piled rafts. The authors suggested that the effect of the finite stiffness of the substructure can be inferred from solutions of single piles

and plain rafts. Butterfield and Banerjee (1971c) presented a more rigorous analysis using the B.E.M.. In this method the cap is assumed to be effectively rigid but it allows for pile compressibility.

Hain and Lee (1978) considered a raft of finite stiffness supported by a random group of identical piles with the soil mass idealized as an elastic continuum. The raft comprises thin rectangular plate bending finite elements. It is assumed that the connection between the raft and the pile is a sliding ball joint. Thus the model cannot accommodate applied lateral loading. Also, local raft slopes need to be insignificant because no moment is transferred from the raft to the pile. This is generally only valid for axisymmetrically loaded rigid rafts.

Interaction between units is accommodated by various interaction factors which were developed for a homogeneous continuum. However, Hain (1977) claimed:

"that the settlement of a single pile in a non-homogeneous soil layer can be predicted with sufficient accuracy using the homogeneous continuum solution and the average soil modulus along the length."

Their analysis requires the use of three separate interaction factors, whereas Davis and Poulos (1972) combine these to form one interaction factor (α_R). Hain and Lee also considered the failure of individual piles at loads less than the total group capacity by employing an approximate excess load cut-off procedure.

Apart from linear elasticity, the I.F.M. also relies on two other important assumptions: (i) the reinforcing effect of the piles within the soil mass is ignored, and (ii) soil anisotropy is accommodated using the Steinbrenner approximation. These two assumptions are in contradiction

with the Mindlin solution of a perfectly homogeneous elastic half-space. However, work by Butterfield and Banerjee (1971b) suggests that the reinforcing effect of the piles should not lead to any significant inaccuracies. Hooper (1979) reported that provided the piles are well spaced and where the soil stiffness is reasonably uniform, the results based on these two assumptions can be treated with a considerable degree of confidence.

To avoid making these assumptions a full three dimensional analysis is necessary. Ottaviani (1975) carried out such an analysis for a 5x3 group of square piles having a stiff pile cap in contact with the ground and subject to vertical loading. Despite only one quarter of the piled raft being modelled, the mesh for the F.E.M. comprised 3300 nodes and 2700 eight noded solid elements. The results indicated the shear stress contours to be markedly asymmetric, in contrast to the axisymmetric distribution assumed by elastic analyses.

As the cost and general complexity of such three dimensional analyses is high, they tend to be unsuitable for practical design. Their most useful application is in research and in carrying out parametric studies of pile group behaviour to advance the current understanding of the problem.

(d) Non-linear methods.

The subgrade reaction methods of analysis for single piles which utilize non-linear t-z and p-y curves are not readily adapted to pile groups. The group behaviour of very closely spaced piles may reasonably be approximated by

a single large pile. However, Focht and Koch (1973) reported that this approach cannot correctly model the group behaviour of widely spaced laterally loaded piles.

Prakash (1961) and Tamaki et al (1971) proposed methods of analysis for laterally loaded pile groups. These are based on the results of single laterally loaded pile tests. Consideration of group interaction is inferred from the efficiency of other pile groups. However, these methods were developed at relatively low stress levels within the elastic range of the soil. Focht and Koch suggested that these methods are invalid for the analysis of offshore groups. This is due to the soils near the surface of the seabed being stressed into the plastic range.

To overcome the limitations of the above methods Focht and Koch (1973) and Toolan and Horsnell (1979) proposed combined interaction factor/p-y analyses. The procedure assumes that the displacements of individual piles are sufficient to create plastic soil strain. This enables the performance of individual piles to be predicted by the p-y method. The I.F.M. is used to determine the cumulative group deformation. This is because group interaction is primarily due to superposition of small stress increments that remain within the elastic region. Tomlinson (1986) reported that a similar approach is usually adopted for vertically loaded pile groups. In this case the t-z method is combined with the Mindlin (1936) equations to accommodate interaction. It is assumed that

the displacement of a pile within a group can be expressed as:

$$\delta_{Gi} = \delta_{Ii} + Y_L \sum_{\substack{j=1 \\ j \neq i}}^n P_j \cdot \alpha_{ij} \dots\dots\dots 2.1.$$

where,

- δ_{Gi} = group displacement of pile i
- δ_{Ii} = isolated pile displacement of pile i (by p-y or t-z method)
- Y_L = unit elastic displacement of isolated pile (from Poulos and Davis (1974))
- P_j = load on pile j
- α_{ij} = Interaction factor for piles i and j
- n = number of piles in the group.

Where all the piles of a group are connected at their heads by a rigid raft and which undergo the same translation or settlement Tomlinson suggested the equation can be rewritten as:

$$\delta_{Gi} = f(P_i) + Y_L \sum_{\substack{j=1 \\ j \neq i}}^n P_j \cdot \alpha_{ij} \dots\dots\dots 2.2.$$

Where δ_{Ii} is replaced by $f(P_i)$, the load-displacement curve for an isolated pile obtained by the p-y or t-z method. For a prescribed displacement, "n" simultaneous equations are obtained containing "n" unknowns ie. the individual pile loads. The sum of the individual loads is equal to the total group load. Repetition of this computation for a number of prescribed displacements enables a curve of total group load against displacement to be plotted.

The method computes the axial loads at the pile heads. The distribution of force and moment along the shaft may be approximated by using single pile solutions subjected to an equivalent loading system.

A more appropriate method used to determine the variation of force and moment along a pile within a

laterally loaded group is the "y" modifier, or "y" factor method. A single pile is analysed using a p-y approach with the value of y selected to equate the pile head and group displacement. Focht and Koch considered the resulting bending moment distribution to be valid for pile design. However, Chow (1987) observed that the y-modifier assumption generally overestimates the bending stresses in the pile.

Kay et al (1983) used the added soil displacements, determined from a finite element analysis, at the positions of the other piles in the group to offset the p-y curves. This is termed the "pile in moving soil" method. It enables the response of a single pile in the group to be assessed. As explained by Chow (1987):

"if the geometry of the group is such that the individual piles do not behave in a similar manner... then the procedure may be difficult to implement".

Wood (1979) developed the program LAWPILE for the non-linear analysis of a laterally loaded pile group embedded in heterogeneous layered soils. The non-linear soil behaviour is modelled by evaluating the local yield pressures which are then incorporated within the solution. The program is reasonably versatile. The pile head is modelled as free or restrained. The structural and soil properties can be varied along the pile shaft and also from pile to pile. The results were compared to the measured behaviour of laterally loaded piles and were of "sufficient accuracy for design purposes".

O'Neill et al (1977) presented a method of analysis for three dimensional pile groups with non-linear soil response and pile-soil-pile interaction. The method is

iterative and cumbersome in nature. The raft is uncoupled from the pile in the analysis. The various modes of loading on a single pile are also uncoupled. From pile load tests on isolated piles, the authors developed unit soil reaction curves (t-z or p-y) to model the pile head response.

Pile-soil-pile interaction is accomplished in a similar manner to that described by Tomlinson (1986). The authors recognised the inconsistency of superimposing added displacements from an elastic Mindlin approach on inelastic primary displacements computed from non-linear unit soil curves. They contended that although the:

"use of the finite element method could obviate the need for such an approximation...the finite element method is presently poorly suited to general analysis of pile groups because computer storage and computation time requirements have precluded the development of algorithms that can handle arbitrary pile geometry. The method described herein thus represents the best current [1977] method for studying the behaviour of large groups of piles driven in arbitrary attitudes".

O'Neill et al (1982a) performed a similar analysis which was correlated with test results. They observed that the strain level outside the immediate vicinity of the piles is low in comparison to the high distortion at the pile-soil interfaces. This confirmed the validity of a combined t-z/Mindlin approach. The analysis procedure is outlined by O'Neill et al (1982b).

Chow (1986a) and Leung and Chow (1987) presented a refinement of the approach of O'Neill et al (1977) to "accurately" consider pile-soil-pile interaction. Chow (1986b) extended the method to non-homogeneous soils whereby the interaction between the piles is limited to the soil in the same layer. Interaction between the various

soil layers is assumed to be negligible.

Chow (1987) presented an iterative analysis of pile-soil-pile interaction. Good agreement is generally obtained when the accuracy of the iterative method is compared with that of their direct method. The iterative method enables the stiffness matrix of individual piles to be uncoupled from the group. The stiffness matrix to be solved at any one time is therefore limited to that of a single pile. However, it was not shown whether this method can be extended to analyse piled foundations with ground contacting rafts of finite stiffness.

Trochanis et al (1991a) applied the F.E.M. to a three dimensional non-linear analysis of single and pairs of piles. They proved that the interaction between piles undergoing non-linear displacement is significantly less than that predicted by elastic analyses.

2.5. SOIL STRUCTURE INTERACTION.

Few methods of analysis directly model the superstructure stiffness. The finite stiffness of the raft is often not considered in an interactive analysis. Analysis of the superstructure to calculate the magnitude of redistributed loads may result in the loads being so high that the structural frame suffers considerable distress. In practice, the structure departs significantly from the ideal behaviour and distress is probably minimal, which is assisted by distortions being "built-out". However, an understanding of interaction enables the selection of appropriate and economic options for the design of foundations.

Because of the complexity of modelling the complete system, approximate methods are usually employed to accommodate the effects of soil-structure interaction. A common approach is to determine the relative stiffness of the structure to the soil. This enables design charts to be used to determine differential settlements, such as those presented by Fraser and Wardle (1976).

Meyerhof (1953) suggested a simplification which enables the superstructure stiffness to be incorporated in the analysis. An equivalent raft is modelled with the same total second moment of area as the sum of that of the raft and floor slabs of the superstructure. The application of this approach to frame superstructures comprising panels and shear walls is also endorsed by de Simone (1966). However, the Institution of Structural Engineers (1977) reported that successive storeys above ground make progressively smaller contributions to the total effective stiffness of the system. They suggested that an estimate of the overall structural behaviour could be determined by fully analysing a certain number of lower storeys and ignoring the stiffness of the storeys above. There is little guidance given on the numbers of storeys to be considered in particular cases. Thus, where possible, they recommend that the full superstructure should be modelled, preferably three dimensionally.

Hooper and Wood (1976) showed that the measured differential settlements of a particular building were one tenth of those computed for a raft foundation ignoring the superstructure stiffness. However, a reduction in the raft differential settlements and bending moments was

accompanied by increased wall stresses. It is therefore necessary to consider these stresses in the design process where the superstructure stiffness is utilized in the analysis.

King and Chandrasekan (1974) and Majiid and Cunnell (1976) studied the influence of soil-structure interaction on the bending moments of frame structures. King and Chandrasekan observed that the bending moments in the superstructure and raft are significantly different where the interaction between the superstructure and raft is considered. Whilst Majiid and Cunnell reported that the stiffness of the superstructure assists in reducing differential settlement between pad foundations of an irregularly loaded space frame. This is probably due to the more lightly loaded pads being induced to play a part in stabilizing the remainder.

The Institution of Structural Engineers (1977) reported comparative interactive results for a single plane frame. These include the semi-graphical method of Meyerhof (1947), Larnach's (1970) iterative technique and results computed by Wood (1972). The results obtained from the three methods agree well with one another and show that differential settlement will be overestimated without consideration of interaction. The results of Wood et al (1977) for a multi-bay two storey building, originally described by Webb (1975), were also reported. By not considering interaction there was an underestimate of a particular column load of 40%, and a 23% underestimate of settlement at the same column.

Wardle and Fraser (1975) compared the computed results from various representations of the superstructure stiffness. The model comprised a seven storey structure supported by a raft, resting on an elastic layer of depth equal to the raft breadth. In each case the total settlements were similar, but the differential settlements for a raft with no superstructure were approximately double those where the superstructure stiffness was included. The differential settlements and column loads determined from an equivalent raft analysis compared well with the full analysis. However, the equivalent raft analysis grossly overestimated the raft moments. The raft moments computed from the model of a superstructure condensed to a single storey were in good agreement with those of the complete structure. Therefore, where it is not practical to analyse the full structure, an equivalent single storey will provide more satisfactory results than an equivalent raft.

Hooper and Wood (1976) described various equivalent modelling systems for a multistorey building. The equivalent raft thickness was based on the combined bending stiffness of the first two storeys. They also proposed restraining rotations of the raft mesh at positions of the cross walls. This approach was successful in this instance, because rotation of the raft at positions of the cross walls was minimal.

Hooper (1978) concluded that direct modelling of the superstructure is impractical in almost all cases. However, a simplified representation of the superstructure stiffness can usually be made. This enables the designer to

assess the effect of substructure movements on the integrity and serviceability of the superstructure.

2.6. DISCUSSION.

Soils are often idealized as elastic materials although they do not generally behave in a strictly elastic manner. Elastic theory enables an understanding to be gained of the short term load-deformation behaviour of structures. The load transfer mechanisms from the substructure to the soil can also be interpreted. Accordingly, an assessment can be made of possible long term consolidation settlement.

Common numerical techniques for solving a substructure supported by an elastic continuum are the Finite Element Method (F.E.M.) and the Boundary Element Method (B.E.M.). The F.E.M. is versatile in that it can be applied to the analysis of the complete superstructure-substructure-supporting soil. A disadvantage of the method is that discretization of the soil domain by finite elements tends to involve a time consuming and expensive solution process. The B.E.M. only requires the boundaries of the soil mass to be discretized, with a subsequent saving in cost. Solution of an idealized pile group usually requires strict boundary conditions to be imposed, such as a rigid or perfectly flexible overlying raft. The Winkler type foundation employed by the Subgrade Reaction Theory (S.R.T.) is often mistakenly used as a simplified elastic model. The Winkler model differs from that of a continuum because only the ground in contact with the load deforms ie. there is no interaction between springs.

Consequently, uniformly loaded non-rigid substructures settle uniformly, in contrast to the concave settlement profile from elastic solutions.

For the analysis of general raft foundations a simplified B.E.M., referred to as the Surface Element Method (S.E.M.) has proven to be a satisfactory and adaptable technique. The finite stiffness of the raft and variable loading on the plan of the raft are directly considered by the approach. Standard elastic solutions are utilized by idealizing the soil as a homogeneous isotropic elastic half space. Also, approximate solutions can be obtained for a multi-layered soil profile by making use of the Steinbrenner assumption. The Winkler foundation is not recommended for general raft analysis owing to limitations on its applicability. Although the finite stiffness of the raft and variable loading are considered, the soil is not modelled as a continuum.

Axially and laterally loaded single piles can be analysed assuming either an elastic continuum or a Winkler type ground model. Solutions can be obtained for the elastic continuum model using the B.E.M. and the F.E.M.. Standard elastic solutions are available for a comprehensive set of pile-soil configurations. These are usually presented graphically for ease of use. Winkler type $t-z$ and $p-y$ methods are widely adopted to analyse single piles with non-linear soil behaviour or a complex soil stratification. The methods assume that the soil surrounding the pile can be replaced by a set of non-linear springs entirely independent of each other. The procedure enables load-displacement curves to be determined for a

pile up to failure of the soil. A difficulty with the approach is selecting realistic non-linear parameters.

The simplified analyses which idealize the pile group as a frame generally, either ignore the restraint afforded by the soil, or only consider the lateral restraint of a Winkler medium. To maintain vertical equilibrium the piles are restrained against movement at their tips. This incorrectly assumes that provided the vertical displacement of an isolated pile is satisfactory, then, the pile group vertical displacement will also be satisfactory. The other simplified approach is to idealize the soil as an elastic continuum and replace the piles by an equivalent loaded area at an arbitrary depth. These analyses generally provide realistic estimates of total vertical displacements. However, the approach tends to be limited to the analysis of groups of uniformly loaded vertical piles.

A rigorous analysis of a pile group embedded in an idealized elastic continuum necessitates modelling pile-soil-pile interaction. Elastic methods such as the B.E.M. and the simpler Interaction Factor Method (I.F.M.) are capable of modelling interaction, but cannot generally accommodate rafts of finite stiffness. The degree of interaction predicted by the elastic methods tends to be greater than that observed in practice.

Without resorting to a complex non-linear F.E.M., analysis of heavily loaded closely spaced piles requires a combined p-y or t-z method with a Mindlin equation approach. It is assumed that the p-y and t-z curves adequately model high plastic strain at the pile-soil

interface. The stress transferred through the bulk of the soil mass by pile-soil-pile interaction is assumed to be relatively low and can be analysed using Mindlin's equations. Accordingly, the soil modulus employed in Mindlin's equations is selected independently from the non-linear p-y and t-z curves. Although the procedure is cumbersome and theoretically inconsistent, it has achieved considerable success in the analysis of heavily loaded offshore pile groups. The method can accommodate the finite stiffness of the piled raft, variable loading and arbitrary pile configurations.

Direct modelling of the superstructure is generally impractical. Approximate methods are often employed to model the interaction of the superstructure with the substructure. Although the common approximation of an equivalent raft enables displacements to be satisfactorily estimated, raft bending moments may be grossly overestimated. A better simplification for modelling the superstructure is to condense it to a single storey. However, this requires a method of analysis which can consider three dimensional configurations.

2.7. CONCLUSION.

Rigorous methods of analysis are usually required to "accurately" predict the performance of the loaded substructure. Due to uncertainties in modelling the ground and the difficulty of determining realistic in situ soil properties, results from such analyses should be treated cautiously. These analyses also tend to be costly to undertake.

Simplified methods of analysis are intended to give approximate solutions to the load-deformation behaviour of the substructure. However, the idealizations made are generally so crude that the solutions may bear little resemblance to the actual behaviour.

There is a need for a simple method of analysis which can satisfactorily model the interaction of the superstructure-substructure-supporting soil system. The approach should consider the important features of variable loading on the raft, the finite stiffness of the raft and the superstructure configuration. It is also necessary for the method of analysis to accommodate multi-layered ground models. The idealized ground model should behave as an elastic continuum and exhibit non-linear characteristics under high strain.

In this thesis, it is intended to develop such a method of analysis using a beam-column representation of both the superstructure and substructure. This idealization enables all the above structural considerations to be accommodated. It is proposed to idealize the ground using springs whose stiffness can be modified to model the interaction effects of a continuum in an approximate manner. The spring analogy can also be extended to model non-linear behaviour by iteratively varying the stiffness of the springs. The simplified conceptual model could then be readily analysed using standard structural programs on a microcomputer.

Development of such a method of analysis is in agreement with the Institution of Structural Engineers et al (1989) who concluded:

"Future analytical studies should focus on the need to provide relatively simple aids for design rather than the provision of novel but complex mathematical solutions."

CHAPTER 3.

PROPOSED METHOD.

3.1. INTRODUCTION.

It is proposed to use the stiffness method to analyse a piled raft foundation. The method lends itself to the analysis of both a single pile and a complex structure configuration subjected to external loading or to a prescribed displacement. The structure is idealized as a number of elements of finite stiffness which are connected at their nodal points. A stiffness matrix is then assembled for the complete system using the element properties and their relative positions in the structure. The resulting set of simultaneous equations are solved to obtain the nodal displacements. The forces at each node are determined by back substitution. Due to the standardization of the stiffness method it is well suited to computer solutions.

The substructure to be analysed comprises a piled raft configuration supported by an elastic soil. The raft and piles are idealized as beam-column elements and the ground as a series of springs. This ground idealization is the basis of the simplified subgrade reaction theory (S.S.R.T.). The superstructure can be incorporated into the model using beam-column elements which may be considered as either fixed or pinned to the raft. The ability of the method to model the superstructure configuration is necessary in order to investigate the interaction of the superstructure-substructure-supporting soil system. Furthermore, the raft can be of any specified stiffness, thus avoiding the need to make unnecessary

assumptions regarding its rigidity. The axial shortening of the piles is also directly accommodated in the stiffness method.

The soil support to the raft is idealized using a series of springs in accordance with the theory developed by Terzaghi (1955). The piles, which are either fixed or pinned to the raft, are supported by a series of tangential and normal springs distributed along the pile shaft, which represent the skin friction and passive resistance of the soil respectively. There are several analyses where the lateral response of piles has been idealized with springs eg. Poulos (1980), Tomlinson (1977) and Broms (1964a,b).

There is a general lack of information available for the selection of values for the coefficient of subgrade reaction to represent axially loaded piles. Thus, a simple procedure for calculating the axial, or tangential, linear soil spring stiffness values is required. The use of springs enables a multi-layered soil to be modelled, which tends to be a difficult task using other methods of analysis.

The simplicity of the proposed method permits the use of a standard stiffness program for the analysis of complex soil structure interaction problems. The introduction of spring joint releases beneath the raft and along the pile accommodates the restraint afforded by the soil. A spring joint release is a nodal point in the structure restrained by a spring.

The results determined using this method of analysis are compared to results from the Department Of Transport program PGROUP developed by Banerjee et al (1981). The

soil spring stiffness values are varied to investigate their effect on the load distribution within the substructure and the resulting displacements. The conceptual model represents, as closely as possible, a realistic pile configuration in order to highlight the limitations and capability of the proposed method of analysis.

3.2. THE CONCEPTUAL MODEL.

Although the loading of many substructures is predominantly vertical eg. piles supporting a bridge abutment, significant lateral forces caused by earth pressures, traffic, or by wave and wind forces may also act on the piles. Therefore, a study of a model which incorporated raking piles to resist possible lateral forces was undertaken.

The idealization of the model is shown in Figure 3.1. The group comprised a symmetrical arrangement of two vertical and two raked piles. The rake of the piles was taken as a typical maximum value of 1 in 5. The piles were idealized as 0.5m in diameter, 10m long and formed of concrete with a modulus of elasticity of 30GN/m^2 .

In order to compare results computed by the two methods typical soil parameters were selected assuming a similar soil description of a stiff clay in both cases. The value of the soil modulus E_s was taken as 16MN/m^2 and Poisson's ratio μ_s as 0.25.

Terzaghi's (1955) coefficient of subgrade reaction K_{s1} for a 1ft. square plate was taken as 25MN/m^3 . In order to idealize the substructure model, the piles were

divided into three equal elements. The spring stiffness values beneath the raft and normal to the pile shafts were determined by multiplying the K_{sl}' values by the corresponding element-soil contact area. A first estimate for the tangential modulus K_v , which represents the axial pile-soil behaviour, was determined by dividing the calculated working load by an allowable settlement equal to 10% of the pile diameter. The working load was determined by multiplying the average adhesion at the pile-soil interface by the shaft area and applying a Factor of Safety of 2.5.

The soil modulus and spring stiffness values were selected independently of each other. Hence, it was not expected that the proposed method of analysis and PGROUP would initially give similar solutions. This was because no direct correlation exists between the spring stiffness values and the elastic soil modulus, E_s . In subsequent analyses the spring stiffness values were varied until agreement was achieved with the pile head displacement results from PGROUP for equivalent loading conditions. This enabled the spring stiffness values to be directly related to the soil modulus, E_s , used in the PGROUP analysis.

3.3. CONSTRUCTION OF THE MATHEMATICAL MODEL.

Construction of the model was a relatively easy task using a plane frame stiffness program which allowed springs to be used as joint releases. Firstly, the normal and tangential springs of the raked piles were resolved into global x and y directions. The stiffness values of all the springs located at a particular node were summed in the x

and y directions respectively. Each node was then specified as supported and the x and y joint releases were inputted into the program. This idealization assumed that the soil afforded no resistance to rotation of the node.

As a check that the plane frame program was used correctly, the construction of the stiffness matrix for the frame was also carried out manually. The direct spring stiffness values were simply applied to the appropriate values along the leading diagonal of the structure matrix. An example is shown below to illustrate the construction of the leading diagonal, where the P, K and δ terms represent the load, stiffness and displacement coefficients respectively.

$$\begin{pmatrix} P_{1x} \\ P_{1y} \\ P_{1z} \\ " \\ " \\ P_{7x} \\ P_{7y} \\ P_{7z} \end{pmatrix} = \begin{bmatrix} K(1,1) & & & & & & & \\ & K(2,2) + K_v & & & & & & \\ & & K(3,3) & & & & & \\ & & & " & & & & \\ & & & & " & & & \\ & & & & & K(19,19) + K_h & & \\ & & & & & & K(20,20) + K_v & \\ & & & & & & & K(21,21) \end{bmatrix} \begin{pmatrix} \delta_{1x} \\ \delta_{1y} \\ \delta_{1z} \\ " \\ " \\ \delta_{7x} \\ \delta_{7y} \\ \delta_{7z} \end{pmatrix}$$

In the example, Joint 1 is restrained by a spring of stiffness K_v in the y direction and Joint 7 is restrained in the x and y directions by springs of stiffness K_h and K_v respectively.

The stiffness matrix was then solved and the nodal displacements determined. The bending moments, axial forces and shear forces were computed by back-substitution.

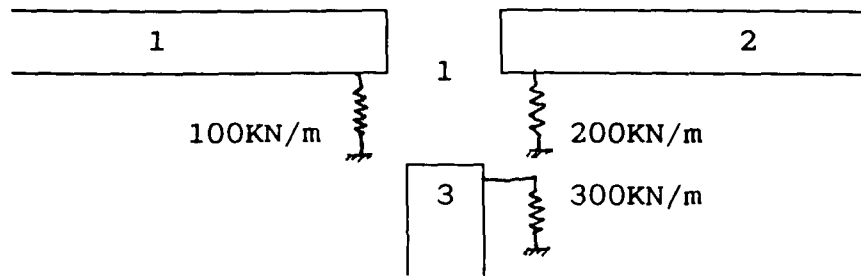
3.4. INTERPRETATION OF OUTPUT.

Solution of the stiffness matrix provides the global displacements at each nodal point. The output also

includes axial force, shear force, bending moment and support reactions at each node. The only distribution along the pile shaft which is obtained directly from the output is that of bending moment, since there is no rotational spring restraint. Typical distributions of axial load, shear force and bending moment along a pile shaft as obtained from the output, are shown in Figure 3.2.

A spring at a nodal point represents the total soil stiffness over the length of an element. Hence the axial and shear forces are transferred from the pile element to the soil in sharp increments at each spring position. The magnitude of the forces transferred to the soil at nodes are represented by the support reactions in the output. To determine the correct axial and shear force distributions a proportion of the respective support reaction is added to the values obtained directly from the output.

For instance, to determine the axial force at the pile head, the value of the support reaction due to skin friction is added onto the axial force value within the pile. However, where several elements meet eg. at a pile head, a number of springs representing the contribution of the soil for each element are combined to form a single spring at the node in a particular direction. In this case the load carried by each spring needs to be assessed. This is achieved by considering the percentage contribution of each spring to the total spring stiffness. The support reactions are then proportioned accordingly. An example is shown below to determine the pile head axial load.



Total spring stiffness at Node 1 = 600KN/m

Proportion of spring stiffness
from Element 3 = $300/600 = 50\%$

Say, axial force at pile head = 1000KN

and, joint reaction
(load in springs) = 500KN

then, proportion of load in spring = 50% of 500 = 250KN
from Element 3

Therefore,
Pile head axial load = $1000 + 250 = 1250\text{KN}$

The shear force at the pile head is treated in the same manner. At intermediate nodes along the pile shaft the forces are averaged for the two adjoining elements to allow for the effect of the spring at these points. At the pile bases the forces are treated in a similar manner to the pile heads ie. the appropriate percentage support reactions are subtracted from the forces given in the output. This process reduces the shear force at the base to zero. Because the bases are assumed to be smooth there are no complementary shears. The axial force at the base is equal to the end bearing resistance of the pile.

3.5. LOADING.

Two load cases were considered. These comprised a vertical downward load of 5000KN and a horizontal load of 500KN from right to left.

3.6. METHOD OF ANALYSIS.

The initial stiffness of the axial spring K_v idealizing skin friction was an estimate, hence an appropriate value for K_v needed to be established. To achieve this, the value of K_v was varied under vertical loading until the computed load distribution at the pile heads approximated to that from the PGROUP results. A comparison of load distributions rather than displacements was made because this form of simplified analysis is most commonly employed to assess the load distribution within piled foundations. The soil stiffness normal to the piles, supporting the raft and at the base of the piles was maintained constant whilst K_v was varied. Having determined an appropriate value for K_v , the lateral spring stiffness normal to the pile shafts, K_h , was varied under horizontal loading. This was necessary since the initial K_h value was an approximate value for a stiff clay and needed to be related to the E_s value used in the PGROUP analysis.

3.7. RESULTS.

3.7.1. General.

Both the substructure geometry and loading were symmetrical, hence, only the distribution of forces in one vertical and one raked pile are presented. The raked and vertical pile are referred to as Piles 1 and 2 respectively. Furthermore, as bending moment is a function of shear force, the bending moments are not shown. Where good agreement was achieved for shear force, there was also good agreement between bending moments.

The axial and shear forces in Piles 1 and 2 computed by PGROUP for vertical and horizontal loading are presented in Table 3.1.

3.7.2. Discussion Of Results.

(a) Vertical loading.

For vertical loading, the axial and shear forces in Piles 1 and 2 computed by the S.S.R.T. for various values of K_v and K_h are presented in Table 3.2.(a).

In Figure 3.3. the value of the lateral spring soil stiffness K_h was kept constant at 17,730KN/m as the axial soil stiffness K_v was varied from 1507 to 15065KN/m. Figure 3.3.(a) indicates the variation in the ratio of the S.S.R.T. axial load, P , to the PGROUP axial load, P_g , at the pile heads. By increasing K_v from 1507 to 15065KN/m the axial load carried by the vertical pile ie. Pile 2, was approximately doubled from 505 to 1040KN. The increase in the axial load carried by the raked pile ie. Pile 1, was only 2%. The variation in the ratio of the S.S.R.T. shear force, T , to the PGROUP shear force, T_g , at the pile heads is presented in Figure 3.3.(b). There was a 46% increase in the shear force carried by Pile 1 from 13 to 19KN, whereas the shear force in this pile computed by PGROUP was -5KN. The shear forces were less than 1% of the applied vertical loading and were therefore negligible.

When the value of the axial pile-soil spring stiffness K_v was increased from 1507 to 15,065KN/m the load carried by the raft reduced from 25% to 10% of the total applied load. For an E_s value of 16MN/m^2 the load carried by the raft as computed by the PGROUP program was 6.2%.

From the above comparisons, the best accuracy was achieved using an axial spring stiffness value of 15,065KN/m. The corresponding P/Pg ratios were 0.92 and 0.99 in Piles 1 and 2 respectively. On this basis further comparisons were carried out for vertical loading taking the axial pile-soil spring stiffness K_v as 15,065KN/m.

Table 3.2.(a). and Figure 3.4. indicate the effect of increasing the value of the lateral pile-soil spring stiffness K_h from 4433 to 88650KN/m whilst K_v was kept constant at 15065KN/m. This caused the axial load carried by Pile 1 to increase by 40% from 1110 to 1550KN. There was a resulting decrease of 30% in the axial load carried by Pile 2 from 1125 to 780 KN. The shear forces were also reduced as K_h was increased, giving better agreement with PGROUP, but as previously explained, the shear forces were negligible for the vertical loading case. Figure 3.4.(a) indicates that the original estimation of a K_h value of 17,730KN/m gave good agreement with PGROUP results. The corresponding P/Pg ratios were 0.92 and 0.99 in Piles 1 and 2 respectively.

For vertical loading, it is concluded that the best agreement obtained between S.S.R.T. and PGROUP results for the pile head load distributions was achieved with K_v equal to 15,065KN/m and K_h equal to 17,730KN/m.

(b) Horizontal loading.

For the horizontal loading case, the axial and shear forces in Piles 1 and 2 computed by the S.S.R.T. for various values of K_v and K_h are presented in Table 3.2.(b).

In Figure 3.5. the axial spring soil stiffness K_v was kept constant at 15065KN/m whilst the value of the lateral soil stiffness K_h was increased from 4433 to 88650KN/m. Figure 3.5.(a) indicates the axial forces to be sensitive to K_h . When the value of K_h was increased from 4433 to 88,650KN/m the axial load carried in Pile 1 reduced from 230 to 60KN, whereas the value given by PGROUP was 260KN. The corresponding axial load in Pile 2 was reduced from 75 to 10KN. The axial load in Pile 2 computed by PGROUP was 30KN.

The shear forces in all piles were also relatively high. PGROUP computed the shear forces in Piles 1 and 2 to be 98 and 104KN respectively ie. approximately 20% of the applied horizontal loading. The shear forces at the pile heads were relatively insensitive to K_h under horizontal loading as shown in Figure 3.5.(b). The best T/T_g value of 1.23 in Pile 1 was at K_h equal to 17,730KN/m. For this ground model the S.S.R.T. shear force was 121KN in comparison to 98KN from PGROUP. The corresponding T/T_g value in Pile 2 was 1.05.

In Figure 3.6. the lateral spring soil stiffness K_h was kept constant at 17730KN/m and the value of the axial soil stiffness K_v increased from 3013 to 15065KN/m. Figure 3.6.(a) indicates the axial load in Pile 2 to be very sensitive to changes in K_v under horizontal loading. Whereas the axial force in Pile 1 was less sensitive to changes in K_v but consistently underestimated the PGROUP value.

As shown in Table 3.2.(a), for values of K_v of 15065KN/m and K_h of 17730KN/m the S.S.R.T. axial loads in

Piles 1 and 2 were 117KN and 39KN respectively under horizontal loading. The corresponding PGROUP axial loads were 260KN and 30KN respectively.

The variation between the shear forces determined by the S.S.R.T. and PGROUP as K_v was varied is presented in Figure 3.6.(b). The agreement between the shear forces from both methods was generally good. The S.S.R.T. results were relatively insensitive to the value of K_v adopted. As shown in Table 3.2.(b), for horizontal loading with values of K_v of 15065KN/m and K_h of 17730KN/m, the S.S.R.T. shear forces in Piles 1 and 2 were 121KN and 110KN respectively. The corresponding PGROUP shear forces were 98KN and 104KN.

(c) Summary.

The analyses of the model indicate that selection of K_v and K_h values of 15,065KN/m and 17,730KN/m respectively enable good agreement to be achieved between the axial loads at the pile heads for vertical loading. The ratio of the S.S.R.T. to PGROUP pile head axial loads P/P_g was between 0.92 and 0.99. The shear forces were insignificant in magnitude. By using these stiffness values for the horizontal loading case, the ratio of the S.S.R.T. to PGROUP pile head shear forces T/T_g was between 1.04 and 1.23. The ratio of P/P_g under horizontal loading was quite poor, being 0.45 in Pile 1 and 1.29 in Pile 2. The axial force in Pile 2 was insignificant under horizontal loading. PGROUP computed the compressive and complementary tensile axial force in Pile 1 to be approximately 50% of the applied load as the group rotated.

The load distributions within the piled raft from the S.S.R.T. generally compared reasonably well with the PGROUP solutions. The exception was the agreement between the pile head axial load computed by the two methods under horizontal loading. This may have been due to PGROUP overestimating the loads. However, as the axial loads induced in piles due to vertical loading are generally much greater than those from lateral loading, this difference should not significantly effect pile design.

3.7.3. PGROUP Parametric Studies.

(a) General.

Parametric studies were carried out using the PGROUP program for the same piled raft model as described in Section 3.7.2. The parameters not varied during these studies were:

- (i) Substructure geometry
- (ii) Poisson's ratio for soil $\mu_s = 0.25$
- (iii) Young's Modulus of concrete $E_c = 30\text{GN/m}^2$

The elastic soil modulus E_s was increased from 16 to 320MN/m^2 in order to investigate its effect on the axial and shear force distributions for both horizontal and vertical loading. The variation of raft displacement with E_s was investigated. Corresponding results with a variation of K_v and K_h for the S.S.R.T. analysis were produced for comparison. The effect of pile element refinement on the PGROUP results was also considered.

Results are discussed for both vertical and horizontal loading by examination of Figures 3.7. to 3.12.

(b) Vertical loading.

Figure 3.7.(a) shows the variation of axial load at the pile head for vertical loading. By increasing E_s from 16 to 320MN/m^2 , the axial load carried by Pile 1 decreased from 1320 to 1000KN. The axial load in Pile 2 remained constant at about 1070KN for the same variation of E_s . To maintain equilibrium of vertical forces, the proportion of load carried by the raft increased as E_s was increased.

The variation in the shear forces in the piles is shown in Figure 3.7.(b). The shear forces fluctuated considerably as E_s was increased. However, the values were insignificant in magnitude, the greatest being 6.8KN in Pile 1.

Figure 3.9.(a) shows the variation of raft displacement against E_s . The displacement decreased as E_s was increased, ie. increased stiffness resulting in decreased deformation. In Figure 3.10.(a) the variation of displacement with K_v is shown; the trend of the graph being the same as in Figure 3.9.(a). For values of K_v of 15065KN/m and K_h of 17730KN/m , the displacement determined by the S.S.R.T. analysis was 22mm. A displacement of 31.5mm was computed by PGROUP for the E_s value of 16MN/m^2 used in Section 3.7.2.

Under vertical loading, the load distribution in the piled raft was insensitive to a variation in the number of pile elements within the range from 3 to 11 and is not presented.

(c) Horizontal loading.

The variation of axial load at the pile head against E_s is presented in Figure 3.8.(a). At an E_s value of 16MN/m^2 the axial loads at the heads of Piles 1 and 2 were 260KN and 30KN respectively. However, at an E_s value of 320MN/m^2 the corresponding loads were 40 and 210KN respectively ie. a complete reversal in the distribution. This may be due to a convergence problem with PGROUP at low ratios of E_p/E_s . By examination of Poulos and Davis' (1974) interaction factors, an increase in E_s corresponds to decreased interaction. Thus, the central piles, ie. Pile type 2, should carry more load as E_s is increased.

Figure 3.8.(b) indicates that the shear forces in both Piles 1 and 2 increased as E_s was increased.

The variation of raft displacement against E_s is presented in Figure 3.9.(b). The horizontal displacement of the raft decreased from 10.5 to 1.5mm as E_s was increased from 16 to 320MN/m^2 . In Figure 3.10.(b) the variation of horizontal displacement with K_h is shown, the trend of the graph being the same as Figure 3.9.(b), with the displacement decreasing from 8.2 to 3.2mm as K_h was increased from 17730 to 88650KN/m. For values of K_v of 15065KN/m and K_h of 17730KN/m, the horizontal displacement was 8.2mm compared to 10.5mm from PGROUP for the E_s value of 16MN/m^2 used in Section 3.7.2.

Results showing the sensitivity of the axial loads to the number of elements used for the idealization of each pile are presented in Figures 3.11.(a) and (b). By refining the number of pile elements from 3 to 9, there was a reduction in axial load at the head of Pile 2 from 1050

to 950KN and a corresponding increase in Pile 1 from 1320 to 1420KN. The variation in axial load at a depth of one-third the pile length was unchanged.

As the number of elements was varied the shear force distribution remained generally unaltered up to 9 elements, as presented in Figures 3.12.(a) and (b). For more than 9 elements the variation of shear forces in Piles 1 and 2 was irregular. This suggested a poor solution procedure within the program.

The PGROUP User Manual recommended that between 6 and 11 elements should be used to model each pile.

3.8 INVESTIGATION OF RELATIONSHIP BETWEEN K_v , K_h AND E_s .

3.8.1. General.

Comparison between the S.S.R.T. and PGROUP results for the piled raft foundation indicated that the S.S.R.T. could satisfactorily model the load distribution. The displacements computed by the S.S.R.T. were generally lower than those from PGROUP.

In this section, comparison of displacements for single piles from PGROUP and the S.S.R.T. will enable subgrade reaction stiffness values for K_v and K_h to be determined more precisely. Modification Factors, M_v and M_h , are presented which relate K_v and K_h values to the more familiar soil modulus, E_s . Application of M_v and M_h factors to the soil spring stiffness values effectively enables the S.S.R.T. to model the load-deformation behaviour of a pile embedded in an elastic continuum.

3.8.2. Background To The Work

In order for this work to be completely general, K_v and K_h are taken as $M_v.E_s.L'$ and $M_h.E_s.L'$ respectively; where L' is the pile element length. The end bearing stiffness K_{eb} is taken as $M_v.E_s.b$; where b is the equivalent breadth of a square pile. It is recognised that this treatment of the end bearing stiffness is crude because its load-deformation behaviour is dissimilar to that of skin friction. However, for piles with L/d ratios greater than 20, the contribution of the end bearing resistance is minimal when compared to the skin friction.

The Modification Factors were found to be a function of both the L/d ratio and the relative stiffness of the pile to soil. For axial loading the relative stiffness of the pile to soil is denoted by K , where:

$$K = \frac{E_p.R_A}{E_s}$$

and,

E_p = pile modulus

$$R_A = \frac{\text{area of pile section}}{\pi.d^2/4}$$

Similarly, for lateral loading the relative stiffness of pile to soil is given by K_R , where:

$$K_R = \frac{E_p.I_p}{E_s.L^4}$$

and,

I_p = second moment of area of pile section
 L = pile length.

The Factors M_v and M_h are similar to the Influence Factors I_μ and $I_{\mu h}$ presented by Poulos and Davis (1974) which are also functions of the L/d ratio and relative stiffness of pile to soil. However, Poulos and Davis'

Influence Factors are applied to the whole system ie. to pile and soil, whereas M_v and M_h are envisaged to apply to the soil only.

For example, for a compressible pile subjected to axial loading, the pile head displacement δv as given by Poulos and Davis is:

$$\delta v = \frac{P \cdot I_{\mu}}{L \cdot E_s}$$

where:

P = applied axial load
 L = pile length
 E_s = soil modulus
 I_{μ} = Influence Factor.

Thus, for a given L/d ratio and E_p value, I_{μ} can be determined from graphs presented by Poulos and Davis. This enables the axial displacement of a single pile to be calculated manually. However, problems arise when this method is applied to pile groups. A few limitations are outlined below:

- (i) The method relies on the principle of superposition. Hence, a variation in soil stiffness from pile to pile cannot be accommodated and all piles have to be of uniform length and cross-section.
- (ii) The pile cap must either be idealized as rigid or perfectly flexible.
- (iii) For a group of vertical piles, subject to horizontal loading only, no axial load is induced in any piles. Whereas analyses using both the S.S.R.T. and the PGROUP program computed significant axial loads in piles off the line of rotation as the pile cap rotated.

These limitations can be overcome using the proposed method. The parameters M_v and M_h can be determined for

individual piles with different load-deformation characteristics. These can then be applied to the soil stiffness values of K_v and K_h for each pile element. A stiffness matrix for the complete structure-foundation-soil system can then be constructed in the usual manner. Interaction between piles can either be ignored or accommodated as outlined in Chapter 5.

3.8.3. Method Of Approach.

Values for M_v and M_h were determined for a comprehensive range of L/d ratios. Although the method was proposed for friction piles with L/d ratios from 20 to 50, a wider range of L/d ratios was considered in order to determine an extensive set of M_v and M_h values. The pile modulus E_p was limited to the practical construction materials of steel, concrete and wood, with values of 200, 30 and 10GN/m^2 respectively. The soil modulus E_s was varied from 500KN/m^2 to 1GN/m^2 .

As a means of comparison, displacements for a series of single axially and laterally loaded piles were obtained from the PGROUP program. To maintain accuracy at high values of soil moduli, a load equal to the soil modulus was applied in each case. To obviate problems of convergence with the PGROUP analysis, 10 pile elements were used to model each pile shaft.

To correlate S.S.R.T. and PGROUP results, the M_v and M_h parameters were varied until the pile head displacements agreed to within 1% of those achieved by PGROUP. In order to satisfactorily distribute the soil springs at nodal

points along the pile shaft, 20 elements were used to idealize the pile in the S.S.R.T. model.

3.8.4. Results.

(a) General.

For the idealization of a circular concrete pile, with E_p equal to 30GN/m^2 , M_v and M_h were determined for L/d ratios from 5 to 100. For a L/d ratio of 20, E_p values of 10 and 200GN/m^2 were also considered in order to assess the effect of pile stiffness on M_v and M_h .

(b) Analysis of axial behaviour.

In Figure 3.13. M_v is plotted against the relative pile to soil stiffness K for various L/d ratios. For any given L/d ratio, M_v remained approximately constant for K values from 6×10^4 to 300 ie. for an E_p value of 30GN/m^2 with E_s varied from 500 to 10^5KN/m^2 . By definition R_A is equal to unity for circular piles. At K values less than 300 the displacements computed by PGROUP became irregular. This could be due to a convergence problem with PGROUP. However, for consistency, comparisons were made with the PGROUP results for all stiffness values. Therefore M_v reflects the value required to achieve agreement between the S.S.R.T. and PGROUP results.

During back analysis of the results, the calculations indicated that, for any given L/d ratio, M_v remained approximately constant as the pile head displacement increased steadily with an increase in E_s and the applied load. This was as expected since the axial shortening of

the pile became more significant in relation to the pile-soil displacement as E_s increased relative to E_p .

As the L/d ratio increased from 5 to 100, M_v reduced from a value of 0.77 to 0.44 for relatively high values of K . For practical L/d ratios of 20 and 50, the M_v values were generally between 0.59 and 0.50 respectively. Therefore, it is satisfactory to take M_v as 0.5 for friction piles with L/d ratios between 20 and 50 and relative stiffness values of K from 0.3×10^6 to 60×10^6 e.g. for an E_p value of 30 GN/m^2 with soil modulus values between 500 and 10^5 KN/m^2 . For pile-soil systems not within these limitations, M_v should be determined from Figure 3.13..

To validate the results presented in Figure 3.13. the pile was analysed with different stiffness characteristics to those initially used. For a L/d ratio of 20 the pile modulus E_p was assigned values of 10 and 200 GN/m^2 to represent wood and steel respectively. The following results were computed:

$$\text{For } K = 200 \quad M_v(\text{steel}) = 0.570 \text{ and } E_s = 1.00 \text{ GN/m}^2$$

$$K = 200 \quad M_v(\text{wood}) = 0.575 \text{ and } E_s = 0.05 \text{ GN/m}^2$$

For given values of K and L/d ratio, M_v was approximately constant for different values of E_s . These results confirm that M_v should be selected on the basis of the relative stiffness K not the value of the soil modulus E_s .

(c) Analysis of lateral behaviour.

The Modification Factor, M_h , for lateral behaviour is plotted against the relative stiffness K_R for various L/d ratios in Figure 3.14..

For a given L/d ratio, the value of M_h varied with the relative stiffness K_R . This variation was more pronounced for the larger L/d ratios and lower K_R values. For most L/d ratios, the unit lateral displacement of the pile head, δh , increased steadily up to an E_s value of 0.10 GN/m^2 , then rose sharply at about 1 GN/m^2 for an E_p value of 30 GN/m^2 .

The displacements computed by PGROUP for the laterally loaded pile were inconsistent. For example, for a given soil modulus, say 500 kN/m^2 , the displacement δh decreased from 0.602 to 0.214m as L/d was increased from 5 to 30. By increasing the L/d ratio from 30 to 100 the corresponding displacement δh increased from 0.214 to 0.243m. This is clearly unrealistic and is considered to be due to PGROUP convergence difficulties. In this case, it is recommended that the value of δh should be confined to 0.214m above L/d ratios of 30 ie. no benefit is achieved by increasing the length above 30m for a 1m diameter pile under lateral loading.

As the L/d ratio increased from 5 to 100, M_h reduced from 1.325 to 0.71 for an E_s value of 500 kN/m^2 . At an E_s value of 1 GN/m^2 , M_h reduced from 1.48 to 0.006 as the value of L/d was increased from 5 to 100. The very low M_h value of 0.006 at L/d of 100, could be due to convergence difficulties with PGROUP at low values of K_R . Poulos and Davis (1974) did not present results for K_R values less than 10^{-6} , whereas K_R was equal to 10^{-8} for an E_s of 1 GN/m^2 with E_p equal to 30 GN/m^2 and a L/d ratio of 100. Although this pile system may be impractical, M_h reflects the value required to achieve agreement with the PGROUP program.

For circular concrete friction piles with L/d ratios of 20 to 50, the M_h value varied between 0.82 and 0.96 for E_s values less than 10MN/m^2 . For practical purposes, it is satisfactory to take M_h as 1.0 ie. K_h equal to $E_s.L'$, for this limited range. However, for general pile-soil systems beyond these limitations, it is imperative that the M_h value is selected from Figure 3.14..

To examine the effect of varying the pile stiffness on the M_h value, E_p values of 10 and 200GN/m^2 were considered for a L/d ratio of 20. The results indicate that M_h was approximately constant for wood, concrete and steel. For example:

For $K_R = 6.14 \times 10^{-5}$

$M_h(\text{Steel}) = 1.100 \quad E_s = 1.00\text{GN/m}^2$

$M_h(\text{Concrete}) = 1.080 \quad E_s = 0.15\text{GN/m}^2$

$M_h(\text{Wood}) = 1.065 \quad E_s = 0.05\text{GN/m}^2$

The agreement between the results was excellent. This confirmed that the M_h values presented in Figure 3.14. were applicable for general pile analysis. By employing appropriate M_h values in the S.S.R.T. analysis, the resulting value of δh would be equal to that determined by PGROUP for a laterally loaded pile embedded in an elastic continuum.

(d) Summary.

The S.S.R.T. has been modified to model single axially and laterally loaded piles embedded in an elastic continuum. The displacement of an axially loaded pile can satisfactorily be determined by taking the value of K_v as $E_s.L'/2$ for a limited range of practical pile-soil systems.

This relationship is valid for friction piles with L/d ratios between 20 and 50 and relative stiffness values of K from 0.3×10^6 to 60×10^6 e.g. for an E_p value of 30 GN/m^2 with soil modulus values between 500 and 10^5 KN/m^2 .

The relationship of K_h equal to $E_s L'$ is valid for laterally loaded piles with L/d ratios between 20 and 50 and relative stiffness values of K_R from 10^{-1} to 10^{-5} e.g. for an E_p value of 30 GN/m^2 with values of E_s from 500 to 10^4 KN/m^2 .

For pile-soil systems not within the above range it is necessary to select Modification Factors M_v and M_h from Figures 3.13. and 3.14.. These are then applied to the spring stiffness values to be used in a S.S.R.T. analysis. The resulting displacements for a single pile embedded in an elastic continuum will agree with those determined from the PGROUP program.

3.9. DISCUSSION AND CONCLUSIONS.

The applicability of the S.S.R.T. for piled raft analysis was investigated by comparison with PGROUP results. The substructure considered comprised both raked and vertical piles. The S.S.R.T. generally computed a satisfactory load distribution within the idealized piled raft. The exception was the agreement between the pile head axial forces computed by the S.S.R.T. and PGROUP under horizontal loading. This may have been due to PGROUP overestimating the force. However, as the axial forces induced in piles due to vertical loading are generally much greater than those from lateral loading, the difference in results should not significantly effect pile design.

The S.S.R.T. idealization of the piled raft utilized three elements to model each pile. It is now appreciated that this was not a satisfactory idealization for piles subject to horizontal loading. Initially, solutions were computed manually and the stiffness matrix was large and cumbersome with just three elements. Use of standard structural analysis programs enable groups to be analysed with the piles subdivided into several elements. A further development of this approach would be to idealize the pile elements as shedding load continuously, rather than at sharp increments at nodal points. This would enable the number of elements used to be reduced.

Parametric studies were carried out using PGROUP to investigate the influence of various parameters on substructure behaviour. The results indicated that the relative stiffness of the substructure to soil had a significant effect on the load distribution, which was also an observation of the S.S.R.T.. PGROUP results of piles subject to horizontal loading were shown to be sensitive to pile element refinement. Convergence problems were detected for a number of pile-soil systems using PGROUP.

The analysis of a substructure by elastic methods generally requires a value for the soil modulus E_s . Having selected a value of E_s , stiffness values for both the lateral and axial soil springs K_h and K_v can be readily determined from an extensive set of Modification Factors M_v and M_h . This enables the S.S.R.T. to be applied to the analysis of piles embedded in an elastic continuum.

Loading	Pile head forces (KN)			
	P1	P2	T1	T2
Vertical	1320	1050	-5	2
Horizontal	260	30	98	104

P1 = Axial force in Pile 1 T1 = Shear force in Pile 1
P2 = " " " " 2 T2 = " " " " 2

Table 3.1.: PGROUP pile head forces.

Stiffness (KN/m)		Pile head forces (KN)			
Kv	Kh	P1	P2	T1	T2
1507	17730	1200	505	13	1
3013	17730	1220	670	16	1
12052	17730	1225	995	18	1
15065	17730	1225	1040	19	1
15065	4433	1110	1125	26	1
15065	70920	1425	875	10	-1
15065	88650	1550	780	8	-1

Table 3.2.(a):: S.S.R.T. pile head forces for vertical loading.

Stiffness (KN/m)		Pile head forces (KN)			
Kv	Kh	P1	P2	T1	T2
15065	4433	230	75	125	84
15065	70920	60	15	120	118
15065	88650	60	10	120	118
3013	17730	72	18	118	117
6026	17730	89	27	120	115
12052	17730	110	36	121	110
15065	17730	117	39	121	110

Table 3.2.(b):: S.S.R.T. pile head forces for horizontal loading.

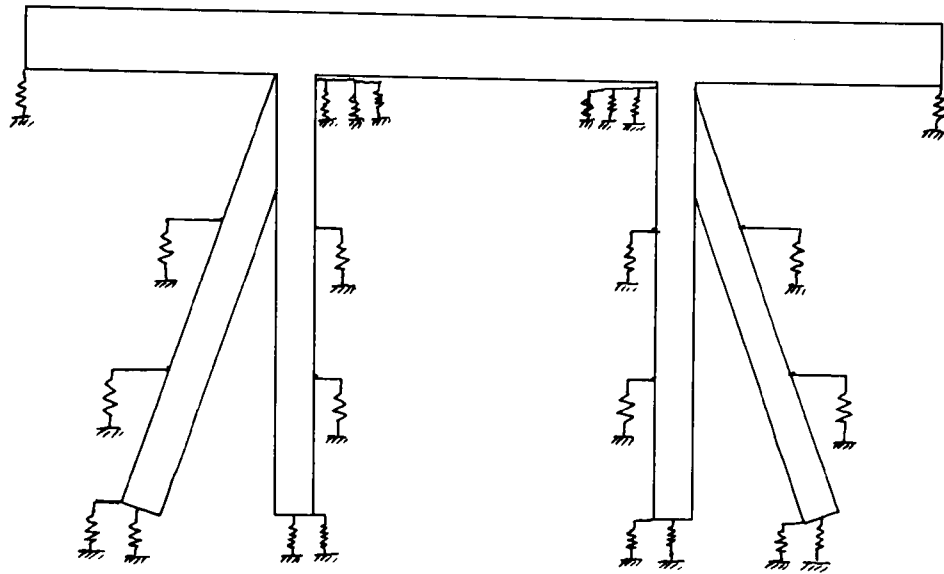


Figure 3.1.: Idealization of the model.

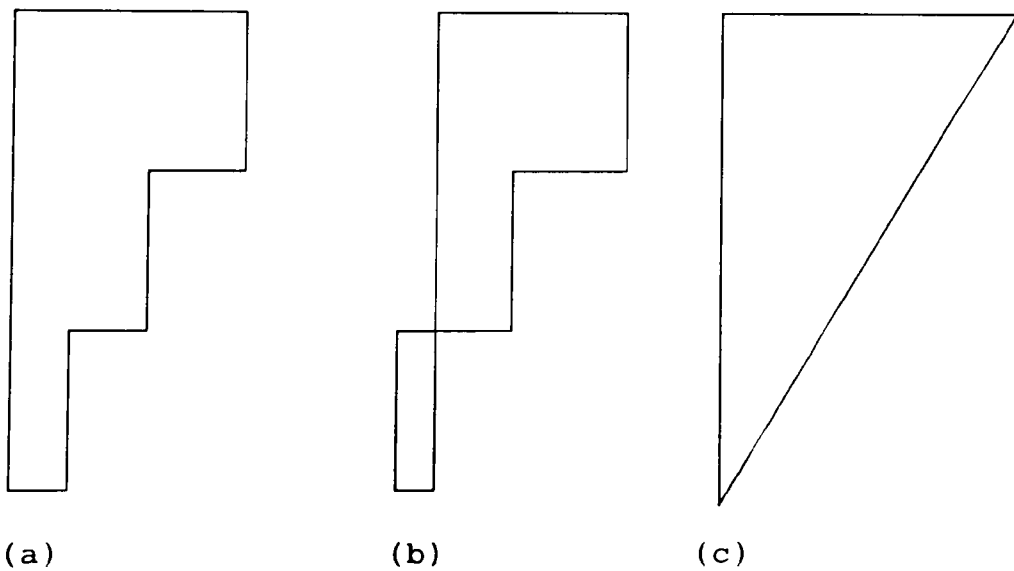
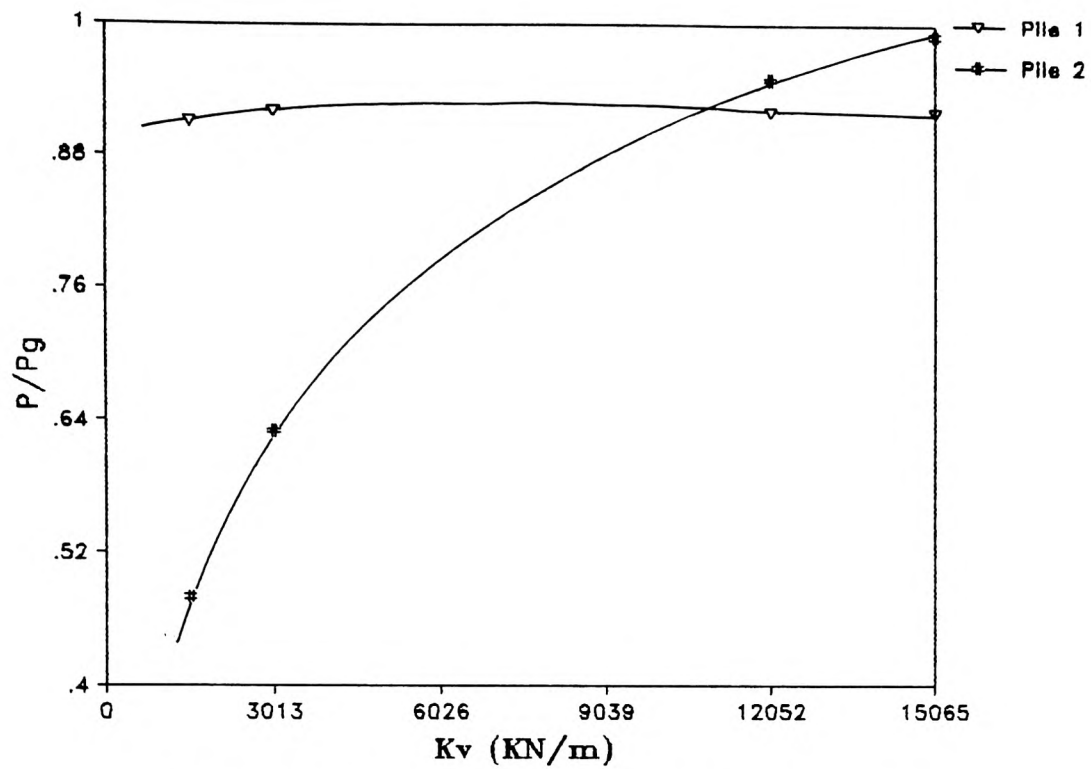
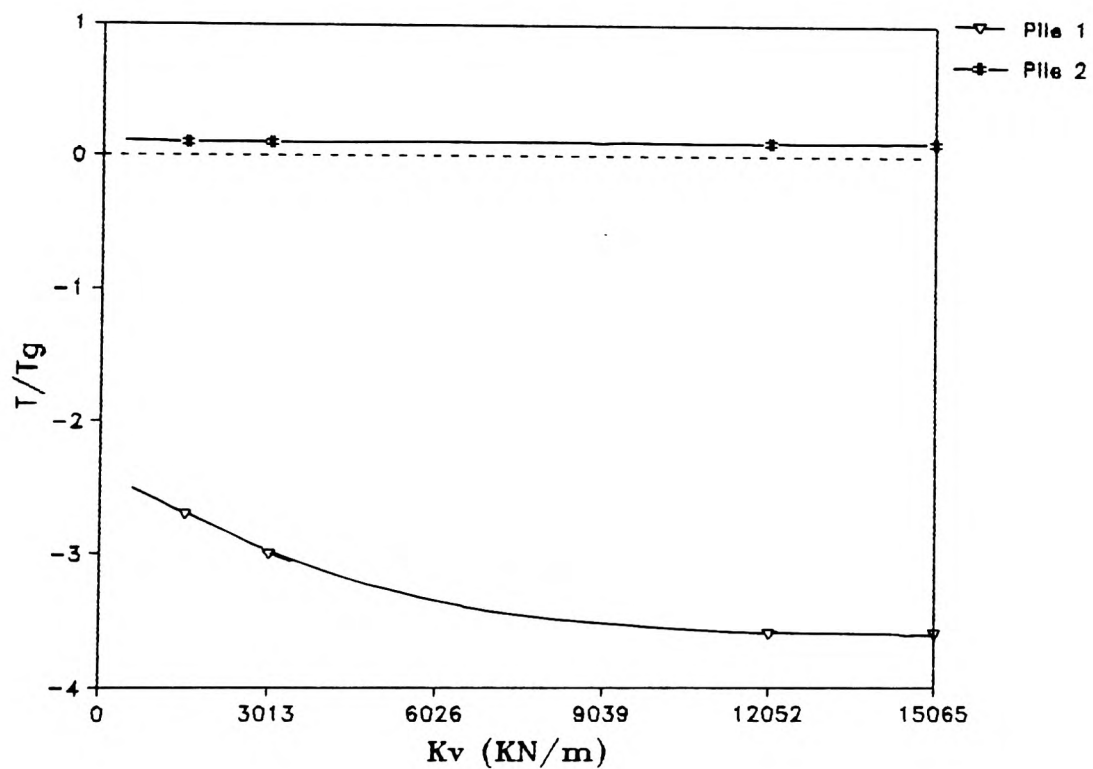


Figure 3.2.: Typical distributions of (a) Axial load, (b) Shear force and (c) Bending moment.

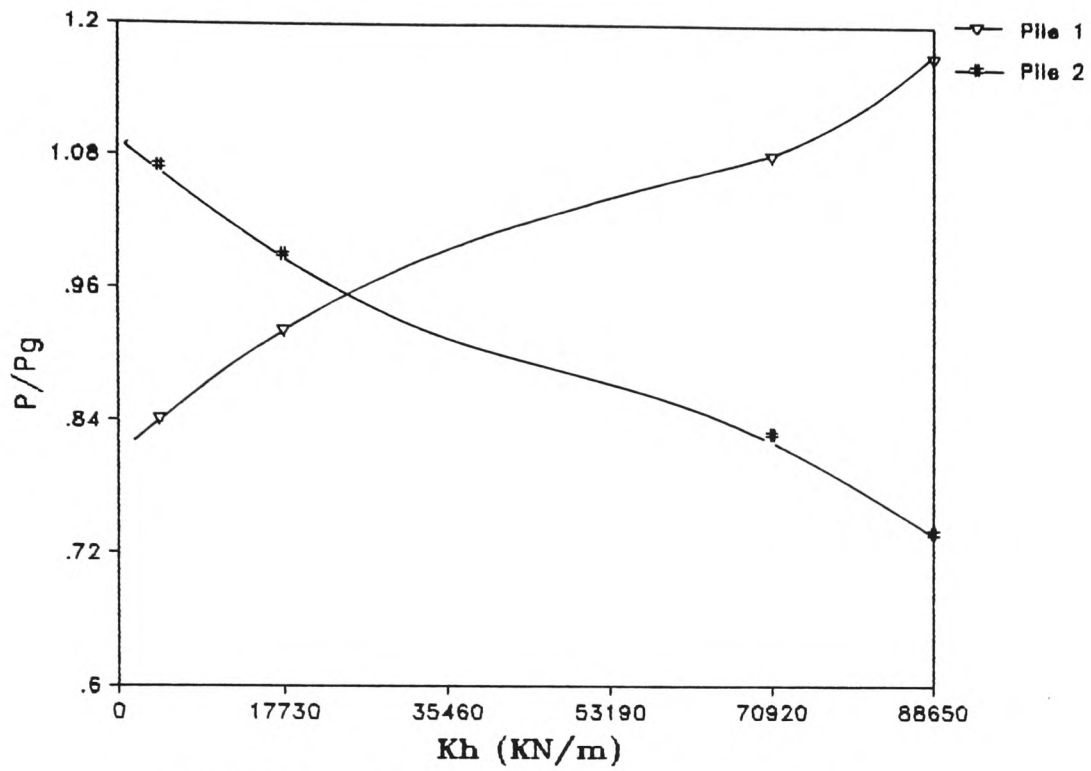


(a) Ratio of axial loads at the pile head.

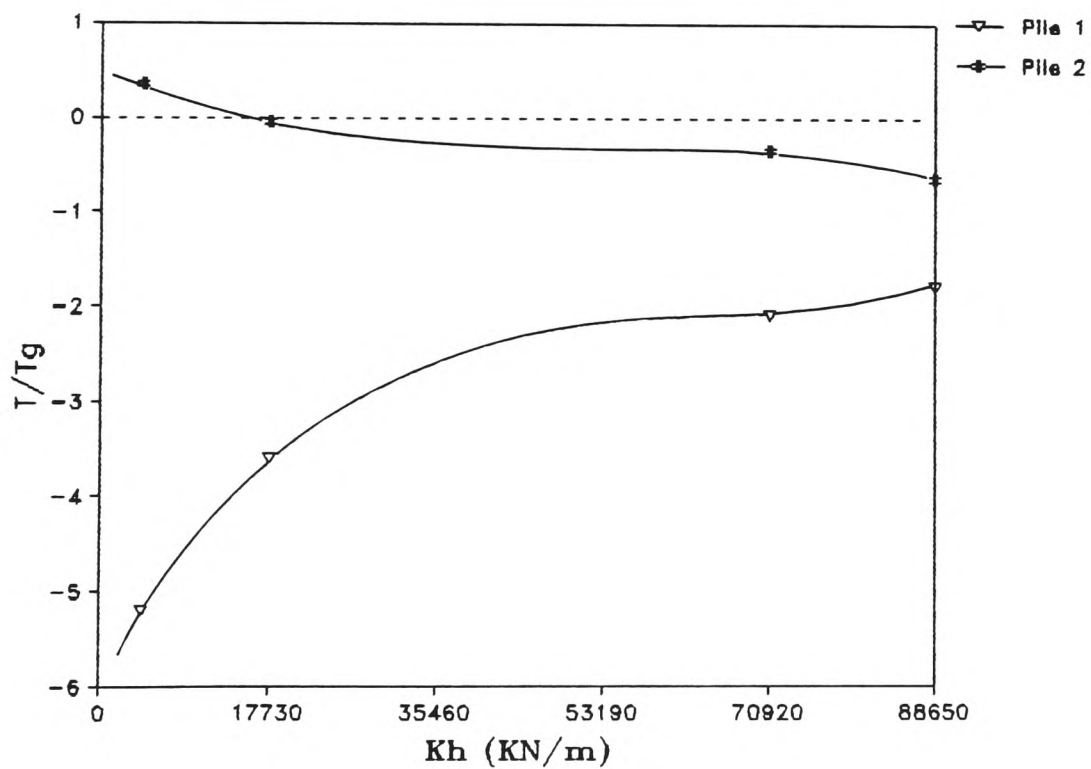


(b) Ratio of shear forces at the pile head.

Figure 3.3.: Effect of K_v on accuracy for vertical loading.

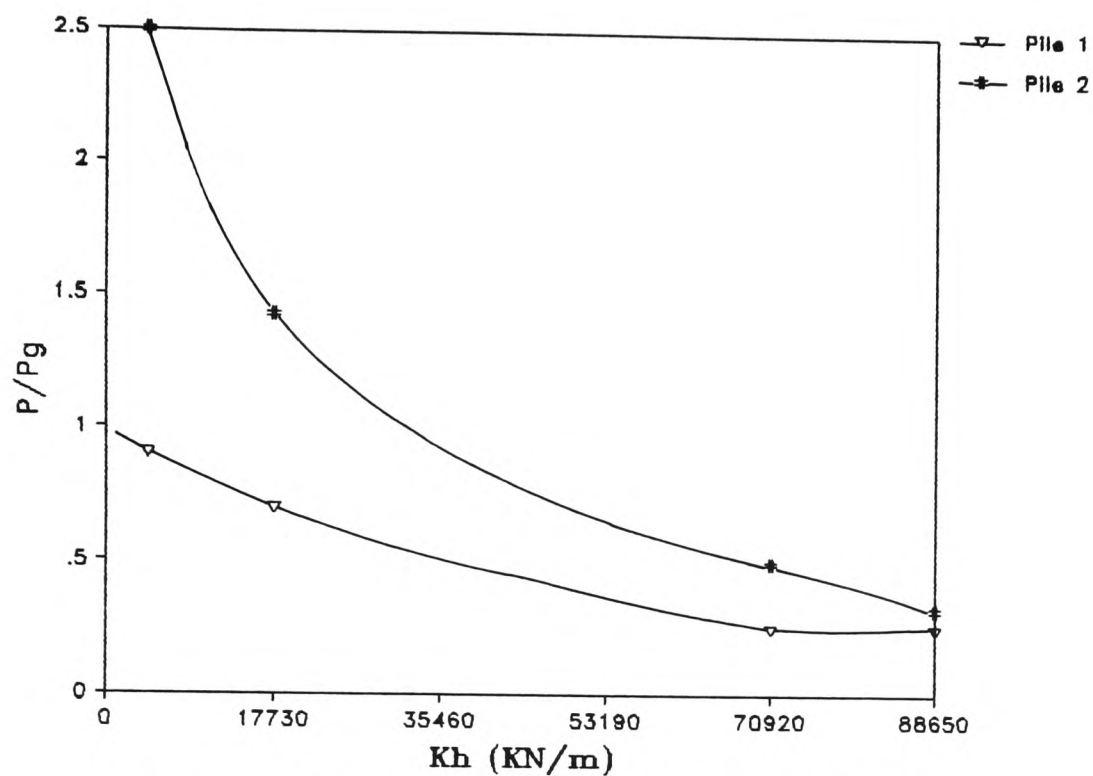


(a) Ratio of axial loads at the pile head.

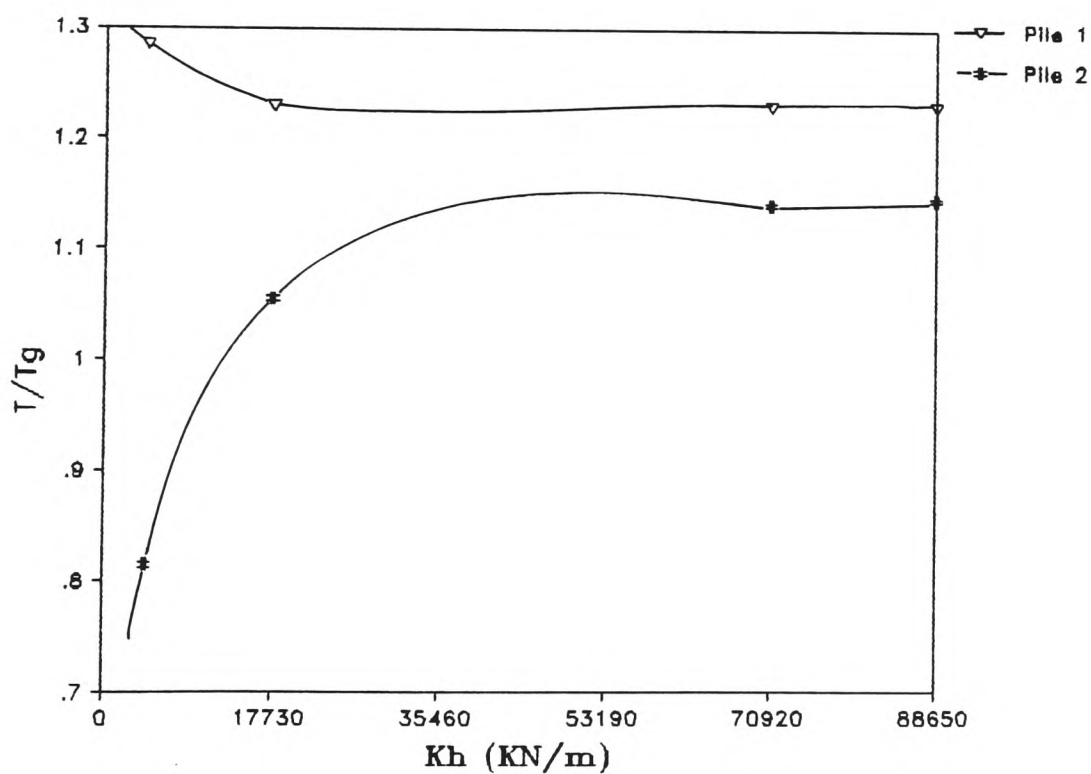


(b) Ratio of shear forces at the pile head.

Figure 3.4.: Effect of Kh on accuracy for vertical loading.

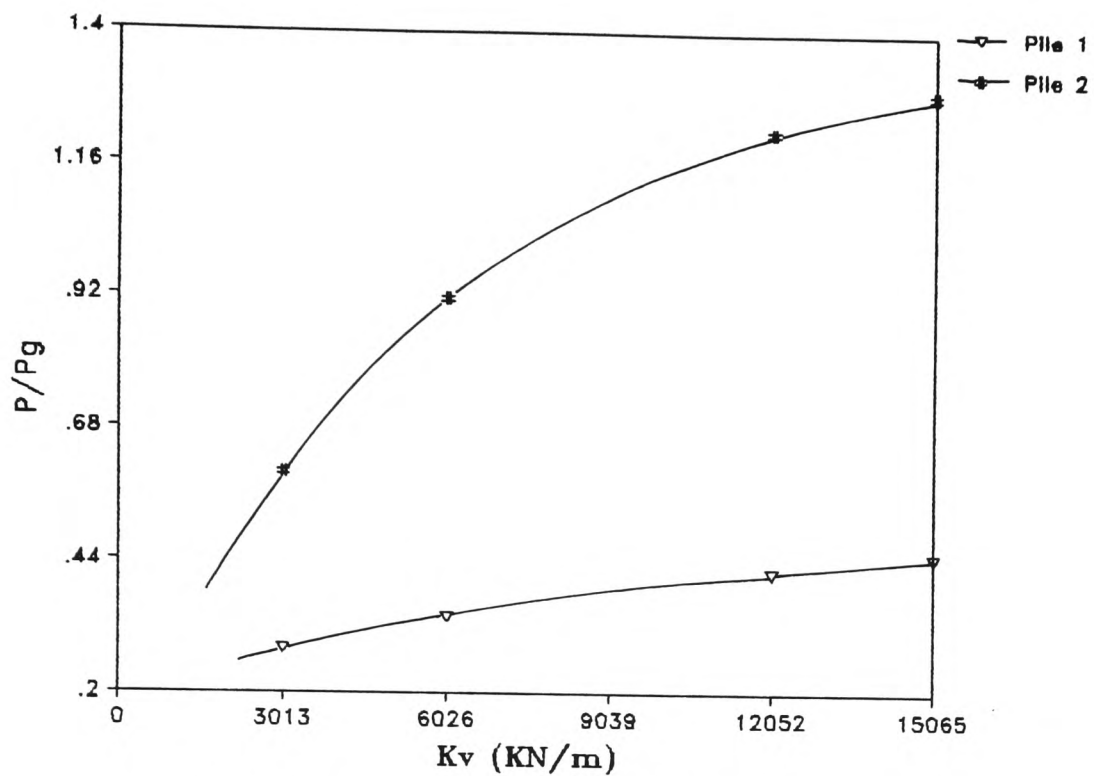


(a) Ratio of axial loads at the pile head.

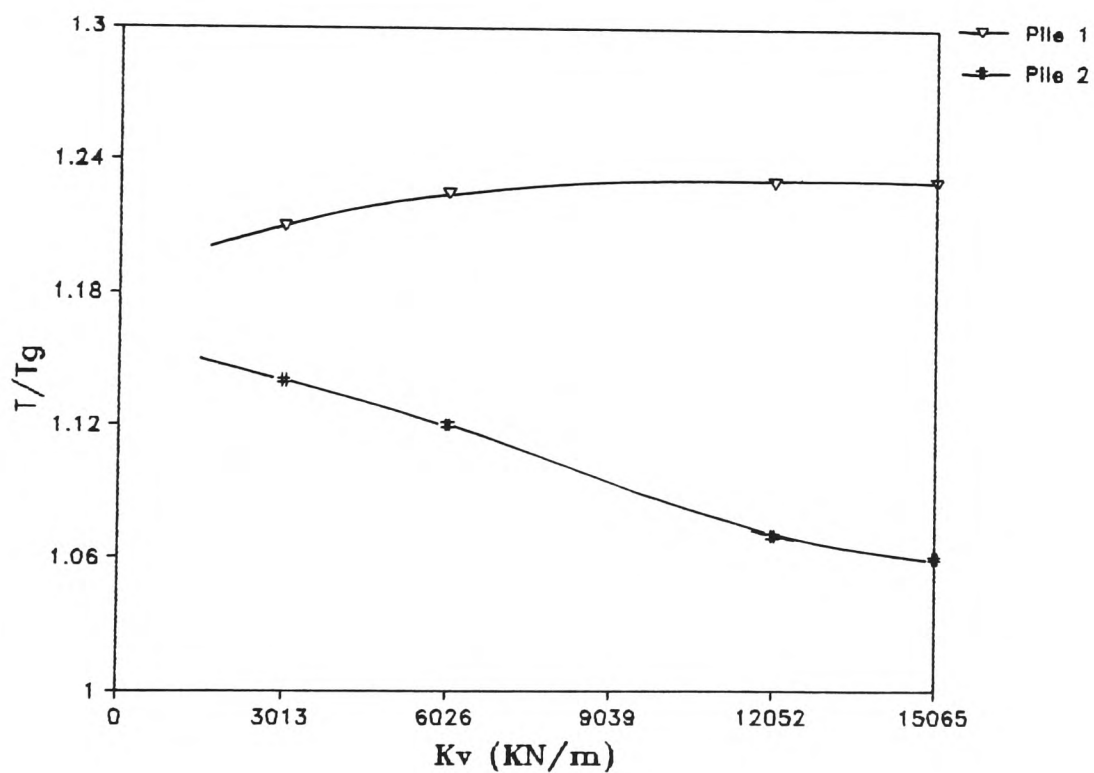


(b) Ratio of shear forces at the pile head.

Figure 3.5.: Effect of K_h on accuracy for horizontal loading.

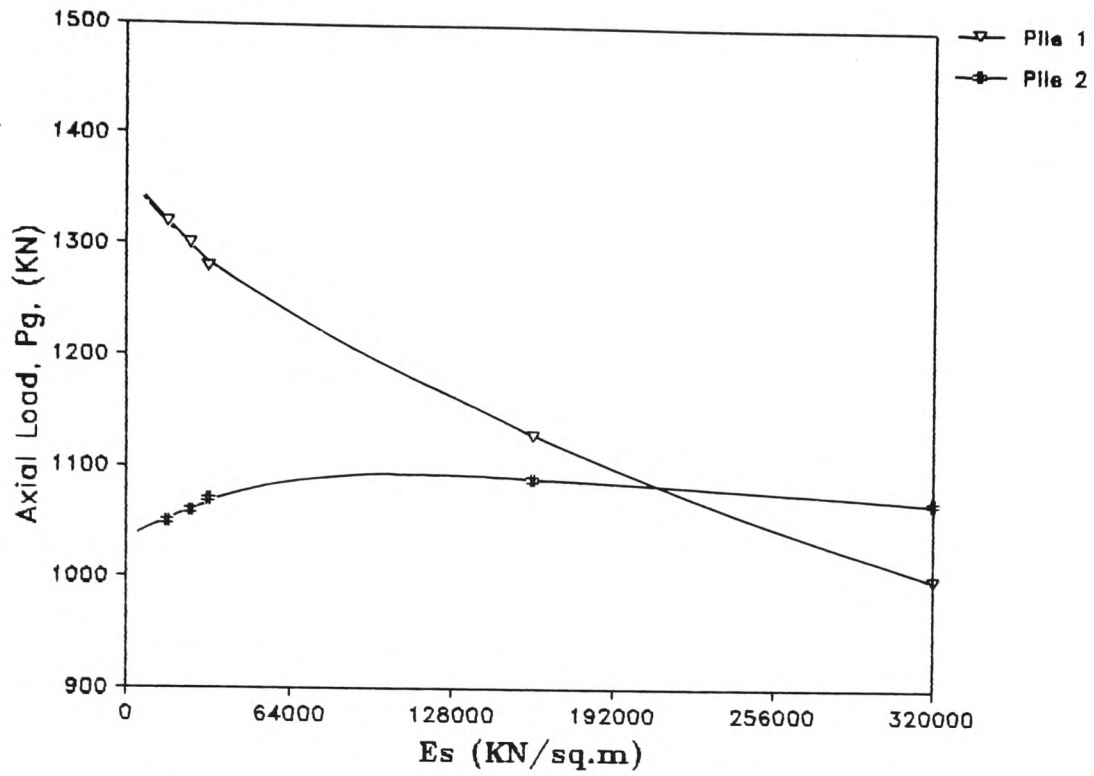


(a) Ratio of axial loads at the pile head.

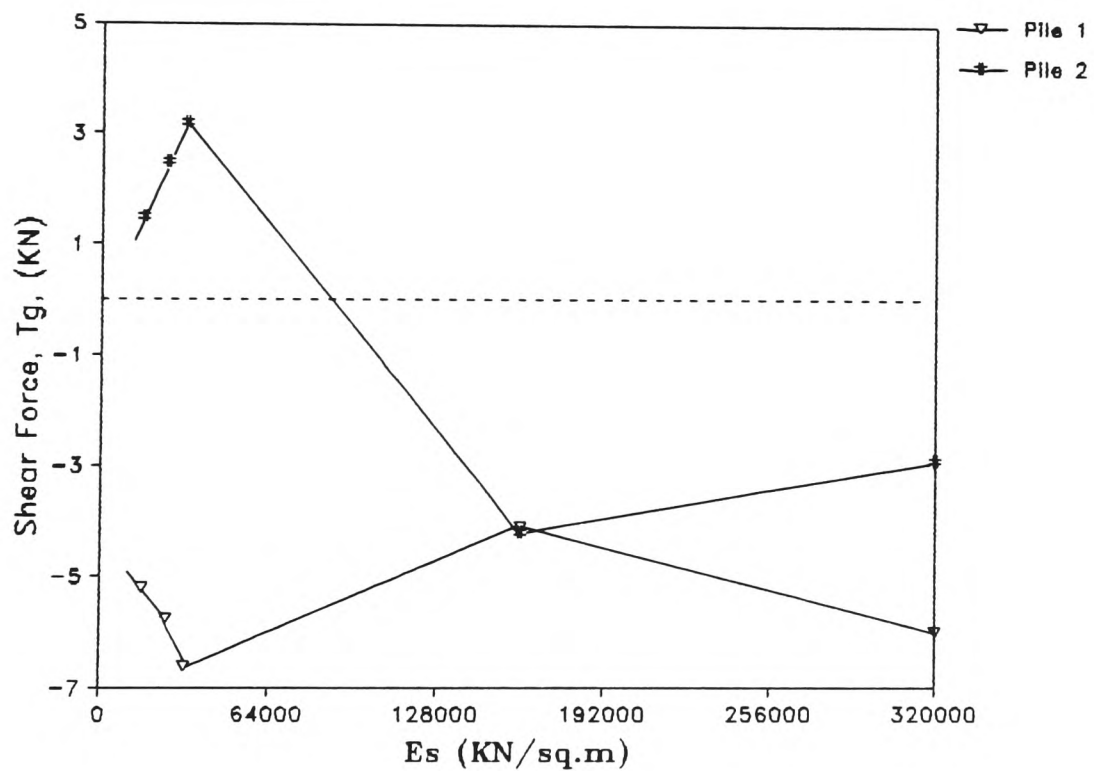


(b) Ratio of shear forces at the pile head.

Figure 3.6.: Effect of K_v on accuracy for horizontal loading.

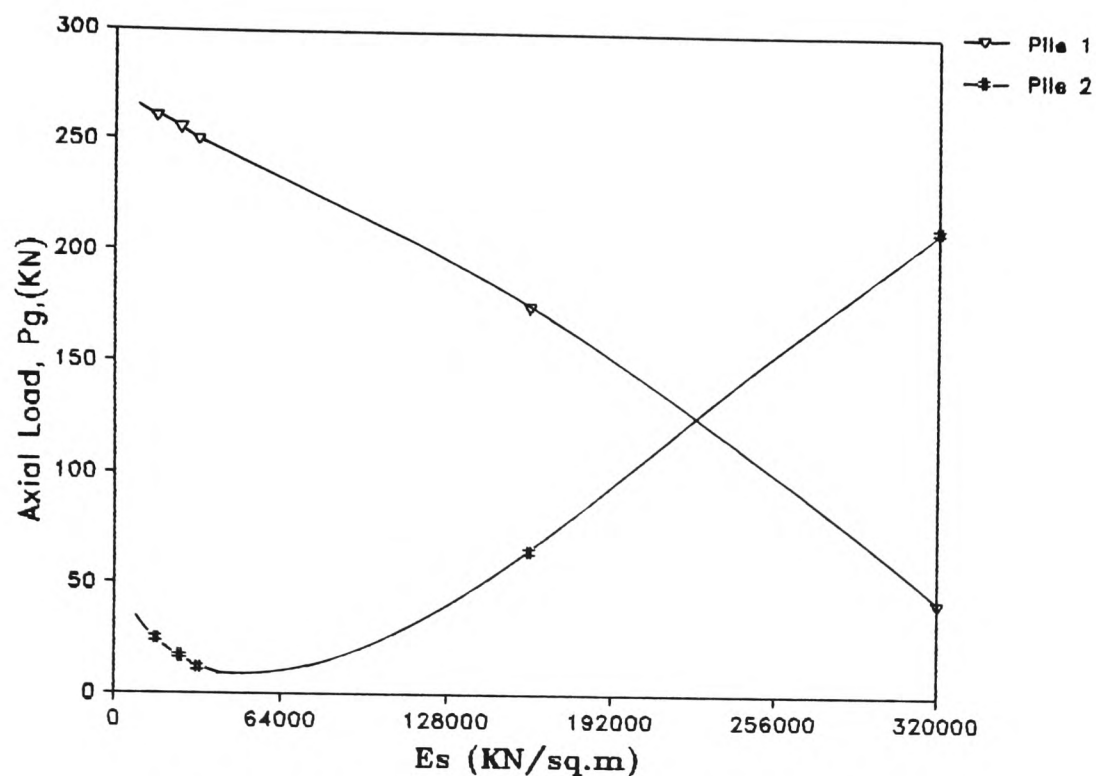


(a) Ratio of axial loads at the pile head.

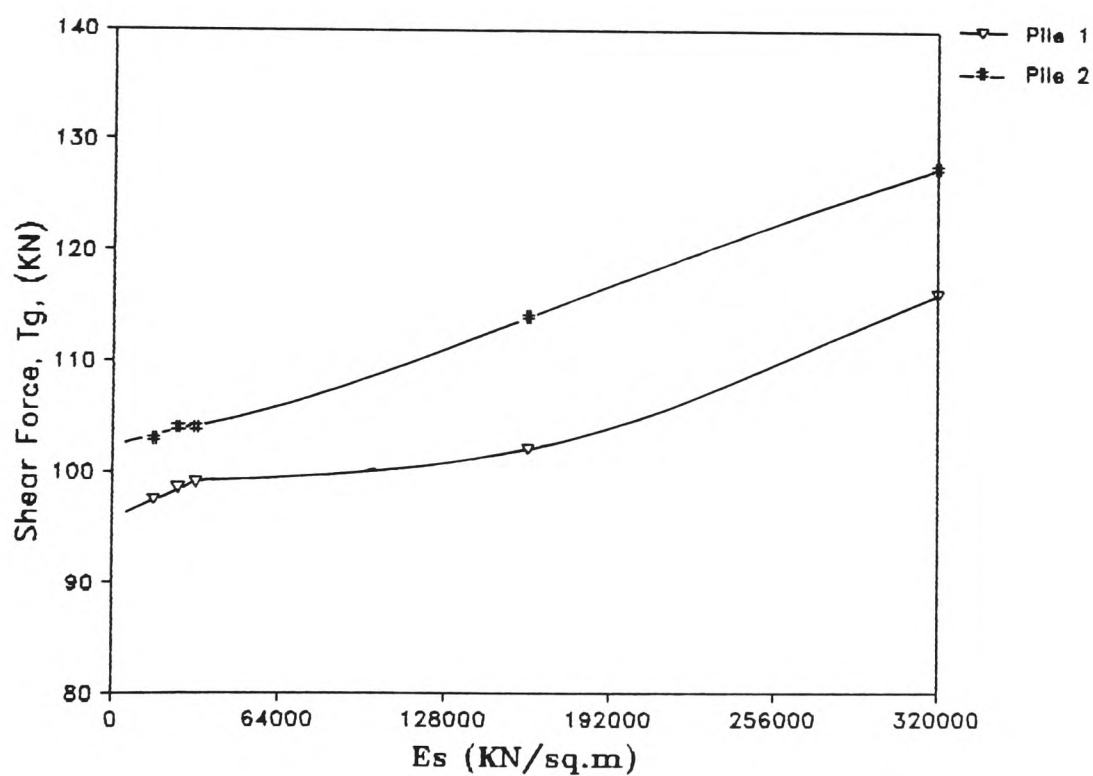


(b) Ratio of shear forces at the pile head.

Figure 3.7.: Distribution of loads against E_s for vertical loading.

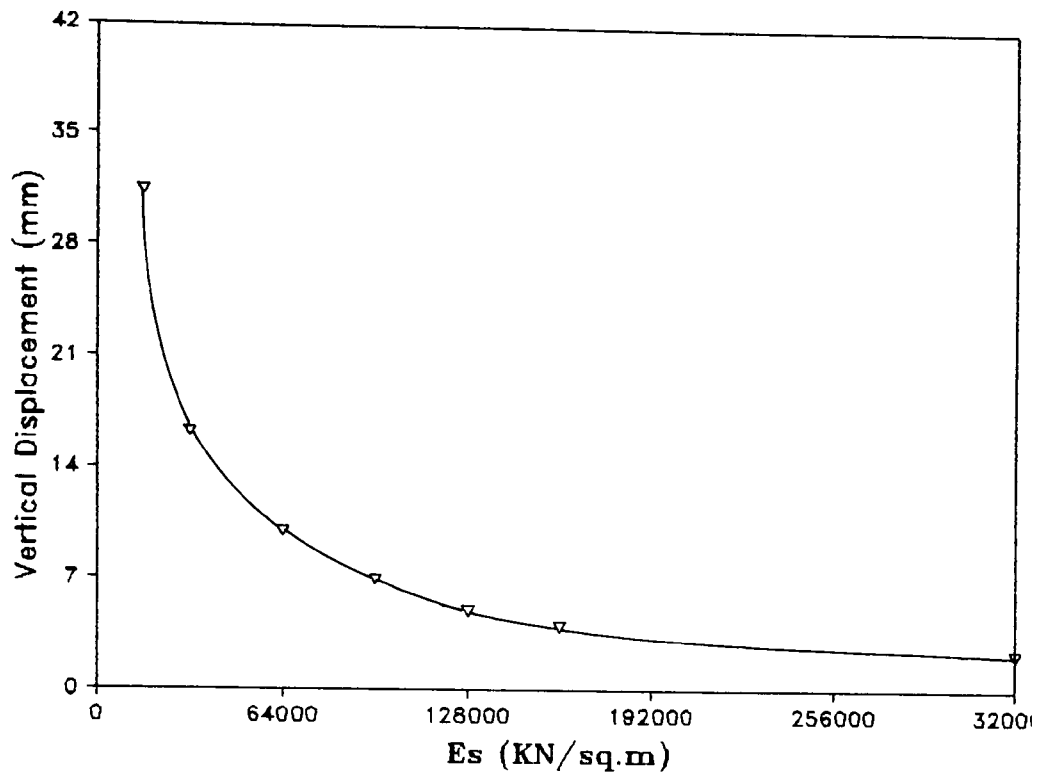


(a) Ratio of axial loads at the pile head.

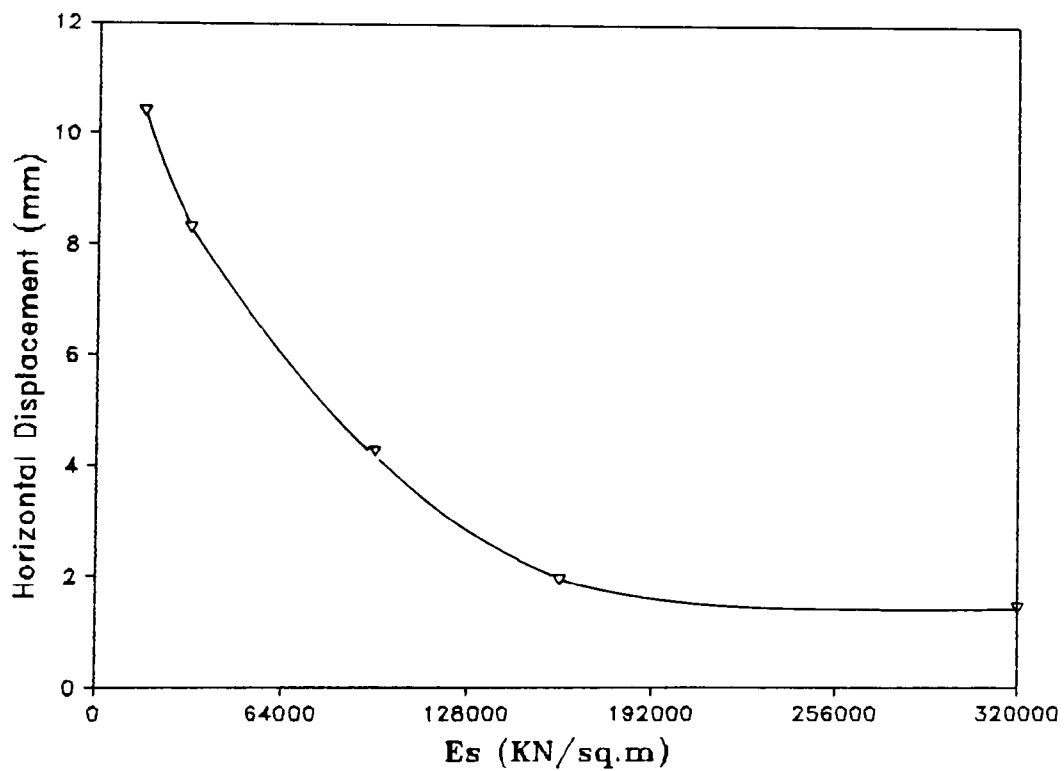


(b) Ratio of shear forces at the pile head.

Figure 3.8.: Distribution of loads against E_s for horizontal loading.

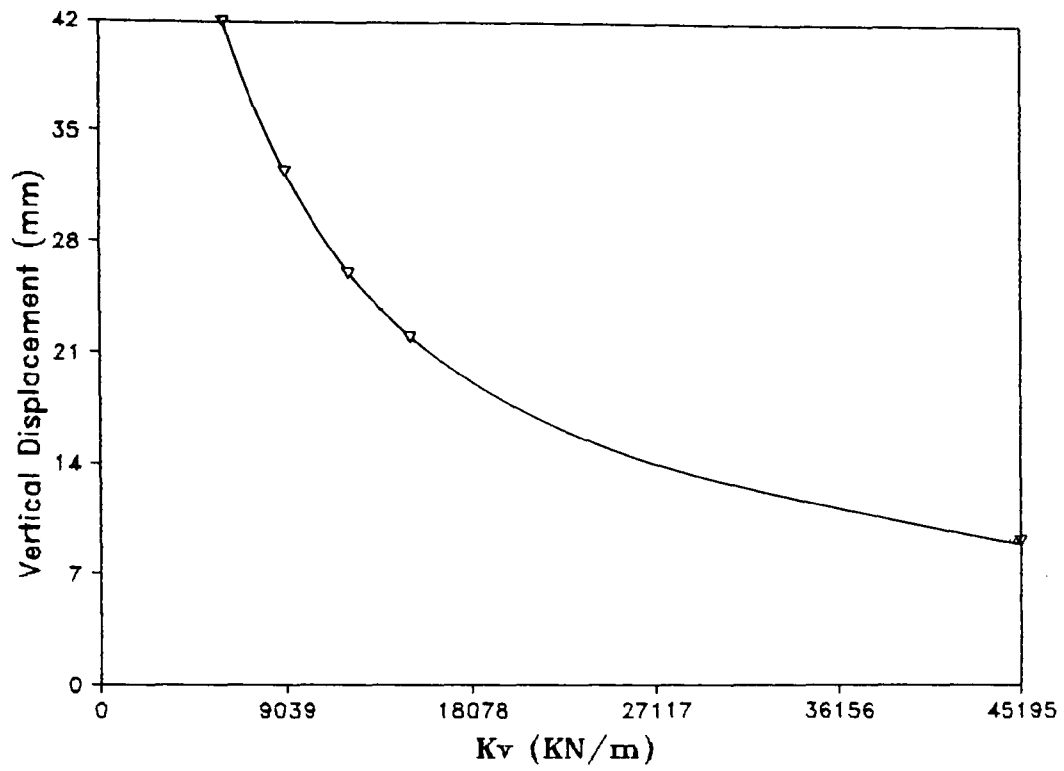


(a) For vertical loading.

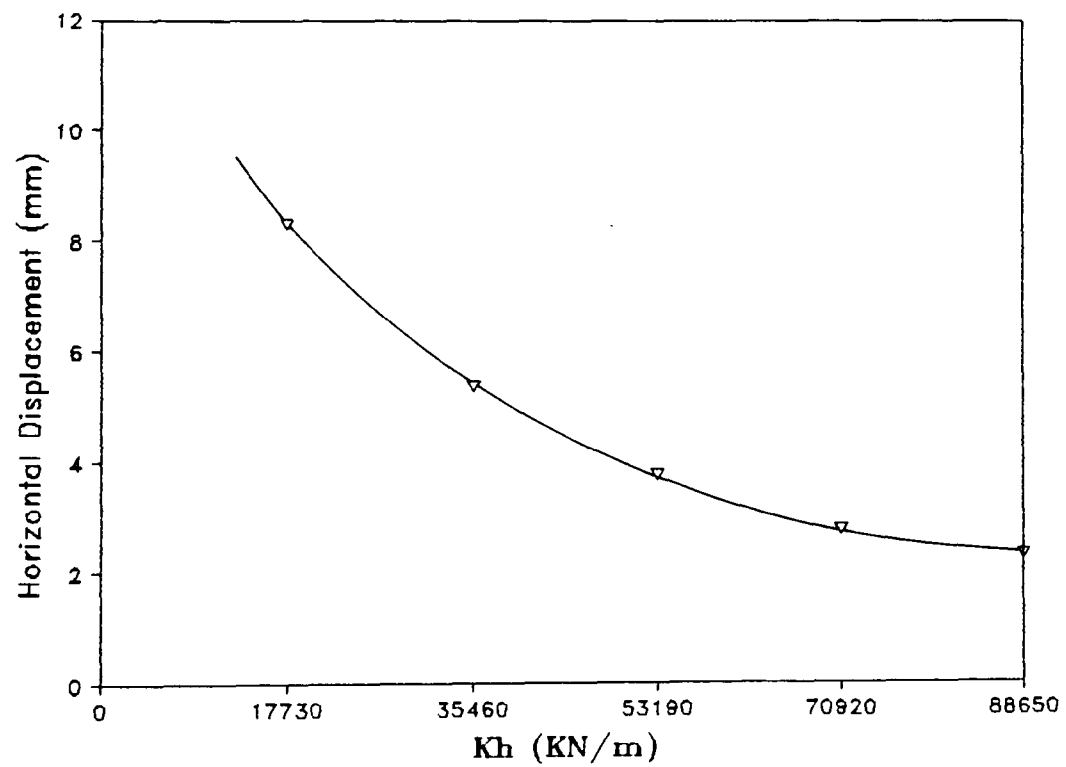


(b) For horizontal loading.

Figure 3.9.: Displacement against E_s .

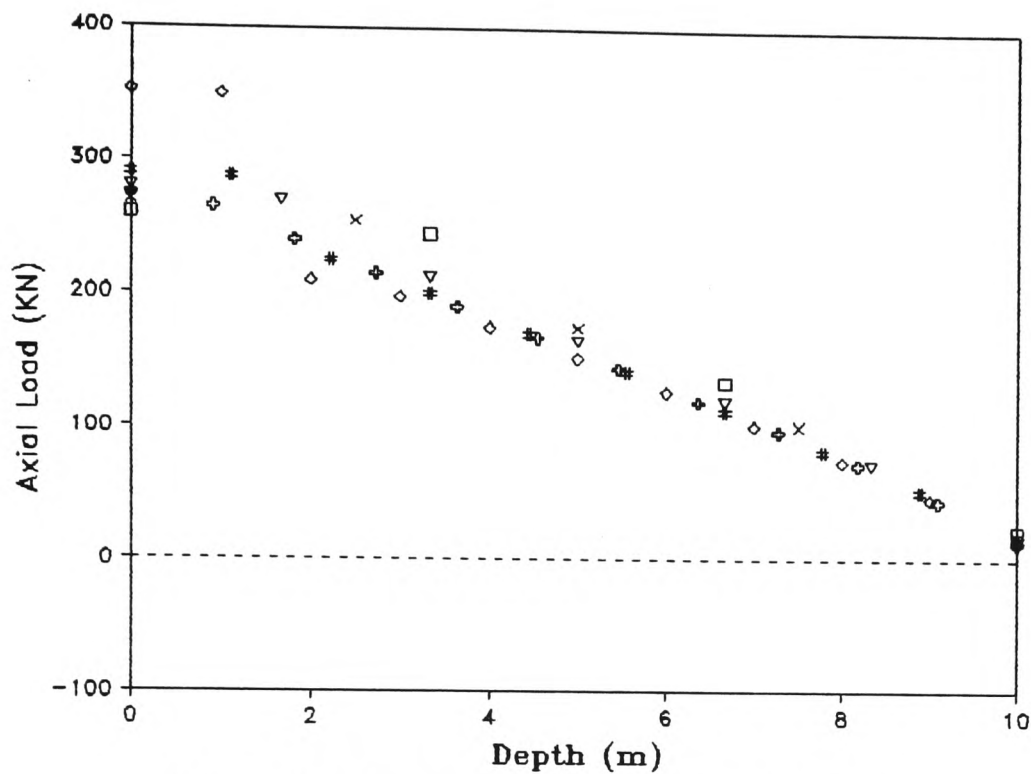


(a) For vertical loading.

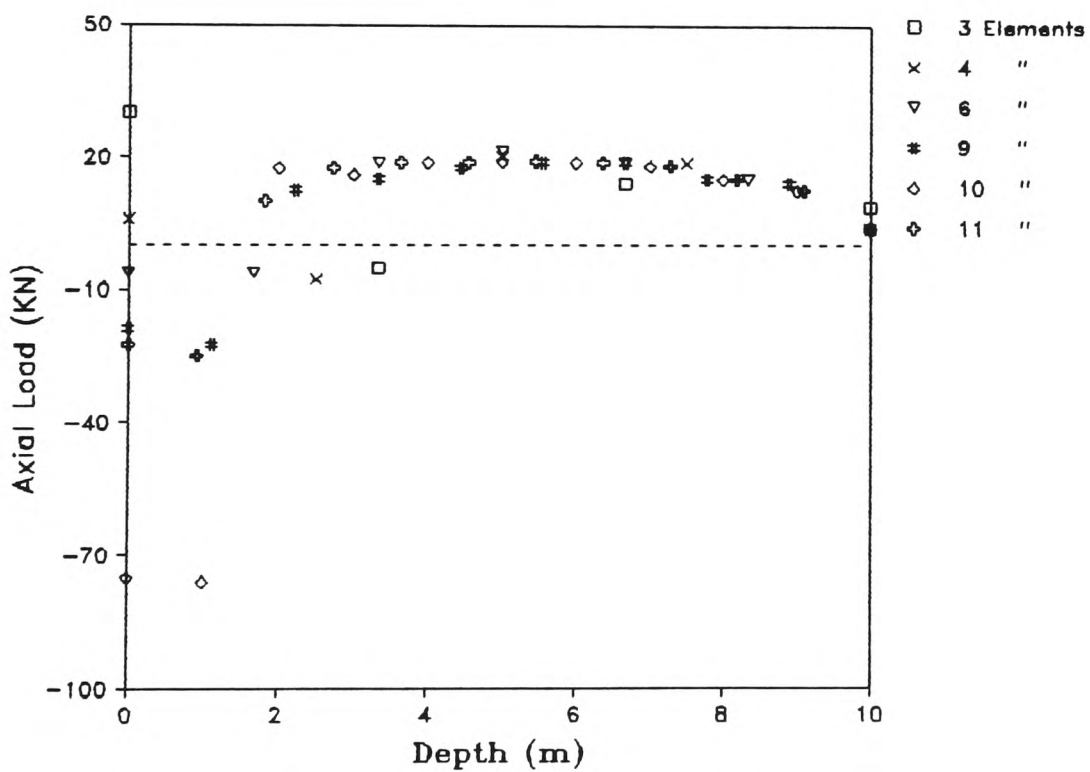


(b) For horizontal loading.

Figure 3.10.: Displacement against K_v and K_h .

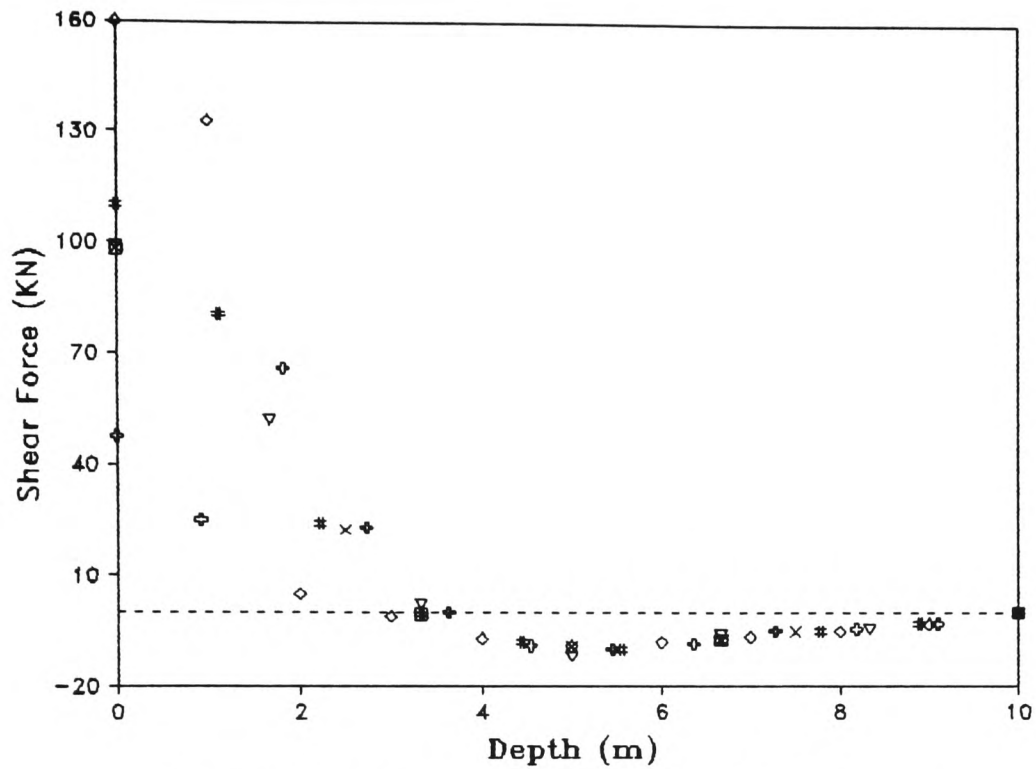


(a) Axial load distribution for Pile 1.

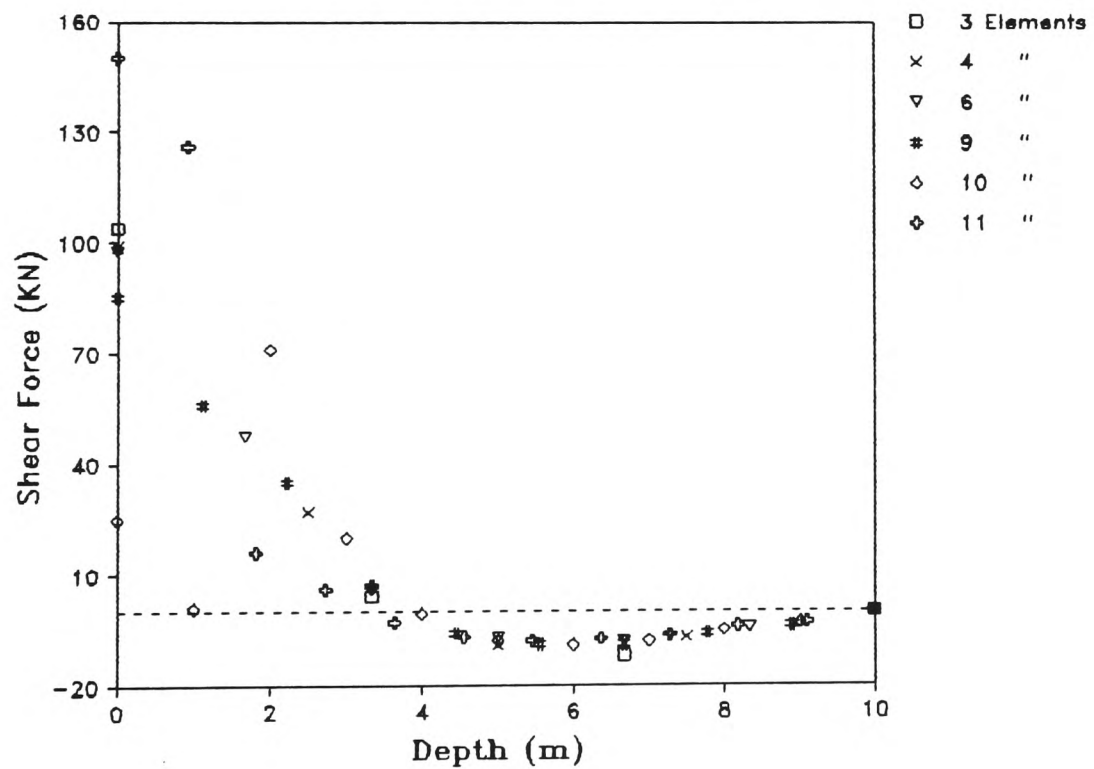


(b) Axial load distribution for Pile 2.

Figure 3.11.: Sensitivity of PGROUP axial load distribution to number of elements for horizontal loading.



(a) Shear force distribution for Pile 1.



(b) Shear force distribution for Pile 2.

Figure 3.12.: Sensitivity of PGROUP shear force distribution to number of elements for horizontal loading.

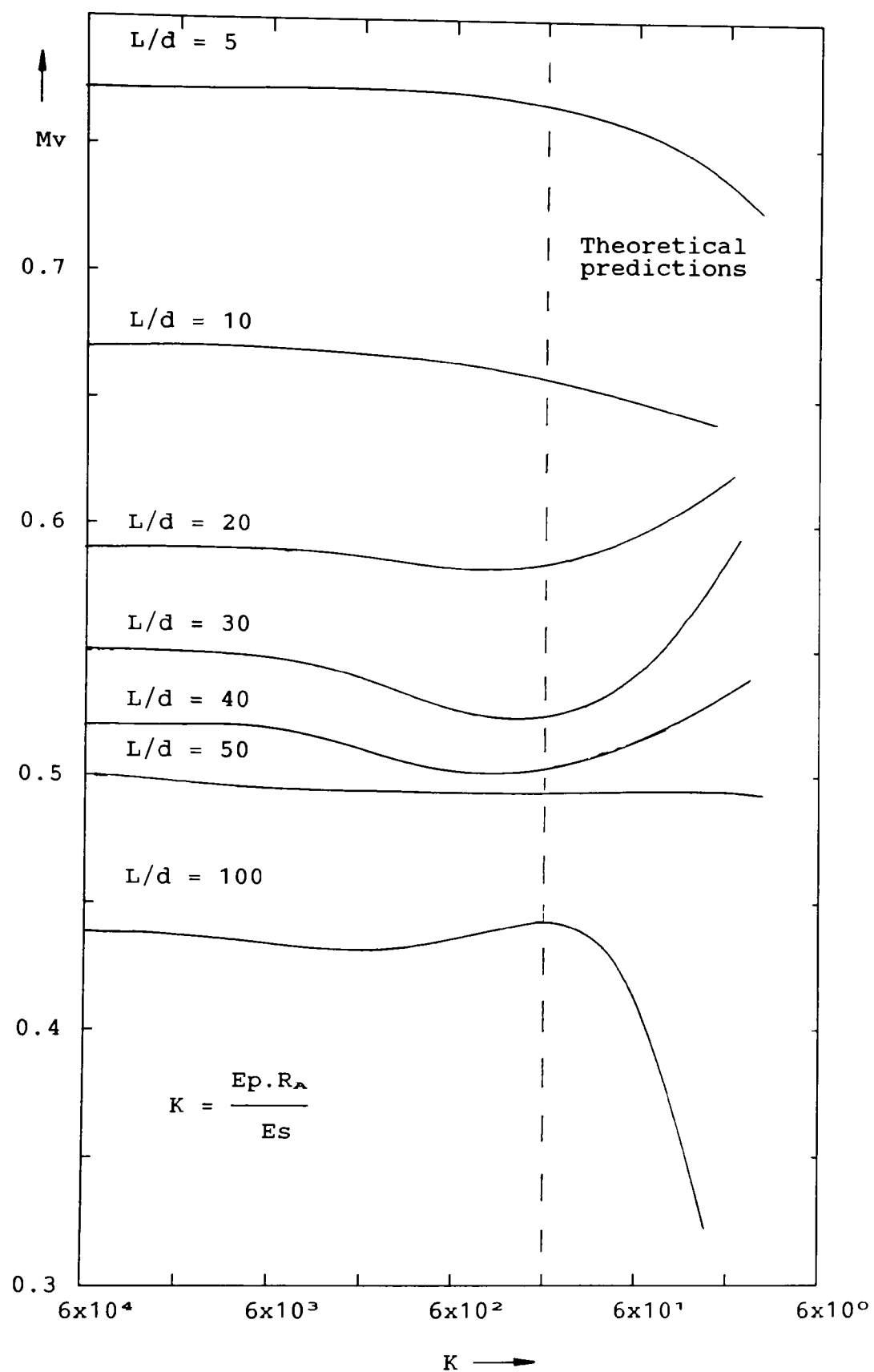


Figure 3.13.: Modification Factor M_v against K .

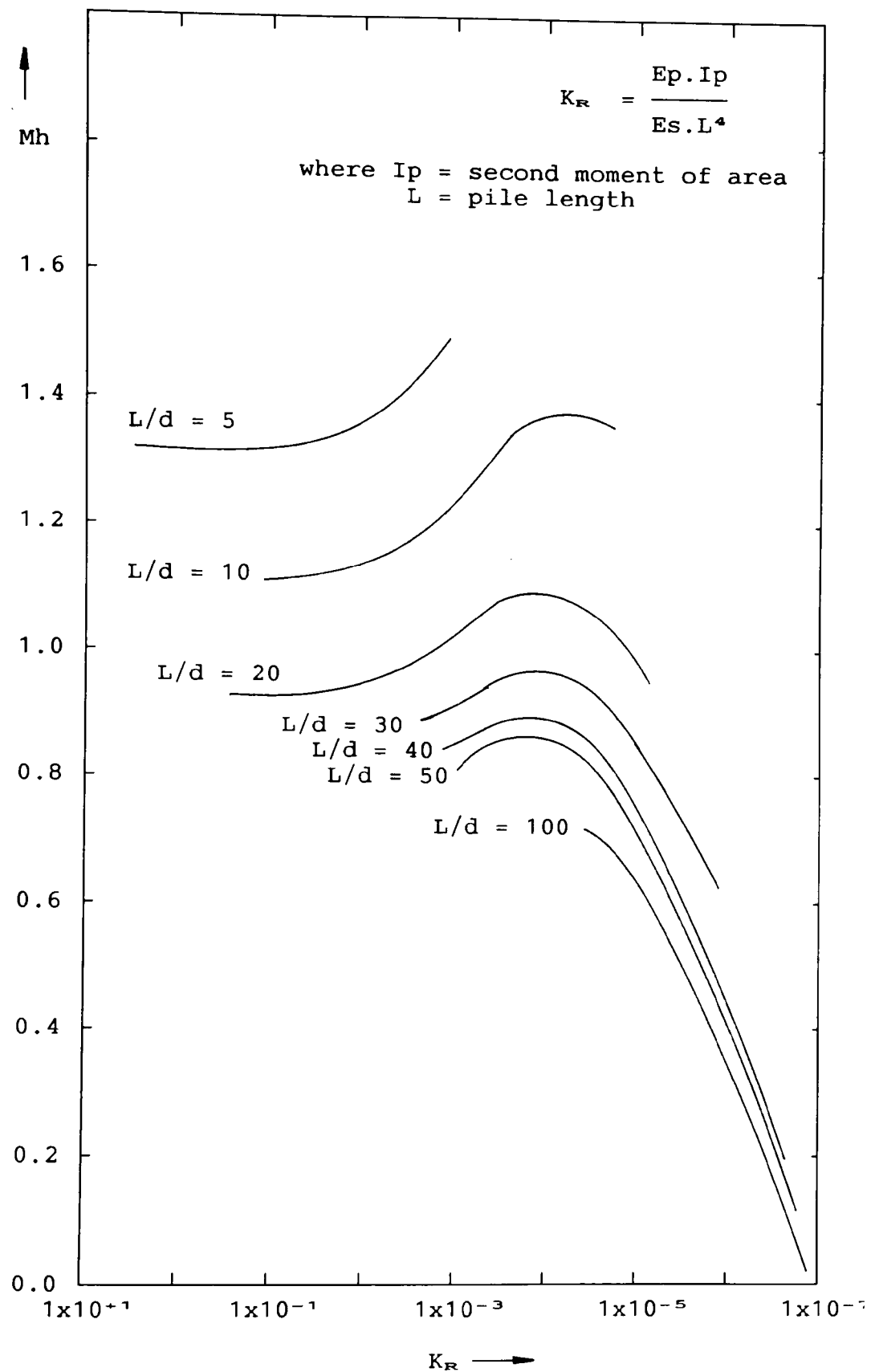


Figure 3.14.: Modification Factor M_h against K_R .

CHAPTER 4.

ANALYSIS OF PILES WITH NO GROUP INTERACTION.

4.1. INTRODUCTION.

Solutions determined by the proposed simplified method are compared with more rigorous analytical data, experimental and field results. The piles considered have L/d ratios between 20 and 50, relative axial stiffness values, K , from 0.3×10^6 to 60×10^6 and relative bending stiffness values, K_R , from 10^{-5} to 10^{-1} . These being the ranges over which the following simplified relationships were shown to be valid in Chapter 3.

$$K_v = E_s.L'/2$$

$$K_h = E_s.L'$$

The application of these relationships to general pile analysis is validated using the proposed S.S.R.T. method. This is achieved by analysis of the experimental and field data used to verify the PGROUP analysis and reported in the PGROUP User Manual. Comparisons are made with both the measured behaviour and PGROUP solutions. Finally, the proposed method is used to analyse an instrumented piled bridge abutment and associated pile loading tests. The results computed by the proposed S.S.R.T. method are compared to the measured performance, PGROUP results and data from a number of other simplified analyses of the piled abutment.

4.2. COMPARISON OF RESULTS.

4.2.1. General.

In order to validate the PGROUP results, comparisons were made with the measured performance of a variety of

single piles and pile groups under various loading conditions. Both the experimental data and the analytical results reported by the PGROUP authors are compared with results computed using the proposed S.S.R.T. method. The graphs presented in the PGROUP User Manual are reproduced here. The PGROUP results were determined by adopting 6 elements per pile and Poisson's Ratio of the soil μ as 0.5. For piles without group interaction μ is not required for the S.S.R.T. analysis.

The pile element lengths are reduced locally to determine S.S.R.T. results in critical regions. This is not possible with the PGROUP program where the elements must be of equal length. To obtain results in critical regions the PGROUP program subdivides the whole pile into a greater number of elements.

Comparison of results for pile performance in each case is at an applied loading of half the ultimate value.

The reported results are not generally in S.I. units since they are presented in their original form.

4.2.2. Field Results Of Reese and Cox.

Reese and Cox (1969) conducted full scale tests on laterally loaded hollow aluminium tube piles driven into a silty clay. The significant parameters are listed below:

Shear Strength of soil at ground level (Unconfined compression test)	= 0.2 kgf/cm ²
Increase in strength with depth	= 3.0×10^{-4} kgf/cm ² /cm
Length of pile (L)	= 5.30m
Depth of soil layer	= 13.0m

Outer diameter of pile	= 0.3m
Inner diameter of pile	= 0.2936m
Modulus of pile material (E_p)	= 5.3×10^9 kgf/m ²

The measured performance of two test piles, Nos. 7 and 8, are compared to analytical results from PGROUP and the S.S.R.T. in Figure 4.1.. The PGROUP results were computed using a Gibson soil model where the soil modulus profile with depth $E(z)$ is of the form $(E_0 + mz)$. E_0 is the soil modulus at the ground surface and m is the rate of increase of modulus with depth z . By taking the ratio of E_s/C_u as 350, values of $E_0 = 0.7 \times 10^6$ kgf/m² and $m = 0.2 \times 10^6$ kgf/m²/m were used for the PGROUP soil idealization. These parameters were converted to spring stiffness values for use in the S.S.R.T. analysis. The S.S.R.T. pile idealization comprised element lengths of $L/24$ for the upper third, $L/12$ for the middle third and $L/6$ for the lower third of the pile shaft. This produced 15 pile elements including the single element above ground level.

The S.S.R.T. results were approximately double those presented in the PGROUP User Manual. When this pile idealization was analysed using the PGROUP program the computed displacements and rotations were found to be double the values presented in the Manual. This suggested an error in the scales reported by the PGROUP authors. The graphs reproduced in Figure 4.1. have their displacement and rotation axes magnified by a factor of 2.

Having made the necessary modifications, the linear load-displacement relationships from PGROUP and the S.S.R.T. agreed satisfactorily with the measured field

results. Excellent agreement was achieved on comparing the PGROUP and S.S.R.T. displacement and rotation results.

4.2.3. Field Results Of Alizadeh.

Alizadeh (1969) carried out four full scale load tests on tapered timber piles driven into a silty clay. The necessary details of the tests are given below:

Average undrained shear strength (C_u) = 4.50 lbf/in^2

Average diameter of the pile heads = 1.04ft.

Average diameter of the pile bases = 0.84ft.

Average length of piles = 36.6ft.

Pile modulus of elasticity (E_p) = $2.2 \times 10^6 \text{ lbf/in}^2$

The measured field results are compared to those determined from PGROUP and the S.S.R.T. in Figure 4.2.. The PGROUP results were computed by taking the ratio of E_s/C_u as 110, giving a value for E_s of 500 lbf/in^2 . The pile analysed by PGROUP comprised a constant shaft and base diameter of 1ft.. This simplification was not necessary for the S.S.R.T. analysis. The second moment of area of each pile element was determined from the average diameter of each element. For direct comparison with PGROUP results a constant pile diameter was also analysed.

The sensitivity of the PGROUP results to changes in the soil modulus are presented in Table 4.1.(a). Better agreement with measured values of displacement, rotation and maximum bending moment was achieved using the Gibson soil rather than the homogeneous soil model.

The S.S.R.T. results presented in Figure 4.2. and case (iii) in Table 4.1.(b) were computed for a pile of constant diameter of 1ft. embedded in an homogeneous soil

with an E_s of 500 lbf/in². The pile element mesh was graded as follows:

elements 6" in length for 0-10ft.

elements 12" in length for 10-15ft.

elements 36" in length for 15-24ft.

elements 72" in length for 24-36ft.

The displacement and rotation results from the S.S.R.T. analysis presented in Figures 4.2.(i) and (ii) were consistently lower than both PGROUP and measured field values. The distribution of the ratio of the moment in the pile to the applied lateral load, M/P , with depth is presented in Figure 4.2.(iii). The maximum M/P test value was 2.3 compared to 2.7 from PGROUP and 3.66 from the S.S.R.T.

S.S.R.T. results for various pile idealizations are presented in Table 4.1.(b). As the pile element lengths were graded finer, both the pile head displacement and M/P ratio increased. This resulted in a better agreement with the measured pile displacement but an overestimate of the M/P value. S.S.R.T. results for the tapered pile with a coarse element mesh were relatively poor. This indicated that an adequately graded pile element mesh was more important than an accurately modelled pile taper, in this instance.

4.2.4. Field Results Of McClelland and Focht.

McClelland and Focht (1956) carried out a full scale test on a 24in. circular pile driven into the sea bed. The

details of the test are given below:

Total length of pile	= 81ft.
Embedded length of pile (L)	= 75ft.
Diameter of pile (D)	= 2ft.
Flexural rigidity ($E_p I_p$)	= 1.62×10^{11} lbf.in ² .
Horizontal load at the pile head (H)	= 6.0×10^4 lbf.
Applied moment at the pile head (M)	= -6.0×10^6 lbf.ft.

The clay layer extended to a depth of 146ft. below the mudline which was submerged beneath 33ft. of water. Laboratory tests of subsoil samples indicated a near linear increase in shear strength with depth from a value of 1.6 lbf/in² at the sea bed level to 10.1 lbf/in² at a depth of 40ft..

The results of several PGROUP analyses using the Gibson model ($E(z) = E_0 + mz$) and the two layer (E_0, E_1) soil model are shown in Table 4.2.(a). The results for a homogeneous soil with $E_0 = 400$ lbf/in² are shown in Figure 4.3.. The distribution of moment with depth from the S.S.R.T. analysis agrees satisfactorily with that computed by the PGROUP program. Both analytical methods underestimated the measured maximum moment, possibly due to the soil model not being an appropriate idealization.

Although the measured shear strength increased linearly with depth, several PGROUP analyses were carried out using the two layer soil model, because the measured bending moment distribution indicated that very little resistance was afforded by the upper 15ft. of subsoil. This is indicated by the PGROUP results presented in Table 4.2.(a). where changes in E_0 for the top 15ft. of soil had a significant effect on the horizontal displacement and the

maximum bending moment. Furthermore a 100% increase in the stiffness of the lower layer caused only a small change in the overall behaviour of the system. Although the solution with E_0 equal to 300 lbf/in² and E_1 of 6000 lbf/in² provided one of the best fits with the experimental results, the PGROUP authors stated "the value of E_1 is probably too unrealistic for the lower layer".

The corresponding S.S.R.T. results are presented in Table 4.2.(b). As in the PGROUP analyses, homogeneous, Gibson and two layer soil models were considered.

The effect on the S.S.R.T. results of using a finer grade mesh representation for the pile was investigated for the homogeneous soil. Table 4.2.(b). indicates that the effect of reducing the element lengths over the upper two thirds of the pile shaft from $L/6$ to $L/12$ is minimal for a homogeneous soil with $E_0 = 400$ lbf/in². The agreement with the corresponding PGROUP values for pile head displacement and maximum bending moment was shown to be poor. When the upper third of the pile shaft was further refined to $L/24$ the accuracy of the pile head displacement improved substantially to within 16% of the PGROUP value. The computed bending moment curve was also similar to that determined by PGROUP. It is therefore concluded that a graded mesh representation, with approximate element lengths of $L/24$, $L/12$ and $L/6$ over the upper, middle and lower third of the pile shaft respectively, is required to determine satisfactory results for a laterally loaded pile using an S.S.R.T. analysis.

A parametric study was also carried out for the S.S.R.T. analysis using the two layer soil model in order

to investigate the effect of a variation in soil stiffness for the upper and lower layers. From these studies the same conclusions were reached as those of the PGROUP authors. The upper 15ft. having a significant effect on the overall behaviour of the system, with the behaviour being relatively insensitive to a variation in stiffness of the lower layer.

4.2.5. Field Results Of Alizadeh and Davisson.

Alizadeh and Davisson (1970) conducted several full scale tests on laterally loaded single piles driven in sand. The necessary details of the test are:

Length of piles = 40-55ft.

Diameter or width of piles = 14-20in.

Flexural rigidity ($E_p I_p$) = $3-81.0 \times 10^9$ lbf.in²

Coulomb friction angle (ϕ) = 31°-35°

The authors of PGROUP (1981) contended that although sand is not an elastic material its behaviour can be characterized by a "pseudoelastic" modulus whose magnitude is proportional to the in situ effective stresses. They stated:

"Due to the absence of reasonable alternatives and as a consequence of the consistent results obtained herein, this assumption seems to be justified."

The measured field data, S.S.R.T. and PGROUP results for the lateral load required to produce a 0.1in. displacement plotted against $E_p I_p$ values are presented in Figure 4.4.(i). Both the PGROUP and S.S.R.T. results were determined using the following parameters.

Length of piles (L) = 45ft.

Diameter (d) = 16in.

Young's modulus of piles (E_p) = varied from 1.5×10^6
to 3.2×10^7 lbf/in².

E_0 = 0

m = 30 to 70 lbf/in²/in.

The S.S.R.T. results were computed using 10 elements of equal length to model the pile. The spring stiffness values were again determined by multiplying the soil modulus value at the nodal points by the appropriate element length.

The test results presented in Figure 4.4.(i) show a scatter of $\pm 20\%$ due to variations in length, diameter and soil properties over the site.

Both the S.S.R.T. and PGROUP analyses determined smooth curves for three different values of E_s . The results show the lateral load required to produce a pile head lateral displacement U_0 of 0.1ins. increasing as $E_p I_p$ increases. The agreement between the PGROUP and S.S.R.T. results is encouraging over a wide range of stiffness values for the piles. The S.S.R.T. slightly overestimating the load required to produce a displacement of 0.1ins. at low values of $E_p I_p$ and underestimating the load at high values of $E_p I_p$. The S.S.R.T. results were computed using a Modification Factor M_h of 1, whereas, as shown in Figure 3.14. of Chapter 3, M_h decreases as $E_p I_p$ decreases. By using a lower M_h value the soil stiffness would reduce, requiring a lower load for a specified displacement. Hence, by using a more accurate value of M_h better agreement between the S.S.R.T. and PGROUP results can be expected.

Figure 4.4.(ii) shows the corresponding results for the distribution of $M(z)/H$ against depth, where $M(z)$ is the

bending moment at a depth z and H is the applied lateral load at the pile head. There is good agreement between PGROUP and the measured field results. However, it is unclear which value of $E_p I_p$ the authors had used. S.S.R.T. results are also plotted for $E_p = 3.2 \times 10^6 \text{ lbf/in}^2$ and $d = 15 \text{ ins.}$. The distribution of $M(z)/H$ with depth from the S.S.R.T. analysis is similar in shape to that of PGROUP and the measured field results. The maximum value of $M(z)/H$ from the S.S.R.T. analysis overestimates the PGROUP value by 11% and the measured field value by 8%. The $M(z)/H$ distribution was sensitive to changes in the value $E_p I_p$. For $E_p I_p$ values of 102.9×10^9 and $2.8 \times 10^9 \text{ lbf.in}^2$, the maximum values of $M(z)/H$ from the S.S.R.T. analysis were 4.61 and 2.78ft. respectively.

Tables 4.3.(a) and (b) show the effect of various pile-soil idealizations on the maximum values of $M(z)/H$ from the PGROUP and S.S.R.T. analyses respectively. The S.S.R.T. results were computed using element lengths of $L/6$ for the lower third and $L/12$ for the upper two-thirds of the pile shaft, giving a total of 10 elements. This mesh grading for the pile is now considered to be slightly too coarse. Although, the S.S.R.T. maximum values for $M(z)/H$ were generally greater than the PGROUP values, the S.S.R.T. results indicated $M(z)/H$ to be sensitive to changes in m and insensitive to changes in E_p .

4.2.6. Test Results Of Davisson And Salley.

Davisson and Salley (1970) carried out a series of small scale tests on a single model aluminium pipe pile embedded in sand.

The test details are as follows.

Length of pile and embedded length (L)	= 21in.
Outer diameter of pile (d)	= 0.50in.
Inner diameter of pile (di)	= 0.44in.
Depth of soil	= 48in.
Coulomb friction angle (ϕ)	= 35°

The pile head was subjected to a lateral load of 4 lbf and the distribution of bending moments along the shaft was measured. The comparison of the experimental moment distribution with those from S.S.R.T. and PGROUP analyses is presented in Figure 4.5.. The PGROUP and S.S.R.T. results were determined using the following parameters.

$$E_0 = 0$$

$$m = 40 \text{ lbf/in}^2/\text{in.}$$

$$E_p = 1.2 \times 10^7 \text{ lbf/in}^2.$$

The pile idealized by the S.S.R.T. comprised pile element lengths of $L/6$ over the lower half and $L/12$ over the upper half of the pile shaft, giving a total of 9 elements.

The agreement between the moment distribution computed from both analyses and the measured test values was good. However, both analytical methods tended to shed the moment into the soil too rapidly after the maximum moment had been attained in comparison to the test results.

4.2.7. Field Results Of Mansur And Hunter.

Mansur and Hunter (1970) carried out a series of full scale tests on axially loaded single steel pipe piles driven in sand.

The necessary details of the test are:

Outer diameter of pile = 16in.
Flexural rigidity = 2.1×10^{10} lbf.in²
Length of pile = 55ft.
Coulomb friction angle = 35°

Figure 4.6. shows the comparison between the PGROUP, S.S.R.T. and the test results. Only one axial load distribution at an applied load of 100 Tons is shown for clarity. The agreement between results for the 50 and 150 Tons tests was also good. The PGROUP and S.S.R.T. results were determined using $E_0 = 0$ and $m = 40$ lbf/in²/in and six elements of length $L/6$ to idealize the pile.

The soil spring stiffness value K_v used in the S.S.R.T. analysis was taken as $E_s L/2$ as proposed in Chapter 3. The agreement between the S.S.R.T., PGROUP and measured axial load distributions was excellent.

The agreement between the displacements determined by the S.S.R.T. and PGROUP was good. At a load of 100 Tons the displacements computed by PGROUP and the S.S.R.T. were 1.30 and 1.45ins. respectively, which represents a 11% difference. This confirms the validity of the simple relationship between K_v and E_s .

4.3. INSTRUMENTED BRIDGE ABUTMENT.

4.3.1. General.

Results determined from the proposed S.S.R.T. method are compared to the measured performance of a piled bridge abutment at Newhaven and associated pile loading tests, as reported by Reddaway and Elson (1982). The pile foundation comprises three rows of piles. A section through the

abutment and the general pile arrangement are shown in Figure 4.7. The front and middle row of piles are raked forward at an angle of 1 in 5 and the rear row are raked backward at an angle of 1 in 10. The foundation was constructed using West's Hardrive segmental reinforced concrete piles. These have a 285mm square section and were installed in 10m lengths to a nominal depth of 40m.

The general substrata at the foundation location comprised approximately 12.6m of alluvium overlying 10m of gravel which is underlain by a weathered chalk. The foundations were piled to the underlying chalk. At the design stage it was recognised that the settlement of the overlying alluvial could cause downdrag forces to develop within the piles. Hence, it was considered necessary to establish reasonable parameters for the design of the piled raft. For this purpose, an instrumentation programme was carried out to measure the actual loads carried by the piles. In addition to this, two piles were load tested; one with its shaft slipcoated with bitumen through the overlying alluvium; and one uncoated.

4.3.2. Pile Load Tests.

(a) Load Test On Pile 121 (Uncoated).

As it was difficult to prevent bending of the pile head, this raked pile was only loaded to the Design Load of 1100KN. The results of the pile load test are presented in Figure 4.8.. At the Design Load, approximately 400KN was transferred to the alluvial deposits and only 200KN to the chalk. The report estimated the average ultimate adhesion values in the alluvium and gravel to be 26KN/m^2 and 86KN/m^2

respectively. A summary of the adhesion values calculated from short term pile load tests is reproduced in Table 4.4.

The report authors computed the pile head displacement from the measured load distribution by considering the pile as an elastic member founded in an elastic continuum. Their computed displacement of 6mm "compares reasonably well" with the measured value of 7.5mm presented in Figure 4.8.(ii). For these calculations they assumed the elastic modulus of the pile-remoulded chalk system to be between 250MN/m^2 and 500MN/m^2 , the axial flexibility of the pile was measured as 0.382 microstrain/KN. They did not present modulus values for the alluvium and gravel. Because the load-displacement relationship along the pile shaft was not recorded, these values could not be accurately determined.

(b) Load Test On Pile 122 (Slipcoated).

The pile was slipcoated with bitumen over the upper 10.75m of the pile. This approximately represented the thickness of the alluvium layer. The load test results are presented in Figure 4.9.. The test was terminated at a load of 1550KN due to a compression failure of the pile head. The authors stated that this was "because of inevitable eccentric loading on the raking pile".

The load distribution along the shaft of Pile 122 was similar to that of Pile 121, except that the adhesion of the pile in the alluvium was reduced due to slipcoating. The authors estimated the average ultimate adhesion of the pile in the alluvium and gravel to be 6KN/m^2 and 60KN/m^2 respectively.

The measured load-displacement behaviour of Pile 122 presented in Figure 4.9.(ii) indicates the pile-soil system was less stiff than that of Pile 121. The authors attributed the increased short term settlement of 11.5mm to the lower adhesion of the slipcoat-alluvium interface.

4.3.3. S.S.R.T. Results Of Pile Load Tests.

(a) General.

Several S.S.R.T. analyses of the pile loading tests were carried out using assumed soil modulus, E_s , values. It was necessary to assume E_s values because these were not readily determined from the pile loading test data. For a given value of E_s the axial and lateral subgrade reaction stiffness values, K_v and K_h , were taken as $E_s.L'/2$ and $E_s.L'$ respectively, where L' is the pile element length.

The S.S.R.T. pile idealization comprised 5 elements in the alluvium, 4 elements in the gravel and 3 elements in the chalk.

(b) Pile 121 (Uncoated).

The S.S.R.T. displacement results for this pile are presented in Table 4.5.. Reddaway and Elson (1982) assumed that the elastic modulus of the pile-remoulded chalk system was 250MN/m^2 to 500MN/m^2 . Hence in these comparisons the same E_s values for the chalk were used and the values of E_s for the overlying layers varied.

The results presented in Table 4.5. indicate that the displacement was overestimated by 90% when the assumed value of E_s was equal to the estimated adhesion C_a ie. an E_s/C_a value of 1.

The best agreement between the measured field displacement of 7.5mm as computed by the S.S.R.T. was 5.5mm. This was achieved by taking the E_s of the alluvium and gravel as 26MN/m^2 and 86MN/m^2 respectively ie. an E_s/C_a value of 1000. The S.S.R.T. load distribution curve for case (i) in Figure 4.8.(i) indicates that the magnitude of load transferred was too high to the alluvium and too low in the gravel. This implies that the E_s value of 26 MN/m^2 for the alluvium was too high and 86 MN/m^2 for the gravel was too low. The results suggest that the E_s values are not proportional to the estimated C_a values. The load distributed into a layer depends on its stiffness relative to the other layers. The adhesion values are not constant material parameters which can be applied to general systems.

The S.S.R.T. curve for case (ii) was determined using an E_s value of 5MN/m^2 for both the alluvium and gravel. The load distribution curve indicates these values to be too low as reflected by the low magnitude of load transferred into these strata. The inability to accurately model the load distribution and pile displacement may be due to the E_s value suggested for the weathered chalk being too high. This caused the displacement of the pile to be relatively insensitive to variations of E_s in the upper layers. There were too many unknown variables to readily define soil parameters to satisfactorily model the pile-soil behaviour.

The short term pile test results indicate that initially 36% of the applied load was transferred to the alluvium, 45% to the gravel and 18% to the chalk. However,

the behaviour of the piles in service showed that at the end of construction the whole of the axial load at the pile head was transferred to the chalk. It may therefore be more appropriate to analyse the long term behaviour, provided realistic soil parameters can be determined.

(c) Pile 122 (Slipcoated).

The same procedure used for the analysis of Pile 121 was adopted for this pile ie. the E_s value of the chalk was taken as 250MN/m^2 to 500MN/m^2 and the E_s values of the overlying soils varied.

The S.S.R.T. results are presented in Table 4.6. Initially the E_s/C_a value was taken as 1 giving E_s values of 6KN/m^2 and 60KN/m^2 in the alluvium and gravel respectively. Although, Piles 121 and 122 were only 1.2m apart, the calculated adhesion in the gravel was reduced from 86 to 60KN/m^2 when the pile was slipcoated through the alluvium. An S.S.R.T. analysis with E_s values of 6KN/m^2 , 60KN/m^2 and 250MN/m^2 for the alluvium, gravel and chalk respectively, gave a pile head displacement of 12.0mm in comparison with the measured test displacement of 11.5mm. However, when the E_s of the chalk was doubled from 250 to 500MN/m^2 the displacement was only reduced by 0.2mm. Therefore the S.S.R.T. displacement of 12mm was almost entirely due to the axial shortening of the pile; the displacement at the toe of the pile was 0.067mm and the displacement at the gravel-chalk interface was less than 1mm.

Results were also computed for an E_s/C_a value of 1000, giving E_s values for the alluvium and gravel of

6MN/m^2 and 60MN/m^2 respectively. This set of results is denoted as case (i) in Figure 4.9. The calculated pile head displacement at the Design Load of 1100KN was 8mm which was 30% lower than the measured test displacement. As presented in Figure 4.9.(i) for case (i), the load transferred to the base of the pile was underestimated by over 150%, which indicates that the assumed pile-soil system was too stiff.

The set of results denoted by case (ii) in Figure 4.9. represent a soil model having E_s values of 6KN/m^2 and 60MN/m^2 in the alluvium and gravel respectively. The load transferred to the alluvium was in good agreement with the test results. Although the rate of load transfer was too rapid within the chalk, the curve was of the same general shape as that of the test. This indicates that the assumed E_s value of the chalk was too high.

It is concluded, that provided realistic E_s values can be determined, the S.S.R.T. can adequately model load transfer and subsequent displacement of a pile embedded in a multi-layered soil up to working load. Inspection of the results indicate that E_s for the alluvium-bitumen interface lies between 6KN/m^2 and 6MN/m^2 , E_s for the gravel-pile interface is about 60MN/m^2 and E_s for the weathered chalk-pile interface is less than 250MN/m^2 .

4.3.4. Load Distribution Within The Pile Cap.

The earth pressure acting on the abutment was not recorded. Hence, the actual load on the pile cap was not known and no direct comparisons could be made. However, assumed load cases were correlated with the total vertical

load measured in the foundation. The pile load distribution for the load case of the completed bridge with a rectangular block of PFA resting on the pile cap are reproduced after Reddaway and Elson (1982) in Table 4.7.(a)

The summation of the three observed pile loads was 970KN on the 27:7:77, whilst that of the computed pile loads was generally 770KN. This implies that the imposed load used in the calculations should be 200KN greater for each set of three piles. Hence, it is not practical to make direct comparisons of computed pile loads with observed pile loads. However, the relative distribution of pile loads within the cap can be studied.

Reddaway and Elson (1982) considered that the PGROUP analysis computed the most realistic pile group behaviour. However, Table 4.7.(a) shows that PGROUP overestimated the load in the front row of piles and underestimated the load in the rear row.

A plane frame analysis was also carried out where the piles were considered to be a series of elements supported by a rigid stratum. The lateral stiffness of the overlying soil was modelled by springs normal to the nodes of the elements. This is similar to the proposed S.S.R.T. method where, in addition, the vertical stiffness of the soil is represented by springs tangential to the elements. Thus, the proposed S.S.R.T. overcomes the need to assume a rigid stratum.

Reddaway and Elson (1982) stated that:

"the plane frame analysis also gave a reasonable estimate of the pile loads. However, the model would not predict the deformation of the pile group correctly because of its assumption of soil springs."

They did not present the plane frame deformation results caused by axial compression and bending of the piles. The resulting pile load distribution for the plane frame analysis was less varied than that provided by PGROUP. This is considered to approximate better with the measured distribution.

A series of analyses were carried out using the proposed S.S.R.T. method. Various soil moduli were assumed for the superficial deposits and chalk. The pile cap was modelled having a finite stiffness based on its thickness and also as effectively rigid. These investigations were undertaken in order to examine the sensitivity of the load distribution in the piles to these parameters. The S.S.R.T. results are presented in Table 4.7.(b).

The computed load distribution at the pile heads using the proposed method was insensitive to the variation of E_s for the strata overlying the chalk. Because the chalk had a high E_s value of 500MN/m^2 , the effect of idealizing it as a rigid stratum had a negligible effect on the load distribution. Furthermore, because the pile cap had a relatively high finite stiffness, the consequence of assuming it to be rigid was negligible in this case.

The load distributions computed by the proposed method are similar to that from the ordinary plane frame analysis presented in Table 4.7.(a). The proposed method computed values of load in the rear row of piles which were more representative of the observed values. The better agreement may have been due to more load being transferred to the rear row of piles as the front and middle row settled under load. By comparison of results in Tables

4.7.(a) and (b), the solutions from the proposed method generally agreed more favourably with the observed values in the three rows of piles than other analytical solutions. The proposed method computed a relatively high load in the front and rear row of piles high with a corresponding reduction in the middle row of piles. The pile load distribution from the proposed method was relatively uniform, which is consistent with the observed values.

4.5. DISCUSSION AND CONCLUSIONS.

The proposed S.S.R.T. method can satisfactorily determine the short term performance of laterally and axially loaded piles. The validity of simple relationships developed between spring stiffness values and the soil modulus was demonstrated. This was accomplished by comparison of results for axial load and bending moment distributions along the shaft and load-displacement characteristics of single piles. Good agreement was achieved between the results computed by the proposed method, short term test measurements and results from more rigorous methods of analysis.

To determine acceptable results for laterally loaded piles, it was demonstrated that it was imperative for the element length to be relatively fine, about 1/24th of the embedded pile length, especially over the upper third of the pile shaft. This is because the soil surrounding the pile shaft in this region offers considerable restraint to the lateral displacement of the pile and consequently has a significant effect on the overall behaviour of the system. The modelling of the behaviour of axially loaded piles is

not so sensitive to the grading of element lengths. It was demonstrated that six elements of equal length were adequate to define an axially loaded pile embedded in a Gibson soil.

The proposed method was also applied to the analysis of axially loaded piles embedded in a layered soil. It was demonstrated that provided realistic E_s values can be determined, the method can satisfactorily model the load transfer and subsequent displacement up to working load.

Results from the monitoring of a piled bridge abutment indicated the short term behaviour of pile load tests to be dissimilar to the long term performance of the piled raft. The load distribution within the substructure in the long term was relatively uniform in contrast to that computed by many available analytical techniques. The application of the proposed method to the analysis of the foundation provided a realistic load distribution within the pile heads. The load distribution from the proposed method was relatively uniform which was consistent with observations made in practice. Although displacement calculations for the pile group were not presented for comparison, the proposed method overcomes the necessity to support the pile tips by a rigid stratum as required by traditional simplified methods. This enables an assessment of both the vertical and horizontal group displacement to be made.

E(0) lbf/in ²	m lbf/in ² /in.	δ in.	Θ Rad.	(M/P)Max ft.	Comment
0	10	0.71	0.0133	2.20	G *
0	20	0.49	0.0109	1.85	G
0	30	0.40	0.0102	1.69	G
500	0	0.90	0.0150	2.70	H

Table 4.1.(a): PGROUP analysis of Alizadeh's test data.

E(0) lbf/in ²	m lbf/in ² /in.	δ in.	Θ Rad.	(M/P) Max ft.	Comment
500	0	0.88	0.011	1.21	H (i)
500	0	1.10	0.016	1.75	H (ii)
500	0	1.37	0.020	3.66	H (iii)
0	23.4	0.80	0.013	3.05	G (ii)
0	31.4	0.65	0.011	3.05	G (ii)

Table 4.1.(b): S.S.R.T. analysis of Alizadeh's test data.

Case	S.S.R.T. Idealization
(i)	Tapered pile-constant element length of 6ft.
(ii)	Tapered pile-upper 24ft. refined to 3ft.
(iii)	Uniform pile-upper 10ft. further refined to 6in.

Notation: G - Gibson soil
H - Homogeneous soil
* - Best fit results

E_o lbf/in ²	m lbf/in ² /in	E_1 lbf/in ²	δ in.	Max. B.M. 10 ³ lbf ft	Comments
-	-	-	1.20	360	Test
400	-	-	1.15	210	H
170	1.7	-	1.25	270	G
170	2.3	-	1.07	245	G
-	2.3	-	1.55	300	G
-	3.4	-	1.17	200	G
300	-	3000	1.34	280	2L
300	-	6000	1.23	300	2L
225	-	3000	1.58	340	2L

Notation: G - Gibson soil
H - Homogeneous soil
2L - Two layer soil

Table 4.2.(a): PGROUP analyses of McClelland and Focht's test data.

E_o lbf/in ²	m lbf/in ² /in	E_1 lbf/in ²	δ in.	Max. B.M. 10 ³ lbf ft	Comments
-	-	-	1.20	360	Test
400	-	-	0.66	479	H(i)
400	-	-	0.67	495	H(ii)
400	-	-	1.33	189	H(iii)
218	-	-	1.21	480	H(i)
222	-	-	1.21	496	H(ii)
74	0.74	-	1.21	851	G(i)
0	2.58	-	1.12	1065	G(i)
330	-	610	1.32	260	2L(i)
330	-	1220	1.26	282	2L(i)
165	-	1220	1.85	389	2L(i)
252	-	1868	1.21	355	2L(i)

Table 4.2.(b): S.S.R.T. analyses of McClelland and Focht's test data.

Case	S.S.R.T. Idealization
(i)	Constant element length of $L/6$
(ii)	Element length of upper $2/3$ refined to $L/12$
(iii)	Element length of upper $1/3$ further refined to $L/24$

Notation: G - Gibson soil
H - Homogeneous soil
2L - 2 Layer soil

E(0) lbf/in ²	m lbf/in ² /in	[M(z)/H] Max ft.	Comment
-	-	2.90	Test
0	30	3.23	G
0	50	2.82	G *
0	70	2.50	G
3000	0	2.60	H

Table 4.3.(a): PGROUP analyses of Alizadeh and Davissons' test data.

E _o lbf/in ²	m lbf/in ² /in	[M(z)/H] Max ft	E _p lbf/in ²	Comment
-	-	2.90	-	Test
0	50	3.74	1.5x10 ⁶	G
0	50	5.41	16.7x10 ⁶	G
0	50	5.91	32.0x10 ⁶	G
0	75	5.12	16.8x10 ⁶	G
0	125	4.72	16.8x10 ⁶	G
0	175	4.46	16.8x10 ⁶	G
5000	0	2.70	20.3x10 ⁶	H
5000	0	2.48	15.5x10 ⁶	H
5000	0	2.34	13.0x10 ⁶	H

Table 4.3.(b): S.S.R.T. analyses of Alizadeh and Davissons' test data.

S.S.R.T. Idealization
Pile element length of lower 1/3 equal to L/6 Pile element length of upper 2/3 refined to L/12

Notation: G - Gibson soil * - Best fit results
 H - Homogeneous soil

Inferred characteristic	Pile 121 (uncoated)	Pile 122 (slipcoated)
Ultimate average adhesion in alluvium	26KN/m ²	5.6KN/m ²
Ultimate average adhesion in gravel	86KN/m ²	60KN/m ² *
Ultimate average adhesion in chalk	Estimates not possible as insufficient load was transferred to the chalk	>120KN/m ² >7MN/m ²
Ultimate end bearing capacity in chalk		

* Pile uncoated at this depth

**Table 4.4.: Adhesion calculated from short term
pile load tests.**

Es (KN/m ²)			Displacement δ (mm)	Comment
Alluvium	Gravel	Chalk		
250x10 ³	250x10 ³	250x10 ³	1.9	
500x10 ³	500x10 ³	500x10 ³	1.3	
26	86	250x10 ³	13.0	
26	86	500x10 ³	12.0	
500	500	500x10 ³	11.9	
5000	5000	500x10 ³	9.9	Case (ii)
50x10 ³	50x10 ³	500x10 ³	4.4	
26x10 ³	86x10 ³	500x10 ³	5.5	Case (i)
Field measurement			7.5	

**Table 4.5.: Pile 121 - Variation of displacement
with soil modulus.**

Es (KN/m ²)			Displacement δ (mm)	Comment
Alluvium	Gravel	Chalk		
6	60	120	314.0	
6	60	250x10 ³	12.0	
6	60	500x10 ³	11.8	
6	60x10 ³	500x10 ³	9.3	Case (i)
0	19.8x10 ³	500x10 ³	10.7	
6x10 ³	19.8x10 ³	500x10 ³	8.9	
6x10 ³	60x10 ³	500x10 ³	8.0	Case (ii)
Field measurement			11.5	

Table 4.6.: Pile 122 - Variation of displacement with soil modulus.

Method	Load per pile (KN)			Comment
	Front row	Middle row	Rear row	
Static	280	280	240	
Turzynski	240	430	100	**
Minipoint	280	420	100	
Strapp 2 piles pinned to cap piles fixed to cap	230 280	480 390	100 130	
PGROUP Es = 0.5 MN/m ² Es = 10 MN/m ²	380 380	280 270	130 140	
Plane frame	320	270	180	
Observed loads on 27:7:77	320	350	300	Mean values
Observed average loads in 1980	390	450	360	

** - Method used for design of bridge

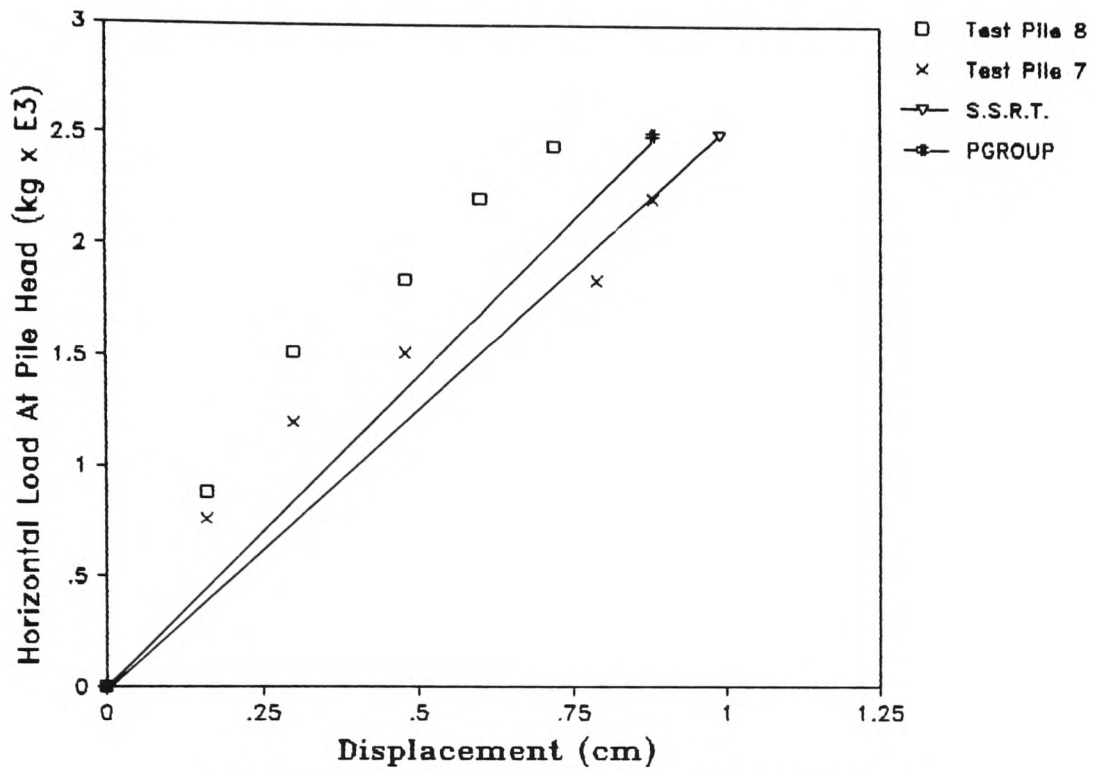
TABLE 4.7.(a): Calculated and observed distribution of pile loads.

Load per pile KN			Es values (KN/m ²)			Comment
Front row	Middle row	Rear row	Alluvium	Gravel	Chalk	
326	267	242	6.0x10 ³	60x10 ³	500x10 ³	S.
323	275	237	6.0x10 ³	60x10 ³	500x10 ³	F.
326	263	244	500	500	500x10 ³	S.
322	266	241	500	500	500x10 ³	F.
326	262	245	500	500	∞	S.
323	266	241	500	500	∞	F.

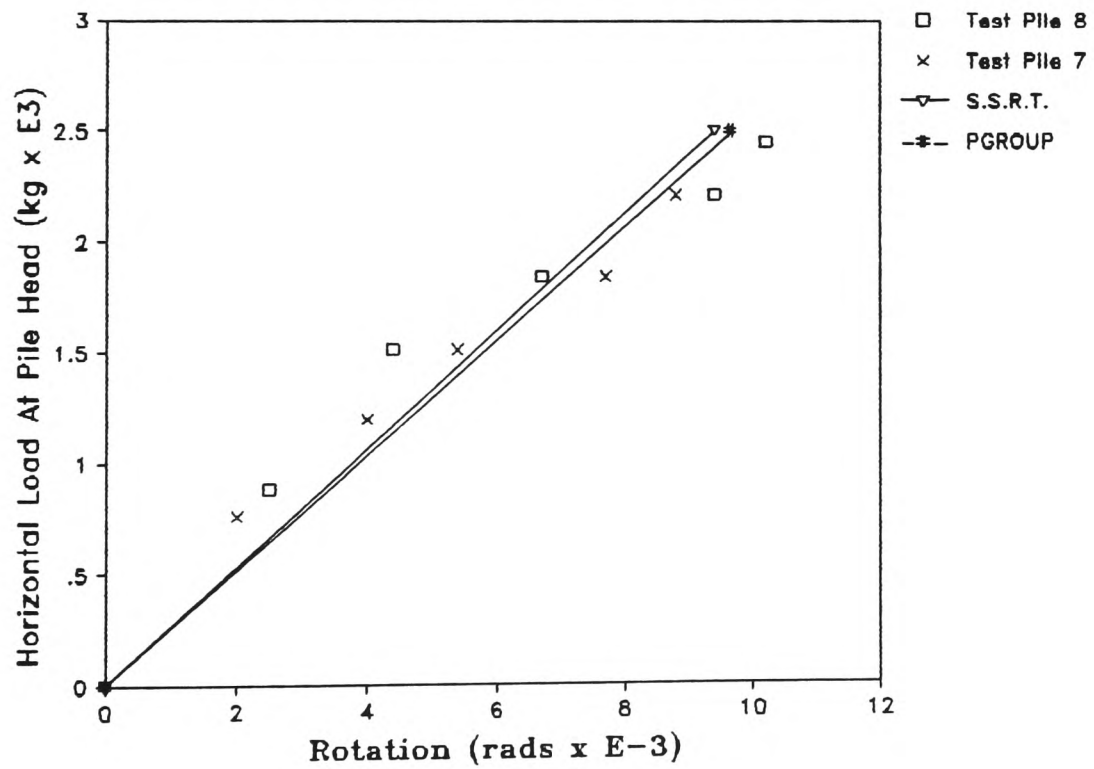
S. Infinitely Stiff Pile Cap

F. Finite Stiffness Pile Cap

Table 4.7.(b): S.S.R.T. results for the distribution of pile loads.

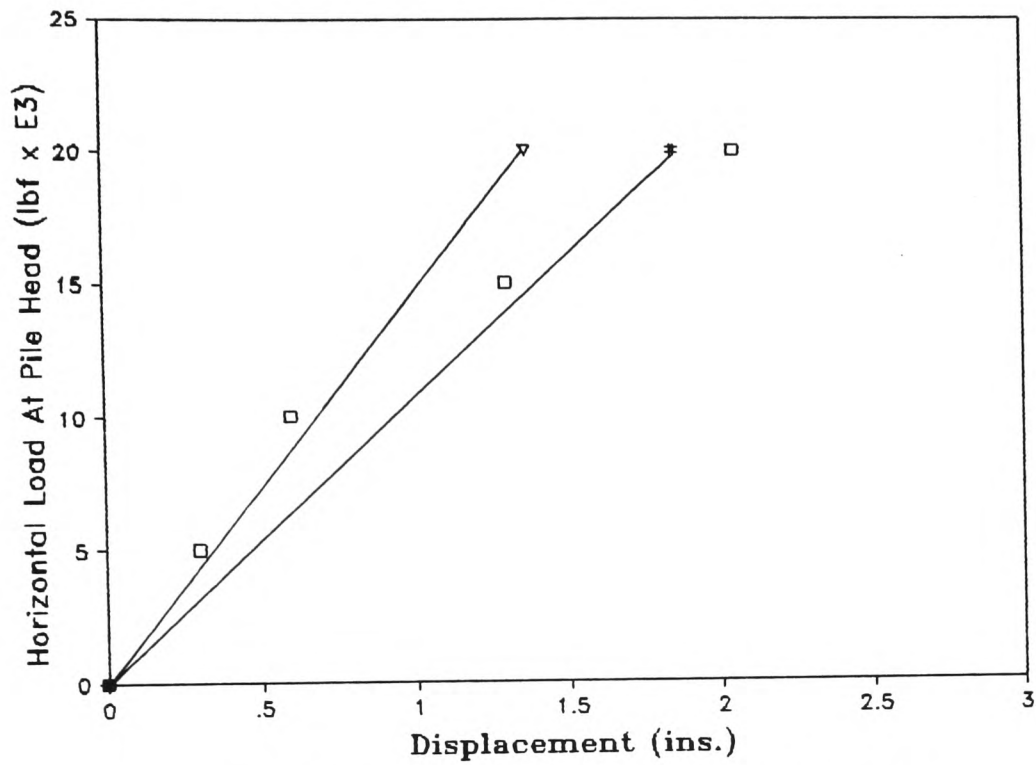


(i) Lateral displacement of pile head.

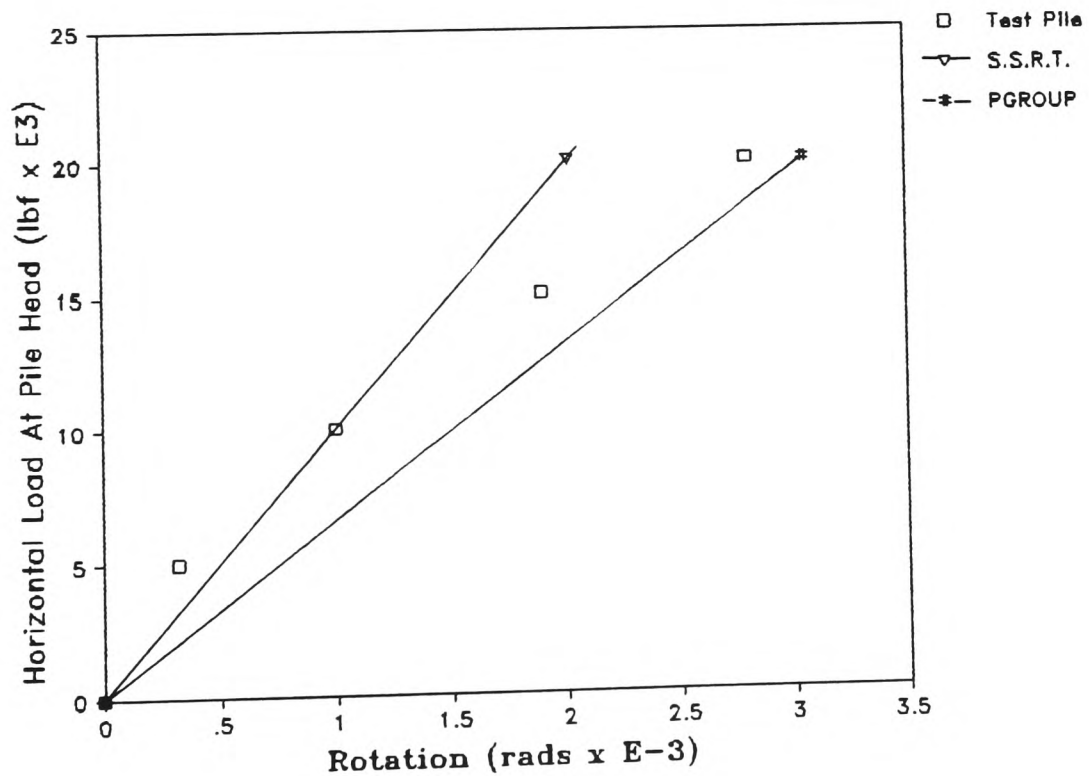


(ii) Rotation of pile head.

Figure 4.1.: Comparison with Reese and Cox.

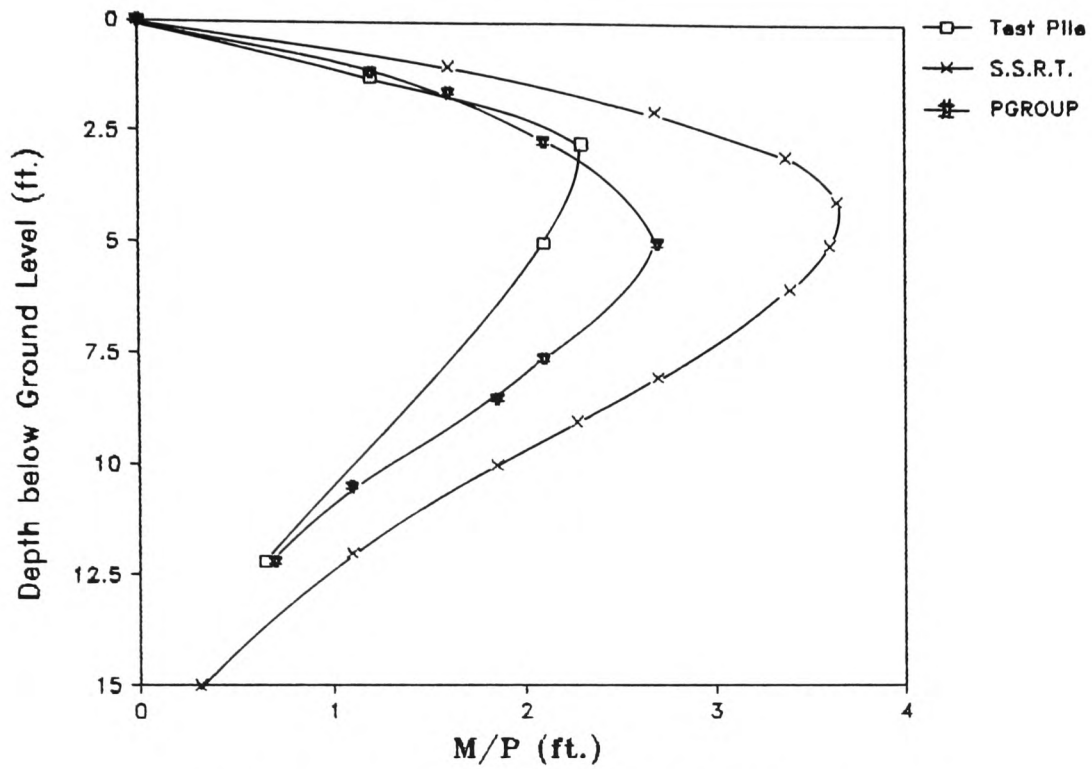


(i) Lateral displacement of pile head.



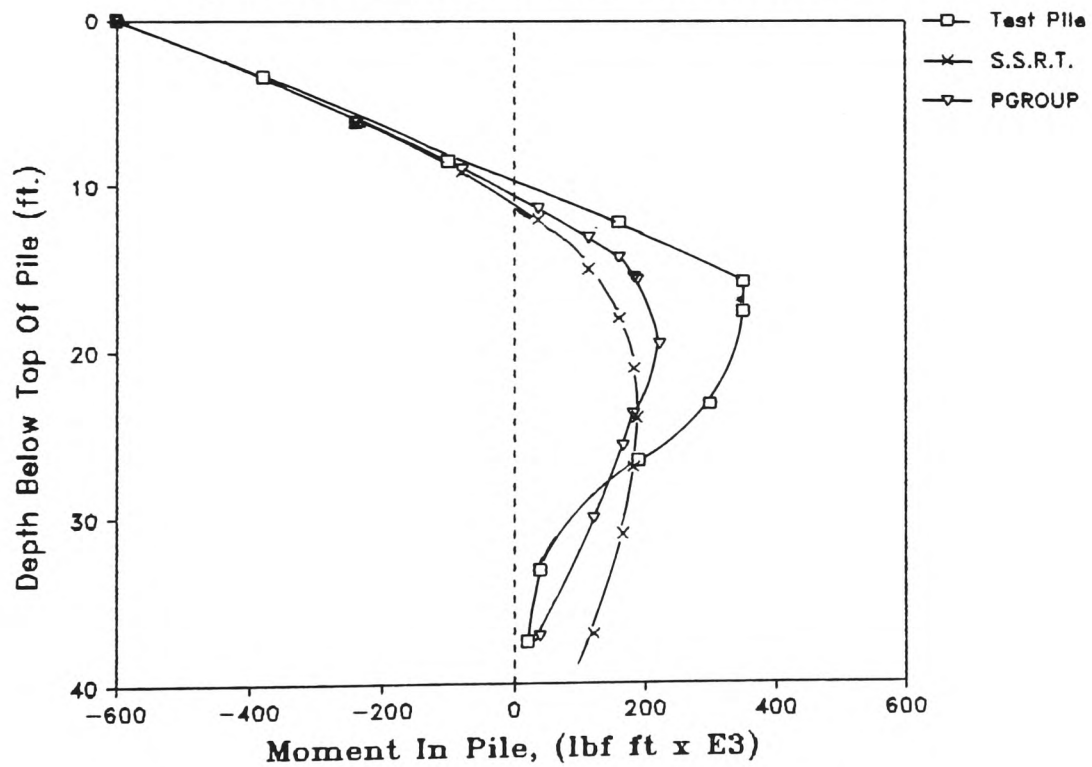
(ii) Rotation of pile head.

Figure 4.2.: Comparison with Alizadeh.



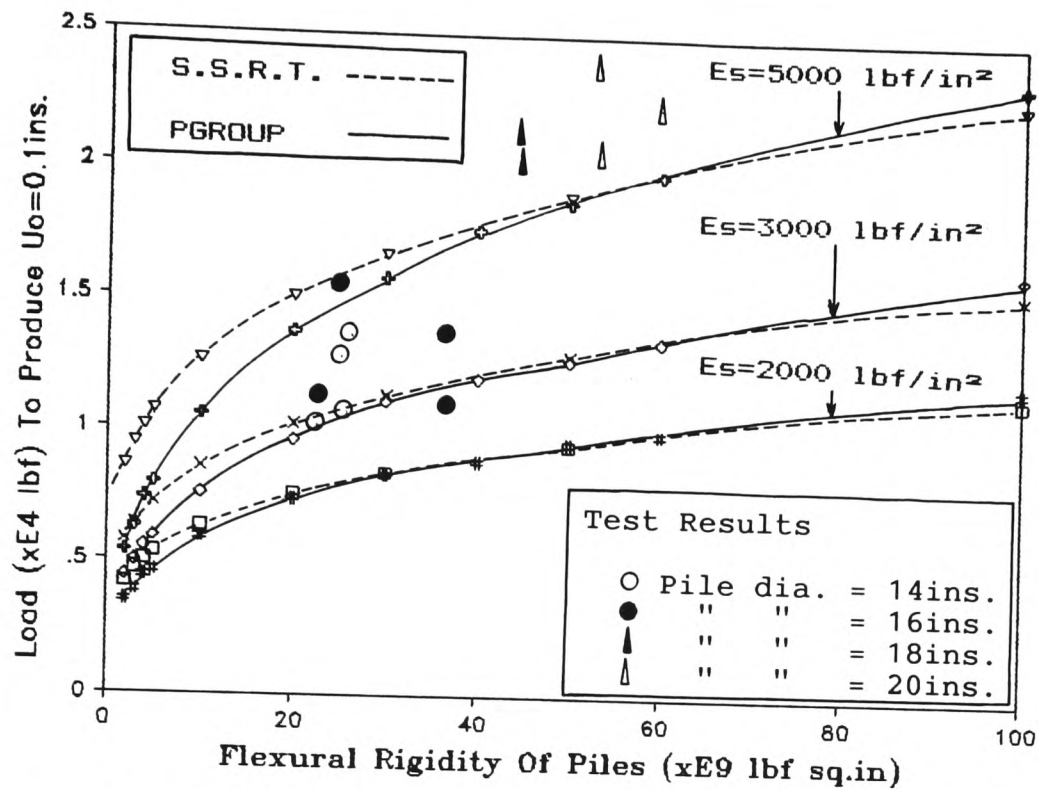
(iii) Bending moment distribution.

Figure 4.2.: Comparison with Alizadeh.

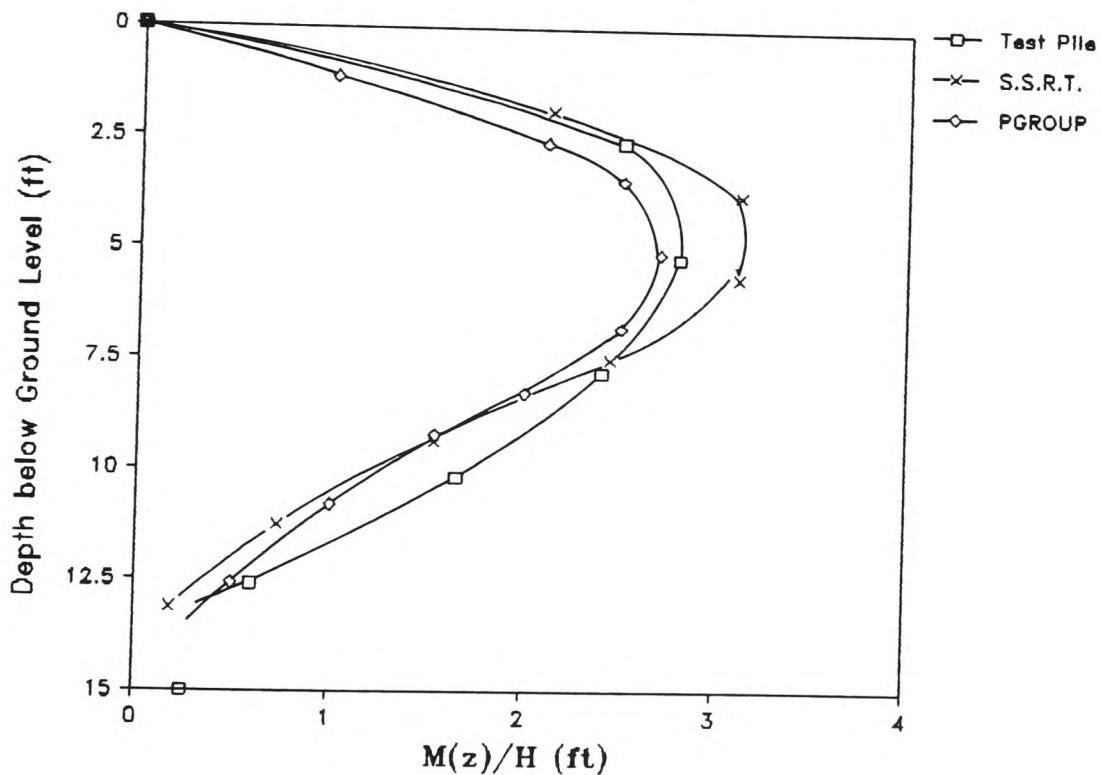


Bending moment distribution.

Figure 4.3.: Comparison with McClelland and Focht.



(i) Load required to produce 0.1in. lateral displacement against flexural rigidity of piles.



(ii) Bending moment distribution.

Figure 4.4.: Comparison with Alizadeh and Davisson.

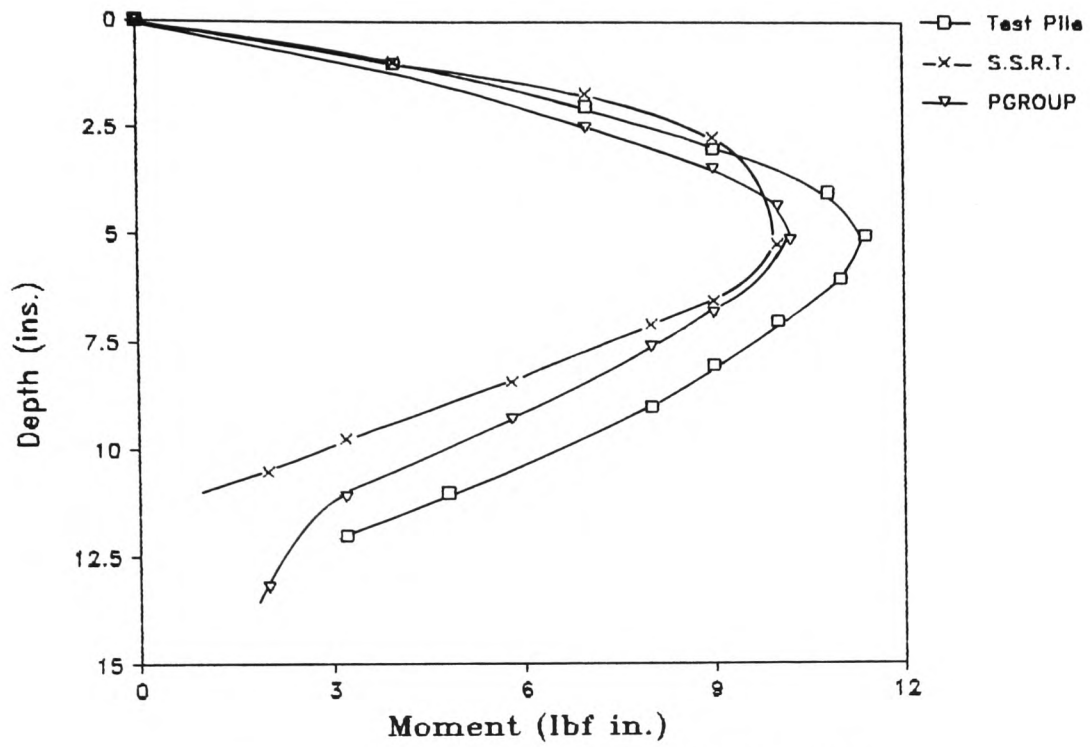


Figure 4.5.: Comparison with Davisson and Salley.

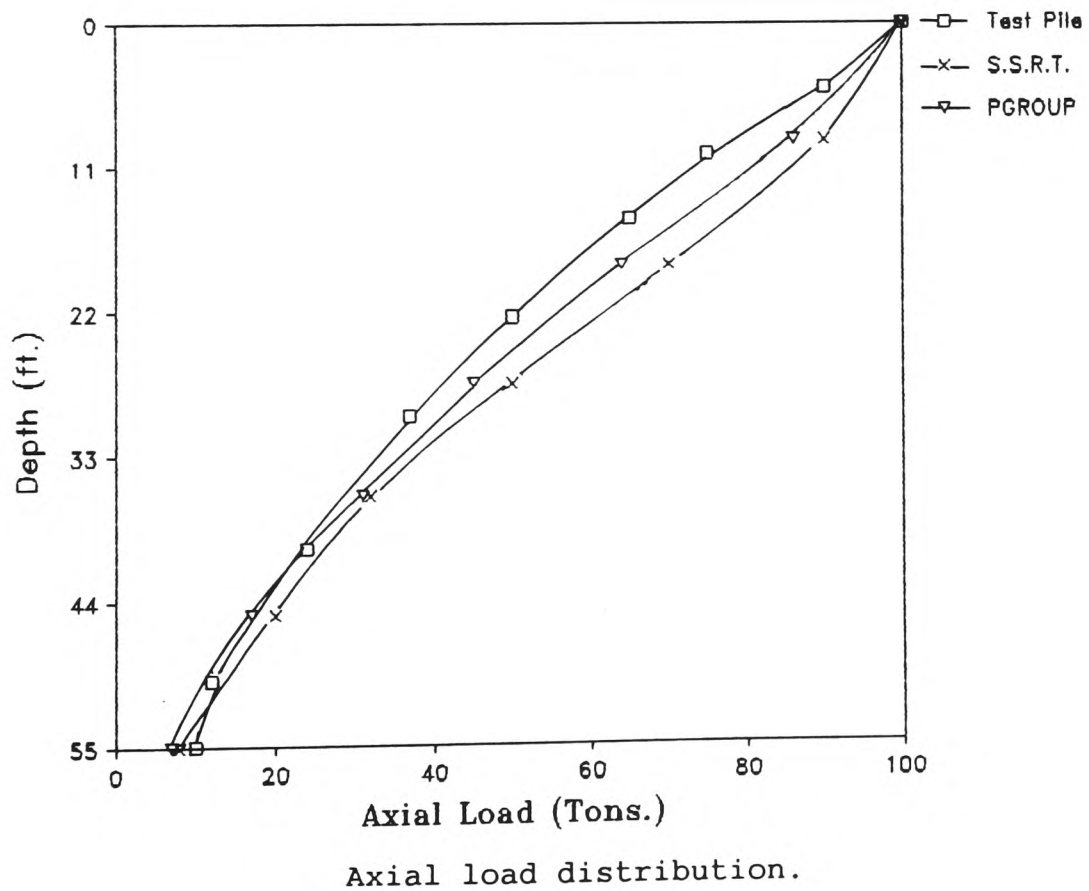
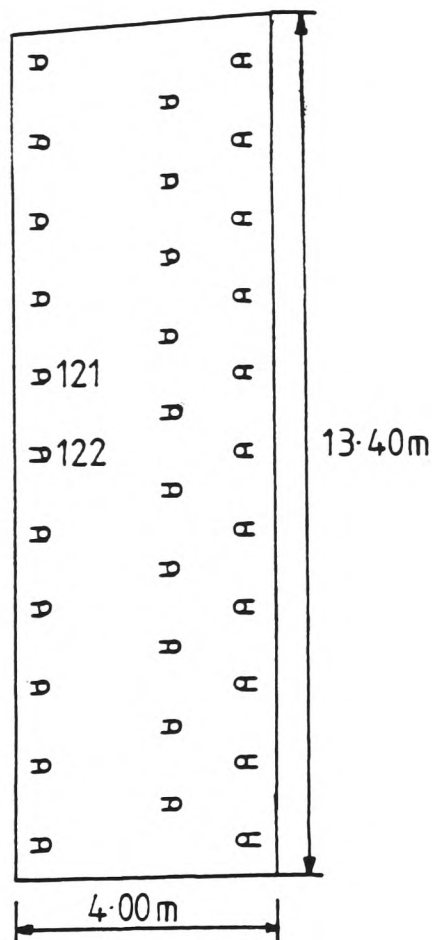
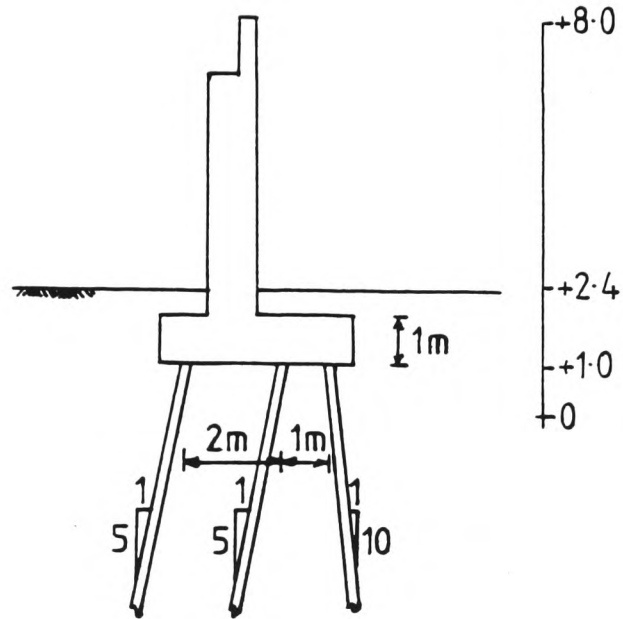


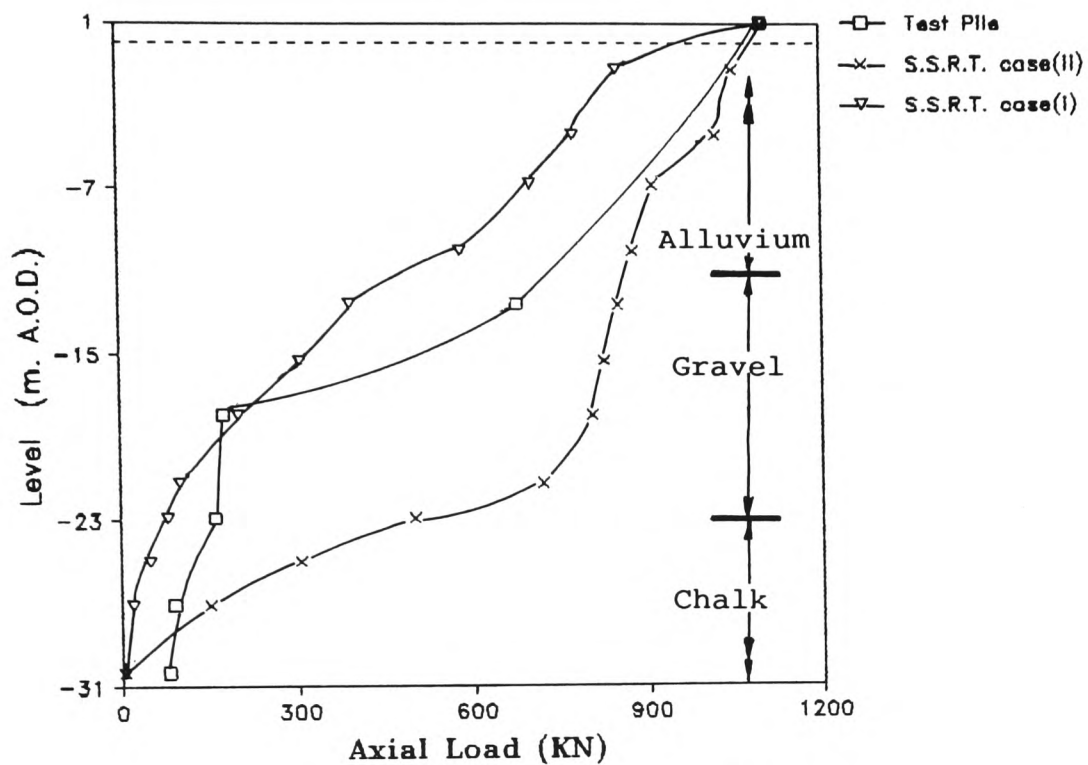
Figure 4.6.: Comparison with Mansur and Hunter.

(a) Section through abutment.

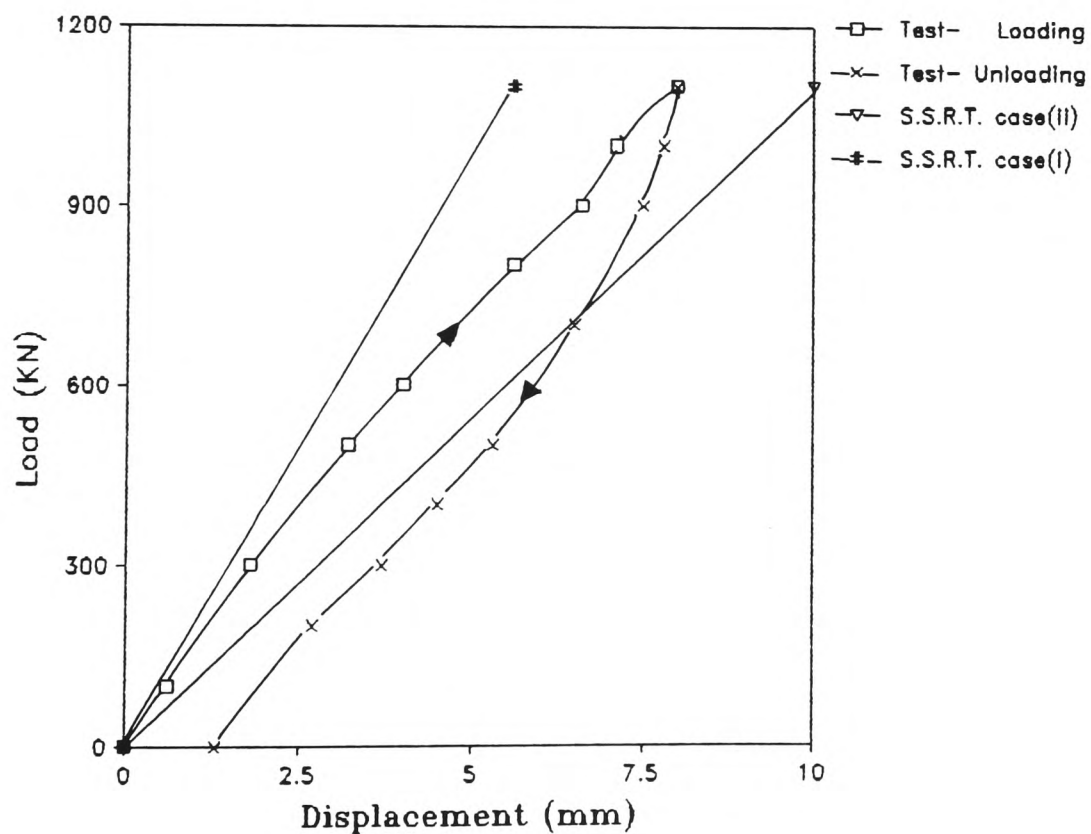


(b) General pile arrangement plan.

Figure 4.7.: Details of piled abutment.

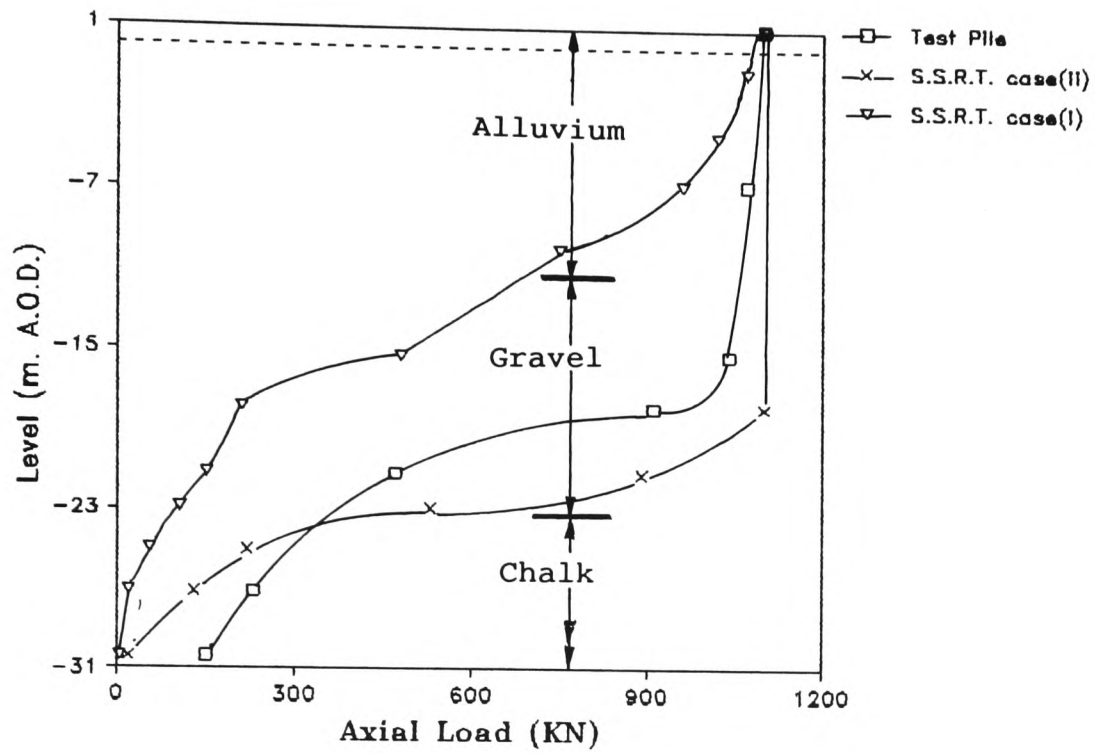


(i) Axial load distribution.

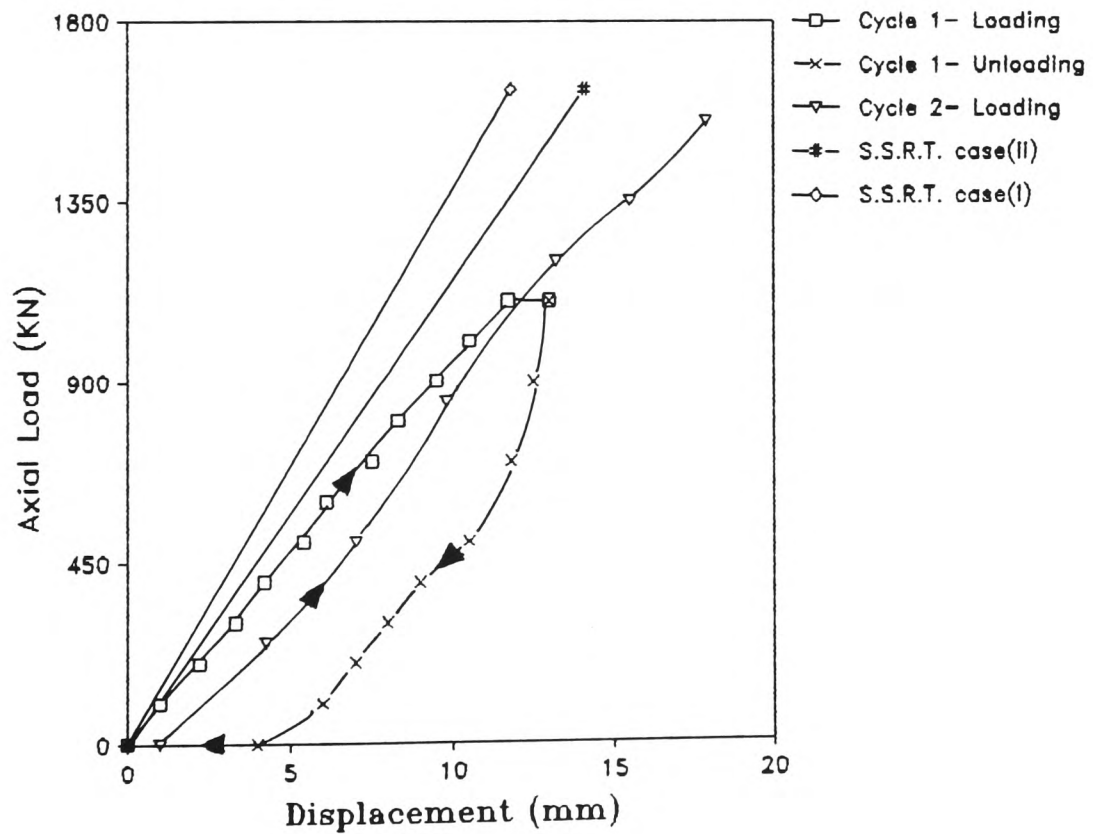


(ii) Load-displacement response.

Figure 4.8.: Results of load test on Pile 121 (uncoated).



(i) Axial load distribution.



(ii) Load-displacement response.

Figure 4.9.: Results of load test on Pile 122 (Slip-coated).

CHAPTER 5.

ANALYSIS OF PILES WITH GROUP INTERACTION.

5.1. GENERAL.

The interaction effects of closely spaced piles tend to be significant. The overall effect is one of increasing the displacement of the group and reducing its load carrying capacity. In this chapter, the interaction of both axially and laterally loaded pile groups and axially loaded piled rafts is considered. The proposed method is presented and the results compared with field measurements, laboratory tests and results from the PGROUP program.

A simplified method of accommodating interaction is presented which enables the overall group displacement to be determined. This implicitly assumes that all piles carry approximately equal loads, which may be true in the long term. A more rigorous method is also presented for the analysis of piles which carry substantially different loads, which tends to be the case for closely spaced piles in the short term.

5.2. SIMPLIFIED ANALYSIS OF AXIALLY LOADED PILES.

5.2.1. General

The proposed simplified idealization of interaction is a combination of methods from Poulos and Davis (1974) and that due to O'Neill et al (1977). The appropriate factors for the interaction between two piles are selected from the work of Poulos and Davis which is reproduced in Appendix B. A modification factor ($1/Z$) similar to that of O'Neill et al is then calculated. The full calculation procedure as performed by O'Neill et al is not carried out.

Application of the simplified modification factor, $1/Z$, to the subgrade stiffness provides a means of successfully accommodating the pile-soil-pile interaction within the analysis.

5.2.2. Procedure

Having determined a pile geometry, appropriate factors for the interaction between two piles are selected from Figure B.3.. The analysis is extended to any general pile group using the principle of superposition. The cumulative displacements due to the presence of the other piles are calculated on the basis that all piles carry an equal load. For groups comprising both vertical and raked piles, the piles are assumed to carry loads determined on a basis of no group interaction. This procedure is in agreement with the approach of O'Neill et al. The procedure enables the $1/Z$ modification factors to be readily determined without the need to solve several simultaneous equations. The $1/Z$ factors are then applied to the soil springs surrounding the piles. A worked example is described below for the interaction due to axial loading of a 3x3 pile group. The pile numbering system is shown in Figure 5.1..

The necessary data for the analysis is given below:

Pile length, L	= 20m	
Pile diameter, d	= 1m	: $L/d = 20$
Pile spacing, S	= 5m	: $S/d = 5$
Pile modulus, E_p	= $10 \times 10^6 \text{ KN/m}^2$	
Soil Modulus, E_s	= 1000 KN/m^2	: $K = E_p/E_s = 10,000$

Applied Load, $V = 9000 \text{ KN}$

and, 10 elements are used to idealize each pile.

From Figure B.3. the respective interaction factors α for the various S/d ratios are presented in Table 5.1.

Interaction is governed by Poulos' equation:

$$\delta_i = \delta_1 \left(\sum_{\substack{j=1 \\ j \neq i}}^k P_j \cdot \alpha_{ij} + P_i \right) \dots \dots \dots 5.1.$$

By assuming no interaction initially , all piles of this group carry an equal load of 9000/9 ie. 1000KN.

Equation 5.1. then reduces to:

$$\delta_i = \delta_1 \cdot P \cdot \left(\sum_{\substack{j=1 \\ j \neq i}}^k \alpha_{ij} + 1 \right) \dots \dots \dots 5.2.$$

The equivalent modification factor Z of O'Neill et al is then given by:

$$Z = \left(\sum_{\substack{j=1 \\ j \neq i}}^k \alpha_{ij} + 1 \right) \dots \dots \dots 5.3.$$

e.g. For Pile 1.

$$Z_1 = 4 \times 0.38 + 4 \times 0.45 + 1 = 4.32$$

and,

$$1/Z_1 = 0.231$$

$1/Z_1$ represents the modification factor for reduction of the soil stiffness to accommodate pile-soil-pile interaction. It is similar in nature to Poulos and Davis' (1974) $1/R_S$ settlement ratio for the complete pile group. The $1/Z$ factor is termed I_v for pile interaction under axial loading and I_h for pile interaction under lateral loading.

Similarly for Piles 2 and 3, the interaction factors I_{v2} and I_{v3} were calculated to be 0.250 and 0.272 respectively.

To calculate the modified soil stiffness to be used in the pile-soil matrix. The following procedure is implemented:

$$K_v = E_s.M_v.I_v.L' \text{ (KN/m)} \dots\dots\dots 5.4.$$

and,

$$K_{eb} = E_s.M_v.I_v.\sqrt{(\text{base area})} \dots\dots\dots 5.5.$$

where K_v = axial soil spring stiffness at nodal point
 K_{eb} = End bearing spring stiffness
 E_s = soil modulus
 M_v = Modification Factor for axially loaded pile
 (from Chapter 3. Figure 3.13.)
 I_v = Interaction factor for axial loading
 L' = pile element length.

e.g. for Pile 1

$$K_{v_1} = 1000 \times 0.59 \times 0.231 \times 2 = 272 \text{ KN/m}$$

and,

$$K_{eb_1} = 1000 \times 0.59 \times 0.231 \times \sqrt{(\pi \times 0.5^2)} = 121 \text{ KN/m}$$

Similarly for Piles 2 and 3

$$K_{v_2} = 296 \text{ KN/m}$$

$$K_{v_3} = 320 \text{ KN/m}$$

$$K_{eb_2} = 131 \text{ KN/m}$$

$$K_{eb_3} = 142 \text{ KN/m}$$

The soil springs at the nodal points of the pile representing the axial behaviour are assigned these stiffness values. A stiffness matrix for the pile-soil system can then be assembled manually as described previously. Alternatively, the spring stiffness values can be input as support releases at the pile nodal points to enable the analysis to be carried out using a standard structural frame program.

As proposed by O'Neill et al, the calculation of the interaction factors can be carried out iteratively by inputting the new pile loads in Equation 5.1 to determine a better approximation of the load distribution. It was found that the rate of convergence with results from other

elastic methods was poor using this iterative approach. Provided the piles are reasonably well spaced and an estimate of the overall displacement is adequate for design purposes the proposed method is generally satisfactory as an "easy to use" preliminary design tool. Furthermore, long term pile load distributions are often more uniform than those determined by elastic methods of analysis such as Poulos and Davis' method and PGROUP. This indicates that results from the proposed method may be more representative of the substructure performance in service than more rigorous methods.

5.3. FULL ANALYSIS OF AXIALLY LOADED PILES.

Where it is considered necessary to model interaction effects in a rigorous manner, e.g. for short term loading, the following procedure may be used.

Poulos and Davis' method, as outlined in Appendix B, is applied to the substructure and the simultaneous equations solved by carrying out the full solution process. This is accomplished assuming either a rigid raft, or a uniformly loaded flexible raft. From the computed load distribution and pile cap displacements the stiffness of the pile-soil system with interaction is determined at each location. This is then compared to the stiffness of a single pile-soil system to determine an interaction factor I_v at each pile location. A worked example is shown below.

Let the displacement δ /unit load of a single pile be

δ_1 .

Say $\delta_1 = 2.66 \times 10^{-5} \text{ ins/lbf}$

The stiffness of the pile-soil system is given by:

$$K_1 = 1/\delta_1 = 3.754 \times 10^4 \text{ lbf/in}$$

From a full solution of Poulos and Davis' simultaneous equations the load in Pile i, P_i , and the displacement δ_i are determined.

Say, $P_i = 15.9 \text{ lbf}$ and $\delta_i = 1.35 \times 10^{-3} \text{ ins.}$

Then, the stiffness of Pile i with interaction is K_i

Where,

$$K_i = \frac{15.9}{1.35 \times 10^{-3}} = 1.1778 \times 10^4 \text{ lbf/in}$$

The reduction in stiffness due to interaction is given by the interaction factor I_i .

Where,

$$I_i = \frac{K_i}{K_1} = \frac{1.1778 \times 10^4}{3.7540 \times 10^4} = 0.314$$

The interaction factors are then applied to the soil stiffness as described in Section in 5.2.2.

The procedure involves carrying out a full analysis using Poulos and Davis' method and back-figuring results to be used as input data for the proposed method. This approach enables the complete system to be analysed comprising a raft of finite stiffness and the superstructure configuration. Thus, by coupling Poulos and Davis' method with the stiffness method and the S.S.R.T., the inability of Poulos and Davis' method to accommodate the above complete system is overcome.

5.4. SIMPLIFIED ANALYSIS OF LATERALLY LOADED PILES.

5.4.1. Procedure.

The simplified analysis of pile-soil-pile interaction under applied lateral loading is accommodated in a similar

manner to axially loaded pile groups. Poulos and Davis' Interaction Factor Method for laterally loaded pile groups is described in Appendix B. The interaction factor for a laterally loaded two pile system is selected from Poulos and Davis' graphs, reproduced in Figures B.10-B.25. The interaction factors, defined in Appendix B, α_{pH} , α_{pM} , $\alpha_{\theta M}$ and α_{pF} are a function of the dimensionless pile spacing, S/d , the length to diameter ratio, L/d , the angle between the line of the piles and the direction of loading, β , and the pile flexibility factor, K_R . The pile flexibility factor is defined as:

$$K_R = \frac{E_p I_p}{E_s L^4} \dots\dots\dots 5.6.$$

Where,
 $E_p I_p$ = pile stiffness
 E_s = soil modulus.

The principle of superposition is used to analyse any general pile group. As before, the added displacements due to the presence of the other piles are calculated on the basis that initially all the piles of a vertical group carry equal loads. In the case of raked pile groups the initial load distribution is determined from an analysis assuming no interaction. For a group of vertical piles carrying equal lateral loads at the pile heads, Poulos and Davis' Equation B.9. reduces to:

$$\delta_i = \bar{\delta}_H \cdot H \left(\sum_{\substack{j=1 \\ j \neq i}}^k \alpha_{pHij} + 1 \right) + \bar{\delta}_M \cdot M \left(\sum_{\substack{j=1 \\ j \neq i}}^k \alpha_{pMij} + 1 \right) \dots\dots\dots 5.7.$$

The parameters of the above equation are defined in Appendix B. For a group subject to lateral loading only,

the modification factor for lateral behaviour is given by:

$$Z_{Hi} = \sum_{\substack{j=1 \\ j \neq i}}^k \alpha_{pHij} + 1 \dots\dots\dots 5.8.$$

Z_H is determined for each pile in the group and the corresponding soil stiffness for each pile is reduced by a factor of $1/Z_H$. The factor of $1/Z_H$ is termed the interaction factor I_h for lateral loading.

The calculation of the modified soil stiffness for lateral loading is similar to that of axially loaded piles. The following procedure is followed:

$$K_h = E_s.M_h.I_h.L' \dots\dots\dots 5.9.$$

Where, K_h = lateral soil spring stiffness at a nodal point
 E_s = soil modulus
 M_h = Modification factor for laterally loaded pile
 (from Chapter 3. Figure 3.14.)
 I_h = Interaction factor for lateral loading
 L' = pile element length.

Values of the soil stiffness K_h representing the lateral behaviour of the piles are applied at the nodal points of the pile. These are included in the stiffness matrix for the pile-soil system as previously described.

5.5. FULL ANALYSIS OF LATERALLY LOADED PILES.

A similar procedure as outlined in Section 5.3. is implemented to analyse the laterally loaded substructure with a rigorous treatment of elastic interaction effects.

5.6. PILED RAFTS.

5.6.1 General.

The analysis of pile raft systems is carried out in a similar manner to axially loaded free standing pile groups. The basic unit is a single pile with an attached pile cap

in contrast to the basic unit of a single pile. The interaction factors α_r , for the interaction between two units, are selected from graphs presented by Davis and Poulos (1972), reproduced in Figures B.5-B.8. The interaction factors determined by Davis and Poulos are confined to units comprising a rigid pile cap and embedded in a semi-infinite mass. To accommodate a unit of finite stiffness, the authors refer the reader to two separate references; Mattes and Poulos (1969) to determine the pile displacements with consideration of pile compressibility; and Brown (1969a) to accommodate the flexibility of the cap. They did not indicate how these two methods should be combined. The authors stated:

"it would appear unlikely that cap flexibility would seriously affect interaction".

This implies that the factors for the interaction between two units are relatively insensitive to the finite stiffness of the unit. It is intended to apply the proposed method to the analysis of piled rafts of finite stiffness. The interaction factors presented by Davis and Poulos should therefore be satisfactory for this purpose. Since the raft stiffness and pile compressibility are accommodated in the structural stiffness matrix, the soil-structure interaction of the system can be readily analysed.

5.6.2. Procedure.

The pile raft system is divided into basic units as suggested by Davis and Poulos. dc/d is then calculated for each unit, where dc is the equivalent cap diameter and d the actual pile diameter. Appropriate factors, α_r , for the

interaction between two units, reproduced in Figures B.5-B.8, are selected for each S/d ratio in the group.

The principle of superposition is used to analyse any general piled raft. As with pile groups, the cumulative displacements due to the presence of the other units are calculated on the basis that all units initially carry equal loads.

This enables a modification factor Z_R to be determined for each unit "i" in a system of "k" units. Where,

$$Z_{Ri} = \sum_{\substack{j=1 \\ j \neq i}}^k \alpha_{Rij} + 1 \dots\dots\dots 5.10.$$

The value of the soil stiffness supporting each unit "i" is reduced by $1/Z_{Ri}$. The factor $1/Z_{Ri}$ is termed the interaction factor I_r for a piled raft system.

The above procedure represents an analysis using a simplified treatment of interaction. As for axially and laterally loaded piles, a full solution of the simultaneous equations can be carried out in order to treat interaction in a more rigorous manner.

The following relationship is proposed to determine an approximate value of the spring stiffness which models the elastic soil beneath a uniformly loaded rigid raft.

$$K_{PR} = E_s \cdot \sqrt{(L' \cdot b)} \dots\dots\dots 5.11.$$

Where,

- E_s = soil modulus
- L' = length of beam element
- b = breadth of beam element
- K_{PR} = soil stiffness at a nodal point.

Determination of K_{PR} values for a raft divided into longitudinal and lateral grillage beams, requires

precautions to be taken to ensure that the total soil area is not considered twice. To avoid the soil stiffness being overestimated, half the K_{PR} value is assigned to each beam.

The raft grillage beams are supported similarly to laterally loaded piles. Hence, it may be more appropriate to take:

$$K_{PR} = Es. \sqrt{(L'.b)} .Mh \dots\dots\dots 5.12.$$

where Mh is the modification factor for a given flexibility of:

$$K_R = \frac{Ep.Ip}{Es.L^4} \dots\dots\dots 5.13.$$

where L is the length of the raft. No values of Mh have been determined for low aspect ratios with a high relative stiffness. However, Mh is likely to be greater than unity.

To accommodate interaction the K_{PR} value is modified, giving:

$$K_{PR} = Es. \sqrt{(L'.b)}. Ir \dots\dots\dots 5.14.$$

Also, for a piled raft, the soil surrounding the axially loaded piles should be modified to:

$$K_v = Es.Mv.Ir.L' \dots\dots\dots 5.15.$$

$$K_{eb} = Es.Mv.Ir.\sqrt{(base\ area)} \dots\dots\dots 5.16.$$

Because the contribution of the adhesion between the soil and raft to the axial load carrying capacity of the piled raft is generally low, it is reasonable to assume that the base of the raft is smooth. Hence, under lateral loading the cap will not alter the stress distribution within the soil. Therefore, determination of interaction factors for the lateral loading of the piled raft is identical to that for pile groups.

5.7. COMPARISON WITH THEORETICAL RESULTS.

5.7.1. General.

Results from the proposed S.S.R.T. method were compared to analytical solutions from both the PGROUP program and Poulos and Davis' method for a free standing pile group subjected to axial and lateral loading. The S.S.R.T. results were determined by treating interaction in a simplified method as described in Sections 5.2. and 5.4.

Because of the manual effort involved in solving Poulos and Davis' equations, the pile group was limited to a 3x3 configuration. The pile group geometries comprised L/d ratios of 10 and 20 with S/d ratios from 2 to 10. The soil modulus was varied from 1.0×10^3 to $1.0 \times 10^6 \text{ KN/m}^2$ and pile moduli of 10, 30 and $200 \times 10^6 \text{ KN/m}^2$ were considered to represent wood, concrete and steel piles respectively. In each case, the pile diameter was taken as 1m and the pile was divided into 10 equal elements. Using the S.S.R.T. approach the soil stiffness values were inputted at the nodal points along the shaft. The applied axial load, V, and lateral load, H, in each instance was 9000KN.

As lateral loading was also considered, the pile numbering system was as shown in Figure 5.2. Under axial loading Piles 2 and 3 carry the same load.

The details of three pile configurations considered are outlined below in Cases I, II and III.

CASE I

$d = 1\text{m}$	$E_p = 30.0 \times 10^6 \text{ KN/m}^2$
$L/d = 10$	$E_s = 10.0 \times 10^3 \text{ KN/m}^2$
$S/d = 2$	$V = H = 9000\text{KN}$

CASE II

$$\begin{array}{ll} d = 1\text{m} & E_p = 10.0 \times 10^6 \text{KN/m}^2 \\ L/d = 20 & E_s = 1.0 \times 10^3 \text{KN/m}^2 \\ S/d = 5 & V = H = 9000\text{KN} \end{array}$$

CASE III

$$\begin{array}{ll} d = 1\text{m} & E_p = 200.0 \times 10^6 \text{KN/m}^2 \\ L/d = 20 & E_s = 1.0 \times 10^6 \text{KN/m}^2 \\ S/d = 10 & V = H = 9000\text{KN} \end{array}$$

The computed results from the three methods are presented in Tables 5.2-5.4.. Results comprise the axial and shear load distributions at the pile heads and the central displacement of the cap. A comparison between the computed displacements for the three cases are shown in Table 5.5..

5.7.2. Discussion Of Results.

(a) Axial loading.

The agreement between PGROUP and Poulos and Davis' axial load distributions was good for the three cases considered as presented in Tables 5.2.(a), 5.3.(a) and 5.4.(a). The axial loads exhibited a considerable variation between the central and corner piles.

Case I represented a system with a high degree of interaction ie. a low S/d ratio and a high relative stiffness K equal to E_p/E_s ; and Case III represented a system with a low degree of interaction ie. high S/d ratio and low value of K . These observations were determined by examination of Poulos and Davis' interaction factors for two floating piles in a semi-infinite mass (reproduced in Figure B.3.).

For Case I, PGROUP computed a central pile load of 32KN and a corner pile load of 1500KN; whereas Poulos and

Davis' method gave a central pile tensile load of -25.6KN and a corner pile load of 1588KN. The corresponding pile axial load distribution for the S.S.R.T. was less varied with a computed central pile load of 942KN and a corner pile load of 986KN. For this case, Piles 2 and 3 were calculated as carrying 4% more load than the corner piles. This is considered to be due to a small accumulative error in the solution process.

For Cases II and III, the S.S.R.T. load distributions were more representative of those from the other solutions, with the central pile carrying the minimum load and the corner piles carrying maximum loads. As the S/d ratio increased, with a corresponding reduction in interaction, the agreement between the load distributions from the S.S.R.T. and the two other methods improved. In Case III, PGROUP results indicated a central pile load of 716KN and corner pile loads of 1130KN in comparison to the S.S.R.T. results of 926KN and 1051KN.

PGROUP computed that Piles 2 and 4 carried shears of 140KN and 149KN which represented 14% and 14.9% of the average pile axial load. This was an error as there was no applied lateral loading on this system and the pile cap was rigid.

The agreement between the cap displacements presented in Table 5.5.(a) was good for the three methods considered. The S.S.R.T. displacements ranged from an overestimation of 8.4% for Case I to an underestimation of -3.7% for Case III. The computed displacements from Poulos and Davis' method were in excellent agreement with PGROUP, ranging from an overestimation of 3% to 0%. The agreement between

the displacements from the S.S.R.T. and the other methods was remarkable considering that the interaction factors were manually extrapolated from Figure B.3. It reconfirmed the validity of the use of interaction factors and gave confidence in the prediction of the vertical displacements for pile groups.

A simplified treatment of interaction for the S.S.R.T. solution gave good agreement between computed total displacements from more rigorous methods of analysis. The load distributions from the S.S.R.T. exhibited a smaller variation between piles, which may be satisfactory for groups of well spaced piles. For groups of closely spaced piles, the load distributions computed by the S.S.R.T. require a more accurate treatment of interaction, as described in Sections 5.3 and 5.5.

(b) Lateral loading.

The shear force distributions determined by the three methods are presented in Tables 5.2.(b), 5.3.(b) and 5.4.(b). For the three cases considered, PGROUP and Poulos and Davis' shear force distributions agreed well with each other. For Cases I and II, where the effect of interaction was significant, the shear forces determined by both PGROUP and Poulos and Davis' method varied considerably from Pile 1 to Pile 4. In Case I, PGROUP computed a central pile shear of 278KN and corner pile shears of 1350KN; whereas Poulos and Davis' method gave a central pile shear of 197KN and corner pile shears of 1397KN. The shear force distribution for the S.S.R.T. was more uniform with a

calculated central pile shear of 868KN and corner pile shears of 1074KN.

As the degree of interaction decreased ie. as the S/d ratio increased and the relative pile stiffness K_R decreased; the agreement between the S.S.R.T. and PGROUP results improved. In Case III, PGROUP computed a central pile shear force of 869KN and a corner pile shear of 1060KN in comparison to values of 954KN and 1014KN, determined by the S.S.R.T..

The agreement between PGROUP and S.S.R.T. results for the axial load carried in Piles 2 and 4 also improved as the degree of interaction decreased. The axial load carried by the piles is intrinsically related to the rotation of the group ie. when the rotations compared favourably, the axial loads from both methods were also in agreement.

The comparison between the cap displacements for the three methods is presented in Table 5.5.(b). The displacements for Case I compared favourably for all methods, with the S.S.R.T. underestimating the cap displacement by -2% and Poulos and Davis' method overestimating by 18%. As the degree of interaction decreased, the agreement between the methods reduced. For Case III, the S.S.R.T. underestimated the displacement by -19% and Poulos and Davis' method overestimated the displacement by 68%. It was expected that the agreement between displacements from the S.S.R.T. and PGROUP would improve with less interaction. This was because the S.S.R.T. results were determined using a simplified treatment of interaction. However, it was possible that

PGROUP was not suited to problems of predominantly lateral loading and thus overestimated the interaction. Poulos and Davis' method grossly overestimated the lateral displacement of the cap in Case III. This was because the method neglected the axial pile loads induced by rotation. Poulos and Davis' did not suggest a procedure to accommodate this effect.

Results for the rotation of the cap are also presented in Tables 5.2.(b)-5.4.(b) for PGROUP and the S.S.R.T.. Rotations were not calculated using Poulos and Davis' method. By comparison of PGROUP and S.S.R.T. results, it was observed that the agreement improved as the degree of interaction decreased. For a high degree of interaction, in Case I, the S.S.R.T. computed a rotation of 16.2×10^{-3} radians in comparison to 9.12×10^{-3} given by PGROUP. In Case III, for a low degree of interaction, the S.S.R.T. gave a rotation of 4.00×10^{-6} in comparison to a value of 4.78×10^{-6} radians determined by PGROUP.

The difference between rotations may have been due to the small number of 10 equally spaced elements used in the S.S.R.T. idealization of the laterally loaded piles, whereas it is common practice to use as many as 20 graded elements. It may also be appropriate to calculate I_h using $\alpha_{\theta H}$ (the interaction factor for rotation due to a lateral load H) in contrast to α_{pH} (the interaction factor for displacement due to a lateral load H) in cases where rotation is deemed to be the controlling factor for design considerations. However, this was considered to be excessively time consuming in this instance. Furthermore, the rotations computed using the proposed method were

conservative in comparison to those from PGROUP in instances where interaction was significant.

Because the axial load distribution is related to the rotation of the group, an improvement in the computed rotation would lead to a corresponding improved axial load distribution. This may possibly be achieved by increasing the number of elements to model each pile or using $\alpha_{\theta H}$ to calculate I_h for a rotational problem. Alternatively, treating interaction in a more rigorous manner, with a full solution of Poulos and Davis' equations, may result in the load distribution agreeing more closely with the PGROUP solution.

(c) Summary.

The validity of using a simplified treatment of interaction to determine the S.S.R.T. results is demonstrated by comparison of results from other analytical methods.

For axially loaded pile groups, the agreement between the overall cap displacements was good for the three methods considered. The axial load distribution computed by the S.S.R.T. exhibited a smaller variation between piles than that determined by both PGROUP and Poulos and Davis' method.

For laterally loaded pile groups with a high degree of interaction, the displacement results from the S.S.R.T. agreed favourably with those from PGROUP. In cases where interaction was relatively low, the displacement results computed by PGROUP were 19% higher than those from the S.S.R.T.. This may possibly be due to PGROUP

overestimating the interaction for predominantly lateral loading.

The shear force distributions computed by the S.S.R.T. were less varied than those of PGROUP. The S.S.R.T. shear distributions may be more representative of the field behaviour because this tends to be more uniform than that determined by both PGROUP and Poulos and Davis' method. The agreement between the axial load and shear force distributions computed by the S.S.R.T. and those from rigorous elastic methods could be improved by solving Poulos and Davis' simultaneous equations. However, the corresponding solutions may be less representative of the substructure performance in service than those from a simplified treatment of interaction.

Treating interaction in a rigorous manner involves more effort than Poulos and Davis' method. However, the method represents an improvement on their method because the raft finite stiffness and superstructure configuration can also be modelled.

5.8. COMPARISON WITH EXPERIMENTAL RESULTS.

5.8.1. General

To validate the proposed method of raft-pile-soil interaction, comparisons were made with results from a variety of experimental data and other analytical results. The experimental data reported by the PGROUP authors to confirm their results and the PGROUP solutions were utilized for these comparisons. The graphs and figures presented in the PGROUP User Manual are reproduced here.

The comparisons reported in the User Manual were limited to cases of a rigid pile cap.

10 elements were used to model each pile in the following S.S.R.T. analyses. In all cases the soil spring stiffness values were computed using a simplified treatment of interaction as described in Sections 5.2, 5.4, and 5.6 of this Chapter, unless otherwise stated. In order to idealize the rigid cap, the grillage beams connecting the piles were assigned very high stiffness values.

5.8.2. Comparison With Davisson And Salley.

Davisson and Salley (1970) carried out a small scale test on a group of raking piles subjected to combined vertical and horizontal loads and moments. The pile group was embedded in a dry, fine and fairly uniform sand. The load distribution at the pile heads and the horizontal displacement were recorded. Group configuration details are presented in Figure 5.3. The parameteric details of the test are given below.

Length of piles (L)	= 21in.
Outer diameter of piles	= 0.50in.
Inner diameter of piles	= 0.44in.
Young's modulus of piles (Ep)	= 1.00×10^7 lbf/in ²
Angle of rake	= 18.5°

The analytical results for both PGROUP and the S.S.R.T. are also presented in Figure 5.3. Both analyses were carried out taking the pile cap to be perfectly rigid and the group as free standing. The results presented in Figure 5.3. were determined assuming that the soil modulus increased linearly with depth at a rate, m , of 40 lbf/in²/in.

Because the piles were raked, the interaction decreased as the pile spacing increased with depth. Ideally the interaction factors for the S.S.R.T. should have been calculated for each element along the pile. This would have required a considerable effort, hence, interaction factors I_v and I_h were computed at one appropriate depth. For axially loaded piles the distribution of shear stress along the pile is nearly constant as shown by Poulos and Davis (1974) (their Figure 13.1). This idealization is also in agreement with Burmister (1940) and Vesic (1970a). Consequently, I_v for all piles was determined at a position of half the pile length. The majority of the applied lateral load on a pile is transferred to the soil along the upper third of the pile shaft as shown in Chapter 4. I_h was therefore calculated midway along the upper third of the pile shaft, at a depth of one-sixth the pile length. These approximations were not rigorously validated, however, the results obtained were acceptable.

The sensitivity of the analyses to changes in the elastic parameters are presented in Table 5.6. Three soil conditions were considered, two Gibson soils with m of 40 and 50 $\text{lbf/in}^2/\text{in}$ and a homogeneous soil with an E_s value of 500 lbf/in^2 . The closest agreement of both PGROUP and the S.S.R.T. results with the experimental lateral displacement was with m equal to 40 $\text{lbf/in}^2/\text{in}$. The experimental displacement was 0.0074ins. in comparison to 0.0077 and 0.0078 computed by the S.S.R.T. and PGROUP respectively.

The S.S.R.T. results agreed more closely with the experimental moment and shear forces in the piles than those from PGROUP. The axial load determined by the S.S.R.T. in Piles 1 and 3 was 13.3 lbf in comparison to an average of 15.4 lbf experimentally, which represented a -13.6% underestimation. The computed axial load in Piles 2 and 4 from the S.S.R.T. analysis was 4.2 lbf in comparison to the experimental average value of 2.9 lbf, which represented an overestimation of 44.8%. Piles 2 and 4 carried the lowest load, hence, an overestimation of this load would not significantly effect the design.

The S.S.R.T. analysis satisfactorily computed the performance of the loaded pile group. The solutions from the S.S.R.T. also generally agreed more closely with the measured behaviour than those from PGROUP, which treated interaction in a rigorous manner. Consequently, a simplified treatment of interaction was satisfactory for analysis of this loaded pile group.

5.8.3. Comparison With Ghosh.

Ghosh (1975) carried out tests on model groups of vertical piles subject to vertical loading. A combination of 2x2 and 3x3 pile group configurations were driven into a remoulded London Clay. The 3x3 pile group numbering system is presented in Figure 5.4.. Other details of the tests are given below.

Clay undrained shear strength (C_u)	= 14.5 lbf/in ²
Young's modulus of pile material (E_p)	= 3.0×10^7 lbf/in ²
Pile outer diameter	= 0.50 in.
Pile inner diameter	= 0.25 in.
Length/diameter ratio (L/d)	= 20, 30 and 40
Spacing/diameter ratio (S/d)	= 2.5 and 5.0

The analytical solutions were determined assuming a homogeneous soil with a modulus of 7500 lbf/in^2 ($E_s/C_u = 500$) and a Poisson's ratio μ_s of 0.5. The results are also presented in Figure 5.4.

The experimental results for the 3x3 groups indicated that an increase in the S/d ratio from 2.5 to 5.0 increased the group stiffness by approximately 10%. For the same increase in the S/d ratio both PGROUP and the S.S.R.T. computed an increase in stiffness for the system of about $35.0 \times 10^3 \text{ lbf/in}^2$, which represented approximately a 40% increase.

For the 3x3 pile group, the S.S.R.T. and PGROUP results of group stiffness were in good agreement with one another. However, for the 2x2 pile configuration the S.S.R.T. and PGROUP results diverged as the L/d increased, with the experimental values lying between the two curves.

Also presented in Figure 5.4. is the comparison of load sharing between piles for a 3x3 group. Results are presented for the experimental, PGROUP and S.S.R.T. studies. For the central pile, the PGROUP results grossly underestimated the experimental values, whereas the S.S.R.T. results were in close agreement with the experimental loads. For intermediate peripheral piles, the agreement between all results was good. However, PGROUP generally overestimated the experimental load in the corner piles. The S.S.R.T. results for the corner pile were generally lower but in some instances agreed more closely with the experimental results than PGROUP.

The comparisons presented here indicated that elastic methods of analysis such as PGROUP tend to exaggerate the

interaction between piles. The presented S.S.R.T. results were derived using the simplified treatment of interaction. The computed displacements were satisfactory and the load sharing between piles agreed favourably with the experimental values.

5.8.4. Comparison With Whitaker.

Whitaker (1957) carried out a series of experiments to investigate the effects of length to diameter ratio (L/d) and spacing to diameter ratio (S/d) for groups of vertical piles. The pile groups were embedded in remoulded London Clay and their load-displacement behaviour was studied under axial loading.

The test details are given below.

For 3x3 pile groups $L/d = 12, 24, 36$ and 40
and 5x5 pile groups $L/d = 24$ and 48

and $H/d = 80$ where H = depth of soil layer.

The results were expressed in terms of an elastic settlement ratio R_S . Where:

$$R_S = \frac{\text{settlement of the group}}{\text{settlement of single pile under same average load}} \quad .5.17$$

The settlement ratios for the 5x5 pile groups are presented in Figure 5.5. and those for the 3x3 pile groups in Figure 5.6.. For the S.S.R.T. analyses H/d was taken as infinity in all cases.

S.S.R.T. results were determined for two 5x5 pile group configurations. In both cases L/d was taken as 24 and the S/d ratio was taken as 2.5 and 5.0. The S.S.R.T. method slightly overestimated the settlement ratio. The PGROUP settlement ratios for $L/d = 48$ were slightly greater

than those for $L/d = 24$. It was unlikely that the S.S.R.T. results would vary significantly from the PGROUP results. Both the PGROUP and S.S.R.T. results were representative of the experimental behaviour.

The results from both the S.S.R.T. and PGROUP analyses of the 3x3 pile groups were in good agreement as shown in Figure 5.6.. Again the results from both methods of analysis were representative of the experimental settlement ratios.

5.8.5. Comparison With Berezantzev et al.

Berezantzev et al (1961) carried out full-scale tests on 2x2, 3x3, 4x4 and 5x5 pile group configurations driven in dense sand. The results were again expressed in terms of a settlement ratio. In all cases the L/d ratio was equal to 20 and the E_p/E_s ratio was taken as 10^5 .

The comparison between the experimental, PGROUP and the S.S.R.T. settlement ratios is presented in Figure 5.7. For each pile configuration, the S.S.R.T. results for the two S/d ratios of 2.5 and 5.0 are presented. Both the PGROUP and S.S.R.T. results were representative of the experimental settlement ratios. The PGROUP and S.S.R.T. results also agreed closely with one another.

5.8.6. Comparison With Whitaker And Sowers et al.

S.S.R.T. results were compared to both PGROUP and experimental results of the load sharing between piles in 3x3 groups. The experimental results were obtained from Whitaker (1957) and Sowers et al (1961). The PGROUP results

were determined using:

$$E_p/E_s = 10^5, L/d = 20, H/L = 1.35$$

Where H was the depth to a rigid stratum. The depth of soil considered beneath the pile tips was therefore relatively shallow. Without inferring solutions for the S.S.R.T. approach, it was necessary to assume H/L to be infinity. The S.S.R.T. analyses therefore ignored the restraining effect of this boundary.

Initially the simplified approach was used for the determination of interaction factors. The computed S.S.R.T. results for the ratio of Load in Pile/Average Load was close to unity in all cases. Agreement with Whitaker was not achieved until a S/d ratio of 8 was reached. The S.S.R.T. computed load distribution was of the correct order ie. maximum load in the corner pile and minimum load in the central pile. However, the load distribution did not vary significantly with the S/d ratio. Hence, the S.S.R.T. results showing the extent of load sharing between piles, presented in Figure 5.8., are those determined from a full solution of Poulos and Davis' simultaneous equations, as described in Section 5.3..

These results and those from the PGROUP analysis agreed well with the experimental loads in the corner and intermediate piles. However, the load in the central pile was underestimated by both analytical methods. PGROUP computed that the central pile carried a tensile load at a S/d ratio less than 2. Between S/d ratios of 2.5 and 8 the difference between both methods was generally less than 10%. Results from both methods also agreed well with the experimental values. The good agreement between results

from both analytical methods suggested that the effect of a shallow rigid boundary on the load distribution was minimal in this case.

5.8.7. Comparison With Ghosh For Cap Contact

Ghosh (1978) carried out model tests on groups of vertical piles embedded in remoulded clay with the pile cap in contact with the soil.

The material properties were the same as given in Section 5.8.3.

A comparison between PGROUP, S.S.R.T. and experimental results is presented in Figure 5.9.(a). The results were computed taking Poisson's ratio μ_s as 0.50. The S.S.R.T. results presented are those determined from a full solution of Poulos and Davis' equations.

The percentage of load carried by the cap from PGROUP agreed well with the experimental values. PGROUP computed that the percentage of load carried by the cap varied from 29% to 21% as the L/d ratio was increased from 20 to 40. The comparative S.S.R.T. values ranged from 21% to 13% ie. the results were generally 8% lower than the PGROUP values. S.S.R.T. values for the load distribution from both a simplified and full analysis are presented in Figure 5.9.(b). The S.S.R.T. results for the percentage of load carried by the cap, determined from a full solution of Poulos and Davis' equations, were identical to those for a simplified treatment of interaction.

The pile load distribution was similar to that for free standing groups, with PGROUP overestimating the load in the corner piles and underestimating the central pile

load. For the simplified treatment of interaction, the S.S.R.T. computed that the percentage of load carried by the different pile types varied between 8% and 11%. This was representative of both the PGROUP and experimental percentage load carried by the corner and peripheral piles. However, the load computed in the central pile was 7% higher than the PGROUP value.

For a full solution of Poulos and Davis' equations the agreement of the pile load distributions computed using the S.S.R.T. and PGROUP was similar to that for the free standing group in Section 5.8.3.. The load computed in all piles by the S.S.R.T. slightly overestimated the PGROUP values but the results were in excellent agreement.

A comparison of group vertical stiffness values for the 3x3 groups is presented in Figure 5.9.(c). The experimental group stiffness values varied from 106.0×10^3 to 150.1×10^3 lbf/in² for L/d ratios of 20 and 40. The comparative values from PGROUP were 116.2×10^3 and 170.8×10^3 lbf/in² in comparison to 124.5×10^3 and 171.2×10^3 lbf/in² from a simplified treatment of interaction using the S.S.R.T.. For a full solution of Poulos and Davis' equations the group stiffness values remained practically unaltered, with a variation from 128.0 to 176.0×10^3 lbf/in² as the L/d varied from 20 to 40.

It is concluded that the S.S.R.T. simplified approach to interaction for the pile group with a ground contacting cap was satisfactory to determine displacements. However, in this case, a full solution of Poulos and Davis' equations was required to model the broad variation of pile loads due to interaction.

5.8.8. Comparison With Feagin

Feagin (1953) carried out a series of full-scale tests on battered wooden pile groups fixed in concrete monoliths. The pile group behaviour was studied under lateral and axial load.

Various pile configurations were load tested to investigate the effects of pile group geometry on the lateral stiffness. The necessary details of the tests are given below.

Embedded length of piles (L) = 30ft.
Mean diameter of pile head = 13in.
Mean diameter of pile base = 9in.
Spacing/diameter ratio (S/d) = 3
Angle of batter = 20°

The piles were embedded in a fine to coarse sand containing occasional gravel. The same conditions prevailed beneath the pile tips with a slight increase in coarseness up to a depth of 75ft. where bedrock was encountered.

Because PGROUP (Version 3.0.) could not accommodate tapered piles, the authors adopted a constant pile diameter of 12ins. as being representative of the critical region of the pile. The pile cap was assumed to be rigid and free standing.

The PGROUP authors idealized the ground as a Gibson soil with a zero surface modulus and adjusted the rate of increase of soil modulus with depth, m , until reasonable agreement with the experimental results for the first test monolith was obtained. Accordingly, a value for m of 40 lbf/in²/in was adopted.

The interaction factor I_h for lateral loading was determined at one-sixth the pile depth, in agreement with Section 5.8.2.. The interaction factor for axial loading I_v was determined at half the pile depth. The results are presented in Figure 5.10..

For the comparison of the "Lateral load required to produce a quarter inch deflection" the results were in overall agreement, with both PGROUP and the S.S.R.T. generally underestimating the required lateral load. By comparison of results from Tests 2, 3 and 6 the effect of battering the piles could be observed. The required experimental lateral load increased from 5.8 to 7.0 to 9.0 Tons/pile for no battered piles, one battered pile and two battered piles respectively. For the same comparison the PGROUP results were 5.3, 7.3 and 8.4 Tons/pile. The S.S.R.T. indicated a similar variation, with results of 5.1, 10.3 and 13.4 Tons/pile.

The most efficient pile configuration was that of Test 8, where the experimental load was measured at 15.8 Tons/pile in comparison to 11.7 Tons/pile from PGROUP and 13.5 Tons/pile from the S.S.R.T.. By comparison of results from Test 6 and Test 8, there was a disproportionate increase in the experimental load capacity of the group due to battering of the two front rows of piles. The increase in the load carrying capacity from both analytical methods for the same comparison was less significant. This suggested that experimental results for Test 8 may have been erroneous.

Because the tests were carried out at a close pile head spacing, with $S/d = 3$, the effect of increasing the

number of battered piles resulted in a decrease in interaction. This effect was only approximately accommodated in the S.S.R.T. analysis. However, the computed S.S.R.T. results were representative of both the measured and PGROUP pile group performance. The S.S.R.T. results enabled the effect of battering various piles on the group performance to be investigated. The lateral stiffness of the group increased as the piles were battered. This was caused by a partial transfer of lateral load due to the development of axial shear stress along the pile shaft. The above effect was accommodated in the S.S.R.T. analysis.

Some of the test results for the lateral deflections due to vertical loading were interpolated by the PGROUP authors because these were not specified accurately by Feagin for each group configuration. The agreement between the experimental results and solutions from both analytical methods was good.

5.9. Case Histories

5.9.1. Hyde Park Cavalry Barracks

(a) General.

The Barracks is a 31 storey building with two basements. The foundation comprises 51 bored piles which are 24.8m long, 0.91m in diameter and under-reamed to 2.44m. The piles are capped by a 1.52m thick concrete raft resting on a deep layer of London clay. The plan area of the raft in contact with the clay is 618m^2 and it is located 8.8m below the ground surface.

(b) Results.

Hooper (1973) used an axisymmetric finite element analysis to compute values of settlement and load for comparison with field measurements taken over a six year period. Hooper increased the actual raft thickness from 1.52m to an idealized value of 3.3m to provide an estimate of the additional stiffness of the structure. He assumed that the soil modulus increased linearly with depth, while Poisson's ratio was constant at 0.5 (undrained) and 0.1 (drained). By comparing computed and measured values of load and settlement at the raft-soil interface he established that the best agreement was obtained when the following relationships were used.

$$E_u = 10 + 5.2z \text{ MN/m}^2 \dots\dots\dots 5.18.$$

$$E' = 0.75E_u \dots\dots\dots 5.19.$$

Where E_u = undrained soil modulus
 z = depth in metres from the ground surface
 E' = drained soil modulus.

Hain and Lee (1978) re-analysed the Barracks as a case history for their work. Two analyses were performed using drained parameters. The ground model for the first analysis comprised a homogeneous soil with a modulus equal to the average value along the piles. The interaction factors were calculated using Mindlin's (1936) equations. The soil parameters used in this case were $E' = 90.2 \text{ MN/m}^2$ and $\mu_s' = 0.1$. The second analysis employed a non-homogeneous soil model with corresponding interaction factors. The soil parameters used in this case were $E' = (41.8 + 3.9z) \text{ MN/m}^2$ and $\mu_s' = 0.1$. Where z was the depth in metres from the base of the raft.

The design loads applied to the raft were 103MN as a uniformly distributed load and 103MN as a parabolically distributed load, both applied vertically downward. The soil pressure at the founding depth of 8.8m was 0.096MN/m^2 .

The two analyses indicated areas of negative raft-soil reaction pressure. This was caused by the large interaction factors associated with the close spacing of piles. They interpreted this to mean that the pile group carried all of the net applied load. Consequently, they repeated the analyses assuming no raft-soil contact.

A plan of one-quarter of the raft indicating the positions of the piles and the grid used for the S.S.R.T. idealization is presented in Figure 5.11.

Hain and Lee did not report details of the parabolically distributed load. For the S.S.R.T. analysis it was estimated to be of the form shown in Figure 5.12. An overall load of 103MN divided by the raft plan area gave an equivalent uniform pressure of 166KN/m^2 . It was assumed that the pressure distribution was three dimensional in nature with a peak value of h . From the relationship between a parabola and a rectangle, the value of h was determined as $(3/2) \times (3/2) \times 166$ which was equal to 374KN/m^2 . The distribution from the peak value to zero at the edges was determined by estimating the best fit curve.

The S.S.R.T. results were determined assuming a 3.3m thick concrete cap. The cap and pile moduli were taken as 15GN/m^2 . A homogeneous soil was assumed with drained soil parameters. Because the base area of the piles in contact with the soil was considerable, the end bearing stiffness was determined by treating the base as a circular load on

an elastic continuum. Hemsley (1987a) recommended that the equivalent K_s value for a circular surface load of radius "a" was given by:

$$K_s = \frac{2Es}{\pi a (1-\mu_s^2)} \text{ KN/m}^3 \dots\dots\dots 5.20.$$

The soil stiffness representing the skin friction was determined in accordance with the procedure given in Chapter 3. This gave an overall flexibility for a single pile of 1.4×10^{-6} m/KN. The equivalent flexibility from Poulos and Davis (1974) for a pile with an enlarged base was 1.6×10^{-6} m/KN, which was 19% higher. The interaction factors were determined from a full solution of Poulos and Davis' equations as described previously in this Chapter.

The calculated and measured pile loads as a function of time for two of the instrumented piles, P1 and P3, are presented in Figure 5.13. After 40 months the measured load carried by the central pile, P3, was slightly greater than the load carried by the outer pile, P1. The results for Hain and Lee's non-homogeneous soil model, with the smaller interaction factors, marginally overestimated the measured values. For Hain and Lee's homogeneous soil model the computed maximum values of P1 and P3 were 4MN and 3MN respectively, compared to the corresponding measured loads of 3MN and 3.4MN. The computed loads from the S.S.R.T. were 4.1MN in P1 and 3.5MN in P3. This was in good agreement with the results from Hain and Lee's homogeneous soil model. Hooper (1973) observed that all piles carried approximately the same load. This supported the use of lower interaction factors associated with the non-homogeneous soil model. Thus a simplified treatment of

interaction using the S.S.R.T., which provides a more uniform load distribution, would compare more closely with the long term measured values.

The observed and computed raft settlements as a function of time are presented in Figure 5.14. After 40 months, the measured central settlement was 22mm and the edge settlement was 15mm giving a differential settlement of 7mm. Hain and Lee's computed settlements provide upper and lower bound results to the measured values. The results for the non-homogeneous soil model underestimated the measured values which were overestimated by the homogeneous soil model. Hain and Lee computed a central settlement of 32mm and an edge settlement of 27mm giving a differential settlement of 5mm. The S.S.R.T. computed a central settlement of 35mm and an edge settlement of 27mm giving a differential settlement of 8mm. The agreement between the settlements from the S.S.R.T. and Hain and Lee's homogeneous soil model was good. However, the differential settlement from the S.S.R.T. agreed better with the measured field value than that from Hain and Lee's method.

(c) Discussion.

The S.S.R.T. analysis was used to model the behaviour of a large piled raft foundation. The computed results agreed favourably with the measured performance. Comparisons were also made with Hain and Lee's method of analysis where three separate interaction factors were required to model the behaviour. Poulos and Davis combined the various elements of interaction and expressed them as

one interaction factor. The agreement between Hain and Lee's method and the S.S.R.T., which uses Poulos and Davis' single interaction factor, was very good. Because there is less effort involved in the S.S.R.T. calculations, using a single interaction factor, there is no real benefit in employing Hain and Lee's method.

The presented S.S.R.T. results were determined from a full solution of Poulos and Davis' equations in order to make comparisons with a more rigorous elastic method of analysis. However, the measured field performance indicated that the piles carried approximately equal loads. This suggested that results from a S.S.R.T. analysis using a simplified treatment of interaction, with an associated relatively uniform load distribution, would compare more closely with the long term measured values. This approach would provide displacements approximately equal to those determined from a full solution of Poulos and Davis' equations. There would also be a corresponding reduction in the amount of effort required to model interaction.

5.9.2. Piled Raft Foundation At Basildon.

(a) General.

Rickard et al (1985) reported a comparison of computed results with the observed performance of a piled raft foundation at Basildon.

The foundation was formed in an excavation 50x75m in plan and 5m deep. The superstructure comprises a reinforced concrete frame construction with brick cladding. Columns are arranged on a 10.8x9.6m grid. A plan and section of the building is presented in Figure 5.15.

The foundation rests upon a deep deposit of London Clay. The variation in shear strength, C_u , with depth is presented in Figure 5.16.

The substructure comprises a 700mm thick reinforced concrete slab, which is thickened in the area of the piles to 900mm. Directly under each column position is a single bored cast-insitu pile 1050mm in diameter, under-reamed to 3150mm and 11m long. The basement walls are generally 600mm thick and at column positions are supported on piles. The wall construction is integral with the basement and ground floor slabs to form a box structure. The piles under the basement and partition walls are 11m long, having diameters of 750 and 900mm with smaller under-reams.

It was anticipated that the maximum gross foundation pressure, dead load plus live load, on the underside of the base was 70KN/m^2 . The estimated dead load pressure from the structure and its finishes was approximately 50KN/m^2 . The pressure relief due to excavation of the clay, assuming a unit weight of 18KN/m^3 , was 90KN/m^2 . Thus the predicted net foundation pressure was -20KN/m^2 on the basis of the maximum gross foundation pressure and -40KN/m^2 on the basis of the dead load alone.

Two main design conditions were considered:

- (i) Short term; maximum building loads, allowing for load sharing between the piles and the raft, but ignoring uplift due to water pressure and heave effects.
- (ii) Long term; maximum uplift forces with minimum building loads; ie. no live loads.

(b) Results.

For the short term condition, Rickard et al carried out a simple soil-structure interaction analysis to compute

bending moments, total and differential settlements. In one part of their analysis, the basement slab was modelled as a grillage of beams. The soil being modelled as an arrangement of discrete springs at the grillage nodal points. The spring stiffness values were initially assigned from their experience. They did not present the values or offer any guidance for their determination. In the second part of their analysis, Mindlin's (1936) equations were applied to calculate the displacement of an array of point loads within an elastic solid. The loads were determined from the first part of the analysis.

Rickard et al modelled the soil as a homogeneous isotropic elastic half-space. The soil modulus, E_s , was assumed to increase linearly with depth by taking $E_s/C_u=400$. A Poisson's ratio of 0.5 was assumed. The piles were simulated by applying the load to the soil at two-thirds the pile depth below the basement slab. From the calculated vertical displacements and applied loads, new spring stiffness values were determined for use in the first part of the analysis. Iterations were made between the two analyses until the spring stiffness values converged. The grillage, computed settlements and pile loads for short term loading are presented in Figure 5.17.(a). The maximum total settlement was 20mm and the maximum differential settlement was 9mm. The results also indicated that in the centre of the slab approximately 50% of the building load was taken by the piles.

A 4.2m thick raft was modelled in the S.S.R.T. analysis. This value was determined by trial and error in an attempt to model the settlement profile from Rickard et

al. The second moment of area for the edge beams was increased by 25m^4 to represent the additional stiffness of a 0.6m thick exterior wall. No details were given of internal walls or column sections. Hence the additional stiffness these contributed to the overall system could not be directly assessed. The elastic modulus for the substructure elements was taken as 15GN/m^2 . The idealized grillage mesh of the raft is presented in Figure 5.17.(b). It was assumed that this was a symmetrical quarter of the raft and zero rotations were specified about the internal centre line boundaries. Three beam-column elements were used to model each pile.

A relationship of $E_s/C_u=400$ was also assumed for the S.S.R.T. soil idealization. The corresponding E_s value was taken as varying from 20 to 78MN/m^2 to model the soil stiffness down the pile shaft.

The S.S.R.T. analysis of the piled raft was carried out by considering a basic unit of a pile overlain by a portion of pile cap as described in Appendix B. Determination of the interaction factors required consideration of the complete raft. The equivalent diameter of the cap above each pile, d_c , was taken as 11.5. Having computed the interaction factors, a full solution of Poulos and Davis' simultaneous equations was carried out to determine K_v for each basic unit. Although there was no applied lateral load on the foundation, K_h was determined for each pile assuming no pile-soil-pile interaction. This was carried out because it was anticipated that the piles could carry shear and moments due to bending rotation of the raft.

The S.S.R.T. computed settlements and column loads for short term loading are presented in Figure 5.17.(b). The maximum total settlement was 23mm and the maximum differential settlement was 20mm. The maximum settlement was near the centre of the raft, as computed by Rickard et al. However, the S.S.R.T. computed a greater settlement at the centre of the edge than at the corner, which was in contradiction with the results of Rickard et al. The applied load distribution used by Rickard et al was not known, which may explain this difference.

The pile load as a percentage of the column load is also presented in Figure 5.17.(b). The piles about the edge carried a greater percentage of the column load than those near the centre which was in agreement with Rickard et al. However, the two computed load distributions were dissimilar. The S.S.R.T. computed the loads in the central piles to vary considerably. The average of the central pile loads as a percentage of column load was 53% which compared well to the Rickard et al estimate of 50%. The difference between individual values may have been due to dissimilar imposed loading conditions or a difference in member stiffness values.

Rickard et al assessed the uplift pressures for the long term case as follows. They estimated that 15% of the uplift pressure was dissipated as immediate elastic heave before the slab was cast. It was estimated that an additional 15% of heave pressure was reduced by the reinforcement of the piles in the soil. The slab was consequently designed for 70% of the overburden pressure. The maximum design pile loads (in both tension and

compression) obtained from the analyses of Rickard et al are presented in Figure 5.18.(a).

The pile design loads as computed by the S.S.R.T. are presented in Figure 5.18.(b). The maximum compressive and tensile loads were 6670 and -3110KN, in comparison to 5400 and -4100KN from Rickard et al. The values were of a similar order, the possible reasons for the differences have been discussed previously.

Observations were made of settlements, pile loads, effective pressure and ground water pressure beneath the basement slab. The piles went into tension during construction, probably as a result of high water pressure beneath the slab, since relatively low effective pressures were measured.

The observed settlements and slab/soil effective stresses at the end of construction are presented in Figure 5.19. The maximum and minimum settlements were 6.5 and 1.7mm across the slab. The effective stress beneath the slab was generally low. Three of the piles were in tension or low compression. Measurements indicated a pore water pressure of 47KN/m^2 beneath the basement slab.

(c) Discussion.

Rickard et al reported that the settlements at the end of construction were much less than the short term computed values owing to low effective pressures. They thus concluded that the short term case was conservative.

The analysis by Rickard et al led to a safe design which allowed successful completion of the basement. It was not possible to accurately compute the actual loads on

the basement at the design stage, hence, a precise determination of settlements could not be expected.

The overall settlements and pile loads computed by the S.S.R.T. agreed reasonably well with those of Rickard et al. However, there were large differences in the load distribution at individual locations. These differences may have been due to a lack of information on the substructure layout and dimensions and the assumed imposed load distribution.

The S.S.R.T. results indicated that bending moments up to 30KNm/m were induced in the raft at pile head locations. This was compatible with the relatively small computed differential settlements. Lateral loads up to 85KN were also computed at pile head locations. Although these values were relatively small in this instance, the results indicate the importance of modelling the lateral pile-soil stiffness of a vertically loaded substructure.

5.10. DISCUSSION AND CONCLUSIONS.

A method of analysis is presented which considers the interaction of axially and laterally loaded pile groups and piled rafts. A simplified treatment of interaction is proposed which enables the overall group displacement to be determined where piles carry approximately equal loads, which is common in the long term. A more rigorous method of analysis is also presented for piles which carry substantially different loads which is usual for closely spaced piles in the short term.

The S.S.R.T. results computed using a simplified treatment of interaction were compared to theoretical

solutions from PGROUP and Poulos and Davis' method for three different pile geometries under axial and lateral loading. Under axial loading, the pile cap displacements computed by the S.S.R.T., for a simplified treatment of interaction, were in good agreement with those from both PGROUP and Poulos and Davis' method. However, the axial load distribution determined by the S.S.R.T. exhibited less variation than that computed by the other methods. For laterally loaded pile groups, the displacements computed by the S.S.R.T. agreed favourably with the PGROUP values for configurations where there was a high degree of interaction. However, the agreement between results diverged as the degree of interaction became lower ie. as the pile spacing increased. At a wide spacing the PGROUP values were approximately 20% higher than those from the S.S.R.T.. This may be due to PGROUP overestimating the interaction of predominantly laterally loaded pile groups. The shear distributions, under lateral loading, were more uniform using the S.S.R.T. simplified approach to interaction than those from both PGROUP and Poulos and Davis' method.

To validate the proposed method for raft-pile-soil interaction, comparisons were made with both measured and PGROUP results from a variety of experimental data. By treating interaction in a simplified manner, the displacements computed by the S.S.R.T. were generally in good agreement with PGROUP and measured values. The computed load distributions were more uniform than those from PGROUP. The observed short term load distributions were also generally more uniform than those computed by

PGROUP. In order to determine solutions for groups exhibiting a considerable variation in pile loads a full solution of Poulos and Davis' simultaneous equations was carried out. The soil stiffness values used as input data for the S.S.R.T. were then back-figured. The benefits of this procedure are that the finite stiffness of the superstructure and raft can also be modelled unlike PGROUP and Poulos and Davis' method. The load distributions achieved using this approach generally agreed well with the PGROUP values.

It was shown that the S.S.R.T. results determined by calculating the interaction factors at one approximate depth for raked piles were acceptable. The interaction factors were calculated at half the pile depth for axially loaded piles and one-sixth the pile depth for laterally loaded piles.

It was demonstrated that the S.S.R.T. was capable of satisfactorily analysing a pile group with the pile cap in contact with the soil.

The S.S.R.T. was also used to model the behaviour of two existing large piled raft foundations. The performance of the foundation of Hyde Park Cavalry Barracks had been well documented which enabled input parameters for analysis to be confidently selected. The computed S.S.R.T. results agreed favourably with the measured performance and Hain and Lee's results.

The presented S.S.R.T. results were determined from a full solution of Poulos and Davis' equations in order to make comparisons with a more rigorous elastic method of analysis. However, observations indicated that the actual

piles carried approximately equal loads. This suggested that a S.S.R.T. analysis using a simplified treatment of interaction would have provided results which compared more closely with the long term measured values. This approach would give displacements approximately equal to those determined from a full solution of Poulos and Davis' equations, with a more uniform load distribution in the piles. There would also be a corresponding reduction in the amount of effort required to model interaction.

The performance of the foundation at Basildon reported by Rickard et al (1985) had been less well documented and there was a degree of uncertainty as to the validity of the idealizations made. The analysis by Rickard et al led to a safe design which allowed successful construction of the basement. It was not possible to accurately compute the actual loads on the basement at the design stage, hence, the computed settlements could not be expected to compare closely with the measured values.

The overall settlements and pile loads computed by the S.S.R.T. agreed reasonably well with those of Rickard et al. However, there were large differences in the load distributions at individual locations. These differences may have been due to a lack of information on the substructure layout and dimensions and the assumed imposed load distribution. This case demonstrated the importance of obtaining and reporting all the relevant information and data for use as a case history. The S.S.R.T. results indicated the need to model the lateral pile-soil stiffness of a vertically loaded substructure.

To conclude, the proposed method of accommodating interaction provided satisfactory results for the comparison of displacements and load distributions within pile groups and piled rafts under both axial and lateral loading. By treating interaction in a simplified manner, the load distribution within the group was more uniform than the PGROUP results. Hence, this approach may be more representative of the long term group behaviour. A full solution of Poulos and Davis' equations enabled interaction factors to be determined for groups exhibiting a considerable variation in pile loads. The corresponding results agreed more closely with those of PGROUP and occasionally short term loading. However, this detracts from the simplicity of the method and is generally considered unnecessary for a preliminary analysis, especially as the computed displacements are acceptable.

5.11. RECOMMENDATIONS FOR INCLUSION OF INTERACTION IN THE ANALYSIS.

(A) Free Standing Groups

- (i) Determine spacing between each pile in the group for all the other piles.
- (ii) Select appropriate interaction factors α for the two pile system.
- (iii) Initially assume all piles carry a load equal to that for no interaction (for vertical piles, all piles carry equal loads under uniform loading).
- (iv) Determine interaction factors I_v and I_h from Equations 5.3 and 5.8.

- (v) If necessary carry out a full solution of Poulos and Davis' equations to determine the interaction factors.
- (vi) Determine K_v , K_{eb} and K_h from Equations 5.4, 5.5 and 5.11 for each pile.
- (vii) Construct pile soil stiffness matrix.
- (viii) Analyse system.

(B) Piled Rafts

The same procedure is followed as in (A) except the basic unit is a single pile with an attached portion of pile cap. The interaction factors are then selected from Figures B.5-B.8. The soil stiffness beneath the raft is given by Equation 5.14, K_v and K_{eb} are given by Equation 5.15 and 5.16 respectively.

S/d	5	7.07	8	10	11.18	14	14.14	15
α	.45	.38	.35	.31	.29	.24	.22	.20

Table 5.1. Interaction Factors α for various S/d values.

	Axial load (KN)				Shear force (KN)			
Pile No.	1	2	3	4	1	2	3	4
PGROUP	32	726	760	1500	0	140	0	-149
S.S.R.T.	942	1029	1028	986	0	0	0	0
Poulos & Davis	-25.6	668	668	1588	-	-	-	-

(i) Axial load and shear force distributions.

	δv (mm)	δh (mm)	θh (rads)
PGROUP	62.8	10^{-6}	10^{-10}
S.S.R.T.	68.1	0	0
Poulos & Davis	64.4	-	-

(ii) Cap displacements.

Table 5.2.(a): Results for axial loading of Case I.

	Axial load (KN)				Shear force (KN)			
Pile No.	1	2	3	4	1	2	3	4
PGROUP	0	881	0	1330	278	897	764	1350
S.S.R.T.	0	491	0	471	868	960	957	1074
Poulos & Davis	-	-	-	-	197	1038	570	1397

(i) Axial load and shear force distributions.

	δv (mm)	δh (mm)	θh (rads)
PGROUP	10^{-6}	108	9.12×10^{-3}
S.S.R.T.	0	106	16.2×10^{-3}
Poulos & Davis	-	127	-

(ii) Cap displacements.

Table 5.2.(b): Results for lateral loading of Case I.

	Axial load (KN)				Shear force (KN)			
Pile No.	1	2	3	4	1	2	3	4
PGROUP	342	831	852	1320	0	117	0	-117
S.S.R.T.	904	984	977	1064	0	0	0	0
Poulos & Davis	294	803	803	1373	-	-	-	-

(i) Axial load and shear force distributions.

	δv (mm)	δh (mm)	θh (rads)
PGROUP	305	10^{-6}	4×10^{-11}
S.S.R.T.	319	0	0
Poulos & Davis	314	-	-

(ii) Cap displacements.

Table 5.3.(a): Results for axial loading of Case II.

	Axial load(KN)				Shear force (KN)			
Pile No.	1	2	3	4	1	2	3	4
PGROUP	0	736	0	959	575	930	881	1200
S.S.R.T.	0	562	0	608	893	970	979	1057
Poulos & Davis	-	-	-	-	601	966	876	1179

(i) Axial load and shear force distributions.

	δv (mm)	δh (mm)	θh (rads)
PGROUP	10^{-5}	527	1.78×10^{-2}
S.S.R.T.	0	106	3.60×10^{-2}
Poulos & Davis	-	127	-

(ii) Cap displacements.

Table 5.3.(b): Results for lateral loading of Case II.

Pile No.	Axial load (KN)				Shear force (KN)			
	1	2	3	4	1	2	3	4
PGROUP	716	932	942	1130	0	70	0	-60
S.S.R.T.	926	997	937	1051	0	0	0	0
Poulos & Davis	701	947	947	1128	-	-	-	-

(i) Axial load and shear force distributions.

	δv (mm)	δh (mm)	θh (rads)
PGROUP	0.27	10^{-9}	10^{-13}
S.S.R.T.	0.26	0	0
Poulos & Davis	0.27	-	-

(ii) Cap displacements.

Table 5.4.(a): Results for axial loading of Case III.

Pile No.	Axial load (KN)				Shear force (KN)			
	1	2	3	4	1	2	3	4
PGROUP	0	140	0	191	869	980	965	1060
S.S.R.T.	19	149	11	156	954	980	1015	1014
Poulos & Davis	-	-	-	-	877	933	955	1087

(i) Axial load and shear force distributions.

	δv (mm)	δh (mm)	θh (rads)
PGROUP	10^{-8}	0.57	4.78×10^{-6}
S.S.R.T.	0	0.46	4.00×10^{-6}
Poulos & Davis	-	0.96	-

(ii) Cap displacements.

Table 5.4.(b): Results for lateral loading of Case III.

CASE	S/d	L/d	K	PGROUP δv (mm)	S.S.R.T. % Diff.	Poulos & Davis % Diff
I	2	10	3000	62.8	+8.4	+2.5
II	5	20	10000	305	+4.6	+3.0
III	10	20	200	0.27	-3.7	0.0

(a) Axial loading.

CASE	S/d	L/d	K_R	PGROUP δh (mm)	S.S.R.T. % Diff.	Poulos & Davis % Diff
I	2	10	0.24	108	-1.9	+17.6
II	5	20	4.90×10^{-2}	527	-12.7	+36.8
III	10	20	9.82×10^{-4}	0.57	-19.0	+68.4

(b) Lateral loading.

Table 5.5.: Comparison of displacements.

		Bending moment lbf in					
E_0 lbf/in ²	m lbf/in ² /in	Piles 1 and 3			Piles 2 and 4		
		Test	PGROUP	S.S.R.T.	Test	PGROUP	S.S.R.T.
-	-	11.4	-	-	12.0	-	-
500	0	-	7.0	6.9	-	8.5	8.4
0	40	-	9.4	10.4	-	10.9	11.4
0	50	-	8.6	9.9	-	9.9	10.8

(i) Bending moment distribution.

Table 5.6.: Comparison with Davisson and Salley.

		Shear force lbf					
E_0 lbf/in ²	m lbf/in ² /in	Piles 1 and 3			Piles 2 and 4		
		Test	PGROUP	S.S.R.T.	Test	PGROUP	S.S.R.T.
-	-	5.1	-	-	4.5	-	-
500	0	-	3.9	4.3	-	4.6	4.9
0	40	-	3.7	4.2	-	4.2	4.5
0	50	-	3.6	4.2	-	4.1	4.8

(ii) Shear force distribution.

		Axial load lbf					
E_0 lbf/in ²	m lbf/in ² /in	Piles 1 and 3			Piles 2 and 4		
		Test	PGROUP	S.S.R.T.	Test	PGROUP	S.S.R.T.
-	-	15.4	-	-	2.9	-	-
500	0	-	15.5	12.1	-	3.2	5.3
0	40	-	15.3	13.3	-	2.2	4.2
0	50	-	15.9	13.1	-	1.6	4.3

(iii) Axial load distribution.

E_0 lbf/in ²	m lbf/in ² /in	Lateral displacement in.		
		Test	PGROUP	S.S.R.T.
-	-	0.0074	-	-
500	0	-	0.0056	0.0042
0	40	-	0.0078	0.0077
0	50	-	0.0066	0.0066

(iv) Lateral displacement.

Table 5.6.: Comparison with Davisson and Salley.

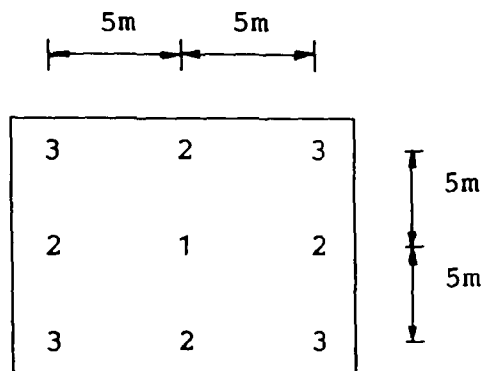


Figure 5.1.: Pile arrangement for axial loading.

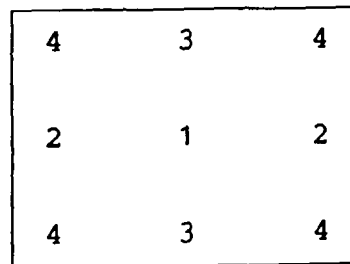
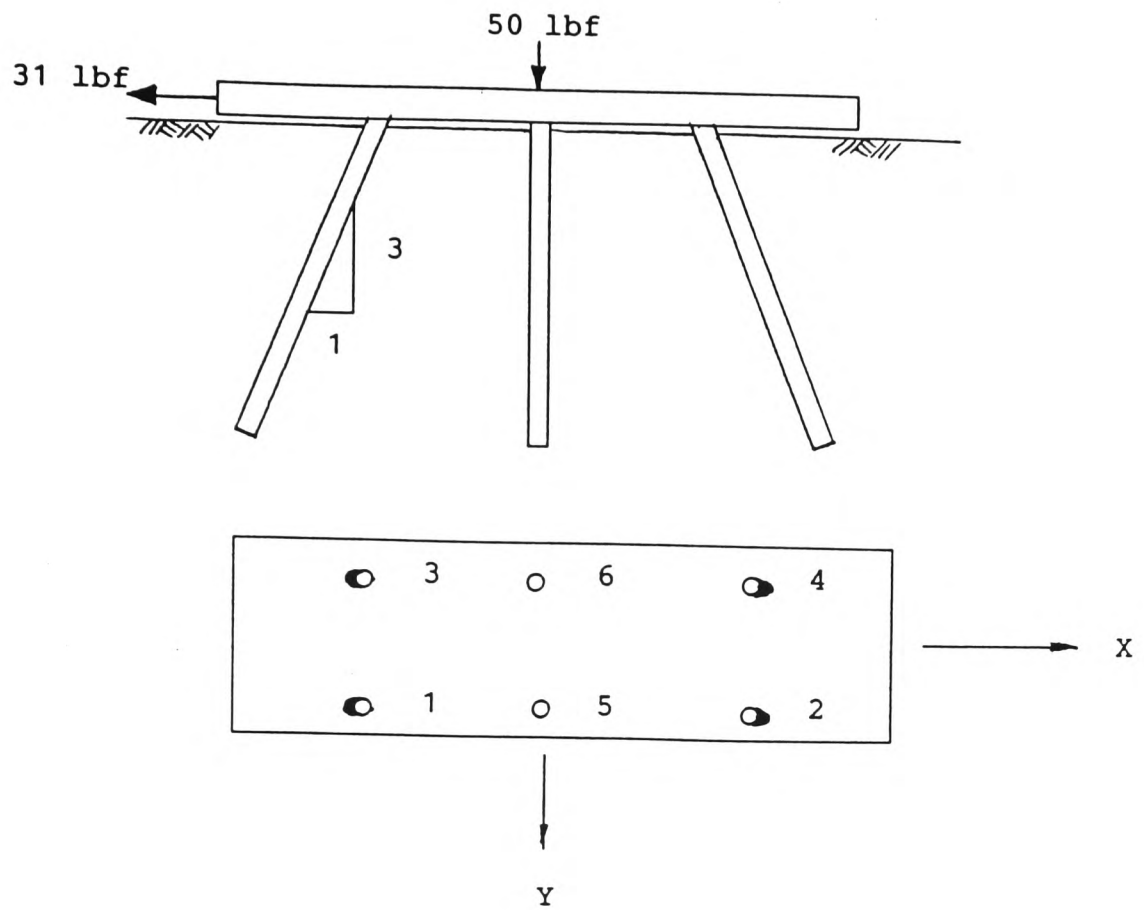
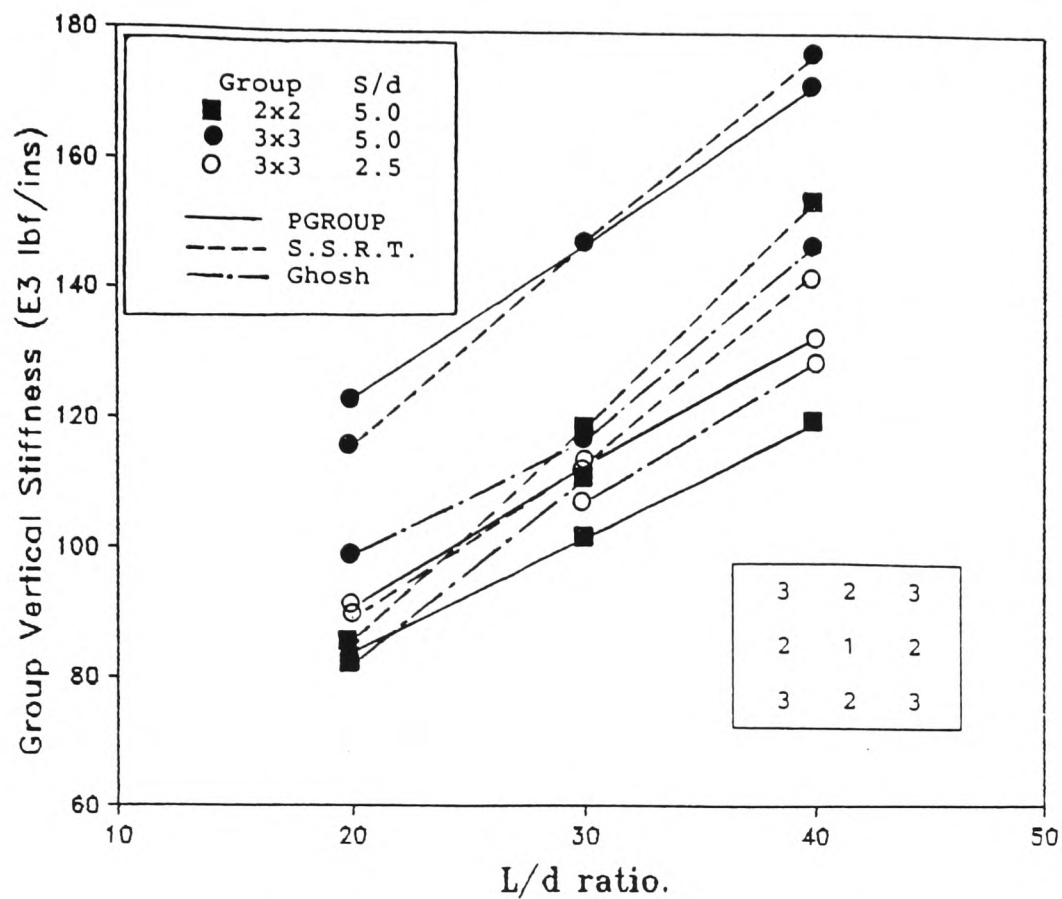


Figure 5.2.: Pile arrangement for lateral loading.



Pile No.	Moment (lbf.in)			Shear force (lbf)			Axial load (lbf)		
	Test	PGROUP	SSRT	Test	PGROUP	SSRT	Test	PGROUP	SSRT
1	11.5	9.4	10.3	5.0	3.7	4.2	18.0	15.3	13.3
2	13.2	10.9	11.4	5.2	4.2	4.5	2.8	2.2	4.2
3	11.2	9.4	10.4	5.2	3.7	4.2	12.8	15.3	13.3
4	10.8	10.9	11.4	3.8	4.2	4.5	3.1	2.2	4.2
5	10.6	10.0	11.0	3.8	3.9	4.4	6.5	8.2	8.2
6	10.4	10.0	11.1	3.6	3.9	4.4	5.4	8.2	8.5

Figure 5.3.: Comparison with Davisson and Salley.



(a) Group vertical stiffness.

		Pile type 1			Pile Type 2			Pile type 3		
L/D	S/D	Test	PGROUP	SSRT	Test	PGROUP	SSRT	Test	PGROUP	SSRT
30	2.5	8.8	3.5	10.5	9.8	9.2	11.0	13.0	14.9	11.6
40	2.5	9.6	4.3	10.5	10.9	9.4	10.9	11.7	14.5	11.5
20	5	8.0	5.4	9.9	8.6	9.7	10.9	14.4	13.9	12.0
30	5	10.0	5.3	10.0	10.4	9.7	11.0	12.1	14.0	12.0
40	5	9.6	5.6	10.1	9.3	9.8	11.0	13.3	13.8	12.0

(b) Axial load distribution at the pile heads (lbf).

Figure 5.4.: Comparison with Ghosh.

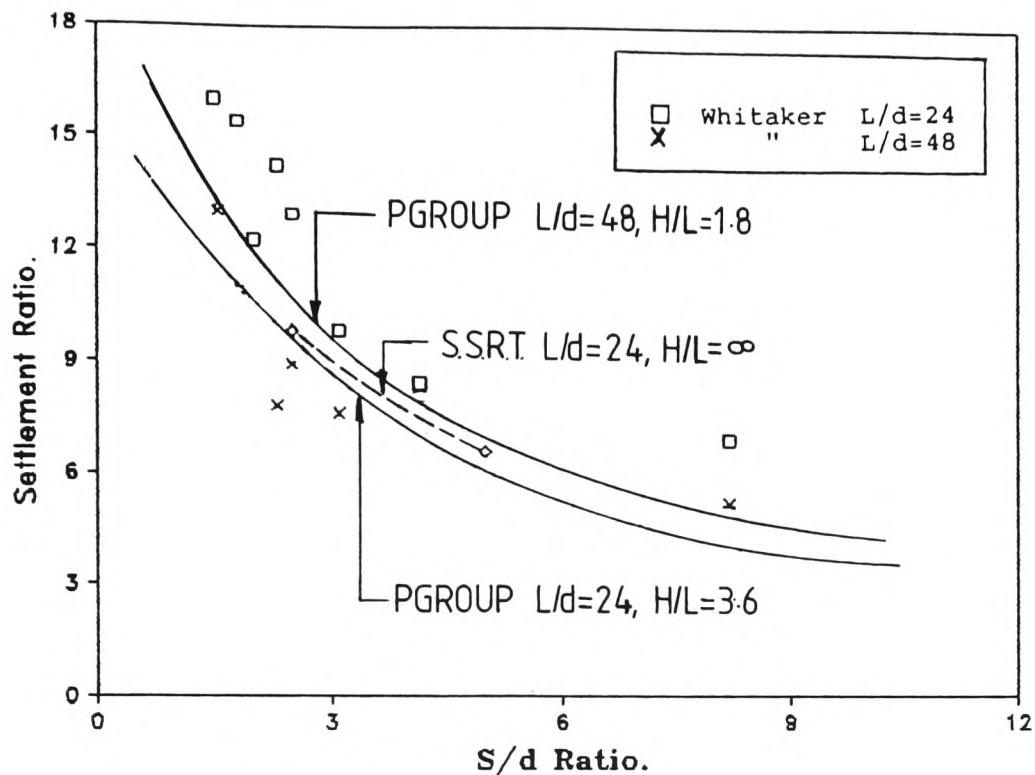


Figure 5.5.: Comparison with Whitaker.
5x5 pile groups.

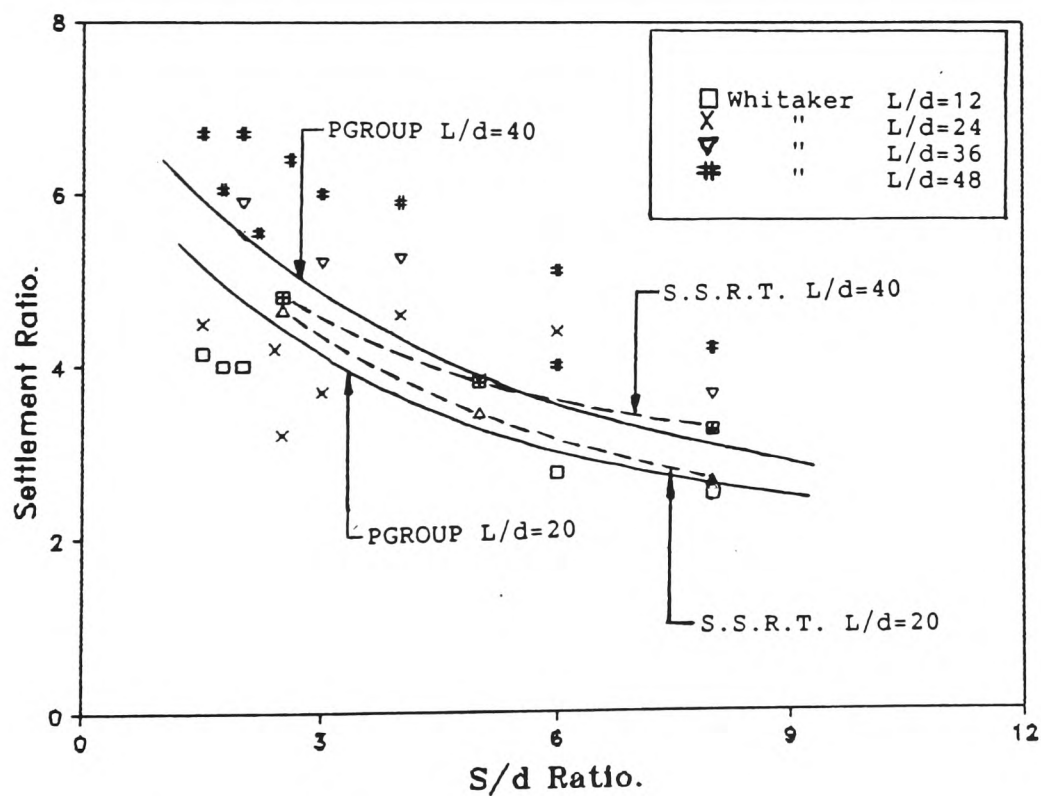


Figure 5.6.: Comparison with Whitaker.
3x3 pile groups.

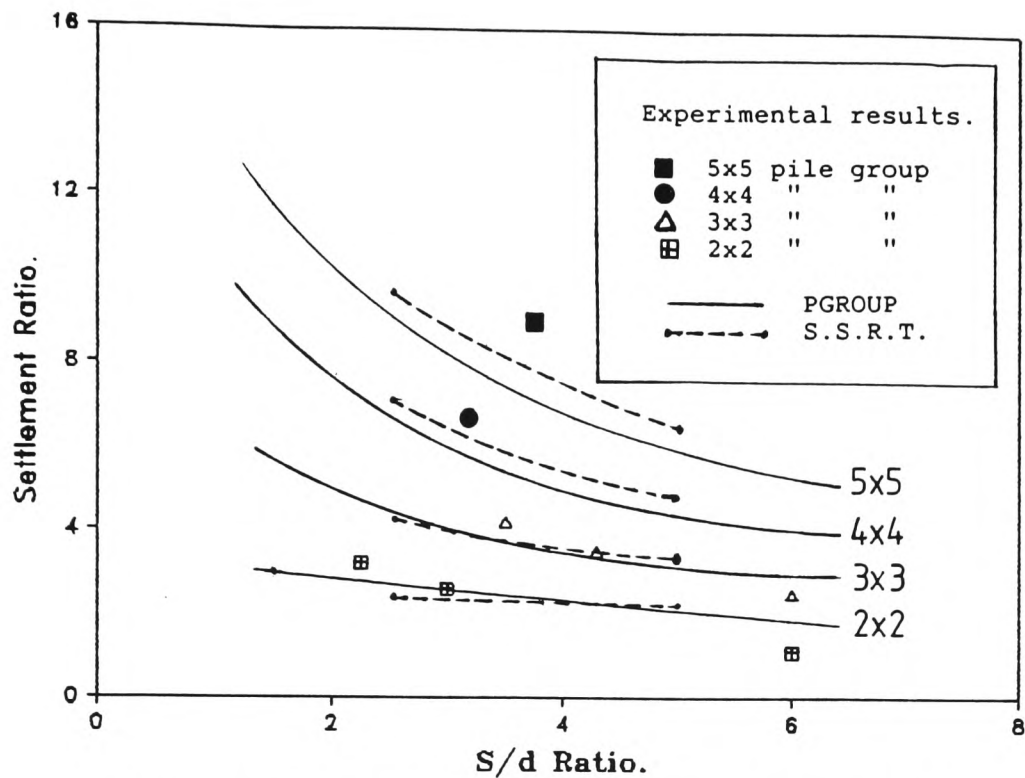


Figure 5.7.: Comparison with Berezantzev et al.

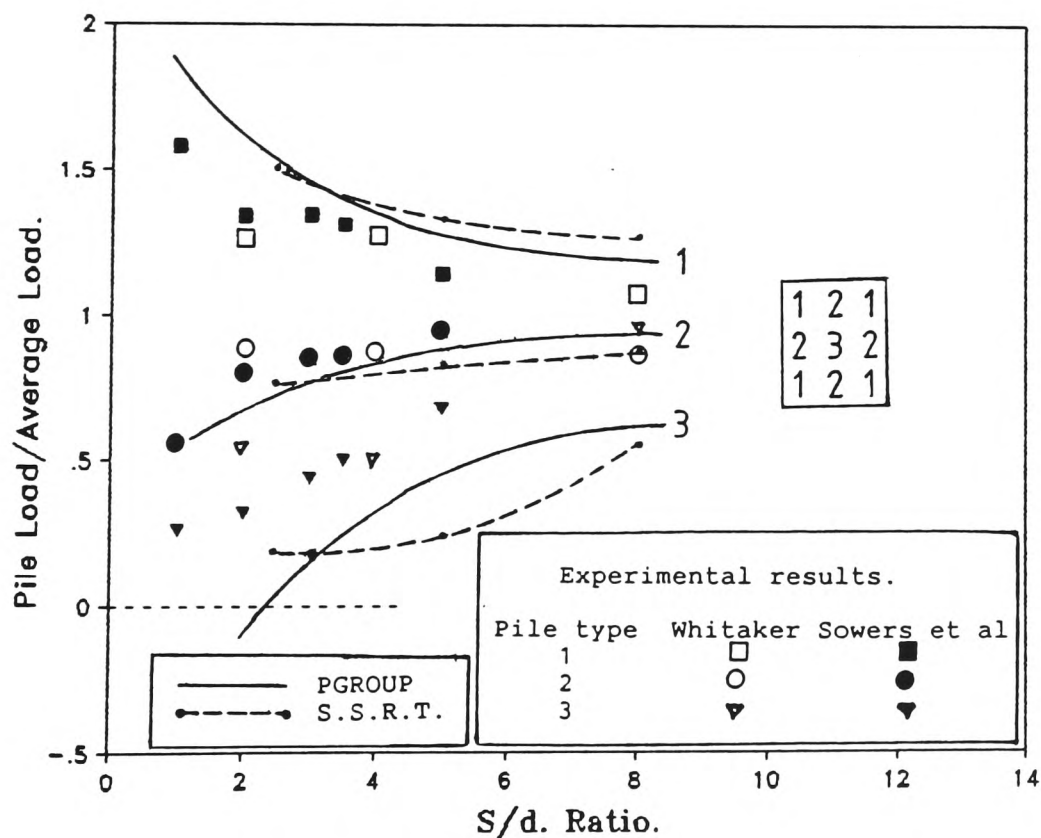
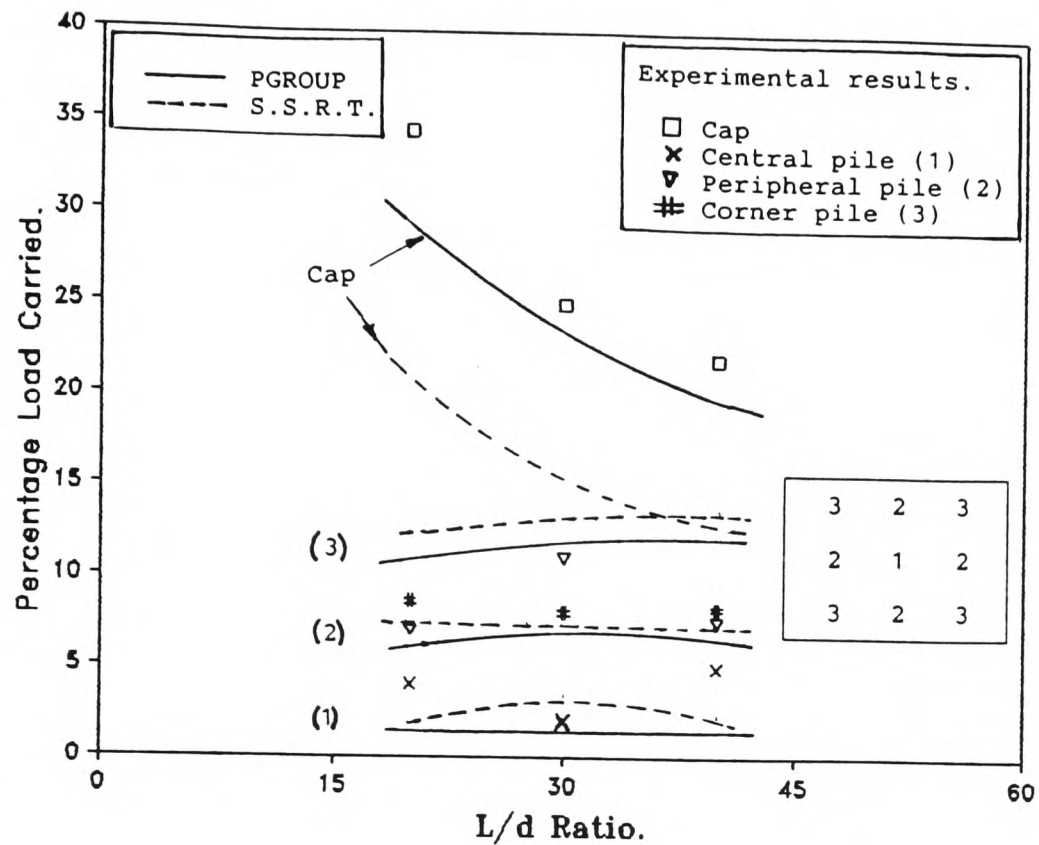


Figure 5.8.: Comparison with Whitaker and Sowers et al.
Load sharing between piles.



(a) Load distribution of 3x3 group with contacting cap.

L/D	Simplified analysis				Full analysis			
	Pile 1	Pile 2	Pile 3	Cap	Pile 1	Pile 2	Pile 3	Cap
20	8.0	9.0	10.5	13.0	1.5	6.0	10.5	13.0
30	8.5	9.5	10.5	15.0	3.5	7.0	13.0	15.0
40	9.0	10.0	11.0	21.0	2.5	7.5	14.0	21.0

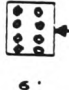
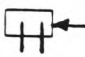
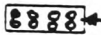
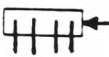



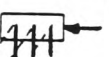

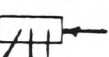

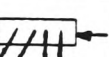

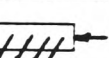
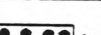
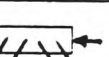
(b) S.S.R.T. axial load distribution (%).

L/D	Test	PGROUP	S.S.R.T.(1)	S.S.R.T.(2)
20	106.0	116.2	124.5	128.0
30	118.3	143.8	147.1	151.0
40	150.1	170.8	171.2	176.0

(c) 3x3 Group vertical stiffness values.
(lbf/in² x 10³)

S.S.R.T.(1) - Simplified analysis.
 S.S.R.T.(2) - Full analysis.

Figure 5.9.: Comparison with Ghosh.

Test No.	Schematic diagram ¹		Result (A)			Result (B)		
	Plan	Elevation	Test	PGROUP	S.S.R.T.	Test	PGROUP	S.S.R.T.
1	12'  6'	5' 	4.8	4.8	3.9	0.0	0.0	0.0
2	6'  12'	5' 	5.8	5.3	5.1	0.0	0.0	0.0
3	6'  12'	5' 	7.0	7.3	10.3	0.04	0.06	0.06
4	9'  10'	5' 	7.1	5.8	4.4	0.05	0.08	0.09
5	6'  9'	5' 	7.3	8.1	7.1	0.05	0.07	0.07
6	6'  12'	5' 	9.0	8.4	13.4	0.07	0.11	0.12
7	6'  12'	5' 	9.0	8.2	7.5	0.21	0.27	0.34
8	6'  12'	5' 	15.8	11.7	13.5	0.0	0.0	0.0

¹ ○ = Vertical pile ● = Battered pile

Result (A) = Lateral load for 1/4 inch deflection, Tons per pile

Result (B) = Lateral deflection due to vertical load
of 20 Tons per pile, in inches.

Figure 5.10. Comparison with Feagin.

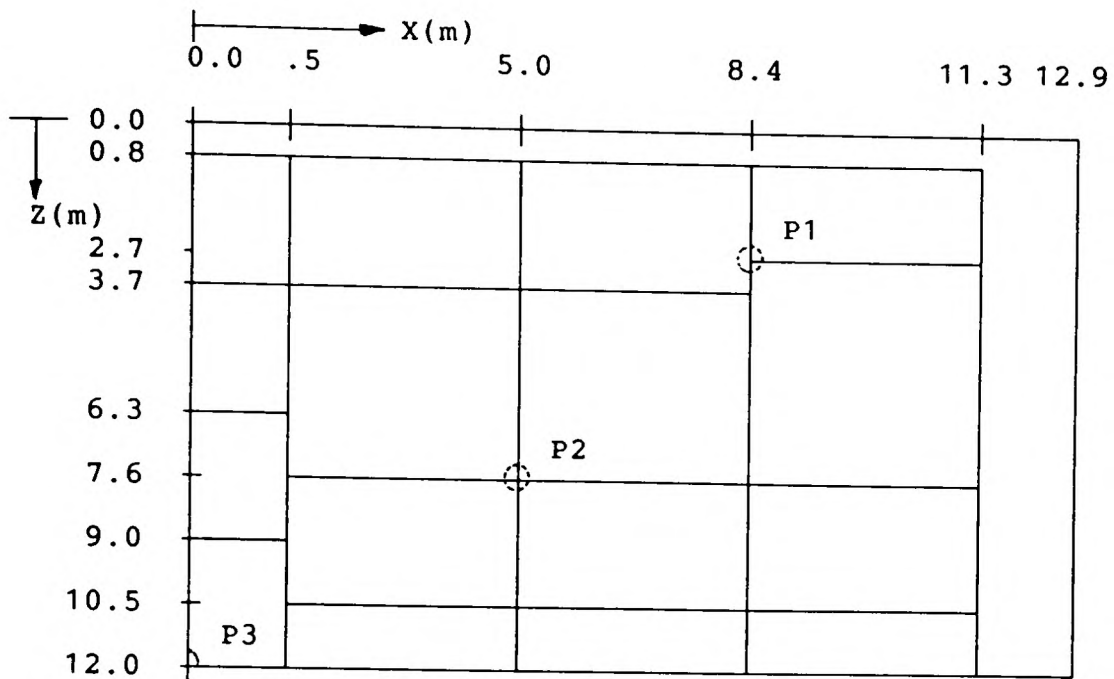


Figure 5.11. Plan Of Raft-Pile Foundation And Idealized Grillage Mesh.

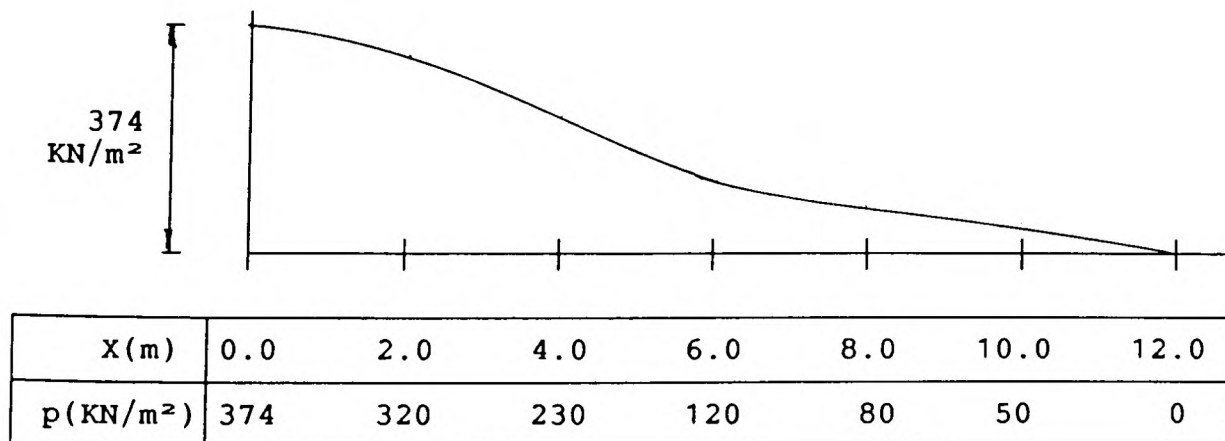
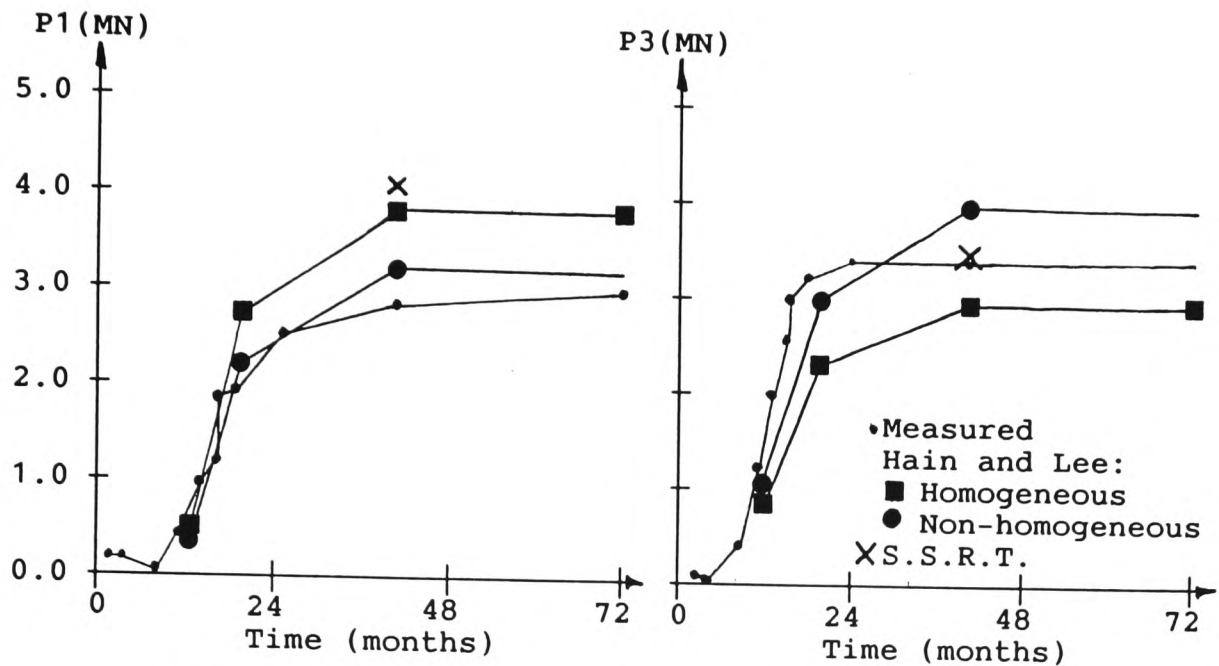


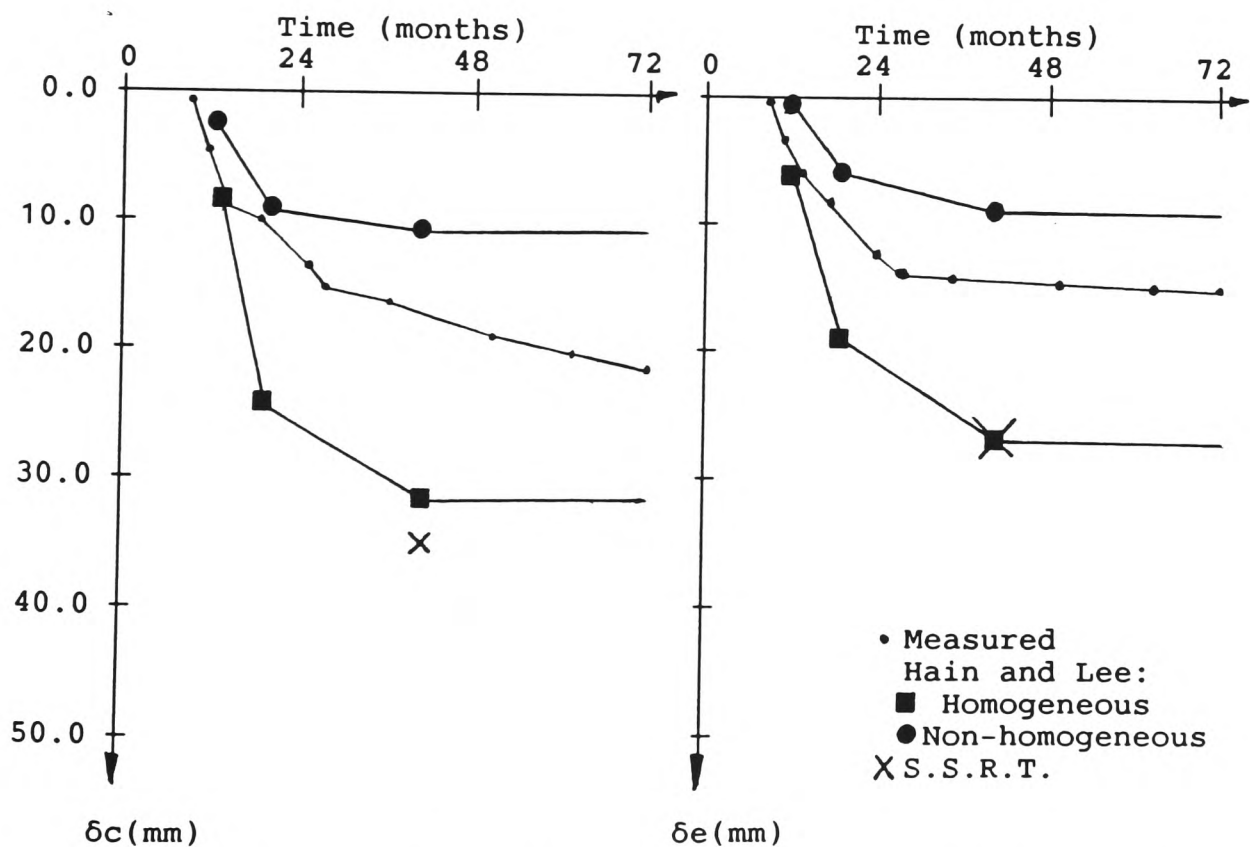
Figure 5.12. Idealized applied loading.



(a) Axial load in P1.

(b) Axial load in P3.

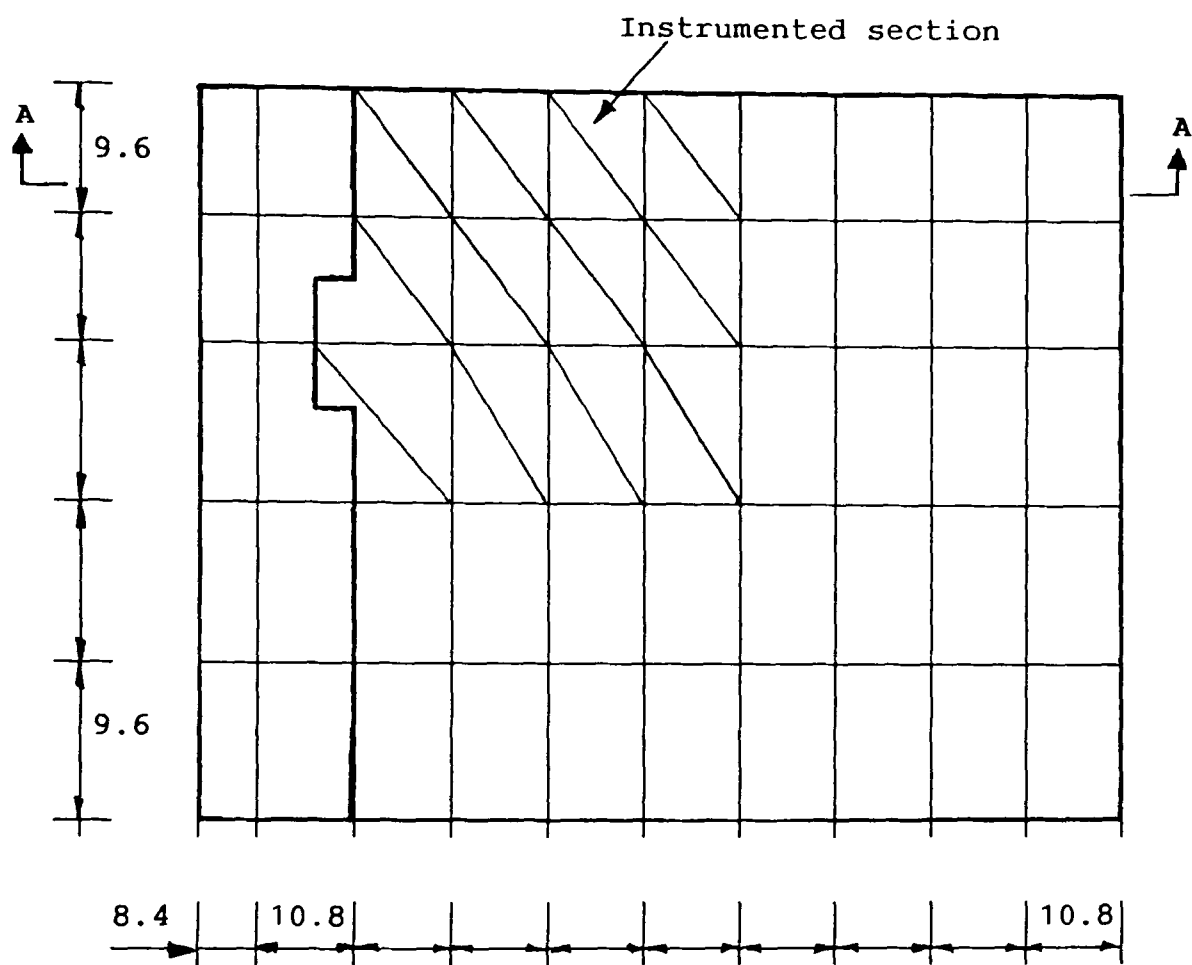
Figure 5.13. Comparison of measured and computed pile loads.



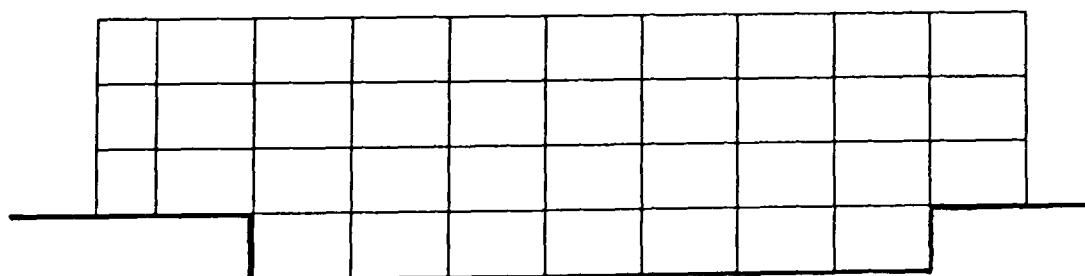
(a) Settlement at centre of raft (δ_c).

(b) Settlement at edge of raft (δ_e).

Figure 5.14. Comparison of measured and computed Settlements.



Dimensions in metres.



SECTION A-A

Figure 5.15.: Plan and section of building at Basildon.

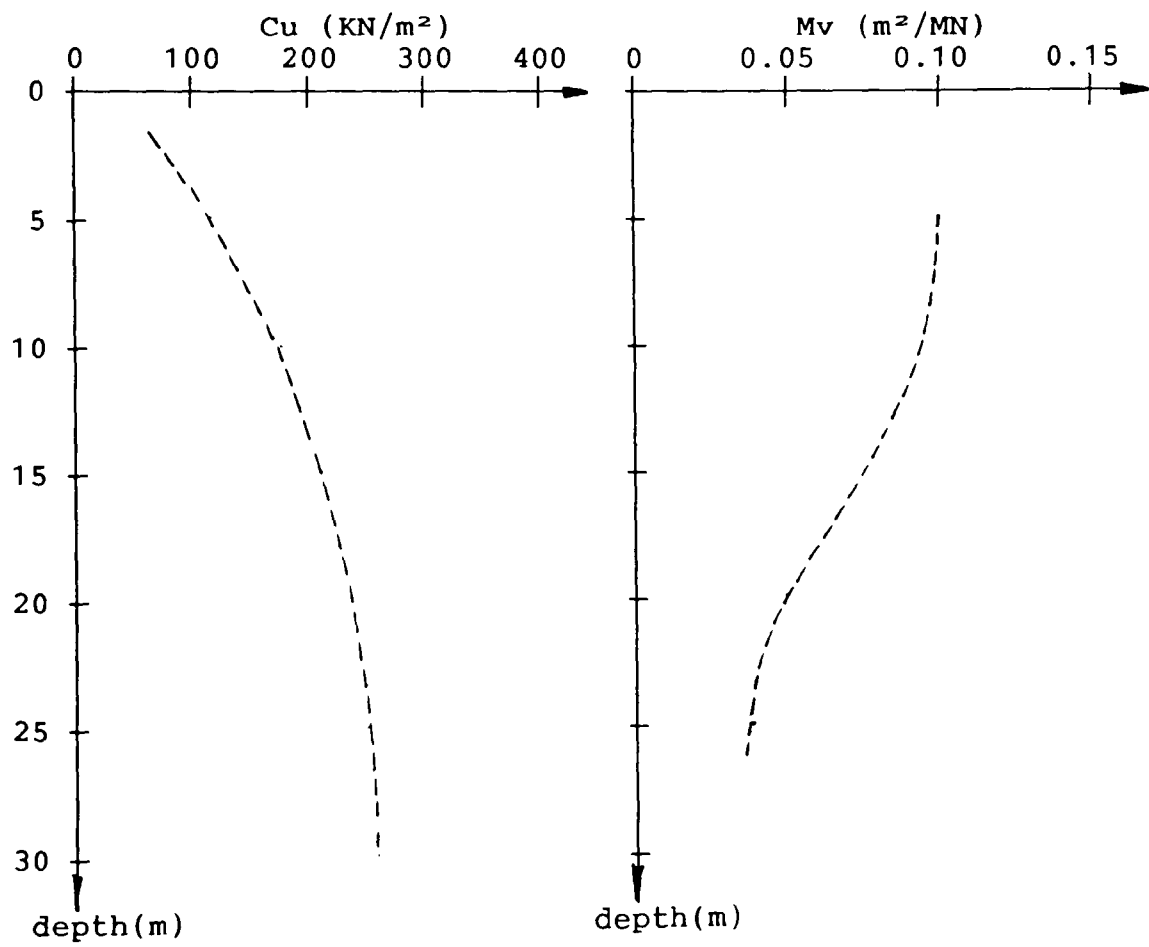


Figure 5.16.: Soil characteristics.

	14	13	12	12	12	11	11	11	11
15	(69)	15	15	(51)	14	14	(36)	14	14
16	(69)	15	17	(55)	16	18	16	18	17
16 17	(64)	16	17	(51)	17	18	(49)	17	18
15	(72)	16	16	(55)	17	19	18	20	18
15	16	16	17	(49)	17	18	(50)	18	18
(70)	(61)	16	19	(55)	17	19	18	19	18
16	(60)		(49)		(50)		(50)		(50)

(a) Results from Rickard et al.

	3	8	12	14
5	(192)	10	(160)	(155)
7	(110)	12	(69)	17
6	(88)		(67)	(47)
8	(100)			(39)
(154)	9	14	19	23
9		(53)	(85)	(27)
8	(117)			
(202)				

(b) S.S.R.T. results.

Figure 5.17. Grillage, Short term computed settlement (mm) and Pile load as % of column load (No. in brackets).

	3150 -500	3000 -500	3950 -1200	3950 -1300	3950 -1300
	3150 -500	2650 -500			
	4300 0	4350 -2950	5400 -4000	5400 -4100	5400 -4100
3250 0	3150 0				
		5400 -4100	5400 -4100	5400 -4100	5400 -4100
3250 0	3050 0				
	4250 -350	5400 -4100	5400 -4100	5400 -4100	5400 -4100

(a) Results from Rickard et al. (negative is tension.)

	1740 -750	2900 -1311	5610 -2610	6670 -3110	
	2000 -920	2490 -1270			
	2400 -1150	3640 -1740	3420 -1710	2830 -1400	
2220 -1020	2810 -1410				
		3830 -1930	6130 -3100	1980 -980	
2910 -1290					
	3260 -1570				

(b) S.S.R.T. results (negative is tension.)

Figure 5.18. Pile design loads

1.7	2.5	3.5	3.3	2.6
(-299)				
x (37.5)	x (6.5)	x (4.5)	x (1.1)	
5.7	4.6	3.8	2.8	2.9
(1192)				
5.8 x (14.7)	x (-24.2)	x (-5.3)	x (2.8)	
6.2	4.1	2.4	2.4	2.3
		(-122)		(-1038)
x (4.4)	x (6.5)	x (-0.4)		x(-8.8)
6.5	4.3	3.1	2.8	3.3

Figure 5.19. Observed Settlements (mm) and Slab/Soil effective stresses (KN/m²) (in brackets, negative is tension).

CHAPTER 6.

DEVELOPMENT OF A CONSISTENT SOIL MATRIX.

6.1. INTRODUCTION.

It has been demonstrated in previous chapters that the stiffness method of analysis coupled with the simplified subgrade reaction theory (S.S.R.T.) can be applied to the analysis of piled foundations.

A disadvantage of the above approach is the need to subdivide the pile into several elements, especially the discretization of laterally loaded piles. This is necessary to enable values of the soil spring stiffness to be distributed at nodes along the shaft. Chow (1987) recommended 15 graded elements to be used for the lateral response and 10 for the axial response. However, for a 3x3 pile group the solution of the stiffness matrix can take over 30 minutes on a microcomputer due to the large number of elements involved. To overcome this problem, consistent soil matrices are presented which represent the continuously distributed subgrade resistance over the length of the element. This enables the number of pile elements required to adequately define pile-soil interaction to be considerably reduced.

6.2. PROPOSED METHOD OF ANALYSIS.

The behaviour of a laterally loaded pile embedded in an elastic subgrade is similar to that of a beam resting on an elastic subgrade. As shown in Figures 6.1.(a) and (b) both elements are resisted in their direction of movement by the subgrade. Thus, the same solution for a beam can be used for a pile. Smith (1982) presented such a solution in

the form of a stiffness matrix $[Ks_h]$ which represents the lateral stiffness of the subgrade surrounding the pile element. The formulation of the stiffness matrix $[Ks_h]$ is analogous to the inertia matrix for a beam in free vibration. The matrix presented below has been rearranged in order to be compatible with the standard formulation of the stiffness matrices.

$$Ks_h = K_h' \cdot L' \begin{bmatrix} 13/35 & 11L'/210 & 9/70 & -13L'/420 \\ 11L'/210 & L'^2/105 & 13L'/420 & -L'^2/140 \\ 9/70 & 13L'/420 & 13/35 & -11L'/210 \\ -13L'/420 & -L'^2/140 & -11L'/210 & L'^2/105 \end{bmatrix} \begin{pmatrix} \delta_{y1} \\ \theta_{z1} \\ \delta_{y2} \\ \theta_{z2} \end{pmatrix}$$

Where,

K_h' = lateral subgrade modulus

L' = length of element

δ_{y1}, δ_{y2} = lateral displacements at ends 1 and 2 of the element

θ_{z1}, θ_{z2} = rotations at ends 1 and 2 of the element.

The stiffness matrix for the pile element Kp_h is given by:

$$Kp_h = \frac{EI}{L'} \begin{bmatrix} 12/L'^2 & 6/L' & -12/L'^2 & 6/L' \\ 6/L' & 4 & -6/L' & 2 \\ -12/L'^2 & -6/L' & 12/L'^2 & -6/L' \\ 6/L' & 2 & -6/L' & 4 \end{bmatrix} \begin{pmatrix} \delta_{y1} \\ \theta_{z1} \\ \delta_{y2} \\ \theta_{z2} \end{pmatrix}$$

in which,

E = Young's modulus of the pile,

I = second moment of area of the pile.

Addition of the two stiffness matrices $[Kp_h] + [Ks_h]$ represents the system shown in Figure 6.2.(a). In this

idealization, $[Ks_h]$ has been determined from consideration of an infinite number of springs acting along the element. $[Ks_h]$ is therefore the consistent soil matrix. This is a significant improvement on the S.S.R.T. where the stiffness $Kh.L'/2$ is added to the pile matrix in the local y direction at each node.

To complement the consistent matrix for the representation of the lateral behaviour of the pile a consistent matrix to idealize the axial behaviour of the pile was developed. Dr R. Delpak suggested that the consistent soil matrix for axial behaviour is analogous to the matrix for a rod subject to free vibration along its axis.

The $[Ks_v]$ matrix shown below represents the stiffness contribution of an infinite number of vertical springs surrounding a vertical rod element of length L' . The derivation of this matrix is presented in Appendix C.

$$Ks_v = Kv'.L' \begin{bmatrix} 1/3 & 1/6 \\ 1/6 & 1/3 \end{bmatrix} \begin{pmatrix} \delta_{x1} \\ \delta_{x2} \end{pmatrix}$$

Where,

Kv' = axial subgrade modulus.

δ_{x1}, δ_{x2} = axial displacements at ends 1 and 2 of the element.

The stiffness matrix for a rod element $[Kp_v]$ is as given below.

$$Kp_v = \frac{EA}{L'} \begin{bmatrix} 1 & -1 \\ -1 & 1 \end{bmatrix} \begin{pmatrix} \delta_{x1} \\ \delta_{x2} \end{pmatrix}$$

Where A = cross sectional area of the element.

Adding $[Kp_v] + [ks_v]$ provides a matrix which represents the axially loaded pile system shown in Figure 6.2.(b). Again the soil matrix has been derived on the basis of an infinite number of springs. This is an improvement on the S.S.R.T. where $K_v.L'/2$ is added to the pile matrix in the local x direction at each node.

The end bearing resistance is represented as a spring having a stiffness of K_{eb} .

Combining the matrices for axial and lateral behaviour yields a 6x6 matrix which represents the general pile-soil stiffness matrix for the solution of two-dimensional problems.

6.3. RESULTS.

Owing to the ease of data preparation, the stiffness matrix for a single pile-soil system can be assembled manually. Having established the stiffness matrix, solutions are obtained utilizing the traditional stiffness approach. The stiffness matrix is inverted and multiplied against the load vector using the Gaussian elimination process. This procedure enables the pile displacement at nodal points along the pile shaft to be obtained directly. The internal axial load, shear force and moment distributions along the pile shaft are determined by multiplying the computed displacement vector by the original element stiffness matrix.

A computer program was developed to carry out the above procedures. This enabled numerous analyses as part of a parametric study to be efficiently carried out. The program was subsequently developed for the analysis of a

general pile raked in two planes in a multi-layered soil.

In order to verify the results and illustrate the applicability of the presented consistent matrix method (C.M.M.), comparisons have been made with the S.S.R.T. and the D.o.T. program PGROUP. Parametric studies were also carried out to assess the sensitivity of the results to the number of elements used to idealize the pile.

6.3.1. Laterally Loaded Pile.

(a) Mathematical modelling.

A pile of length 10m and diameter 0.5m subjected to a lateral load at the pile head of 1000KN was analysed. Elastic moduli were assumed for the soil and pile of 10MN/m^2 and 30GN/m^2 respectively. To study the effect of the fixity of the pile head, two conditions were analysed; one with a free head and the other with the head restrained against rotation.

It was demonstrated in Chapter 3 that the lateral subgrade modulus, K_h , is approximately related to the soil modulus, E_s , for a broad range of pile configurations by the following relationship:

$$K_h = E_s.L' \text{ (KN/m)}$$

where L' is the length of the element. The relative lateral stiffness K_R of the above pile was computed as 9.2×10^{-4} . For a L/d ratio of 20, this pile-soil configuration was within the range where the above relationship would provide satisfactory deflection results. Thus the C.M.M. analyses carried out in this section were based on this relationship. Due to the units in which K_h is defined in

the C.M.M., the following modified relationship is used:

$$Kh' = Es \text{ (KN/m}^2\text{)}$$

(b) Discussion of results.

The sensitivity of the lateral displacement δ_h and rotation θ_h to the number of elements for a pile with a free head is presented in Figure 6.3. The S.S.R.T. was shown to be highly sensitive to the number of elements used. Both the rotation and displacement were grossly underestimated using 1 element. This was because the top spring took a disproportionate load out of the pile. Over the range of 1 to 10 elements, δ_h ranged from 20 to 80mm and θ_h varied from 2×10^{-3} to 33×10^{-3} rads.

The PGROUP results were also sensitive to the number of elements used to idealize the pile. The program failed when 1 element was used, hence, results are presented over a range of 2 to 10 elements. The rotation and displacement were grossly overestimated using 2 elements, at 84×10^{-3} rads and 214mm respectively. These values decreased to 32×10^{-3} rads and 82mm when 10 elements were used.

The best convergence of results was achieved by the C.M.M.. The rotation of the pile head was constant at 36×10^{-3} rads and the displacement increased from 81.5 to 85mm as the number of elements was increased from 1 to 10.

In Figure 6.4. the sensitivity of the lateral displacement of the pile head δ_h to the number of elements for a pile with a restrained head is presented. It was not possible to use PGROUP for this comparison, because the pile head could not be restrained against rotation. The S.S.R.T. results indicate that the sensitivity of δ_h to the

number of elements used to idealize the pile is not as significant as that for the free pile head. In this case δ_h ranged from 20 to 43mm as the number of elements varied from 1 to 10. The lateral displacement for the C.M.M. increased from 30 to 43mm over the same range. For 2 elements δ_h was 40mm, which was within 7% of the lateral displacement for 10 elements. The reason for a poor prediction of δ_h using one element was probably caused by modelling a simplistic displacement pattern along the pile shaft. Hence, when the pile head was not completely free, at least 2 elements are required to satisfactorily predict the lateral pile-soil behaviour using the C.M.M..

The bending moment and shear force distributions for the C.M.M. are presented in Figure 6.5. for a pile with a free head. The results indicate that irrespective of the number of elements employed, the moment and shear force values lie on the curve produced by 10 elements. Superimposed on the same axes are the distributions for the PGROUP program for 10 elements. The agreement between the two curves was good, with the C.M.M. maximum moment being 8% greater than that of PGROUP. It is important that all values lie on the 10 element curve. This indicates that with a reduction in the number of elements to idealize the pile, the correct moment and shear distribution can be obtained using enhanced beam-column elements, such as those presented by Delpak and Peshkam (1984).

In Figure 6.6., the bending moment and shear force distribution for the C.M.M. are presented for a pile with a restrained head. For 1 element the bending moment was overestimated by 17%. However, all moment and shear values

computed using more than 1 element lay on the same curve for 10 elements. This was in agreement with the results presented in Figure 6.4.

6.3.2. Axially Loaded Pile.

(a) Mathematical modelling.

Piles of length 10 and 40m with diameters of 0.5 and 1m subjected to an applied axial load of 1000KN at the pile head were analysed. This gave a range of L/D ratios from 10 to 80. Again a value of 10MN/m^2 was assumed for the soil modulus, E_s , and a value of 30GN/m^2 for the pile modulus, E_p .

The work presented in Chapter 3 indicates that the axial subgrade modulus, K_v , is approximately related to the soil modulus, E_s , for a broad range of pile configurations by the following relationship:

$$K_v = E_s \cdot L' / 2 \text{ (KN/m)}$$

where L' is the length of the element. The computed relative axial stiffness K of the above piles was 3000. These pile configurations were generally within the range where the above relationship would provide satisfactory displacement results. The exception was the pile with a L/d ratio of 10, in which case the displacement would be overestimated by approximately 20% by inspection of Figure 3.13.

Due to the units in which K_v is expressed in the C.M.M., the following modified relationship is used:

$$K_v' = E_s / 2 \text{ (KN/m}^2\text{)}$$

(b) Discussion of results.

The sensitivity of the axial displacement δ_v to the number of elements for the various piles are presented in Figure 6.7.. The axial displacement from both the C.M.M. and S.S.R.T. was insensitive to the number of elements used. The two sets of results were practically coincident. Although the S.S.R.T. tended to underestimate the axial shortening of the pile, especially for a large spacing between springs, there seemed to be no advantage for using the C.M.M.. However, since the matrix formulation for the C.M.M. was almost as simple as that of the S.S.R.T., it should be used for the axial behaviour in order to be compatible with the lateral behaviour where the use of the C.M.M. was clearly advantageous.

The axial displacements computed by the S.S.R.T. using 10 elements and the C.M.M. using 1 element, overestimated those obtained from PGROUP by 20% at an L/D ratio of 10. At a L/d ratio of 80, the corresponding PGROUP displacements were underestimated by 7%.

Whereas the axial displacements from the C.M.M. and S.S.R.T. were insensitive to the number of elements, at least 3 elements were required by the PGROUP program to determine consistent results.

The axial load distributions along the various pile shafts from C.M.M. analyses are presented in Figure 6.8.. All load distributions were essentially uniform from the pile head to the tip. The load distributions were constant irrespective of the number of members used. Also superimposed on Figure 6.8.(a) is the distribution determined for 10 elements using PGROUP. This was almost

identical to the C.M.M. load distribution, except for an increased shedding of load near the pile tip.

In Figure 6.9. the axial load distributions along the pile shaft determined by PGROUP are shown. The load distributions determined from idealizations using various numbers of elements were basically identical. However, as the number of elements increased the load at the tip decreased. For a 10m long pile with a diameter of 1m, the load transferred to the tip decreased from 132 to 75KN as the number of elements used was increased from 1 to 10.

6.4. CONCLUSIONS.

Consistent soil matrices are presented which represent the continuously distributed axial and lateral subgrade resistance over the length of a pile element. Results from the proposed method were compared with those from PGROUP and the S.S.R.T. Parametric studies were carried out for each method of analysis considered. This was undertaken to examine the convergence of results with the number of elements used.

The convergence tests were carried out for the simple case of a single pile loaded both laterally and axially. The effect of pile head fixidity was also examined.

The S.S.R.T. displacement results for an idealized laterally loaded pile with a free head were highly sensitive to the number of elements used. The PGROUP results were also sensitive to the number of elements ie. the convergence of results was poor. The convergence of results computed by the C.M.M. was excellent.

For a laterally loaded pile with a restrained head, the S.S.R.T. displacement results were not as sensitive to the number of elements as those for a free head. The C.M.M. results for a pile with a restrained head were slightly more sensitive to the number of elements than those for a free head. However, the discrepancy between the results obtained using 2 and 10 elements was only 7%. Hence, when the pile head was not completely free, at least 2 elements were required to adequately idealize pile-soil behaviour using the C.M.M.. For the restrained head it was not possible to use the PGROUP program as the pile head could not be restrained against rotation.

Results for axially loaded piles from both the C.M.M. and the S.S.R.T. were insensitive to the number of elements used. Because the matrix formulation of the C.M.M. is simple, it is recommended that it is also used to model the soil response of axially loaded piles. This is in order to achieve compatibility with the lateral behaviour, where the use of the C.M.M. was clearly advantageous. Whereas the C.M.M. and S.S.R.T. were insensitive to the number of elements used, at least 3 elements were required by the PGROUP program to determine consistent results.

Due to the very encouraging results achieved, the use of consistent soil matrices in a large pile configuration would be clearly beneficial. This would result in a considerable reduction of the size of the stiffness matrix for the whole system. Thus the computer time would be reduced with a corresponding reduction in the cost of analysis of a given problem. Because the C.M.M. is incorporated within the stiffness matrix for the system,

current standard analysis packages cannot be used. Thus specific programs would have to be developed for piled foundation analysis such as the one developed for the analysis of single piles in this work.

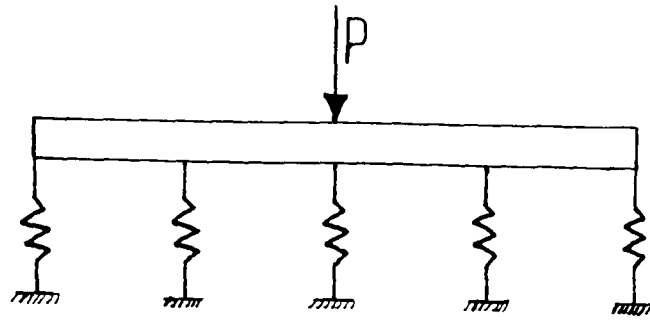


Figure 6.1.(a): Beam resting on an elastic subgrade.

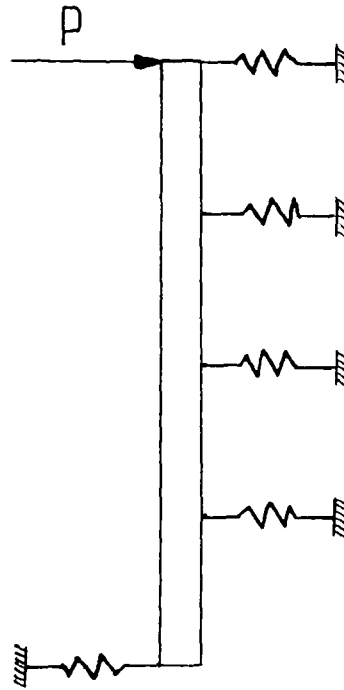


Figure 6.1.(b): Pile embedded in an elastic subgrade.

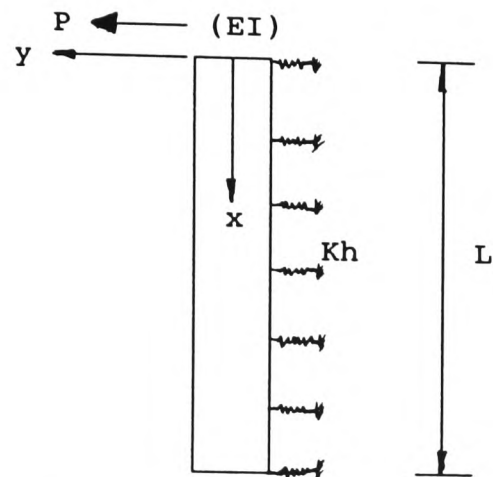


Figure 6.2.(a): Pile system subjected to a lateral load.

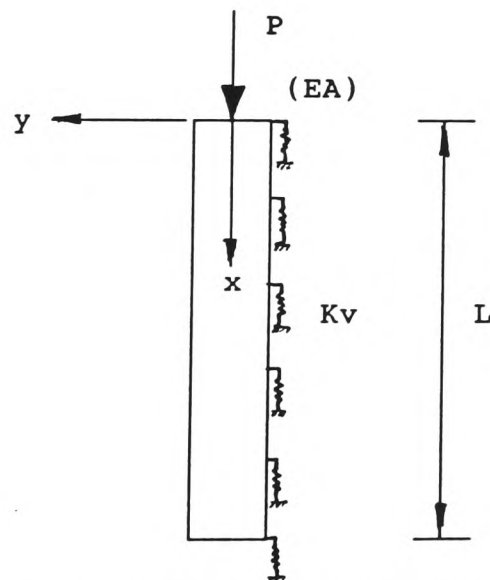
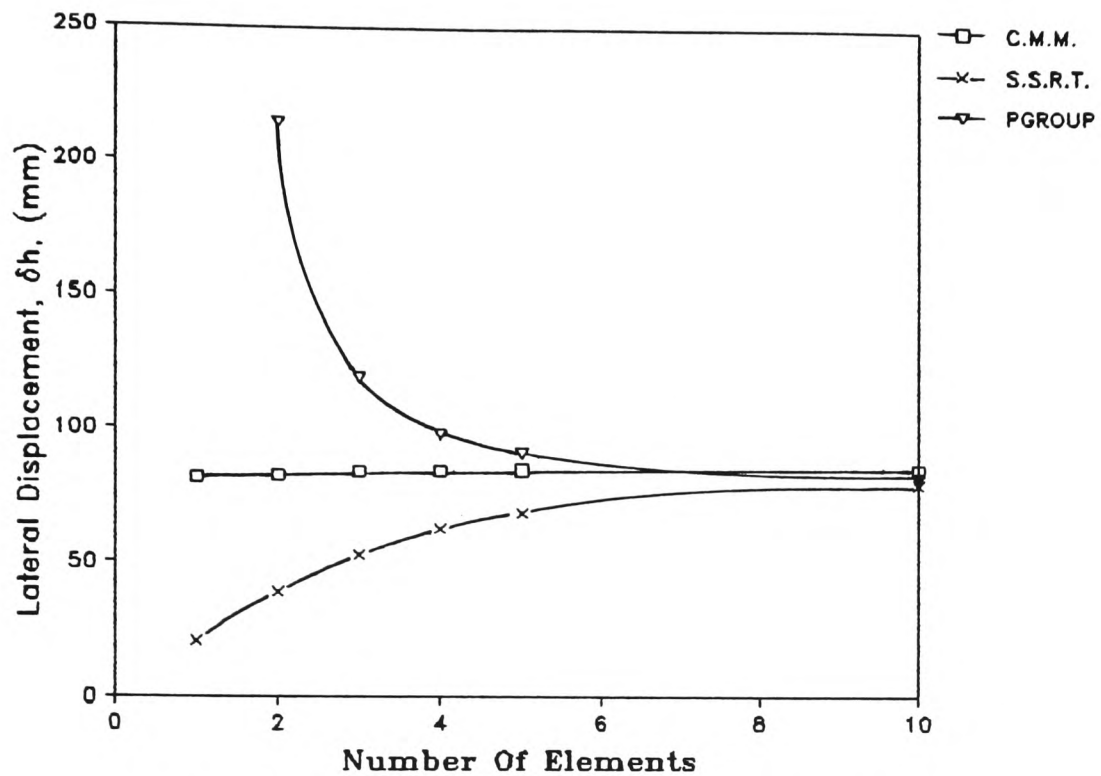
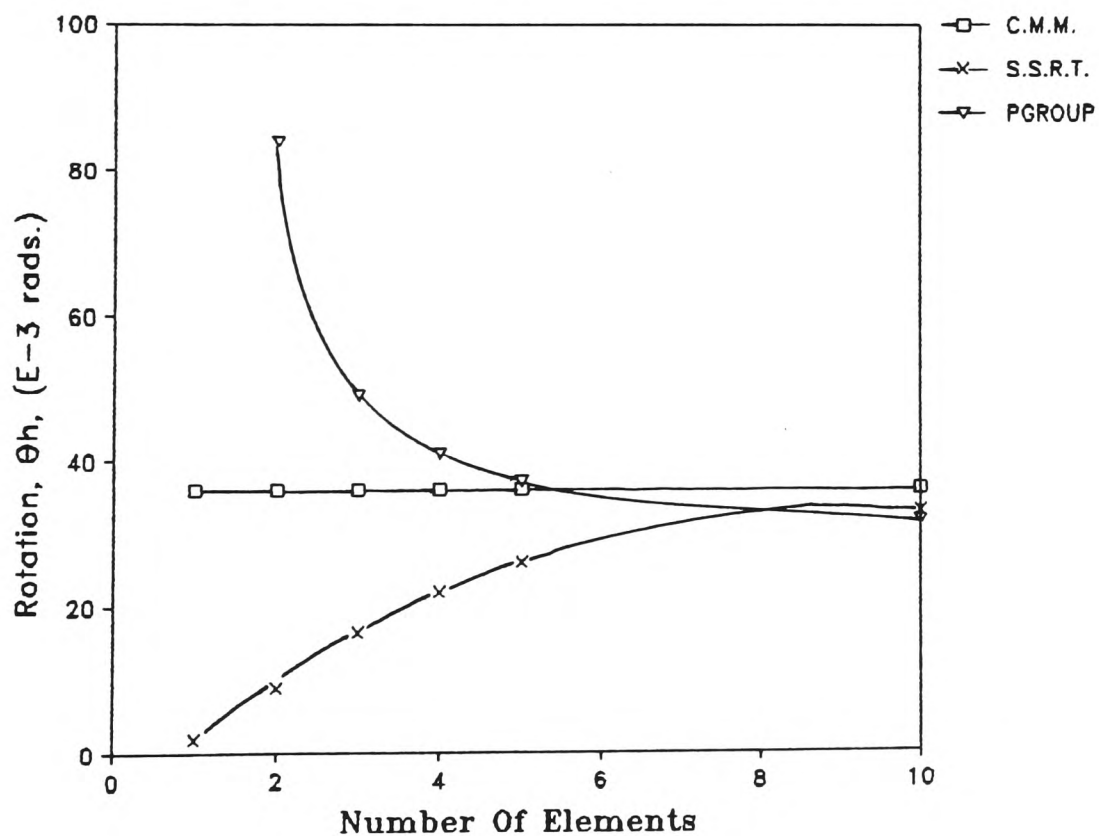


Figure 6.2.(b): Pile System Subjected To An Axial Load.

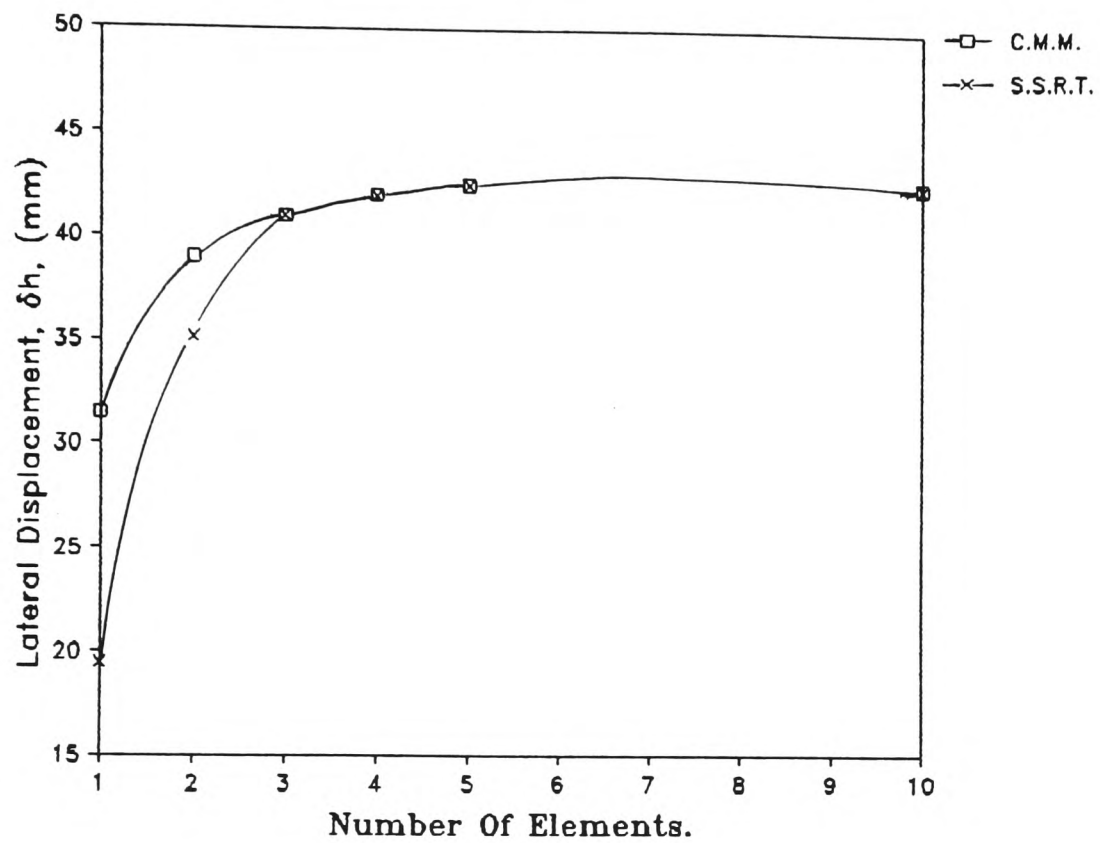


(a) Lateral displacement of pile head.



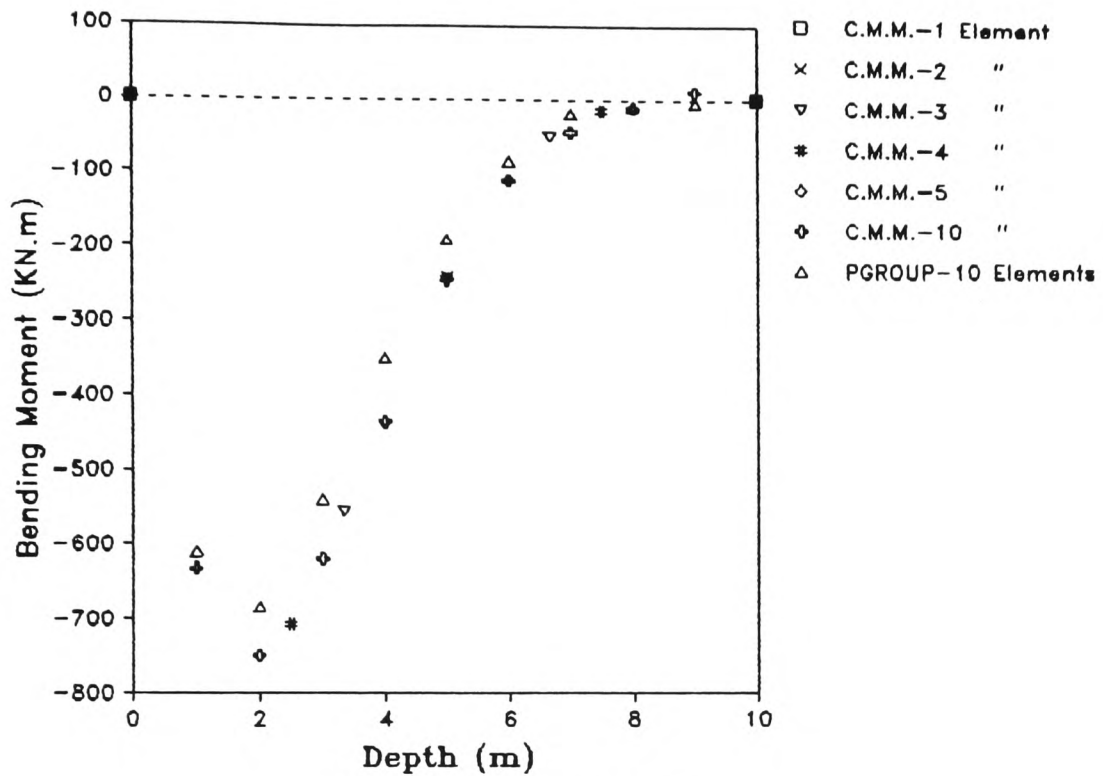
(b) Rotation of pile head.

Figure 6.3.: Results for free pile head.

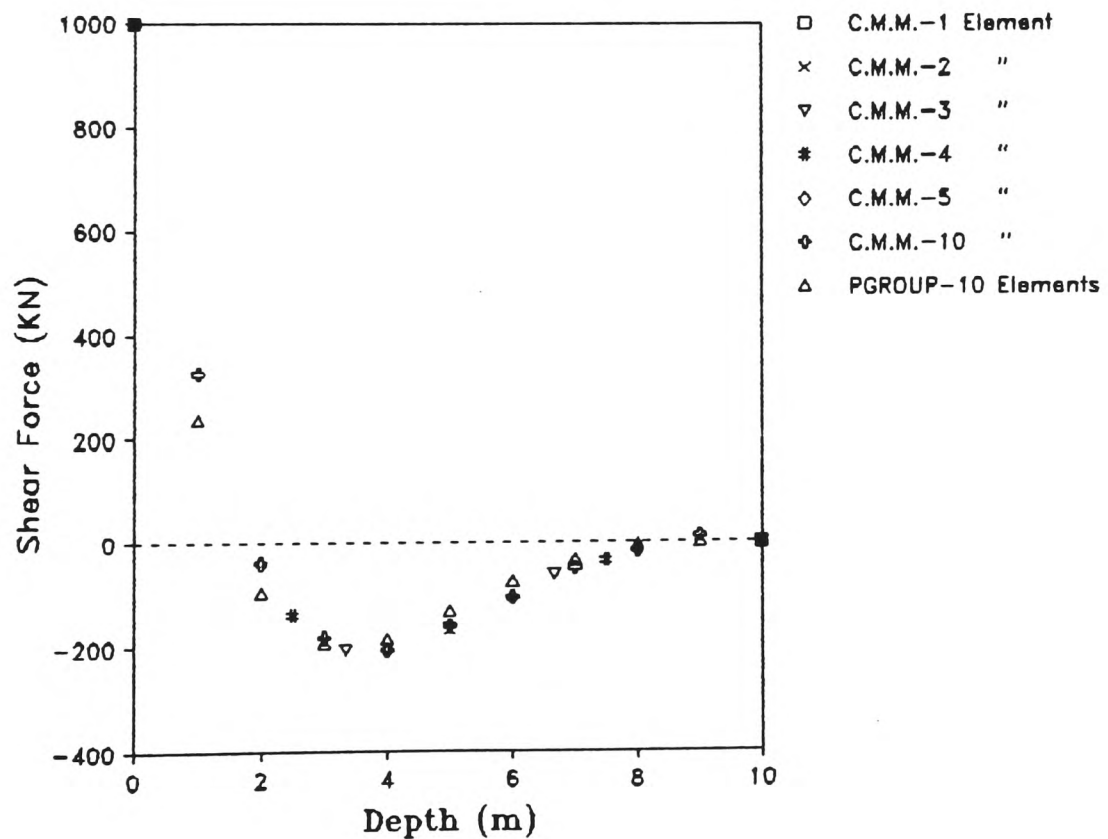


Lateral displacement of pile head.

Figure 6.4.: Results for restrained pile head.

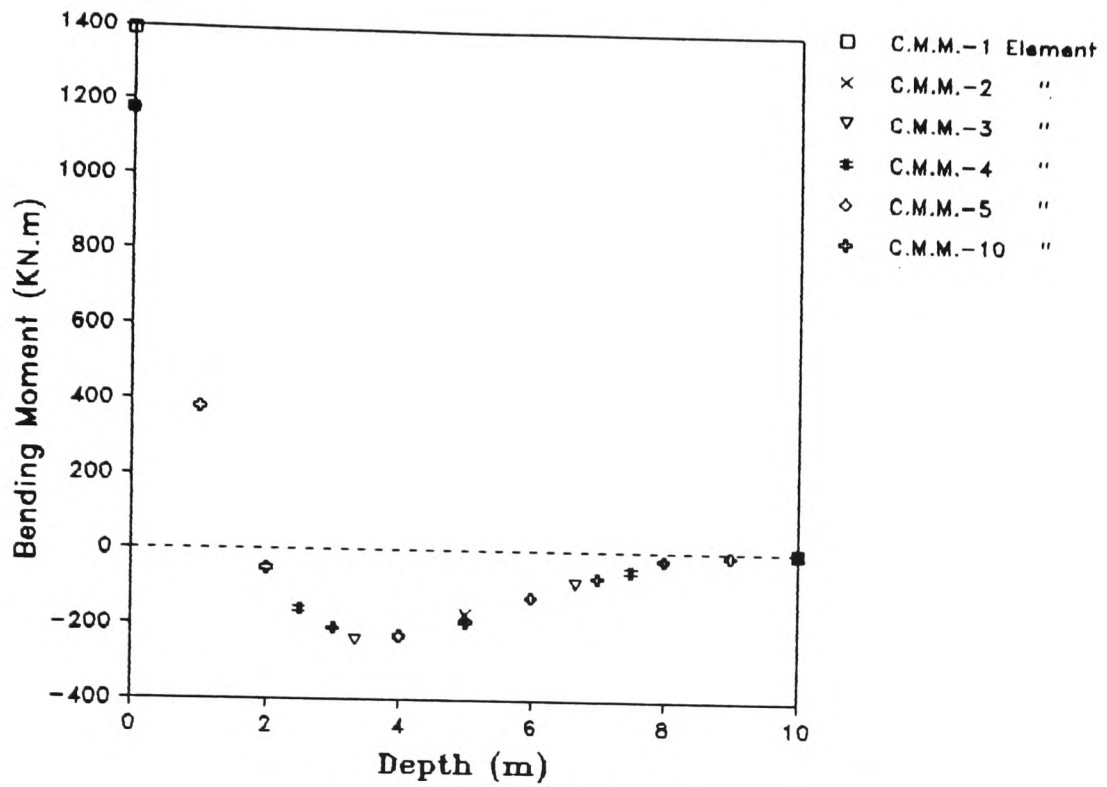


(a) Bending moment.

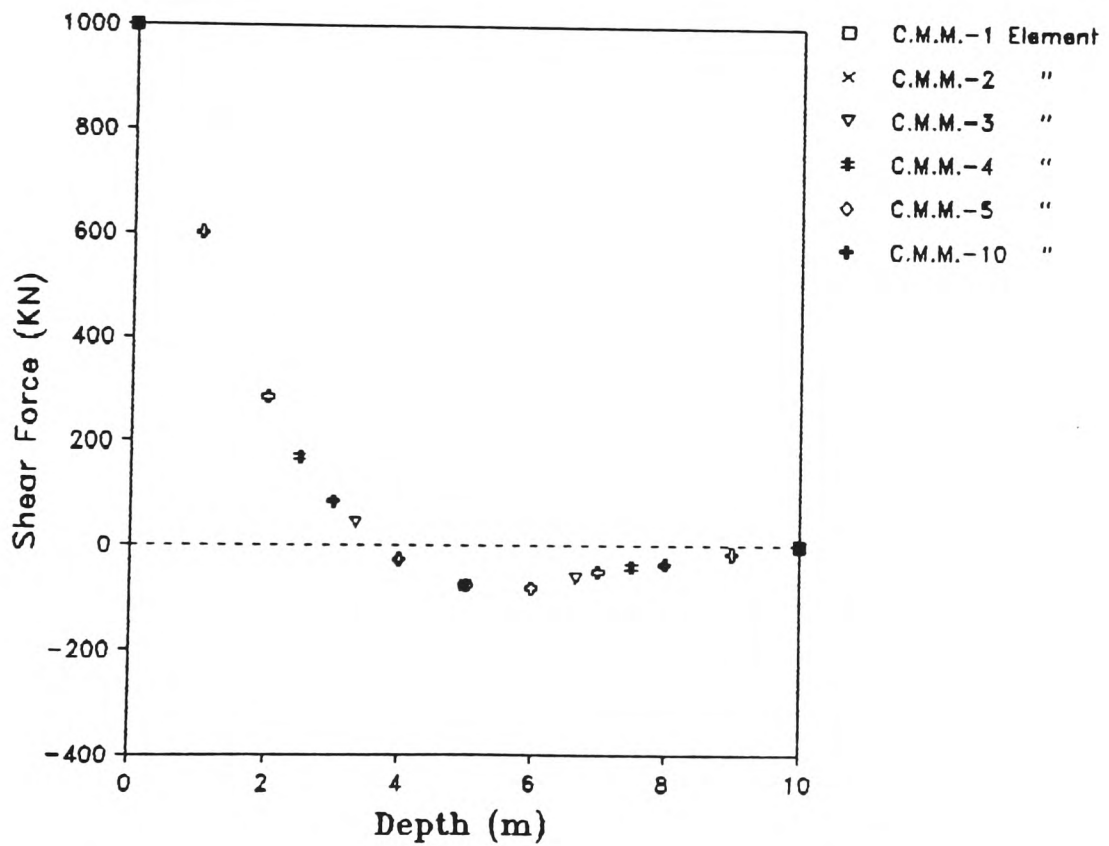


(b) Shear force.

Figure 6.5.: Convergence results for a free pile head.

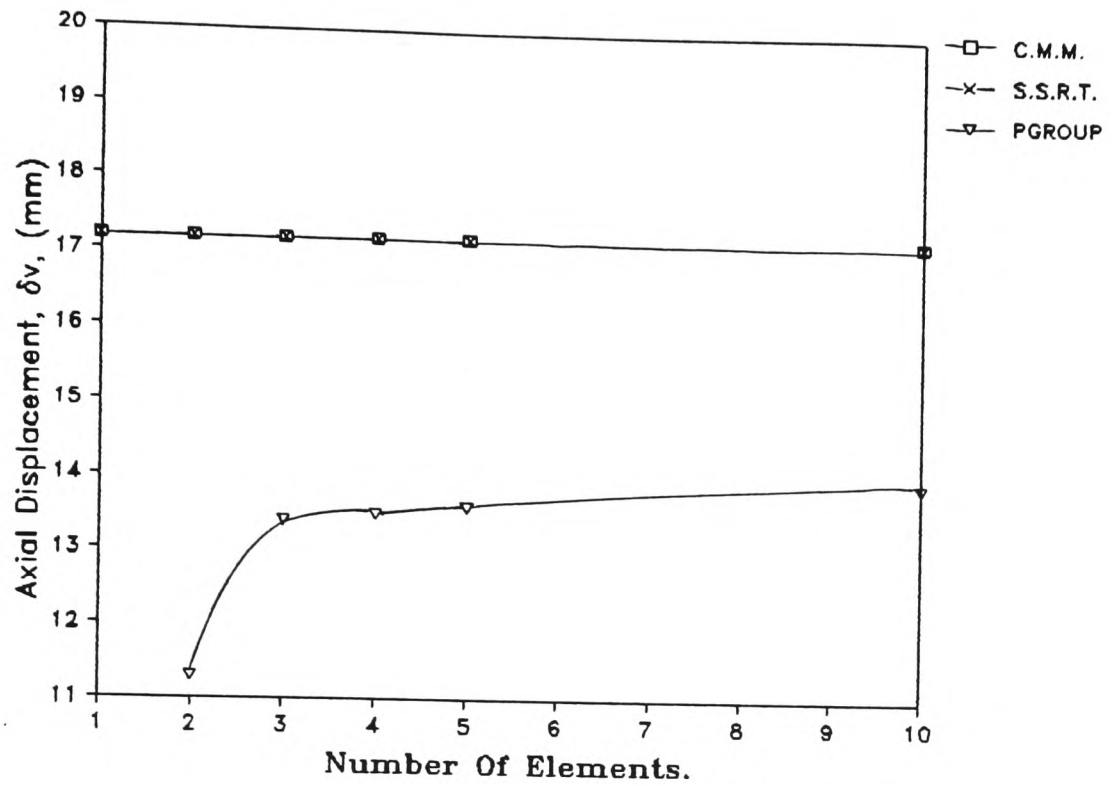


(a) Bending moment.

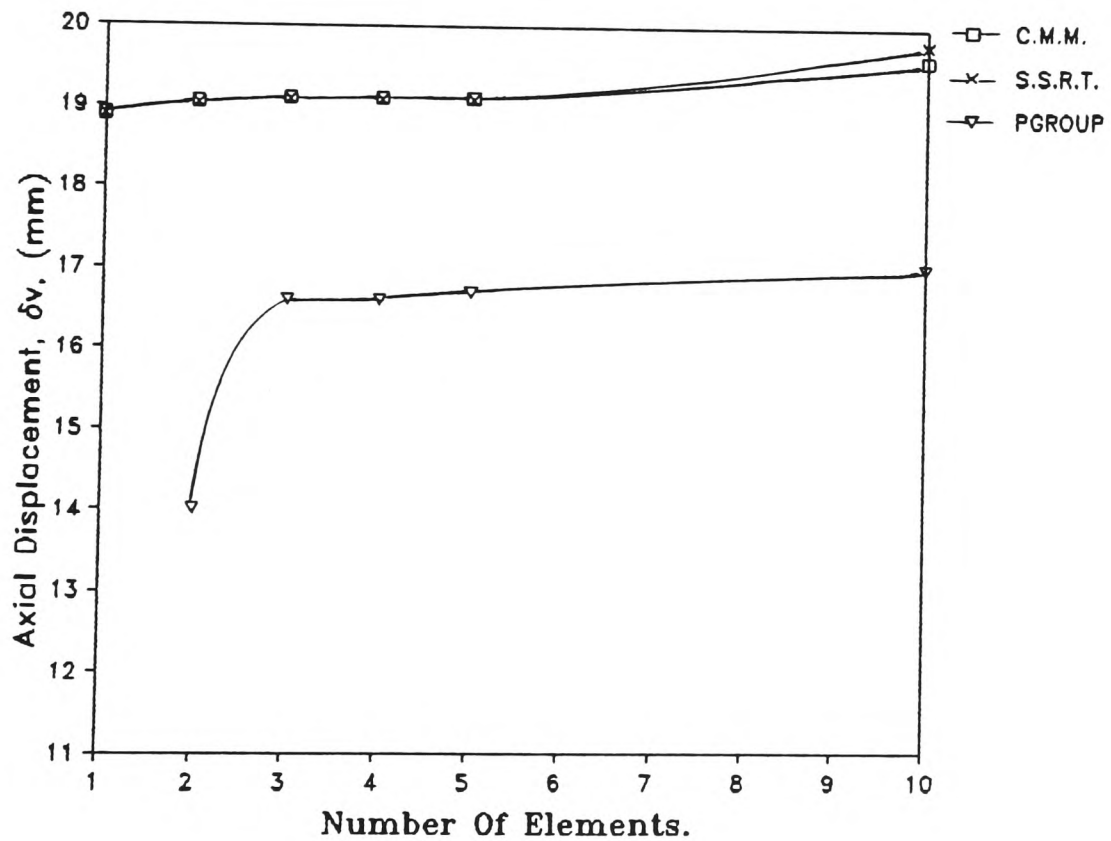


(b) Shear force.

Figure 6.6.: Convergence results for a restrained pile head.

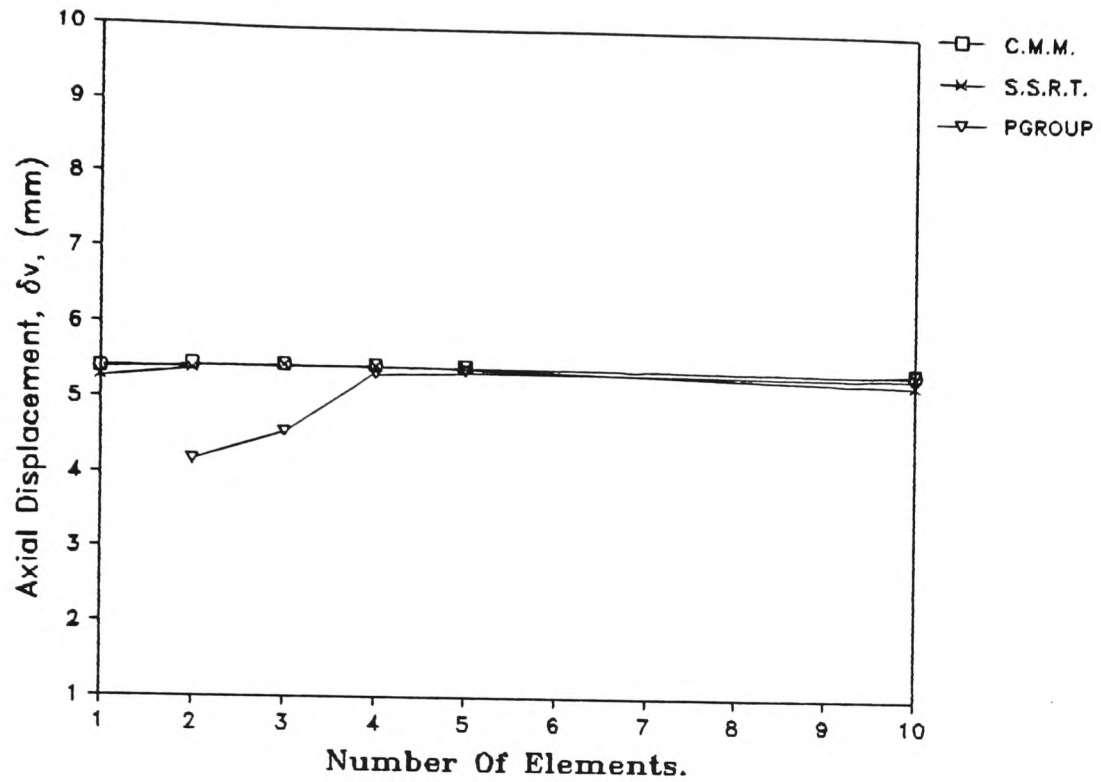


(a) For $L=10.0\text{m}$ and $d=1.0\text{m}$.

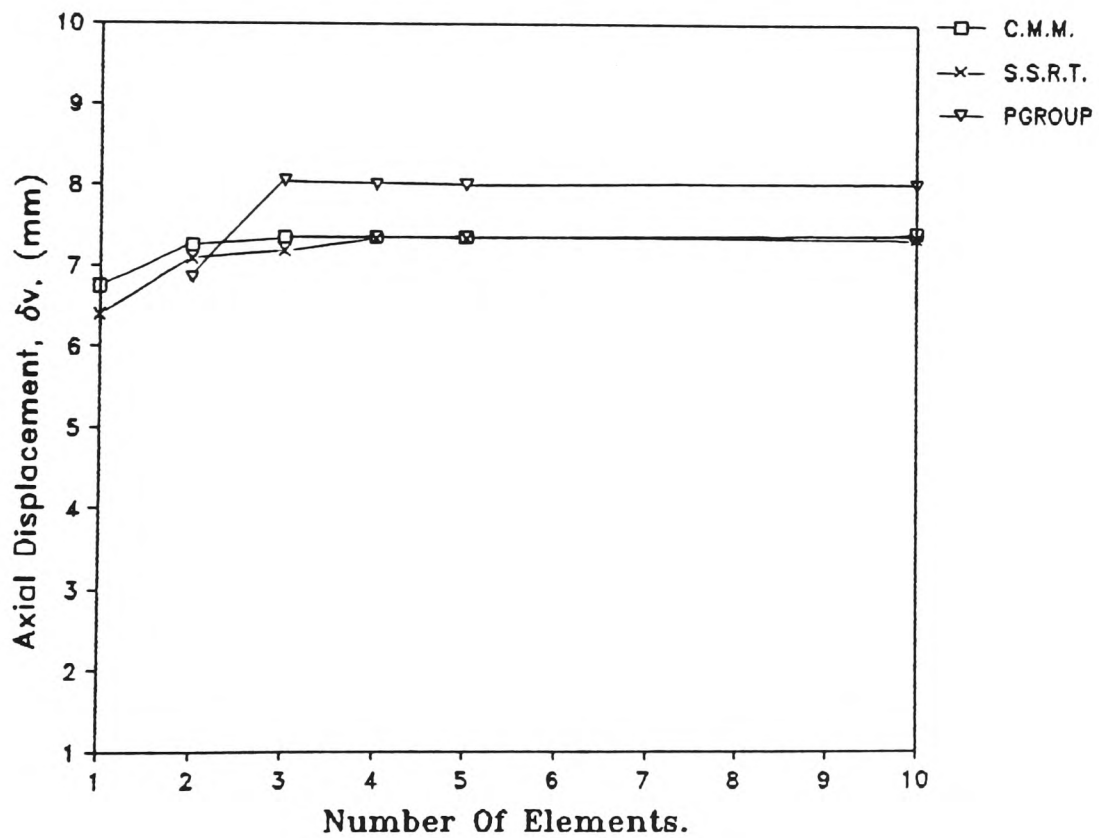


(b) For $L=10.0\text{m}$ and $d=0.5\text{m}$.

Figure 6.7.: Convergence of axial displacement.

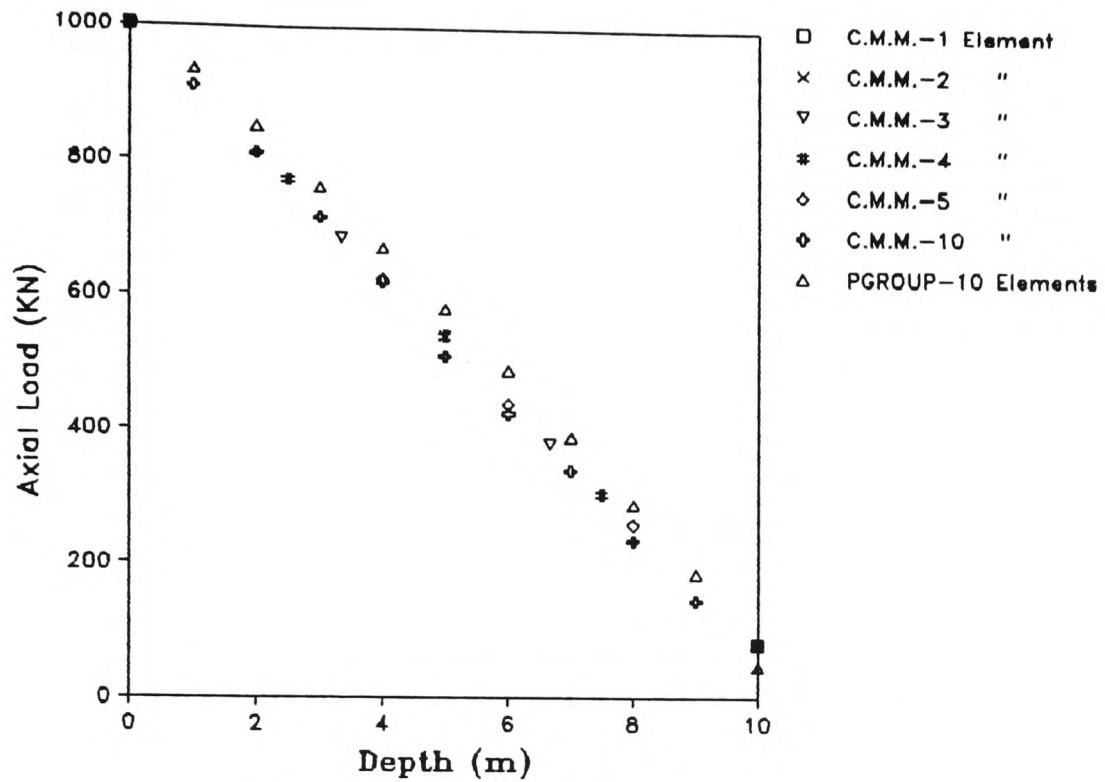


(c) For $L=40.0\text{m}$ and $d=1.0\text{m}$.

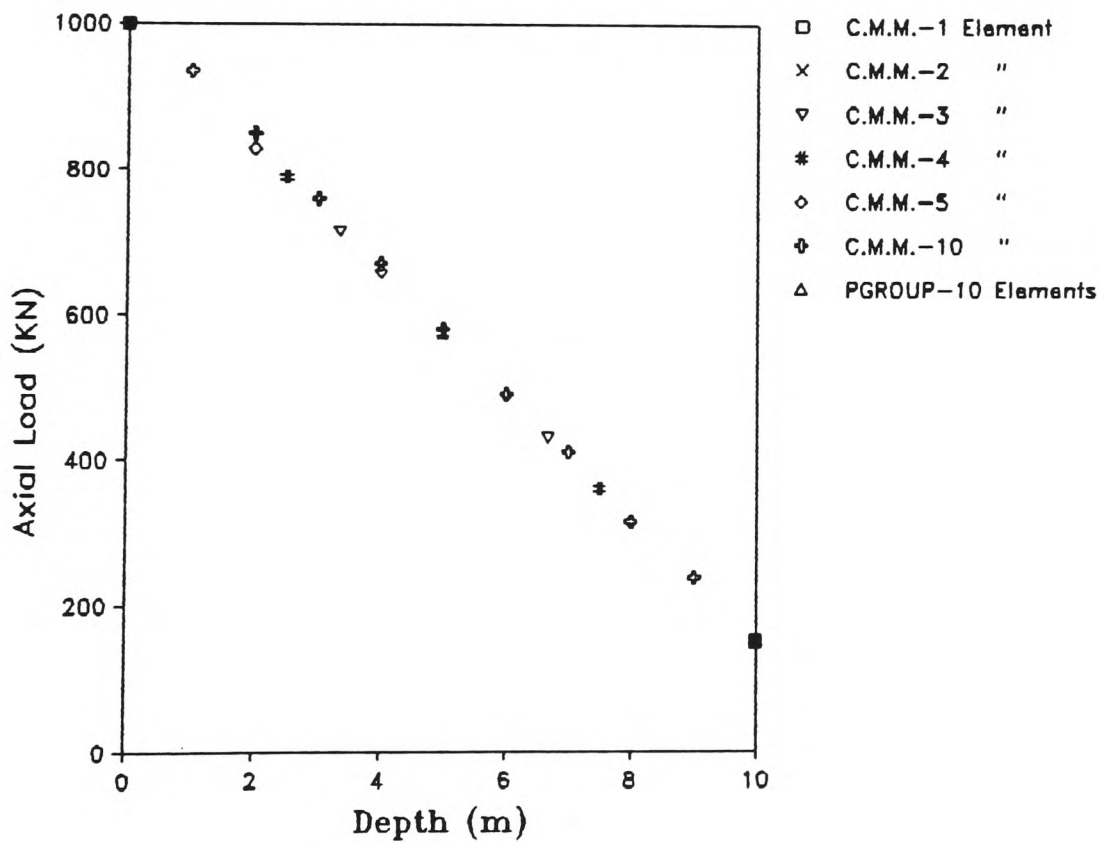


(d) For $L=40.0\text{m}$ and $d=0.5\text{m}$.

Figure 6.7.: Convergence of axial displacement.

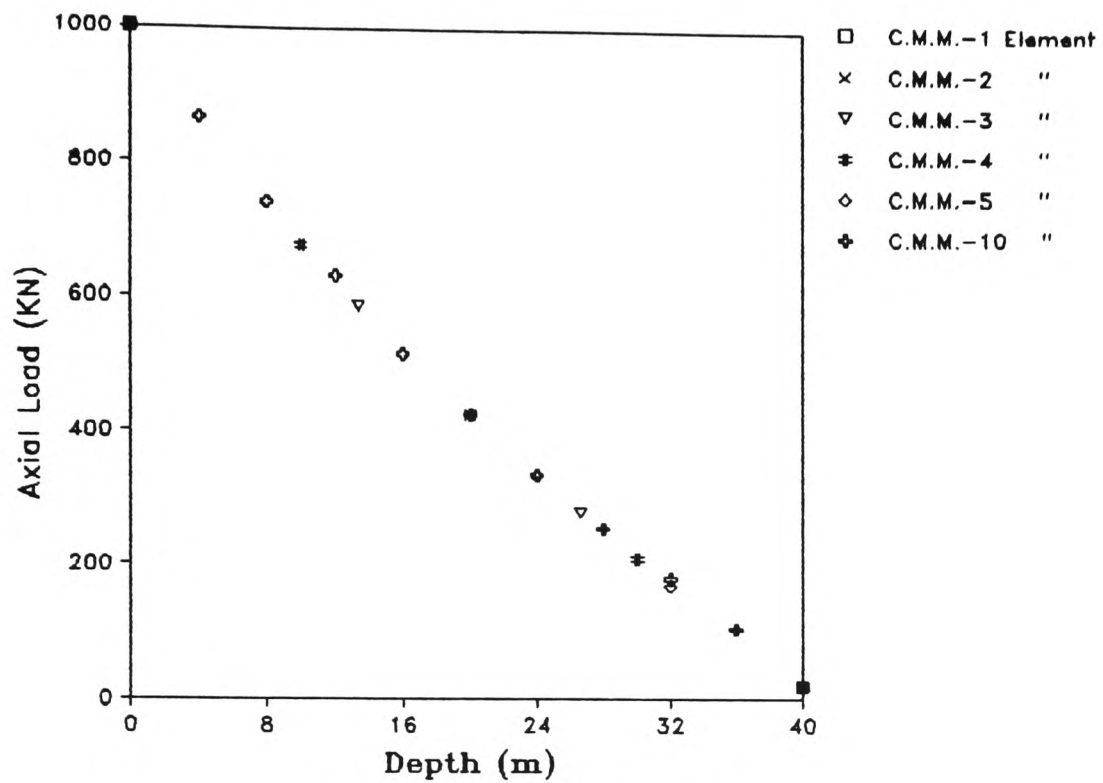


(a) For $L=10.0\text{m}$ and $d=0.5\text{m}$.

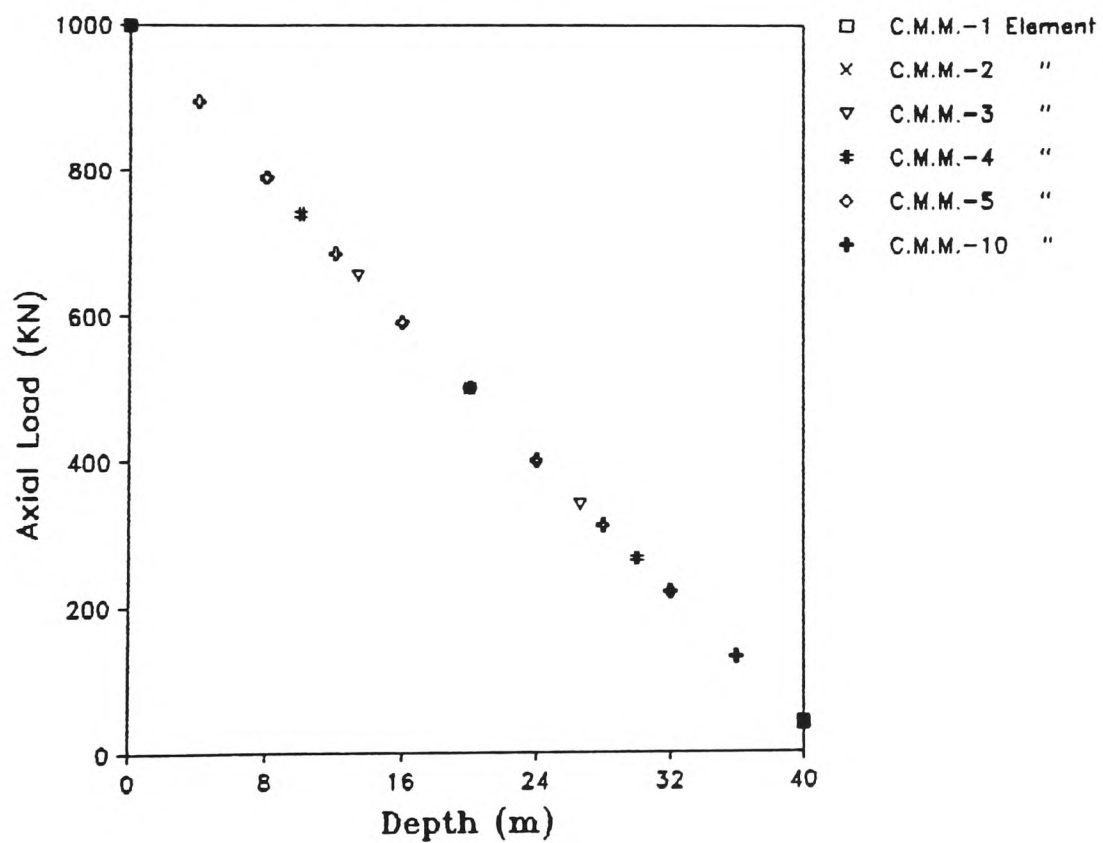


(b) For $L=10.0\text{m}$ and $d=1.0\text{m}$.

Figure 6.8.: Axial load distribution.

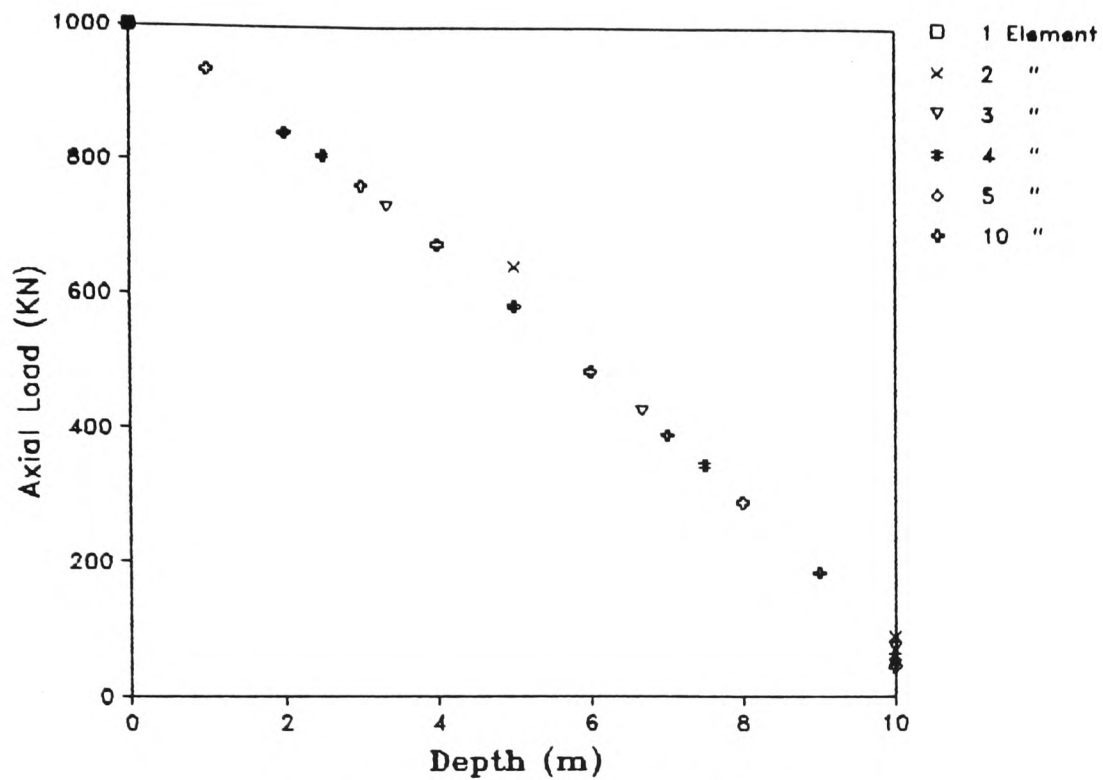


(c) For $L=40.0\text{m}$ and $d=0.5\text{m}$.

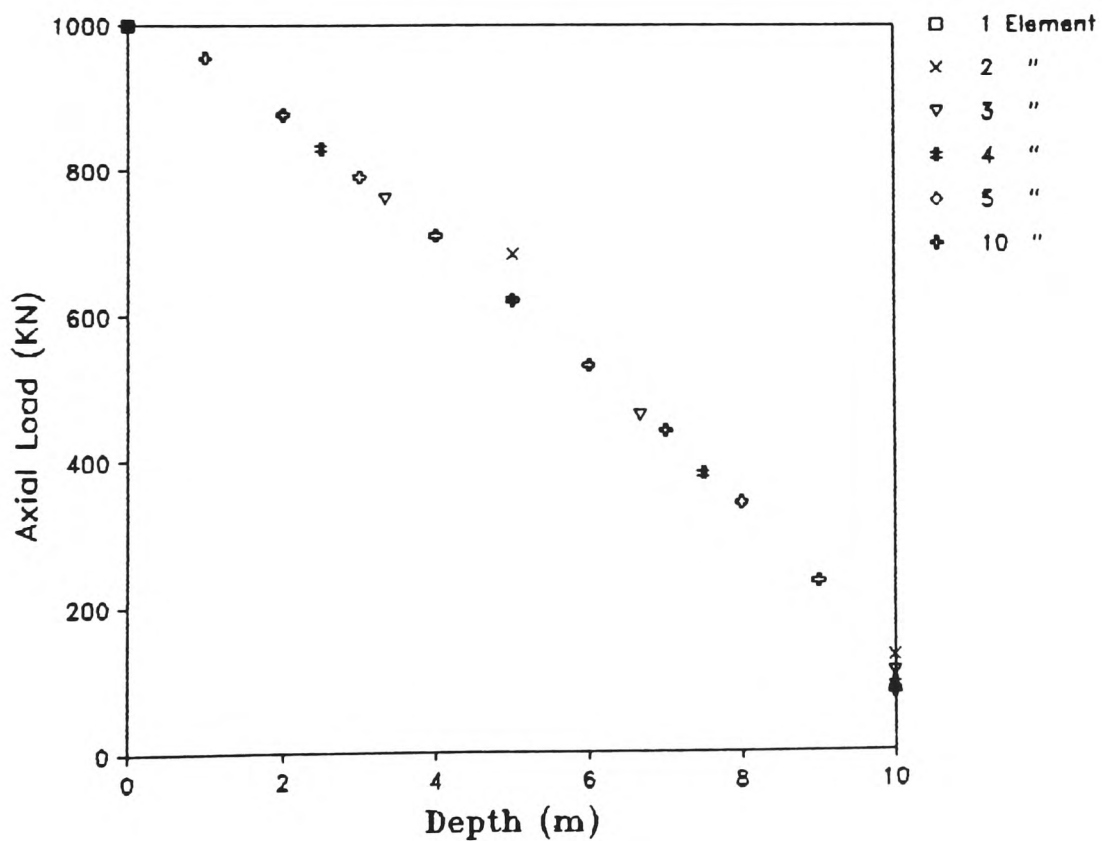


(d) For $L=40.0\text{m}$ and $d=1.0\text{m}$.

Figure 6.8.: Axial load distribution.

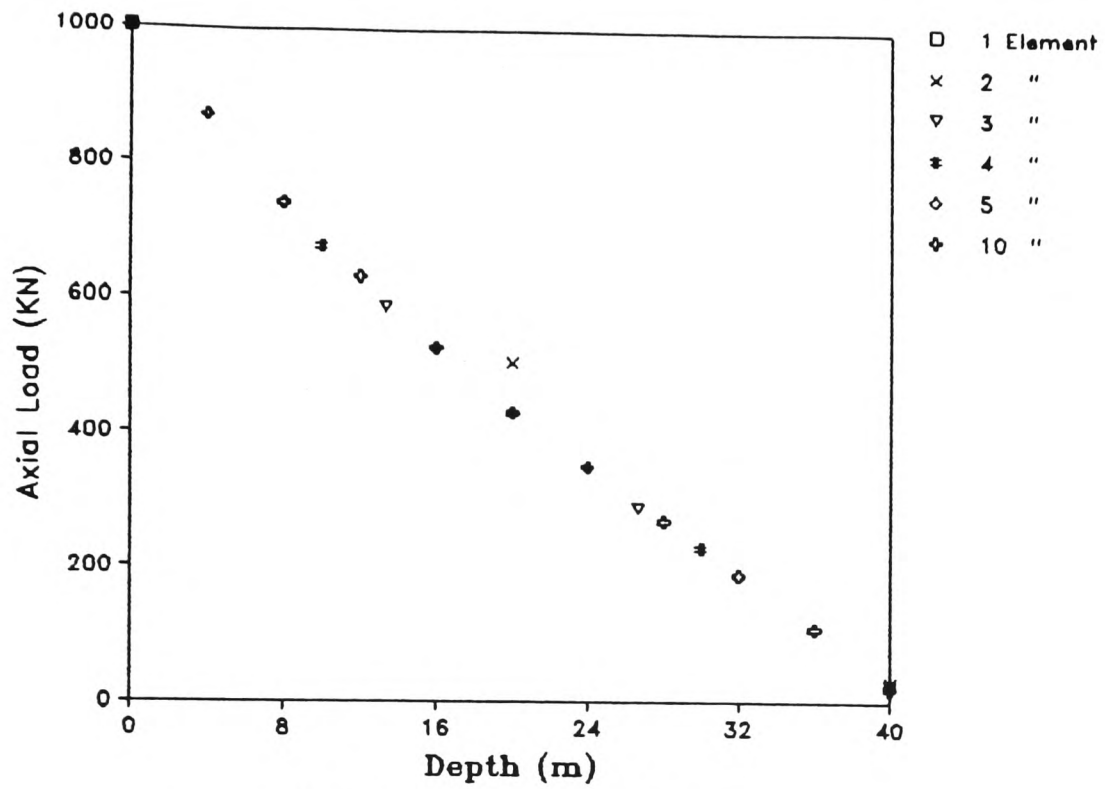


(a) For $L=10.0\text{m}$ and $d=0.5\text{m}$.

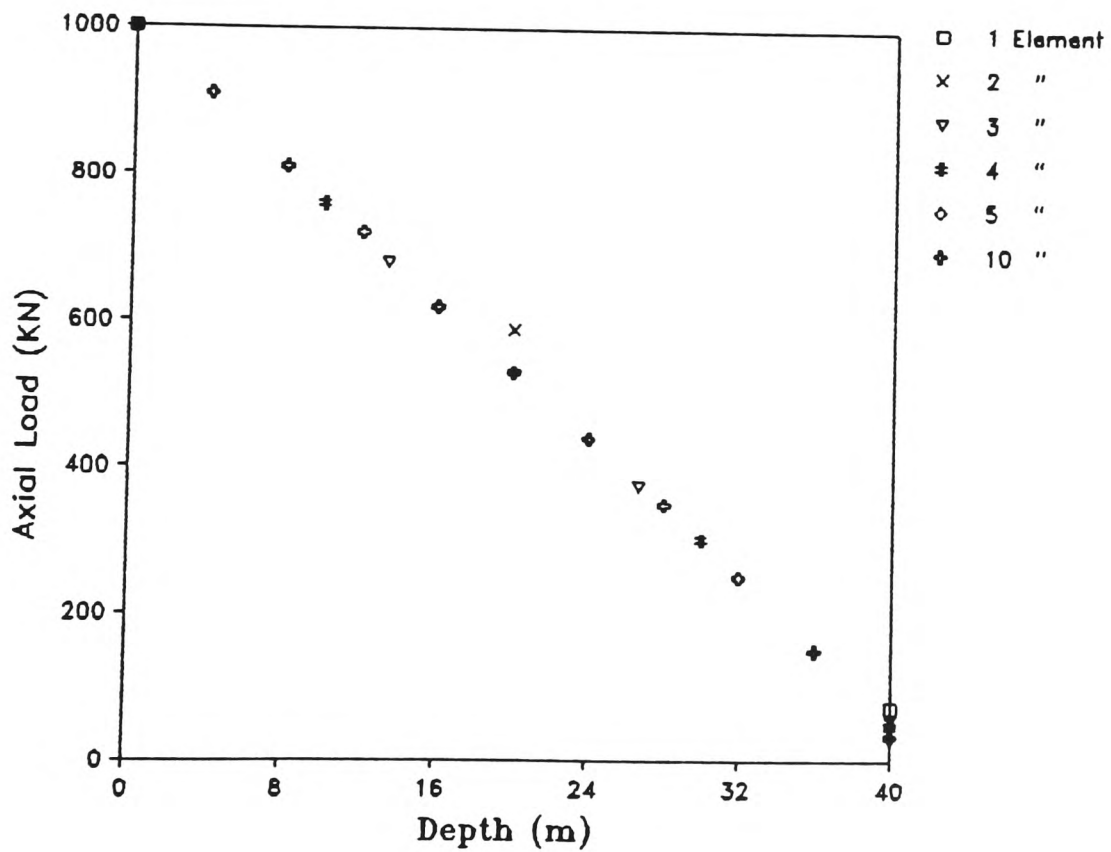


(b) For $L=10.0\text{m}$ and $d=1.0\text{m}$.

Figure 6.9.: PGROUP convergence tests.



(c) For $L=40.0\text{m}$ and $d=0.5\text{m}$.



(d) For $L=40.0\text{m}$ and $d=1.0\text{m}$.

Figure 6.9.: PGROUP convergence tests.

CHAPTER 7.

RAFT FOUNDATIONS.

7.1. INTRODUCTION.

It is widely recognized that a grillage analysis can adequately define the flexural behaviour of a raft foundation. On the other hand, the Winkler foundation is generally criticized for not being able to model interaction between the discretized springs. It is proposed to examine the limitations of a S.S.R.T. approach combined with a grillage analysis to model raft-soil behaviour. Hemsley (1987a) compared results for plates supported by a Winkler foundation and an elastic half-space. An extensive set of results was obtained for circular rafts with free or clamped edges. These indicated that there is a wide disparity in computed raft behaviour using the different ground models. Hemsley's results for the plate on the Winkler foundation and the elastic half-space soil model are reproduced and discussed in this chapter.

Results showing the convergence of settlement and bending moment with mesh refinement for the S.S.R.T. analysis of an edge loaded raft with both free and clamped edges are presented. Comparisons are made between results determined from an elastic half-space model, a Winkler foundation and various S.S.R.T. analyses. In the S.S.R.T. analyses K_s is varied in a controlled manner to accommodate interaction of a circular raft with a perimeter wall.

The limitations of the approach are demonstrated. It is concluded that the S.S.R.T. cannot always be modified to satisfactorily model raft behaviour. Hence, an alternative

method of analysis is developed based on the S.E.M.. The finite stiffness of the raft and the superstructure are idealized by a skeletal frame. The soil is modelled using a surface element representation which can be assigned heterogeneous properties. A program is developed to carry out the analysis. The solution procedure used by the program and user manual are presented in Appendix D. The results computed by the program are compared with case histories and other analyses of raft foundations. Comparisons are also made with analytical results which consider the superstructure stiffness.

7.2. AXISYMMETRICALLY LOADED CIRCULAR RAFT.

7.2.1. Convergence Of S.S.R.T. Results With Mesh Refinement.

(a) General.

To investigate the convergence of S.S.R.T. results with mesh refinement comparisons were made with results for a plate on Winkler springs. The worked example comprised an idealized raft of finite stiffness subjected to both concentrated and uniform applied loading. The raft was of 10m radius and thickness 0.5m, with elastic properties of $E=20\text{MN/m}^2$ and $\mu=0.2$. The idealized elastic soil properties were $E_s=20\text{MN/m}^2$ and $\mu_s=0.2$.

Hemsley defined K_s such that the vertical displacement of an axially loaded rigid circular raft on Winkler springs was equal to that of an identical raft in frictionless contact with the surface of a homogeneous isotropic elastic half space. He presented the following

relationship which is more exact than those proposed previously.

$$K_s = \frac{2 E_s}{\pi a (1-\mu_s^2)} \text{ (N/m}^3\text{) } \dots\dots\dots 7.1.$$

Where a = raft radius. Using this relationship for the worked example described above, a value of 1.33MN/m^3 was determined for K_s .

The S.S.R.T. results were determined by considering a quadrant of the raft and enforcing rotational compatibility along the radial boundaries. The second moment of area, I , for each grillage beam was calculated using $I=b.d^3/12$, where d = raft thickness. The torsional constant, J , was taken as $2I$. The spring stiffness at each node was computed by multiplying K_s by the plan area covered by the grillage beam. Joint loads were determined by multiplying the applied pressure by the equivalent plan areas.

(b) Results.

The various idealized grillages are presented in Figure 7.1. The convergence of settlement results with mesh refinement for the S.S.R.T. analysis of an edge loaded raft are presented in Figures 7.2.(a) and (b) for the free and clamped edge respectively. The results using the coarse mesh grillages of 1×1 and 2×2 underestimated the differential settlement determined from the plate analysis. However, the results determined from a relatively coarse mesh of 3×3 agreed very well with the plate analysis.

The convergence of bending moment results with mesh refinement for the S.S.R.T. analysis of an edge loaded raft are presented in Figures 7.3.(a) and (b) for the free and

clamped edge respectively. The coarse mesh grillages of 1x1 and 2x2 did not enable the variation of moment across the raft to be modelled satisfactorily. The bending moment variation across the raft determined from the 3x3 mesh agreed well with that from the plate analysis. Thus for an edge loaded raft with a constant value of K_s there is no real benefit in refining the grillage mesh beyond that of a 3x3 grid.

7.2.2. Comparative Results Of Different Ground Models.

(a) General.

Hemsley also compared the raft settlement and radial bending moment for an edge loaded raft determined by idealizing the ground as a elastic half-space and as a Winkler foundation with uniform values of K_s . He reported that the differential settlement computed using the Winkler model was greater than that from the elastic half-space. This was reflected in bending moments calculated using the Winkler model being greater by a factor of 2 to 5.

Because of these shortcomings, it was proposed to vary the K_s value used in the S.S.R.T. analysis to model the variation in contact pressure. An attempt was made to accommodate interaction by consideration of the interaction between two shallow footings which proved to be unsuccessful. Thus the K_s values in the S.S.R.T. were determined by comparison with the contact pressure distributions for edge and uniformly loaded circular rafts on an elastic half-space. This was achieved by specifying values of spring stiffness across the raft in accordance

with the ratio of the elastic contact pressure to applied loading.

This procedure for determining values of spring stiffness from elastic solutions was not practical for general raft analysis. However, this would indicate whether the establishment of empirical relationships to modify the spring stiffness values could adequately model the behaviour of a raft on an elastic half-space.

(b) Results.

The comparison of settlement and bending moment results using various methods for an edge loaded raft with a free edge are presented in Figures 7.4.(a) and (b) respectively.

The differential settlement across the raft as computed by the elastic half-space model was 9mm with a maximum settlement of 18mm. The Winkler maximum settlement was 34mm for a constant value of K_s , in addition, the method computed an upward displacement of 5mm at the centre of the raft. By varying K_s , the agreement between the S.S.R.T. and elastic half-space settlement results improved considerably. The corresponding maximum settlement was 16mm, with a settlement of 2mm at the centre of the raft.

The intensity in radial bending moment of -0.160MNm/m at the centre of the raft using the Winkler model with a constant K_s value considerably overestimated the elastic half-space value of -0.025MNm/m . When K_s was varied across the raft, the agreement between the moments from the S.S.R.T. and the elastic half-space model was very good. The S.S.R.T. distribution was slightly more uniform with a

maximum value of -0.060MNm/m at the centre of the raft.

The equivalent comparisons for the clamped edge are presented in Figures 7.5.(a) and (b). The difference between results from the S.S.R.T. and elastic half-space was reduced for the clamped edge. The maximum settlement from the elastic half-space model was 16mm , with a differential settlement of 4mm . The corresponding maximum settlement from the Winkler with a constant value of K_s was 20mm , with a differential settlement of 12mm . By varying the value of K_s across the raft the settlement profiles from both the S.S.R.T. and elastic half-space model were practically co-incident.

The radial bending moment determined from an elastic half-space solution varied from 0.110MNm/m at the edge to -0.025MNm/m at the centre. A satisfactory bending moment distribution from 0.210MNm/m to -0.100MNm/m across the raft was computed using the Winkler model with a constant value of K_s . The results obtained by varying K_s were in excellent agreement with the elastic half-space solution.

The clamped edge corresponds to the presence of an infinitely stiff perimeter wall joined monolithically to the raft. Thus, the restraint provided by a wall in redistributing bending moment partially compensates for the lack of interaction between the Winkler springs.

The comparison of settlement and bending moment from an elastic half-space, a Winkler model with K_s constant and a S.S.R.T. analysis with K_s varied, for a uniformly loaded raft with a free edge are presented in Figures 7.6.(a) and (b) respectively. There was a uniform settlement of 76mm and corresponding zero bending moment profile across the

raft for the Winkler analysis with a constant value of K_s . Whereas the elastic half space solution computed a maximum settlement of 95mm with the differential settlement of the concave profile being 30mm. The corresponding bending moment profile had a maximum sagging value of 0.130MNm/m. By varying the K_s value across the raft used in the S.S.R.T. analyses the agreement between the results improved. However, the disparity between results, especially bending moment, was considerable. The computed maximum and differential settlements were 83mm and 17mm respectively. The corresponding bending moment at the centre of the raft was 0.030MNm/m. Thus, in this instance, the S.S.R.T. did not adequately model the raft behaviour by varying K_s to approximately idealize the elastic half-space contact pressure distribution. This was because the finite stiffness of the raft effectively reduced the differential settlement by transferring load from lower to higher stiffness springs.

The comparison of settlement and bending moment for a uniformly loaded raft with a clamped edge are presented in Figures 7.7(a) and (b) respectively. The elastic half-space solution computed maximum and differential settlements of 88mm and 18mm respectively. The corresponding bending moment varied from -0.280MNm/m to 0.125MNm/m from the edge to the centre of the raft. Again, there was a uniform settlement of 76mm with a zero bending moment profile across the raft using the Winkler model with a constant value of K_s . With K_s varied, the respective maximum and differential settlements were 85mm and 15mm. The corresponding bending moment profile also improved, varying

from -0.280MNm/m at the edge to 0.065MNm/m in the centre of the raft. The improved agreement between S.S.R.T. and elastic half-space results could possibly be attributed to the clamped edge reducing differential settlements.

The combined loading case modelled by Hemsley comprised a relatively large uniform load in comparison to the peripheral load. Hence, the elastic half-space solution produced concave settlement profiles. The Winkler analyses with K_s constant computed that the edge of the raft settled more than the centre. This is because with K_s constant, the method predicts uniform settlement profiles under uniform loading. Thus the settlement across the raft from both methods was significantly different for this case of combined loading.

The comparison of settlement and radial bending moment results for a raft with a free edge subjected to the combined loading case are presented in Figures 7.8.(a) and (b) respectively. The elastic half-space solution computed a maximum settlement of 103mm at the centre of the raft with a differential settlement of 20mm . With K_s constant, the Winkler model provided a maximum settlement of 109mm at the edge of the raft and a lower settlement of 71mm at the centre. By varying the K_s value across the raft the S.S.R.T. settlement profile became near uniform at 85mm . The bending moment profile from the elastic half-space solution decreased from 0.100MNm/m at the centre to zero at the edge of the raft. Because of the dissimilar settlement profile, the Winkler analysis with K_s constant computed a hogging bending moment of -0.120MNm/m at the centre decreasing to zero at the edge of the raft. By varying K_s ,

the S.S.R.T. analysis calculated a mainly sagging profile across the raft with a hogging bending moment of -0.025MNm/m at the centre. It was therefore demonstrated that modifying the spring stiffness within the S.S.R.T. analysis did not provide a satisfactory ground model for this idealization.

The corresponding results for a clamped edge are presented in Figures 7.9.(a) and (b) for settlement and radial bending moment respectively. The elastic half-space model computed a maximum settlement of 99mm at the centre of the raft decreasing to 86mm at the edge. The Winkler settlement profile using a constant value of K_s had a maximum value of 95mm at the edge reducing to 82mm at the centre. The agreement improved by varying K_s , giving a maximum settlement of 96mm at the centre decreasing to 86mm at the edge of the raft. The moment profile determined from the elastic half-space solution varied from 0.100MNm/m at the centre to -0.170MNm/m at the edge. In contrast, the Winkler model with a constant value of K_s computed a bending moment variation across the raft from -0.100MNm/m at the centre to 0.210MNm/m at the edge. On varying K_s , the agreement improved with a bending moment of 0.050MNm/m at the centre reducing to -0.190MNm/m at the edge.

(c) Conclusion.

The Winkler model with a constant value of K_s was incapable of computing satisfactory results for the loaded idealized rafts. Modifying the K_s value across the raft to approximately accommodate interaction was generally satisfactory for analysis of the edge loaded rafts. The

results determined by this procedure agreed more closely with elastic half-space solutions for rafts with clamped edges than those with free edges. This is considered to be due to the reduced differential settlements associated with clamping the edge. The S.S.R.T. approach, with the K_s values varied, was generally unsatisfactory in modelling the behaviour of uniformly loaded and combined uniform and edge loaded rafts. Because of the limitations on its use, the approach of varying K_s to accommodate interaction is not recommended for general plain raft analysis.

7.2.3. Influence Of Wall Superstructure.

(a) General.

Hemsley (1987b) considered the influence of the superstructure wall on the foundation interaction analysis of a circular raft. The investigation was carried out making the following simplifications.

(i) The vertical load transferred by the wall to the edge of the raft was neglected.

(ii) The effect of the base of the wall being offset from the neutral axis of the raft was neglected.

(iii) The wall was treated as a semi-infinite cylinder but with lateral pressure applied over a full finite height.

An idealized case of an open-topped storage tank monolithically constructed in reinforced concrete was used for the investigation. The configuration is shown in Figure 7.10. The ground was modelled by an elastic half-space, a Winkler subgrade with constant K_s values and an S.S.R.T. model with K_s varied.

Initially, it was assumed that the empty tank was subjected to a line load of 100kN/m acting downward through the peripheral wall. Concrete properties having a Young's

modulus equal to 16GN/m^2 and Poisson's ratio of 0.2 were assumed. The soil modulus was taken as 20MN/m^2 and Poisson's ratio of the soil was taken as 0.2. K_s was taken as 1.33MN/m^3 for the Winkler subgrade .

On filling the tank, it was assumed that the hydrostatic radial pressure on the wall varied from zero at the top to 100KN/m^2 at the base, with a uniform downward pressure of 100KN/m^2 on the base slab. It was also assumed that the vertical wall loading of 100KN/m remained unchanged and the wall flexure induced by such loading was negligible compared to that generated by radial hydrostatic loading.

Solutions were obtained for the S.S.R.T. method by idealizing the structure as a skeletal three dimensional frame with 96 members and 51 joints. The idealized frame is shown in Figure 7.11.

(b) Results.

The raft and wall moments in the storage tank are presented in Figures 7.12.(a) and (b) for the empty and full tank respectively. For the empty tank, the raft radial bending moment from the elastic half-space solution varied from -25KNm/m at the centre to 50KNm/m at the base of the wall. The corresponding meridional wall moment had a value of -15KNm/m at 4m height and 40KNm/m at the base. The Winkler model with a constant K_s value computed the radial raft moment to vary from -115KNm/m at the centre to 130KNm/m at the base of the wall. It also computed the meridional wall moment to have a value of -20KNm/m at 4m height and 105KNm/m at the base. The results improved by

varying K_s to give a raft radial moment at the centre of -25KNm/m and 30KNm/m at the base of the wall. The corresponding wall meridional moment had a value of -20KNm/m at 4m height and 20KNm/m at the base of the wall.

With the tank full, the raft radial bending moment and wall meridional bending moment determined using the Winkler model with K_s constant were generally of opposite sign to those from the elastic half-space soil model. The raft radial bending moment from the elastic half-space had a value of 105KNm/m at the centre and -120KNm/m at the base of the wall. The corresponding wall meridional moment was generally greater than that from the encastre wall having values of 30KNm/m at 3m height and 85KNm/m at the base. With K_s constant, the Winkler model computed the raft radial bending moment at the centre to be -115KNm/m and 135KNm/m at the edge. The corresponding wall meridional bending moment had a value of 15KNm/m at 3m height and 50KNm/m at the base. With a variation in K_s the S.S.R.T. results improved. However, the raft radial moments of -10KNm/m at the centre of the raft and -50KNm/m at the edge were grossly underestimated by the S.S.R.T.. The wall meridional moment from the S.S.R.T. agreed closely with that for the encastre wall having a value of -60KNm/m at the base. However, the value at 3m height determined from this S.S.R.T. analysis was only 15KN/m in comparison to 30KNm/m for the encastre wall.

For the full storage tank, the raft settlement profiles and contact pressure distributions are presented in Figures 7.13.(a) and (b). A maximum settlement of 100mm at the centre and 85mm at the edge of the raft were

computed by the elastic half-space model. With K_s constant, the Winkler model computed a settlement profile opposite in shape to that from the elastic half space soil model with a maximum value of 100mm at the edge and 78mm at the centre of the raft. Where K_s was varied using the S.S.R.T., the settlement profile was near uniform at about 87mm.

The contact pressure determined using the Winkler model with K_s constant was generally greater than that of the elastic half-space model across most of the raft. This was partly due to the elastic half-space model computing a contact pressure infinitely high at the edges. By varying K_s , the contact pressure from the S.S.R.T. agreed reasonably well with the elastic half space model. A maximum value of 355KN/m^2 was computed at the edge for the S.S.R.T. analysis with an idealized 6x6 mesh.

The in-plane raft and wall hoop forces for the full storage tank are presented in Figure 7.13.(c). For the elastic half-space, the in-plane raft force was compressive at -80KN/m by accounting for the offset distance between the mid-depth of the raft and the base of the wall. Hemsley reported that by ignoring this aspect the calculated in-plane tensile force for the elastic half-space is 138KN/m . For the Winkler soil model with K_s constant, the in-plane force grossly overestimated that from the elastic half-space model with a tensile value of 530KN/m . The corresponding maximum wall hoop force was overestimated by a factor of 2. With K_s varied, the S.S.R.T. average compressive in-plane raft force of 87KN/m agreed very well with that from the elastic half-space model. The idealized

structure used in the S.S.R.T. analysis comprised a mesh at the base of the raft and at the outer face of the wall. The maximum wall hoop force of 340KN/m from the S.S.R.T. with K_s varied agreed well with that of about 420KN/m from the elastic half-space solution. However, the wall hoop force profile up the wall from the S.S.R.T. was dissimilar to that from the elastic half-space. This is considered to have been due to the coarse mesh used to idealize the wall; three graded elements were employed of lengths 1m, 1m and 3m from the base to the top of the wall respectively.

(c) Conclusion.

The elastic half-space results indicated that bending moments at the junction of the raft and wall were magnified by consideration of interaction. The Winkler model, with a constant value of K_s , computed an inverted settlement profile and corresponding raft radial bending moments of the incorrect sign. The considerable difference in raft performance from the various ground models was not reflected in the contact pressure distributions. In the S.S.R.T. analysis the variation of K_s was determined by comparison with the elastic half-space contact pressure distribution. Although the computed raft performance improved using this approach, the analytical results were not satisfactory.

7.2.4. Cylindrical Core For Building Structure.

(a) General.

Results for part of the foundation design for a low-rise office development were also presented by Hemsley

(1987b) after Hooper and Philiastides (1986). The design involved anticipating the structural behaviour of the bases to cylindrical core walls around the central area building. The necessary data is presented in Figures 7.14.(a) and (b). The full height of the core was about 15m and the applied vertical loads were characteristic values. The base slab was quite stiff relative to the ground having a K_R of about 1. The walls were not subjected to any significant applied lateral loading.

In one analysis, the perimeter wall was modelled by a beam having flexural properties of a 3m high wall to partly account for wall openings. The axisymmetric structure was modelled using finite elements. As the soil modulus was not constant beneath the foundation, it was analysed using a surface element method (S.E.M.) after Hooper and West (1983).

It was necessary to select a single value of K_s to represent the soil strata in the S.S.R.T. approach. This was based on a soil modulus, E_s , of 33MN/m^2 being the average value over a depth of 2.5 times the base diameter. A corresponding value for K_s of 5.5MN/m^3 was determined. The K_s values across the raft were varied in accordance with an elastic half-space contact pressure distribution for an edge loaded raft with a free edge having a K_R value of 1, taken from Hemsley's Figure 15.(e). A quadrant of the raft was idealized in the S.S.R.T. analysis using a 5x5 grillage.

(b) Results.

The settlement profile and bending moment distributions for the S.S.R.T. and S.E.M. analyses are presented in Figures 7.15.(a) and (b) respectively. The maximum settlement of 22mm at the edge computed by the S.S.R.T. agreed well with that of 20mm from the S.E.M.. However, the S.S.R.T. differential settlement of 19mm overestimated that of 5mm from the S.E.M.. This indicated that the procedure adopted to vary K_s was unsatisfactory because the combined loading and the restraining effect of the wall were not considered. The average settlement of approximately 10mm from the S.S.R.T. was considerably less than the S.E.M. value of about 17.5mm. The overall stiffness of the ground was therefore too stiff in the S.S.R.T. analysis. This is considered to be due to E_s being averaged over a depth of 2.5 times the raft breadth. An arbitrary shallower depth of soil would be more appropriate to determine a representative E_s value.

The S.E.M. computed radial bending moments as varying from -130KNm/m at the centre to 100KNm/m at the edge of the raft. The corresponding tangential bending moment from the S.E.M. varied from -130KNm/m at the centre to -20KNm/m at the edge. The S.S.R.T. underestimated the maximum radial and tangential moments at the centre and grossly overestimated the respective moments at the edge of the raft. It computed a relatively uniform distribution of tangential bending moment across the raft from -80KNm/m at the centre to -60KNm/m at the edge. The corresponding radial bending moment varied from -80KNm/m to 170KNm/m. Because bending moment is a function of displacement the

poor results were reflected in the comparison of settlements.

(c) Conclusion.

The agreement between settlement and bending moment results from the S.E.M. and the S.S.R.T. was poor. The S.S.R.T. analysis was carried out by varying K_s across the raft based on the contact pressure distribution of an edge loaded raft with a free edge resting on an elastic half-space. This modelling procedure is considered to be inaccurate and simplistic. The approach ignored the effects of a heterogeneous finite soil layer, combined loading and restraint afforded by the wall.

7.2.5. Discussion and Conclusions.

A study was made of the effect of mesh refinement on the settlement and radial bending moments from S.S.R.T. analyses. The results were compared with those from a plate analysis on Winkler springs. It was concluded that for a constant value of K_s there was no benefit in refining the mesh beyond that of a 3x3 grid for a quadrant of the raft.

Comparison of results for edge loaded rafts indicated that bending moments obtained from the S.S.R.T. with a constant value of K_s were much greater than those based on an elastic half-space ground model. Under combined edge loading and uniform pressure, the S.S.R.T. with a constant value of K_s computed bending moment distributions of the opposite sign and inverted settlement profiles.

An improvement in results was achieved by varying the K_s value used in the S.S.R.T. analysis to model

approximately the elastic half-space contact pressure distribution. However, the difference between the S.S.R.T. and elastic half-space results was still significant for some cases.

The difference between the results was reduced for the case of a clamped edge, which corresponded to an infinitely stiff perimeter wall joined monolithically to the raft. This was due to the rotational restraint provided by the wall redistributing bending moments which compensated for the lack of interaction in the S.S.R.T. It was thus concluded that the S.S.R.T. could not adequately define the raft behaviour in all cases, even with a controlled variation in K_s .

An investigation was carried out to determine the performance of cylindrical tanks monolithically joined to a raft founded on an elastic continuum. The results indicated that meridional bending moments at the base of the wall and radial bending moments at the edge of the raft may be amplified substantially by soil-structure interaction. The computed structural behaviour of the Winkler soil model with a constant value of K_s was considerably different from that of the elastic continuum model. The distributions of settlements, raft and wall bending moments from the Winkler model were almost inverted in shape to those from the elastic half-space model when the tank was full. Thus the Winkler soil model with K_s constant was not recommended as a means of analysis. Although the results from the S.S.R.T. with a controlled variation of K_s agreed better with those from the elastic half-space model, the disparity in results was still significant. The numerical order of settlement

and moment could be determined, which may be adequate for a preliminary design. However, for the combined loading cases analysed, the S.S.R.T. with a variation in K_s was generally unsatisfactory in modelling the foundation structural behaviour. Thus for general analyses the S.S.R.T. could not be recommended and a more suitable method of modelling was required for raft foundations of this type.

7.3. DEVELOPMENT OF PROGRAM FOR SURFACE ELEMENT ANALYSIS.

7.3.1. General.

Owing to the shortcomings of the S.S.R.T. in adequately modelling the performance of general raft foundations, a method of analysis was developed employing a S.E.M. idealization of the soil. The raft and superstructure were again modelled by a skeletal frame rather than traditional finite elements used for this type of analysis. This procedure enables the soil-structure interaction of modern framed buildings to be investigated more efficiently than using the popular F.E.M.

A computer program was developed for the analysis of general raft foundations which also considers the superstructure geometry. The two dimensional nature of plain raft foundations necessitates only a 6×6 stiffness matrix to model each grillage member. However, for the three dimensional problem, 12×12 matrices are required with a substantial increase in solution time.

The program was developed for use on microcomputers which have a limited memory capacity of 640 kilobytes (kB). In its present stage of development the program is

inefficient and further development is required. However, it enables solutions to be obtained using the proposed method of analysis for two and three dimensional problems.

Two basic programs were written; STEM*.BAS and TRAN*.BAS for two and three dimensional problems respectively. To speed up the solution process, the programs were compiled using a basic compiler into executive programs which have .EXE file extensions. This enables the programs to be run from the disk operating system (DOS) without entering GWBASIC. A controlling menu program SEM.EXE is used to evoke these programs.

Because the memory required to store the full structure matrix generally exceeds the computer memory of 640kB, use is made of the virtual disk space available on the IBM compatible machine. This is created using the VDISK command in the DOS manual. An additional 350kB of space is created by this procedure. The structure matrix is stored in this space by addressing a random access file to drive "D". However, it was found that this memory space was frequently exceeded when using the three dimensional elements utilized by the TRAN*.EXE set of programs. Thus the three dimensional structure matrix is stored in a random access file on the hard disk addressed as drive "C".

7.3.2. The Surface Element Method.

The soil is considered to be an elastic half-space which may have anisotropic properties. Use is made of the Steinbrenner (1934) approximation to accommodate a multi-layered cross anisotropic soil ie. the stress pattern is the same as that of an elastic half space. Although this

is not strictly a valid assumption, the solutions obtained are generally satisfactory, as discussed by Tomlinson (1986).

The raft is idealized using a grillage mesh and the stress in every soil layer beneath each node due to the other loaded nodes is calculated using Boussinesq's (1885) equations. Boussinesq considered a point load acting on the surface of a semi-infinite mass as shown in Figure 7.16. He expressed the stresses at a point within the elastic mass as shown below.

$$\sigma_z = \frac{3 P z^3}{2 \pi R^5} \dots\dots\dots 7.2.$$

$$\sigma_r = \frac{-P}{2 \pi R^2} \left[\frac{-3 r^2 z}{R^2} + \frac{(1 - 2\mu_{hh}) R}{R + z} \right] \dots\dots 7.3.$$

$$\sigma_\theta = \frac{-(1 - 2\mu_{hh})}{2 \pi R^2} \left[\frac{z}{R} - \frac{R}{R + z} \right] \dots\dots\dots 7.4.$$

where σ_z , σ_r and σ_θ are the vertical, radial and tangential stresses.

The corresponding vertical elastic strain ϵ_z at this point due to the load P is given by:

$$\epsilon_z = \frac{\sigma_z}{E_v} - \left[\frac{\mu_{hv} (\sigma_r + \sigma_\theta)}{E_h} \right] \dots\dots\dots 7.5.$$

The vertical displacement δ_z of each soil layer is thus given by:

$$\delta_z = \epsilon_z t \dots\dots\dots 7.6.$$

where t is the thickness of the layer. The vertical

displacement δ_{zi} of each node i at the surface due to the other loaded nodes is then determined by summing the individual displacements δ_z of each layer.

$$\delta_{zi} = \Sigma (\delta_z \text{ of each soil layer}) \dots\dots\dots 7.7.$$

These computations are performed in terms of P . Thus the off-diagonals of a flexibility matrix are determined by expressing:

$$\{ \delta \} = [F_S] \{ P \} \dots\dots\dots 7.8.$$

Equation 7.5. implies that the stress σ_z beneath the point load is infinite when R is equal to zero. Wood (1978) encountered this problem in developing a program using a surface element representation of the soil and finite elements for the raft. He determined the stress beneath the node under consideration by distributing the load over a rectangle of the mesh. It is then possible to calculate the stress in a semi-infinite elastic space beneath a corner of a uniformly loaded rectangle. This enables the leading diagonal terms of the flexibility matrix to be determined.

The same approach used by Wood is adopted in the program to overcome the problem of infinite stress beneath a point load. Having distributed the load over a rectangle, the stresses beneath a corner are determined using Holl's (1940) method presented by Poulos and Davis (1974). The stresses given by Holl are independent of μ . Results obtained using Holl's method were compared with those from Giroud's (1970) equations using a μ value of 0.5 for a worked example. The difference in the computed displacements beneath a corner was 8.5%. Giroud's method relies upon tabulated influence factors. The stresses can

be determined directly from equations presented by Holl. Holl's method is therefore suitable for programming. He considered the stresses at a point beneath the corner of a loaded rectangle as shown in Figure 7.17. The stresses are expressed by the following equations.

$$\sigma_z = \frac{P}{2 \pi} \left[\tan^{-1} \frac{l b}{z R_3} + \frac{l b z}{R_3} \frac{1}{R_1^2} + \frac{1}{R_2^2} \right] \dots 7.9.$$

$$\sigma_x = \frac{P}{2 \pi} \left[\tan^{-1} \frac{l b}{z R_3} - \frac{l b z}{R_1^2 R_3} \right] \dots\dots\dots 7.10.$$

$$\sigma_y = \frac{P}{2 \pi} \left[\tan^{-1} \frac{l b}{z R_3} - \frac{l b z}{R_2^2 R_3} \right] \dots\dots\dots 7.11.$$

where, $R_1 = \sqrt{(l^2 + z^2)}$
 $R_2 = \sqrt{(b^2 + z^2)}$
 $R_3 = \sqrt{(l^2 + b^2 + z^2)}$

The elastic strain ϵ_z is then given by:

$$\epsilon_z = \frac{\sigma_z}{E v} - \frac{\mu_{hv} (\sigma_x + \sigma_y)}{E h} \dots\dots\dots 7.12.$$

The vertical displacement δ_{zi} beneath each point is determined by multiplying the strain ϵ_z by the layer thickness t and summing the individual displacements for each layer as shown below.

$$\delta_{zi} = \Sigma (\epsilon_z t \text{ [for each layer]}) \dots\dots\dots 7.13.$$

This enables the leading diagonal of the flexibility matrix $[F_S]$ to be determined.

An outline of the solution procedures used by the program and the user manual are presented in Appendix D.

7.4. CORRELATION OF RESULTS.

7.4.1. General.

Results from the developed program were compared to those determined by various researchers. A raft of an existing instrumented building was considered. This enabled the results to be correlated to the measured performance. It was therefore demonstrated that the program could be applied to practical problems and was a useful tool for the design engineer in predicting raft behaviour. An investigation was also made into the contribution of the stiffness of a superstructure in resisting differential settlement. The results in this instance were compared to other theoretical solutions.

7.4.2. Ebenezer House.

(a) General.

Hooper and Wood (1977) considered the raft foundation behaviour of a 22-storey building with cross-wall construction located in South London. They carried out an axisymmetric analysis to establish the probable variation of soil stiffness with depth. The raft foundation of asymmetric plan-shape was then analysed using various approximations for the stiffness of the superstructure. Satisfactory agreement was obtained between measured and computed values of total and differential settlement.

(b) Measured performance.

The building is a 22-storey residential block. In situ concrete was used in the construction of the first two storeys (ground plus mezzanine floors). The remaining

superstructure consists of precast concrete units with in situ stitches (Wates system: 180mm walls, 165mm slabs, 115mm exposed aggregate cladding).

Ebenezer House is founded on a 0.91m thick raft having a plan area of 456m^2 . The estimated gross building weight (dead plus live load, excluding wind load) is 114MN, giving a gross applied pressure of 250KN/m^2 . The comparatively rigid cross wall system of superstructure extends over most of the foundation area.

The settlement of the building was monitored using eight observation stations. It was observed that the settlement was almost complete approximately 5 years after the start of construction. The average measured settlement at this time was about 115mm. The measured differential settlement along the length of the foundation was 5.0mm (angular distortion 1/3000 sagging) and across the width of the foundation was 2.9mm (angular distortion 1/3400 sagging) based on the final set of readings after 5 years.

(c) Hooper and Wood's analysis.

From an axisymmetric analysis, the following drained parameters were back-figured to model the measured total raft settlement.

Stratum	Thickness (m)	E_v' (MN/m^2)
Gravel	3	100
London Clay	17	$6 + 1.0z$
Woolwich & Reading Beds	14	200
Thanet Sands & Chalk	66	4000

Where z was measured from the top of the London Clay and E_v' denotes the vertical drained modulus. The gravel thickness was measured from the level of the raft base. The

drained parameters assumed for each layer were horizontal modulus $E_h' = 2.3 E_v'$, Poisson's ratio $\mu_{hh}' = -0.15$, shear modulus $G_{vh}' = 0.66 E_v'$ and Poisson's ratio in the vertical plane $\mu_{vh}' = 0.1$.

Their asymmetric raft analysis was similar to that described by Cheung and Zienkiewicz (1965) but modified to allow for soil layering as presented by Wood and Larnach (1974) and (1975). It was assumed that for a given applied loading the stress distribution in the layered soil was the same as that in a homogeneous elastic half-space. They reported that the test cases considered by Hooper and Wood (1976) based on this assumption provided reasonably accurate settlements over a wide range of soil heterogeneity. It was also assumed that the raft was founded at the ground surface and that the contact between the raft and the soil was frictionless.

The raft mesh, comprising 32 elements and 45 nodes, is presented in Figure 7.18. The applied loading was considered to be uniformly distributed over the entire foundation. The raft was assumed to be isotropic and linearly elastic with a modulus $E = 15 \text{ GN/m}^2$ and a Poisson's ratio $\mu = 0.15$. The Thanet Sands and Chalk were omitted from the asymmetric analysis because the results from the preceding axisymmetric analysis indicated insignificant settlements in these layers.

They carried out both undrained and drained analyses. Only the drained results are presented here because these agreed more closely with the long term measured

performance. Four idealized cases were used to model the raft and superstructure as shown below.

- (a) No raft.
- (b) Unrestrained 0.91m thick raft.
- (c) Restrained 0.91m thick raft.
- (d) Unrestrained 5.6m thick raft.

In order to restrain the raft, as in Case (c), zero rotations were specified at selected nodes. The location and orientation of the nodal restraints are indicated in Figure 7.18. These approximately represented the restraint afforded by the cross-wall layout. Case (d) represented an "equivalent raft" whose thickness was based on the composite bending stiffness of the actual raft and first and second floor slabs. Complete shear connections between floors was assumed. Thus in Cases (c) and (d) an attempt was made to take account of the stiffness of the superstructure.

Hooper and Wood's (1977) results for the four cases are reproduced in Figure 7.18. Settlements are plotted along two grid lines parallel to the long axis of the raft. There was a pronounced concave settlement profile for Case (a) with a differential settlement of about 107mm between Nodes 17 and 21. This was only slightly modified by the presence of the 0.91m thick (unrestrained) raft to give a corresponding differential settlement of about 83mm. Even with the raft subjected to considerable bending restraint, as in Case (c), the differential settlements were much too high with a corresponding value of about 10mm. It was only with Case (d) that corresponding drained differential settlements of about 4mm resembled measured values of 2.8mm to 5mm.

The computed drained settlement profile for the 5.6m thick raft indicated a foundation tilt of $\pm 2.4\text{mm}$ about the short axis and $\pm 1.7\text{mm}$ about the long axis. These movements were equivalent to a vertical tilt of approximately 10mm about both axes. This was compatible with the low measured values.

(d) Analysis using proposed method.

The mesh used to model the raft was identical to that used by Hooper and Wood in Figure 7.18. However, their mesh comprised plate finite elements, whereas the one here represented a total of 76 connected grillage beams. The same four cases as used by Hooper and Wood to model the raft-superstructure were considered.

The uniform loading on the raft was idealized as a series of equivalent point loads at the nodal points. Eleven graded soil layers were used to model the soil strata overlying the Thanet Sands and Chalk.

The computed settlements using drained parameters in Hooper and Wood's analysis agreed well with the long term measured values. Hence, only a drained analysis was considered here. All elastic parameters used in the analysis were equal to those of Hooper and Wood.

The computed results obtained for the four cases are superimposed onto those from Hooper and Wood's analyses in Figure 7.18. The agreement between results from both analyses was favourable. This indicated that a grillage analysis satisfactorily modelled the raft performance. Settlements were generally about 30mm greater using the proposed method, with percentage differences between +16%

and +23%. This suggested a difference between the two methods in modelling the soil. The proposed method also computed a relatively large foundation tilt of about 21mm between Nodes 17 and 24 for the 5.6m raft. The corresponding value from Hooper and Wood was approximately 7mm. However, the form of both sets of curves was similar. As concluded by Hooper and Wood, only the 5.6m "equivalent raft" provided satisfactory values of differential settlement. Bending moment distributions were not reported for comparison.

An attempt was made to identify the reason for the proposed method computing larger settlements than Hooper and Wood. The only variable which they did not specify was the number of soil subdivisions used to model the strata. As a check on convergence of results from the proposed method, the number of soil subdivisions was reduced to 3 giving a decrease in total settlements of 24%. On increasing the number of soil subdivisions from 11 to 22 the settlement was unchanged. It was thus concluded that 11 graded soil subdivisions were sufficient to model the strata in this instance. It is considered fortuitous that the total settlements computed using 3 soil subdivisions agreed well with those of Hooper and Wood.

Other possible causes for the difference between results may be due to a simpler model of the soil being employed by the proposed method. Holl's equations, which are independent of μ , were used to calculate the leading diagonal terms of the soil flexibility matrix. Hooper and Wood also specified a shear modulus which was not required for the proposed surface element analysis. However, the

agreement between settlements from both methods was encouraging, the results computed by this method being more conservative. The variation in results is considered to be due to differences in the soil models not the raft idealizations.

7.4.3. Consideration Of Superstructure.

(a) General.

Wardle and Fraser (1975) presented a method of analysis for rafts on a homogeneous elastic multi-layered soil. A computer program was developed which performed a static elastic analysis of rafts of finite stiffness resting on a layered soil mass. The raft was modelled using conventional plate elements and the superstructure modelled using beam elements. The S.E.M. was used to analyse the soil. Solutions for the layered system were determined using integral transform techniques.

They investigated the effect of superstructure rigidity on soil-raft behaviour. The raft foundation of a seven storey building was analysed by considering the superstructure rigidity using various idealizations. Details of the raft and the open seven storey superstructure are presented in Figures 7.19, 7.20 and 7.21. The soil was taken to be an elastic layer of 18.3m depth.

The alternative superstructure idealizations are presented in Figure 7.22. In Case 1, the superstructure stiffness was taken as zero and the raft analysed as a 18.3m square plate with a thickness of 0.68m. The column loads were computed on the basis of rigid column supports

and applied directly to the raft. Case 2 related to the discretisation of the entire superstructure and full interaction of the superstructure-raft-soil system was considered. In Case 3 the superstructure was condensed to a single storey frame using the method described by Meyerhof (1953). By fully collapsing the structure, an equivalent raft thickness of 0.94m was obtained, as indicated by Case 4.

(b) Wardle and Fraser's results.

The analytical results for the four cases are presented in Table 7.1. The maximum total settlements δ^* in each case were similar, varying from 124mm to 132mm. Differential settlements δ_{OX} and δ_{OC} of 14.6mm and 30.9mm respectively were computed by ignoring the superstructure rigidity. These values were approximately double those when the superstructure stiffness was taken into account.

By ignoring the superstructure stiffness, in Case 1, raft bending moments of 244 and 396KNm/m were induced in the centre and at Column A respectively. The corresponding moments increased substantially to 332 and 481KNm/m when the "equivalent raft", in Case 4, was considered. The more representative idealizations of superstructure stiffness, Cases 3 and 4, indicated that the raft bending moments at the centre and Column A were of the order 120 and 250KNm/m respectively. For these cases, the loads in the corner columns increased considerably. By implication the bending moments in the beams and columns of the corner bays also increased.

It was concluded that completely collapsing the superstructure enabled the total and differential settlements to be satisfactorily computed. However, this idealization overestimated the raft bending moments. For an accurate determination of raft bending moments and column loads a one storey collapsed structure, or the full superstructure, needs to be idealized.

(c) Results from the proposed method.

The developed program was used to analyse Cases 1, 3 and 4 as described by Wardle and Fraser. Case 2 was omitted because the program cannot presently make use of symmetry, thus solving the stiffness matrix for the complete superstructure would have taken an unacceptable amount of time. Also Wardle and Fraser observed that analysis of a single storey idealization enabled raft bending moments and column loads to be computed fairly accurately.

To determine settlements and bending moments at the centre of the raft, the mesh used to idealize the raft was as shown in Figure 7.23. The applied column loads were computed by consideration of the proportion of area supported by each column. The beam element properties were determined by considering the proportion of area they represented. The 18.3m deep soil stratum was idealized using 10 graded layers. Because a three-dimensional idealization was required for analysis of the single storey, for consistency the 3-D programs TRAN*.EXE were also used to analyse the plain raft models.

The results determined using the program TRAN*.EXE are presented in Table 7.1. The total settlements δ^*

computed in each case were similar, varying between 90.3mm and 105.2mm. These values underestimated those of Wardle and Fraser by about 25mm, approximately 25%. The difference could possibly be attributed to the different modelling of the stresses in the soil. In this method the stress was computed at the centre of each layer, whilst Wardle and Fraser used integral transforms to analyse a continuous distribution within the stratum. When more than 10 soil layers were analysed by the proposed method there was no significant change in computed settlements.

Although the total settlements computed by the proposed method were less than those of Wardle and Fraser, the differential settlements from this method were greater by about a factor of 2. This implied that the raft idealized was too flexible. On refining the mesh to that shown in Figure 7.24. the agreement between settlements did not significantly improve. Using the two dimensional program in this instance, values of $\delta_{OX}=25.8\text{mm}$ and $\delta_{OC}=49.2\text{mm}$ were computed for Case 1. This indicated that the grillage idealization of the raft was satisfactory. The difference in results could possibly again be attributed to a difference in modelling the soil.

When the superstructure rigidity was not considered, as in Case 1, the proposed method of analysis computed differential settlements $\delta_{OX}=26.8\text{mm}$ and $\delta_{OC}=54.3\text{mm}$. These values were approximately double those when it was approximated in some manner. This behaviour was in agreement with that reported by Wardle and Fraser.

The agreement between raft bending moments from both methods was acceptable, with the best results being

achieved for Case 3. By considering a single storey, in Case 3, the moments were significantly lower than those for the plain and "equivalent rafts" in Cases 1 and 4 respectively. It was also observed that the loads in the corner columns of the single storey idealization, in Case 3, increased substantially as the load was redistributed. The computed load distribution using this method was more uniform than that computed by Wardle and Fraser. This indicated that the proposed method modelled a higher degree of interaction.

It is concluded that a three dimensional skeletal frame idealization of the raft and superstructure can satisfactorily model soil-structure interaction effects. As demonstrated, this is a necessary requirement because of the poor results obtained using two dimensional models. The variation in results between the proposed method and those of Wardle and Fraser are considered to be due to different analytical procedures for the soil model.

7.5. CONCLUSIONS.

It was established that a grillage idealization can satisfactorily model the flexural performance of raft foundations. This was achieved by comparison of solutions from a plate supported by a Winkler soil model with results from a S.S.R.T. approach using various grillages supported at their connecting nodes by springs. It was demonstrated that a quadrant of an axisymmetrically loaded raft can be satisfactorily idealized using a 3x3 grid.

The limitations of the S.S.R.T. combined with a grillage to model raft-soil behaviour were investigated.

Results determined by the approach were compared with solutions of elastic half-space ground models. Under some loading conditions the bending moment distributions computed using the Winkler foundation with a constant value of K_s were of the opposite sign to those from an elastic half-space ground model. The results improved using the S.S.R.T. with a controlled variation in K_s across the raft to approximately model the contact pressure distribution. However, the difference in results from this method and elastic half-space solutions was still significant for some loading cases, especially for uniformly loaded rafts. The approach enabled the order of settlement to be determined; which may be adequate for a preliminary design. However, the S.S.R.T. could not satisfactorily compute both the settlement and bending moment distribution for general rafts. Therefore, it could not be recommended and a more suitable method of analysis, such as the S.E.M., was required for raft foundations.

An investigation of the interaction between superstructure walls and raft foundations was also carried out. Elastic half-space solutions indicated that bending moments at the junction of the raft and wall were magnified by consideration of interaction. The Winkler soil model with K_s constant and the S.S.R.T. approach with K_s varied indicated that bending moments were induced in the wall. However, the agreement between these results and elastic half-space solutions was not satisfactory.

The S.E.M. was utilized to overcome the limitations of the S.S.R.T. as a ground model for general raft foundations. The raft and superstructure were again

modelled using a skeletal frame. A simplified S.E.M. approach was developed which did not involve integral transform techniques. Development of a computer program enabled the proposed method to be applied to the analysis of both plain rafts and three dimensional structures resting upon rafts. Although, the program was not fully developed, it was capable of solving moderately large practical problems on a microcomputer with a limited memory capacity of 640kB. Convergence tests indicated that about 10 graded soil layers were required to satisfactorily idealize the ground.

The results computed by the program were correlated with those of Hooper and Wood (1977) and the measured performance for an existing instrumented building. The computed total settlements from the proposed method overestimated those of Hooper and Wood with percentage differences between +16% and +23%. The form of the settlement curves from both methods of analysis were similar. The idealization which produced the most realistic settlement profile was that of a raft thickened to approximately represent the superstructure stiffness. The average total settlement for this raft idealization overestimated the average measured settlement by about +25%. Bending moments were not reported by Hooper and Wood.

Wardle and Fraser (1975) also studied the contribution that the stiffness of the superstructure made in resisting differential settlements. Their investigation was confined to a theoretical study. A full three-dimensional superstructure was modelled to examine the effects of simplified idealizations. The various raft and

superstructure idealizations considered by Wardle and Fraser, except the full superstructure, were analysed using the developed program. The computed total settlements in each case were similar and underestimated Wardle and Fraser's values by approximately 25%. The differential settlements were approximately double the values computed by Wardle and Fraser. This is considered to be due to different ground models being employed by the methods. Both methods of analysis indicated that by not considering the superstructure rigidity, the differential settlements were approximately double those where it was approximated in some manner. By consideration of a single storey, the bending moments in the raft were significantly lower than those determined by ignoring the superstructure stiffness and by consideration of a thickened plain raft. It was also observed that the loads in the corner columns of the idealized single storey structure increased substantially as the load was redistributed.

It is thus concluded that collapsing the superstructure completely into a plain raft enabled acceptable predictions to be made of total and differential settlement. However, the bending moments in the raft were overestimated. Thus, for a satisfactory prediction of raft bending moments and column loads to be made, either a single storey collapsed structure, or the full superstructure, needs to be included in the idealization. Furthermore, the developed program was successfully applied to the analysis of the three-dimensional single storey structure. The computed results satisfactorily represented the effects of soil-structure interaction. This

demonstrated that a combined S.E.M. with a simplified skeletal structural frame is a valid method for raft foundation analysis.

Case	Wardle & Fraser's Method				Proposed Method			
	δ^*	δ_{OA}	δ_{OX}	δ_{OC}	δ^*	δ_{OA}	δ_{OX}	δ_{OC}
1	132	-	14.6	30.9	105.2	6.0	26.8	54.3
3	124	-	8.0	14.8	90.3	3.0	14.7	31.2
4	124	-	7.1	15.5	91.2	3.6	15.0	32.4

(a) Settlements (mm)

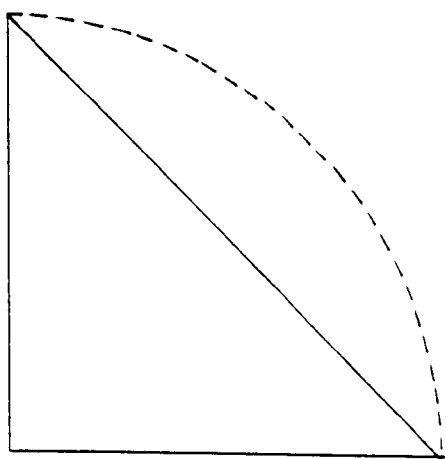
Case	Wardle & Fraser's Method			Proposed Method		
	Col. A	Col. B	Col. C	Col. A	Col. B	Col. C
1	2490	1245	622	2490	1245	622
3	2185	1278	860	1800	1358	1092
4	2490	1245	622	2490	1245	622

(b) Column Loads (KN)

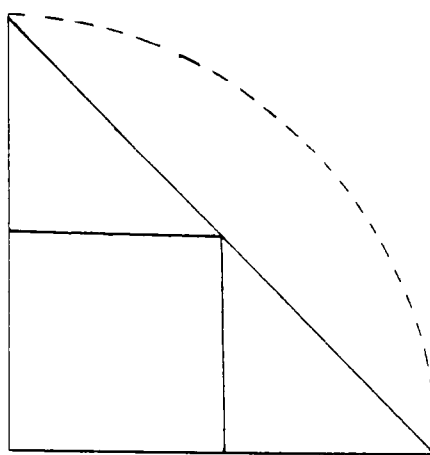
Case	Wardle & Fraser's Method		Proposed Method	
	Centre	Col. A	Centre	Col. A
1	244	396	317	462
3	126	258	159	267
4	332	481	509	641

(c) Bending Moments (KNm/m)

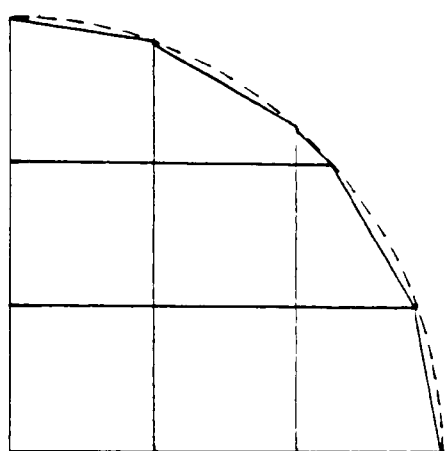
Table 7.1.: Comparison With Wardle And Fraser.



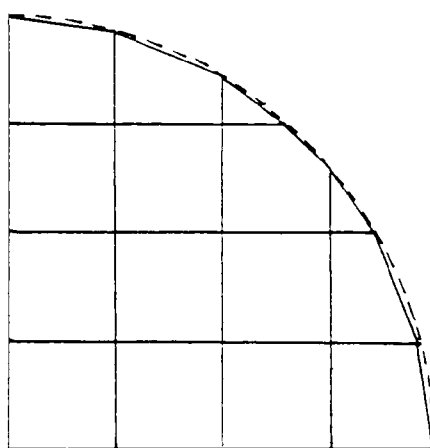
1x1 grid



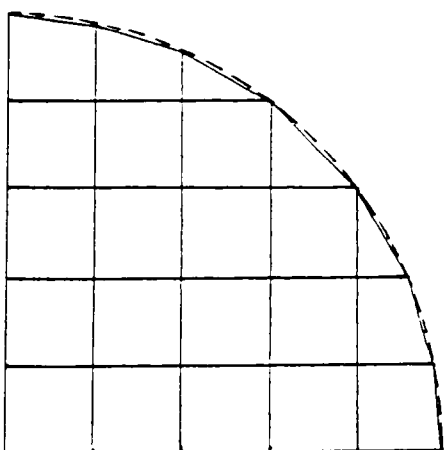
2x2 grid



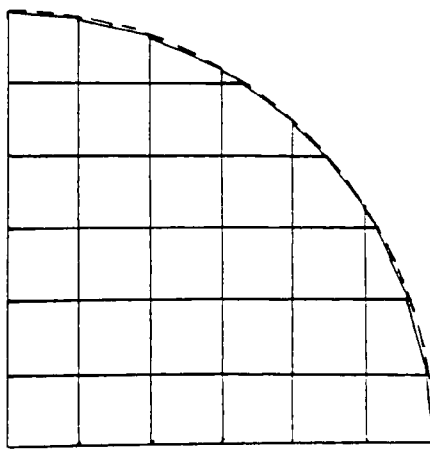
3x3 grid



4x4 grid

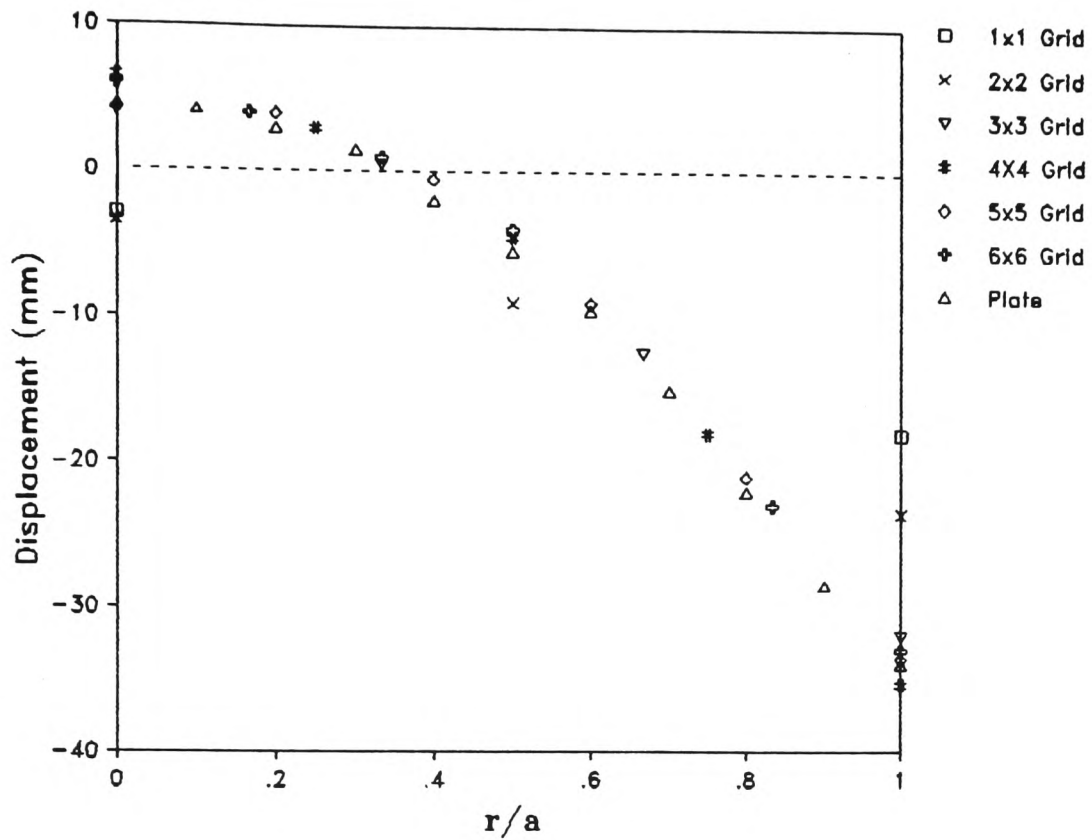


5x5 grid

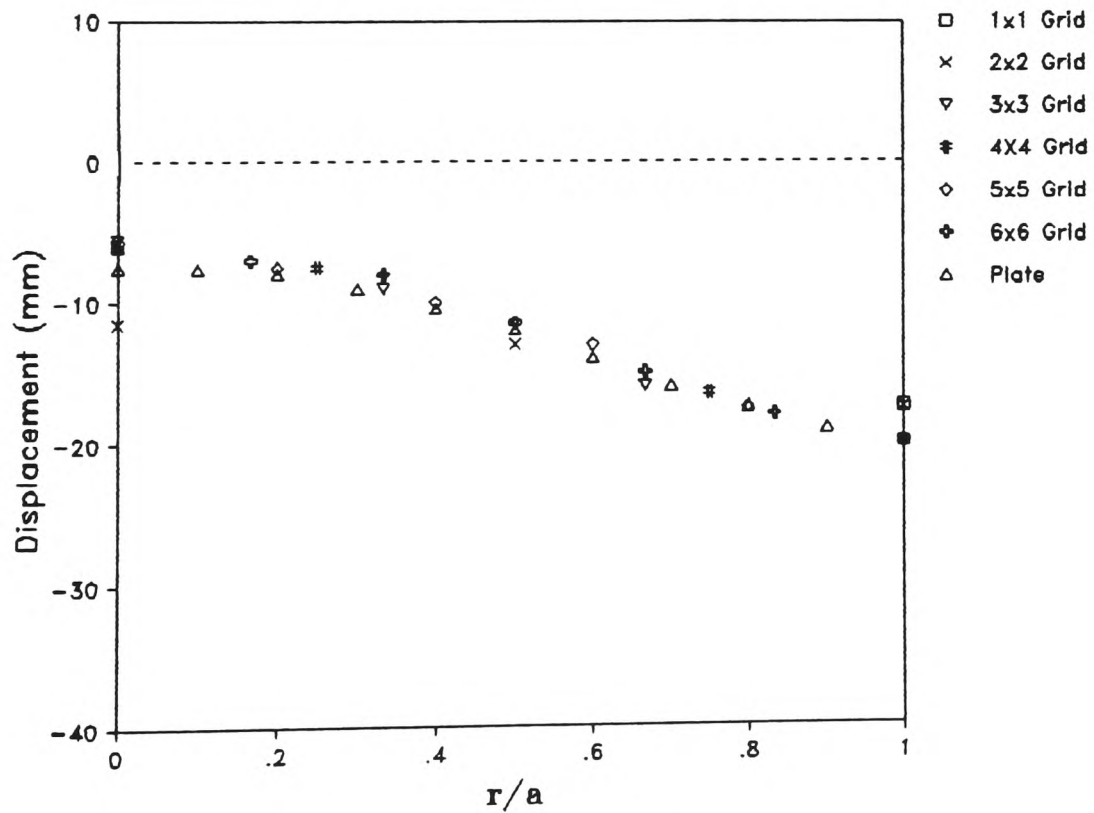


6x6 grid

Figure 7.1.: Grillage idealizations.

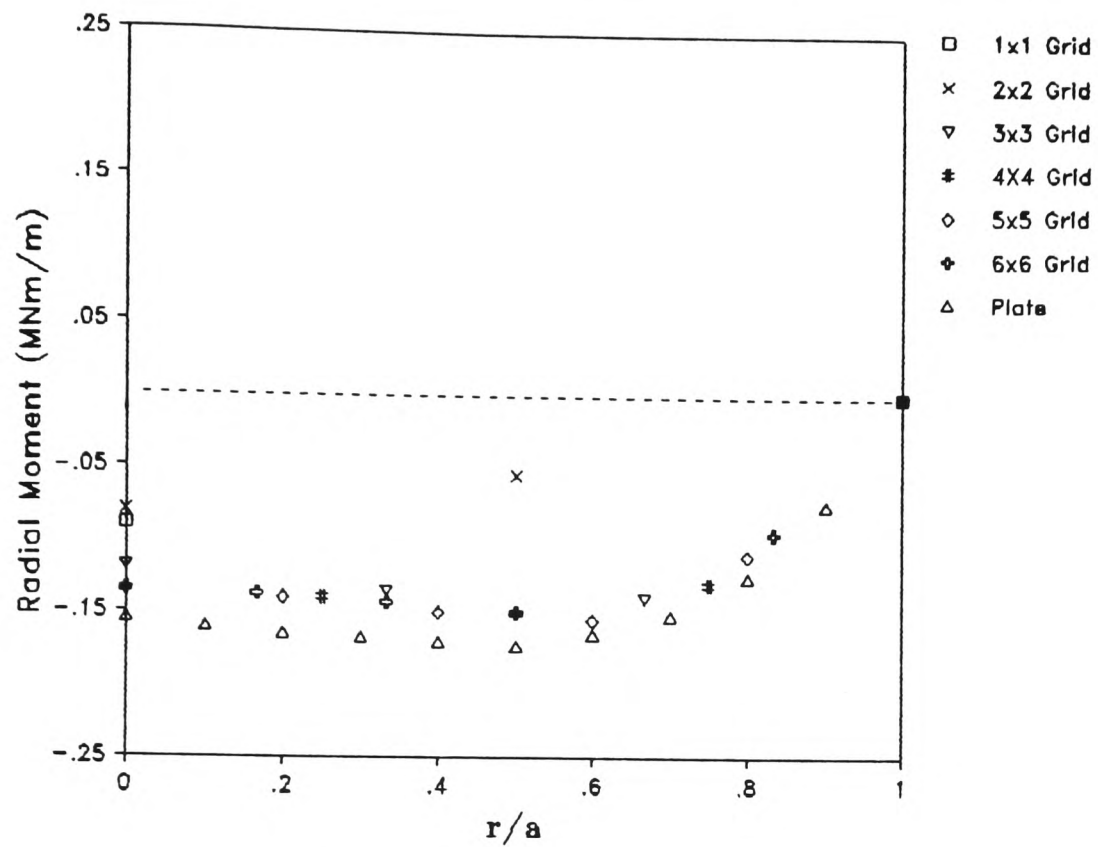


(a) Free edge

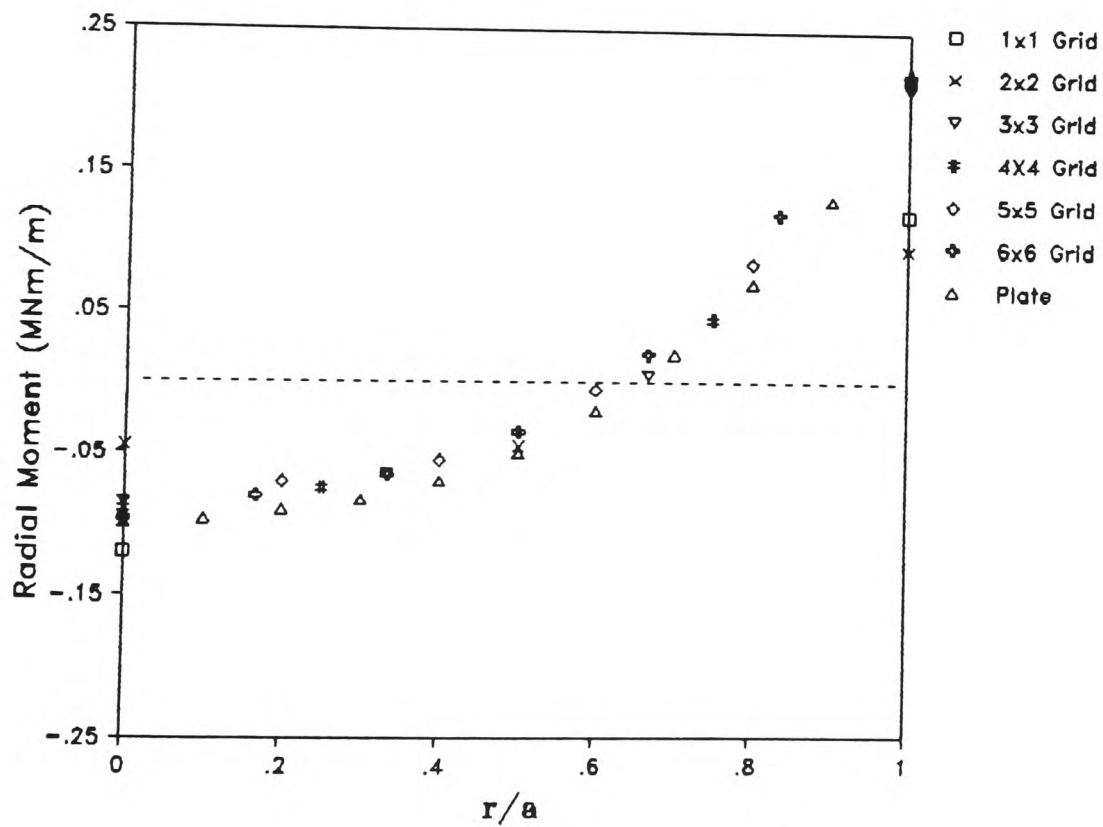


(b) Clamped edge.

Figure 7.2.: Convergence of displacement for edge loaded raft.

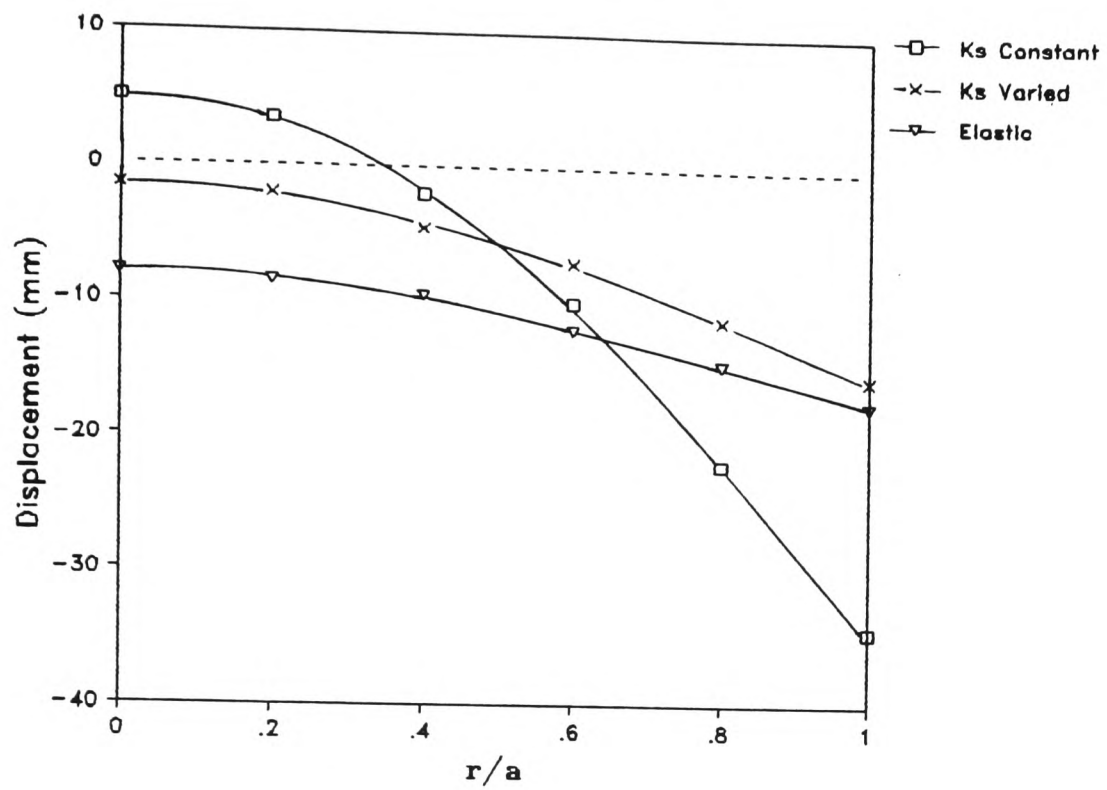


(a) Free edge.

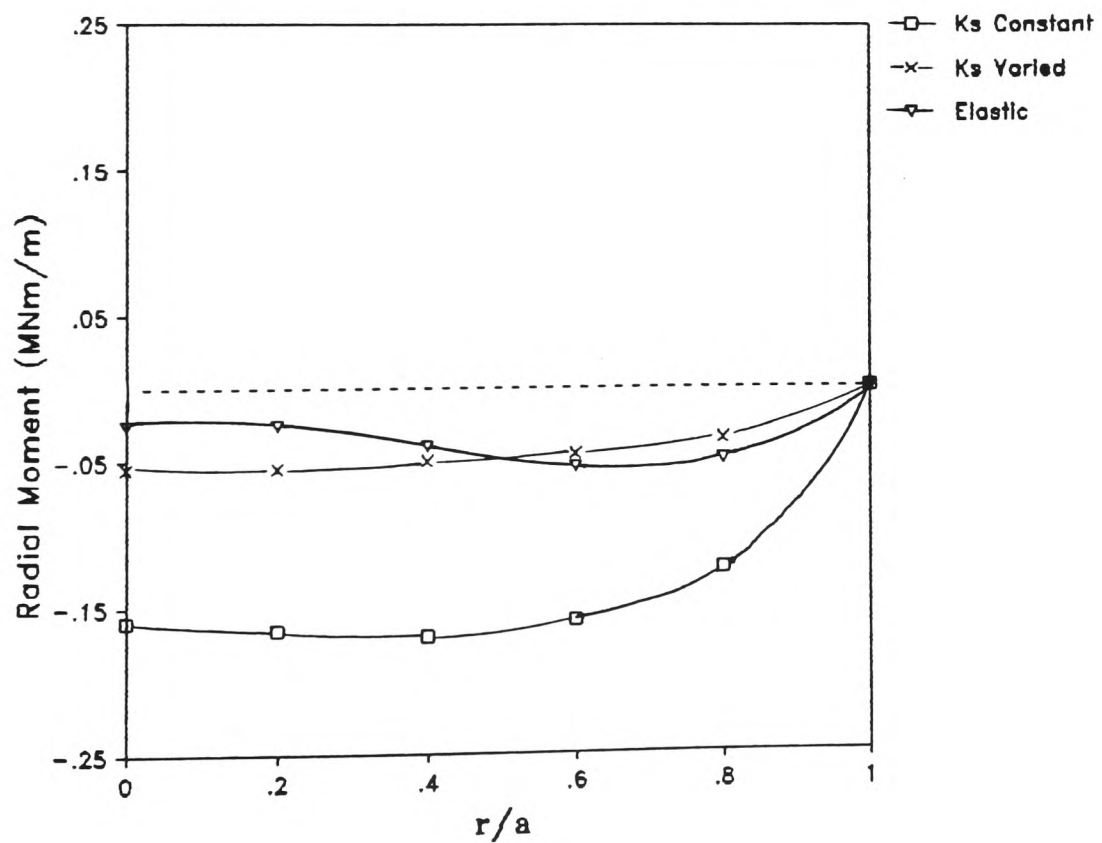


(b) Clamped edge.

Figure 7.3.: Convergence of bending moment for edge loaded raft.

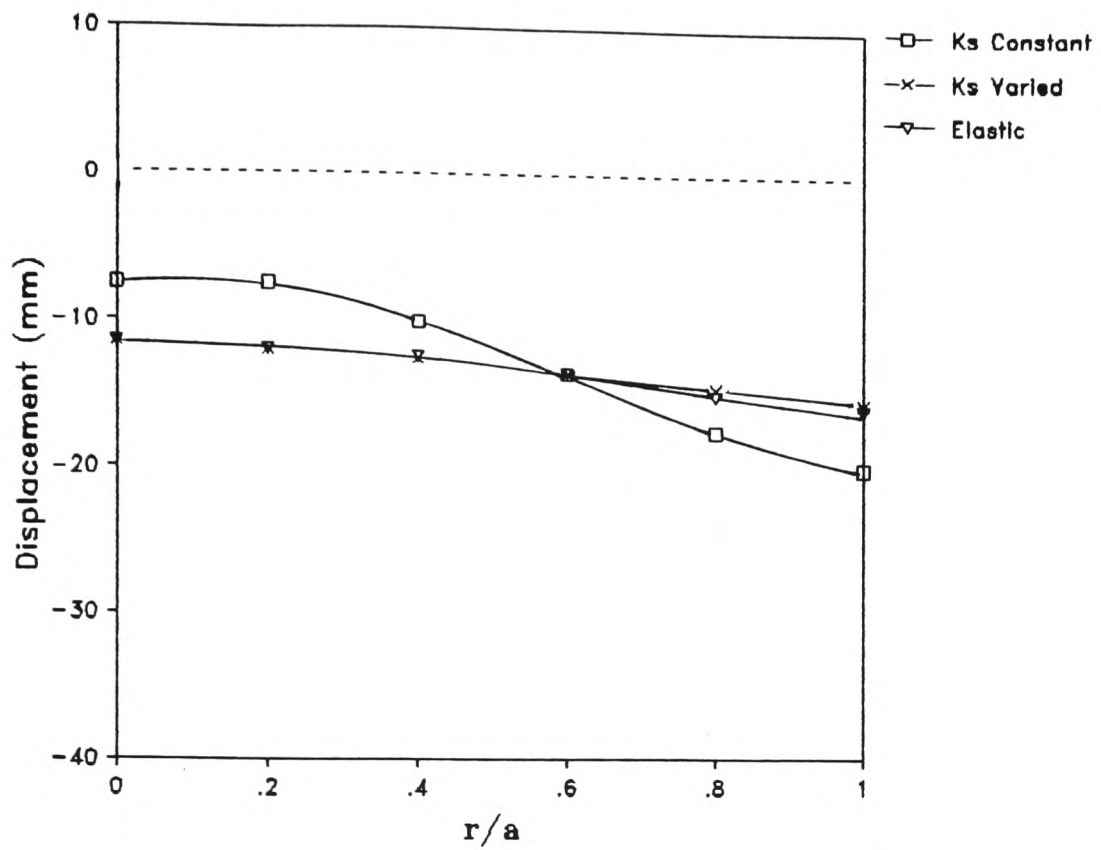


(a) Displacement for free edge.

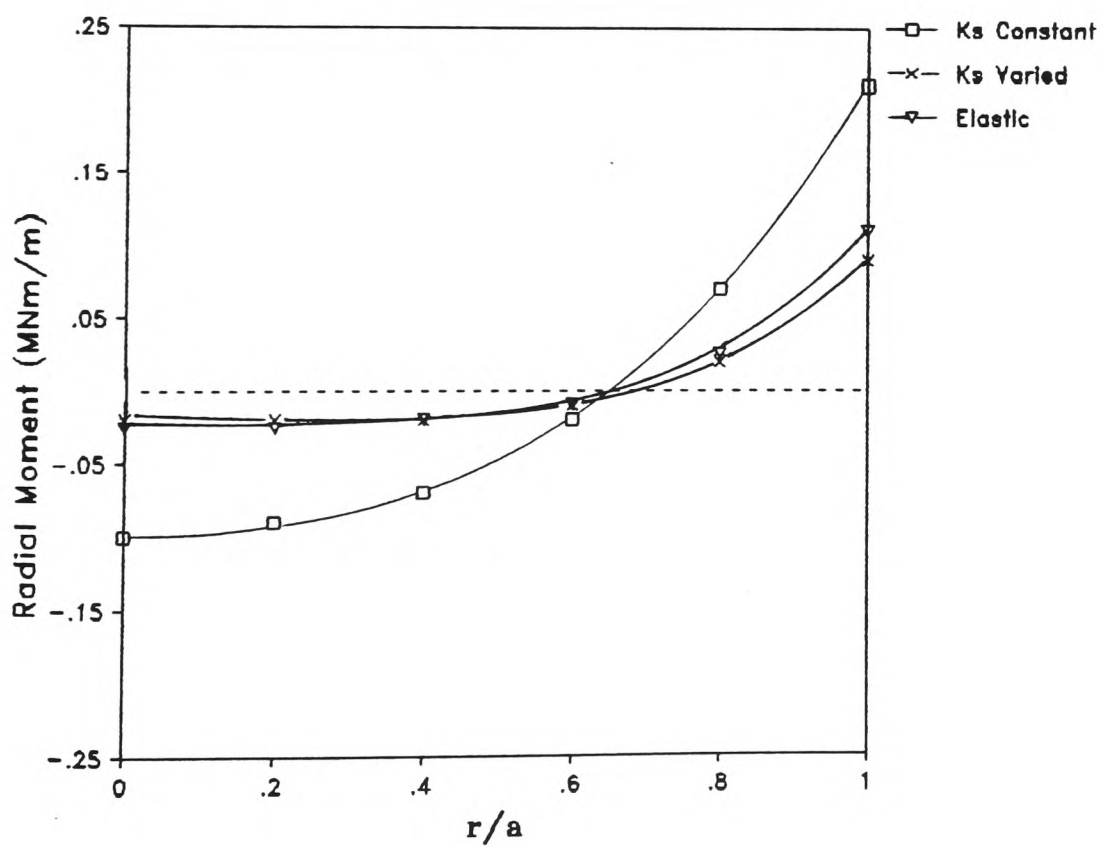


(b) Bending moment for free edge.

Figure 7.4.: Results for edge loaded raft.

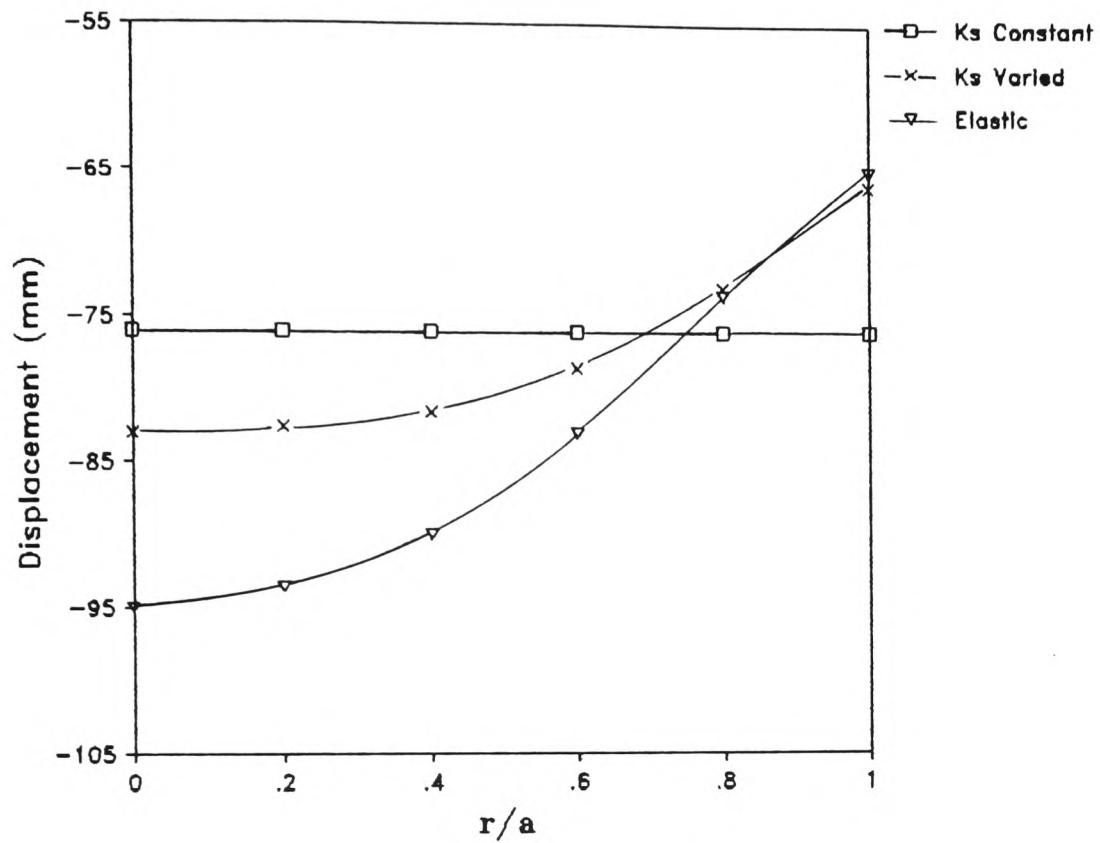


(a) Displacement for clamped edge.

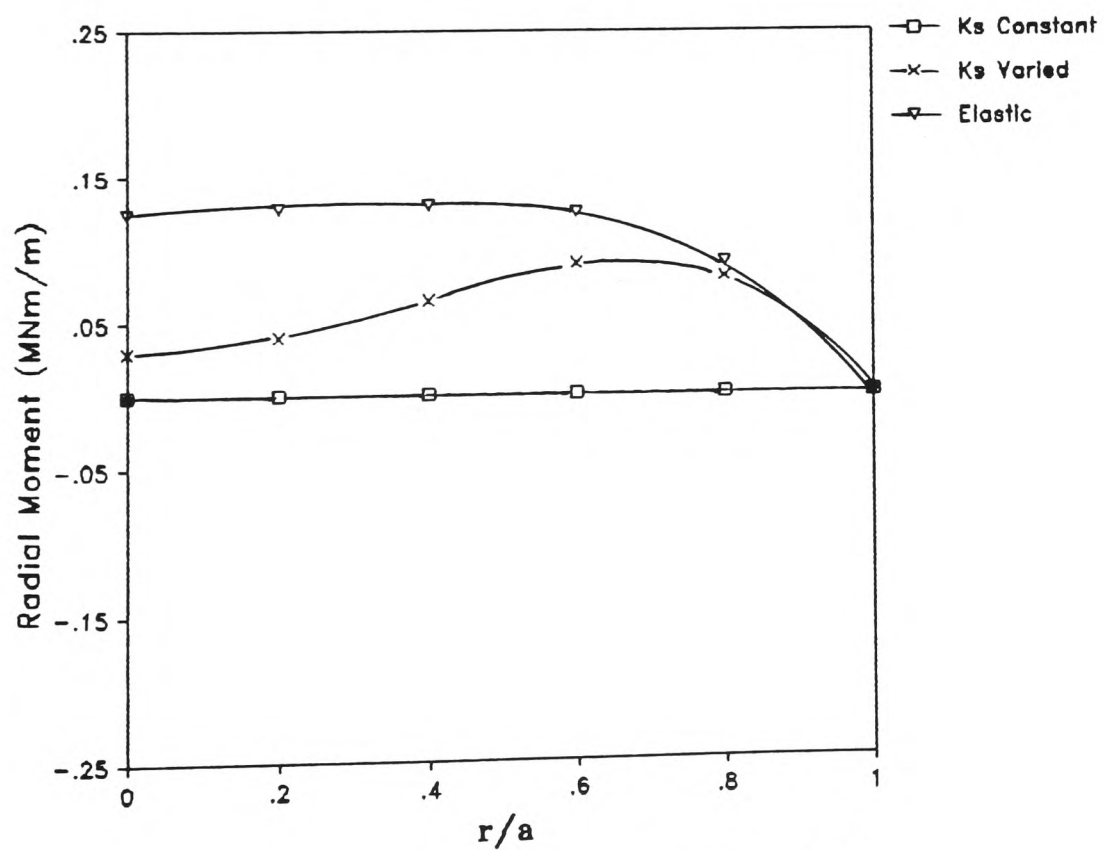


(b) Bending moment for clamped edge.

Figure 7.5.: Results for edge loaded raft.

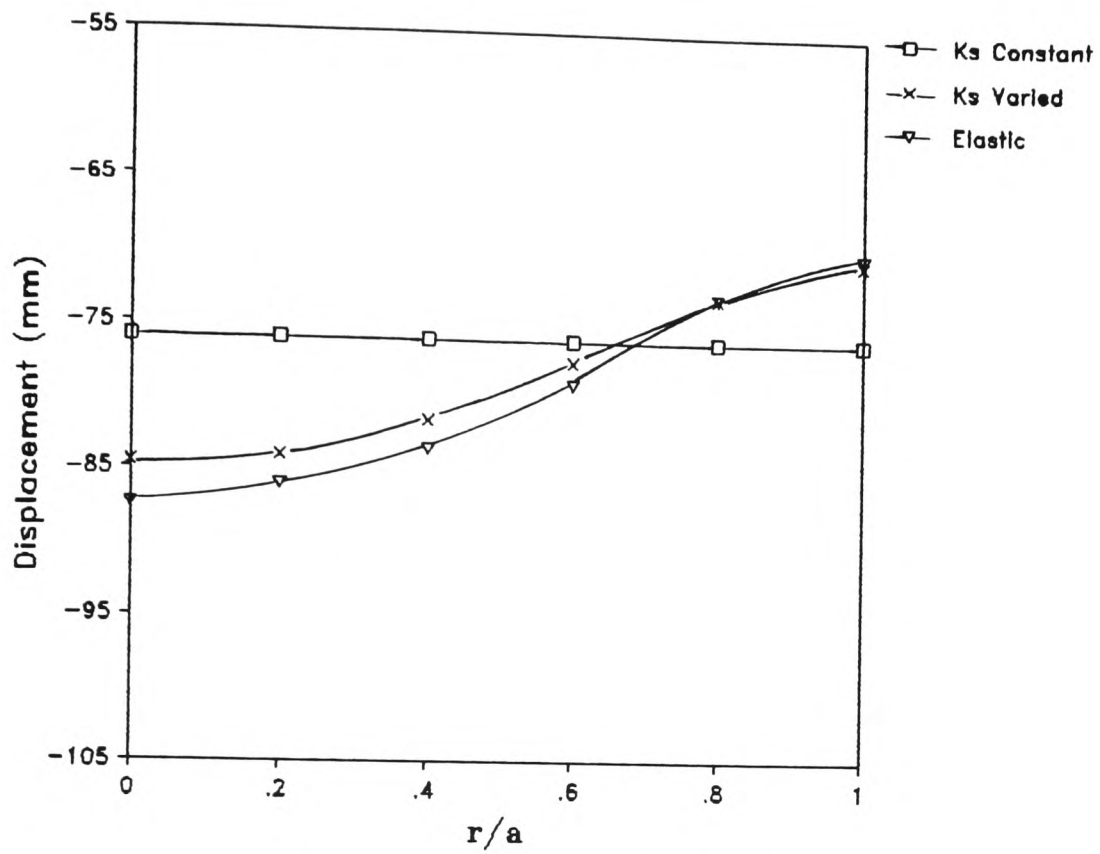


(a) Displacement for free edge.

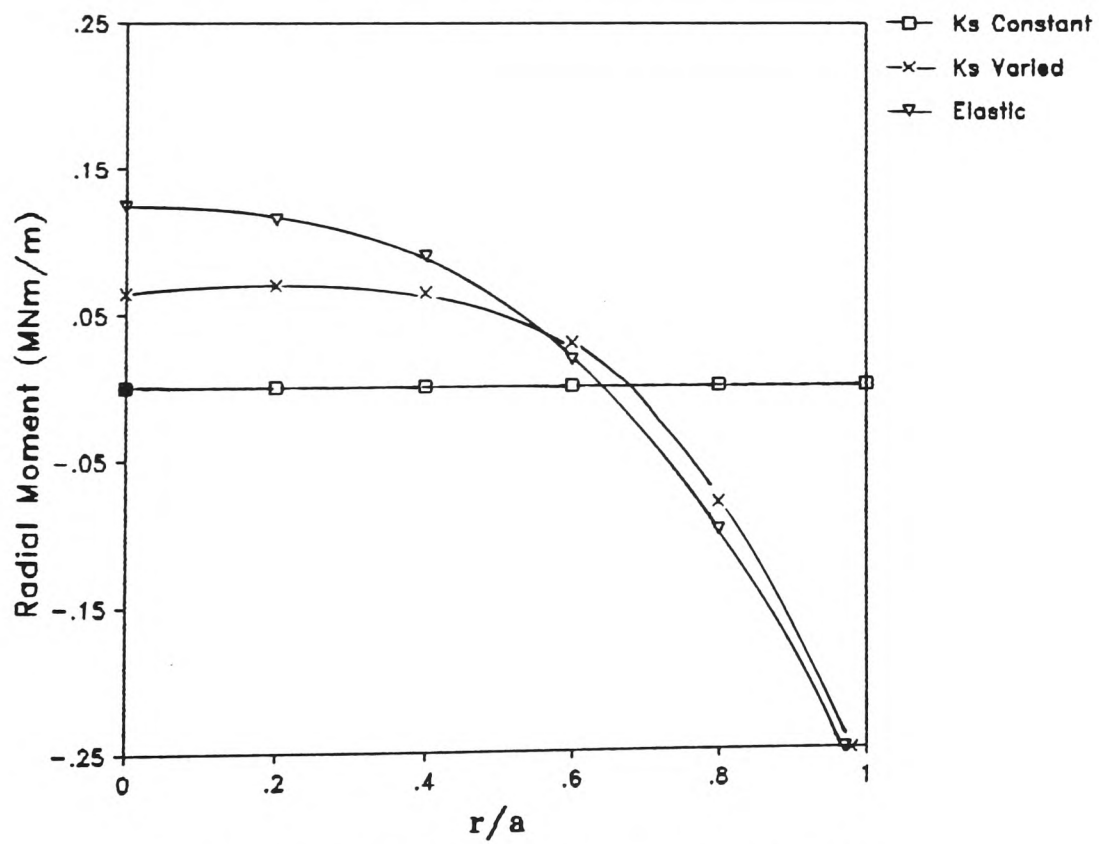


(b) Bending moment for free edge.

Figure 7.6.: Results for uniformly loaded raft.

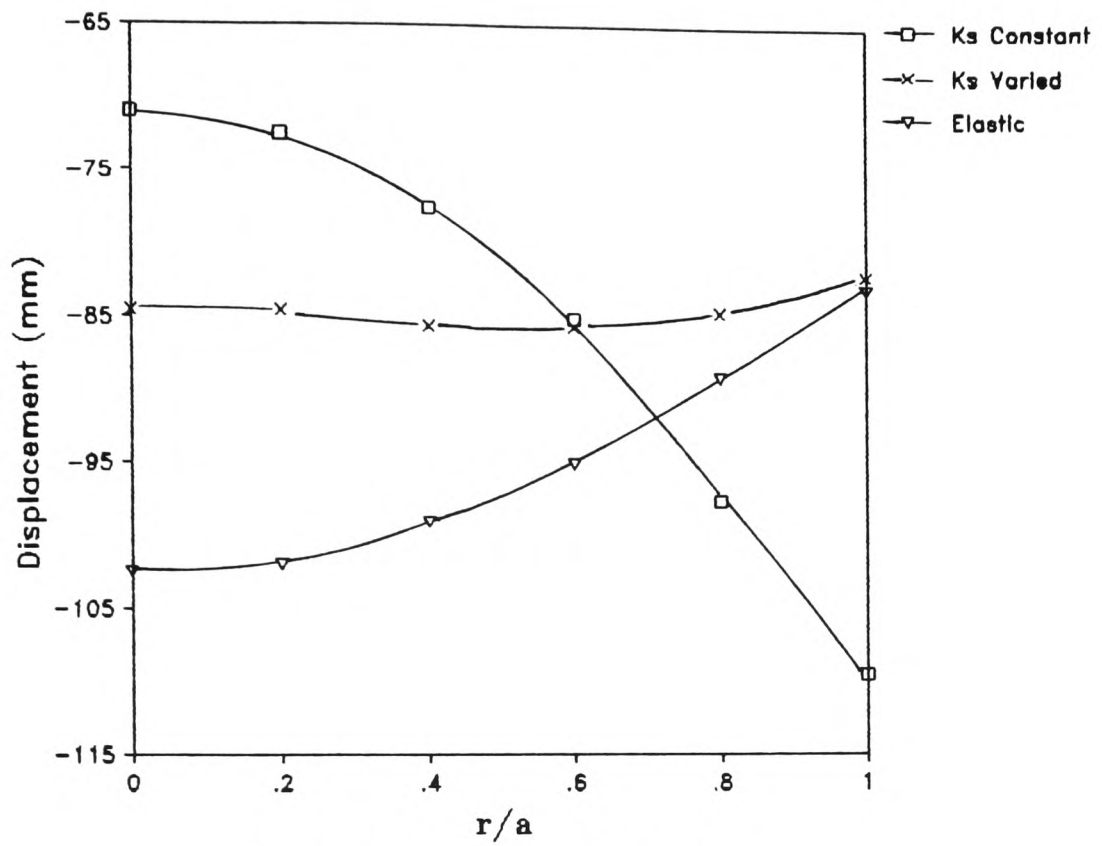


(a) Displacement for clamped edge.

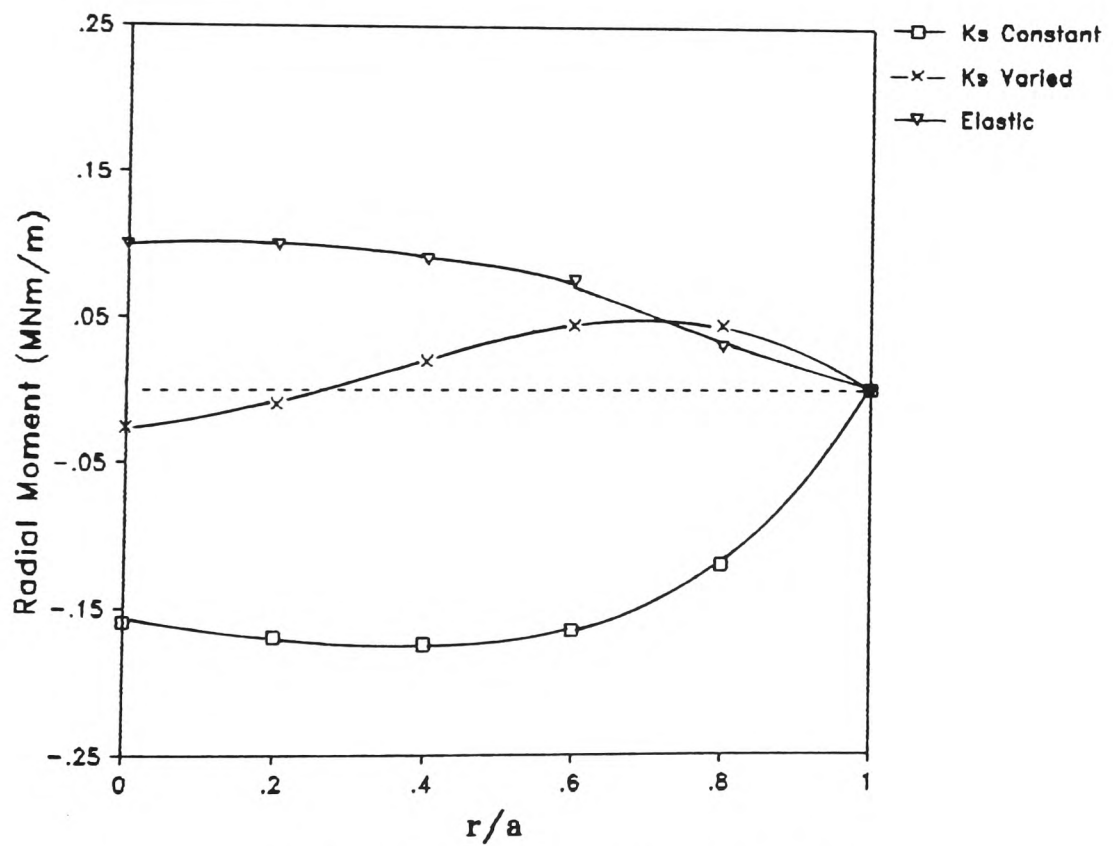


(b) Bending moment for clamped edge.

Figure 7.7.: Results for uniformly loaded raft.

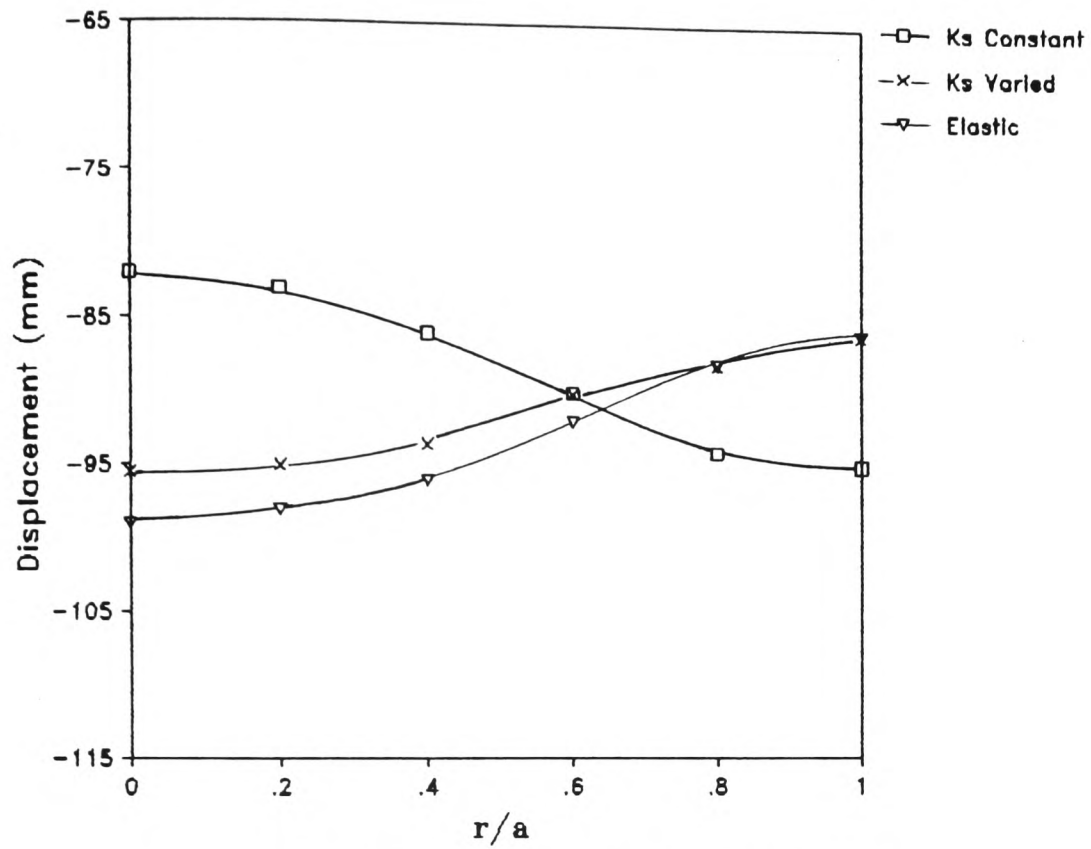


(a) Displacement for free edge.

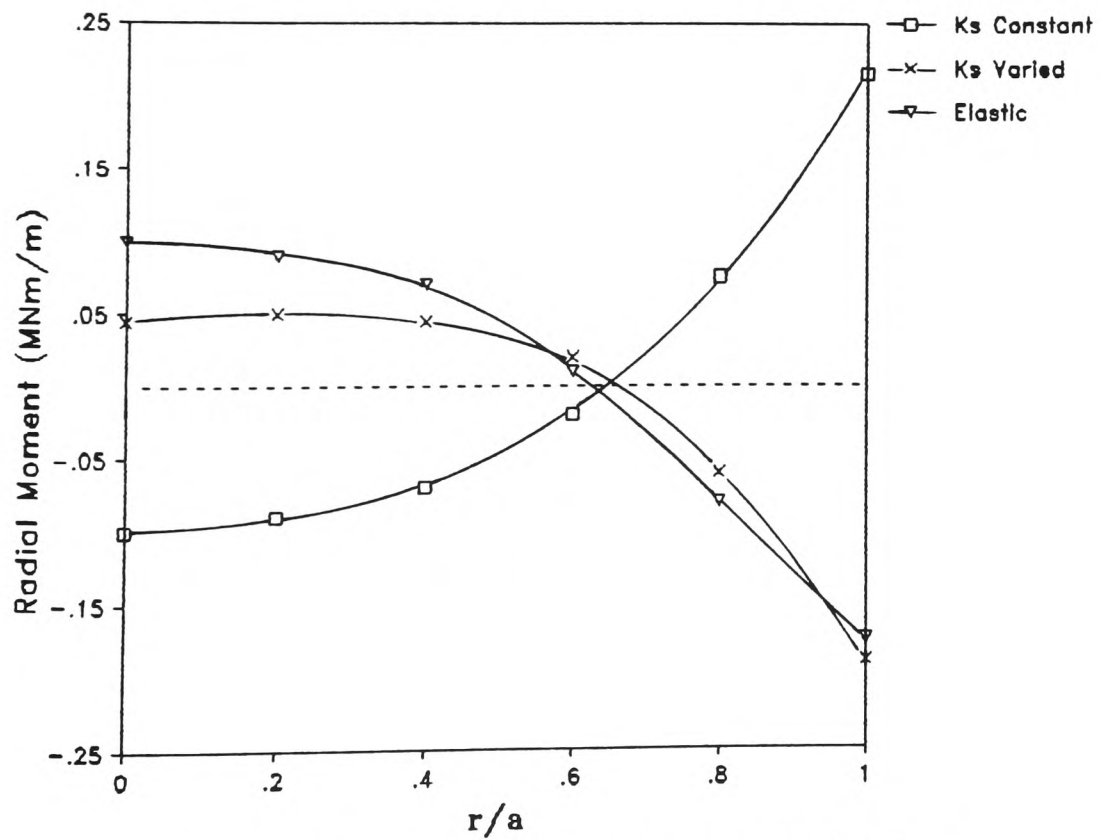


(b) Bending moment for free edge.

Figure 7.8.: Results for combined loading on raft.



(a) Displacement for clamped edge.



(b) Bending moment for clamped edge.

Figure 7.9.: Results for combined loading on raft.

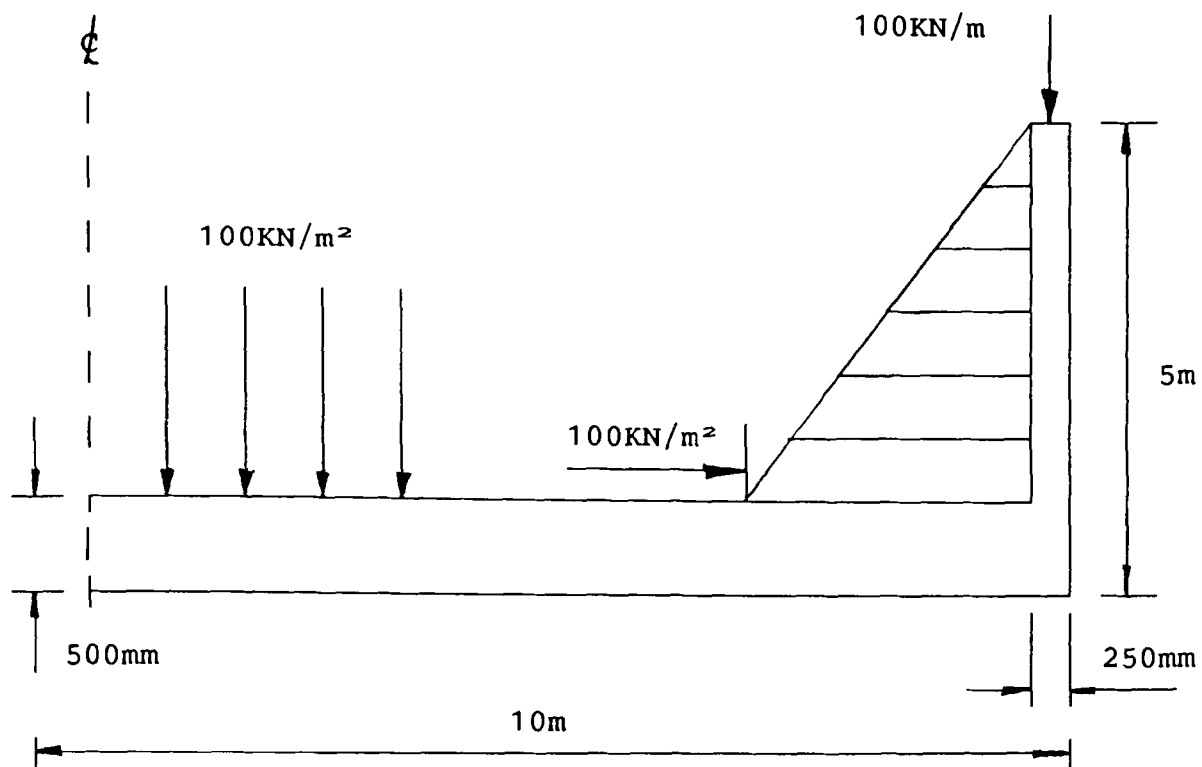
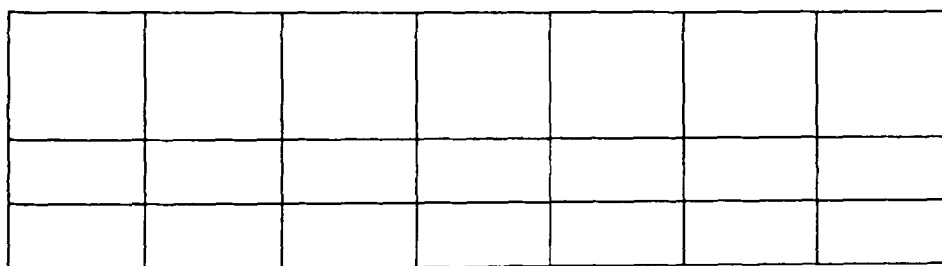
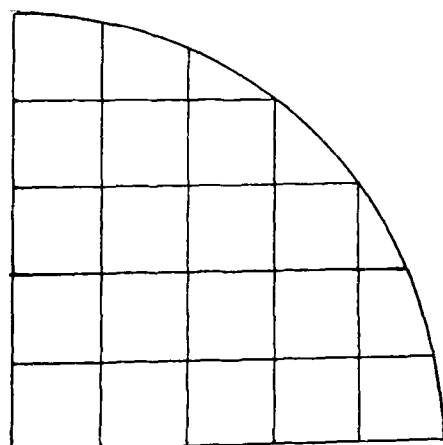


Figure 7.10.: Storage tank configuration.

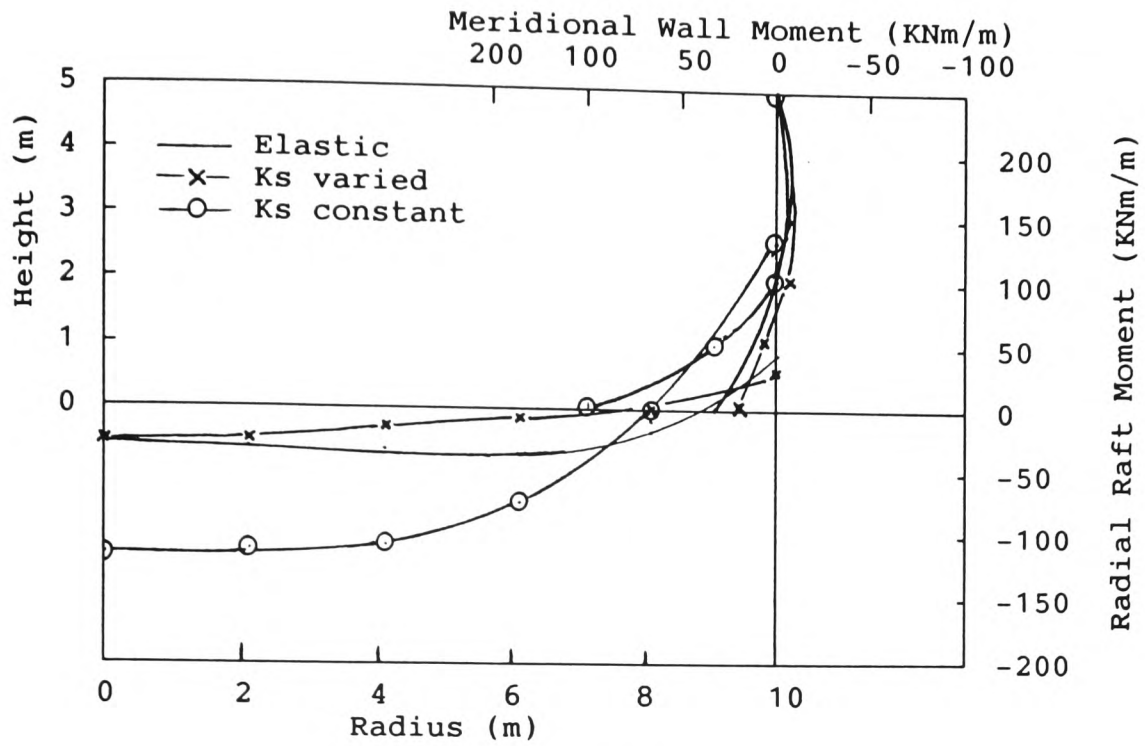


Opened section of wall

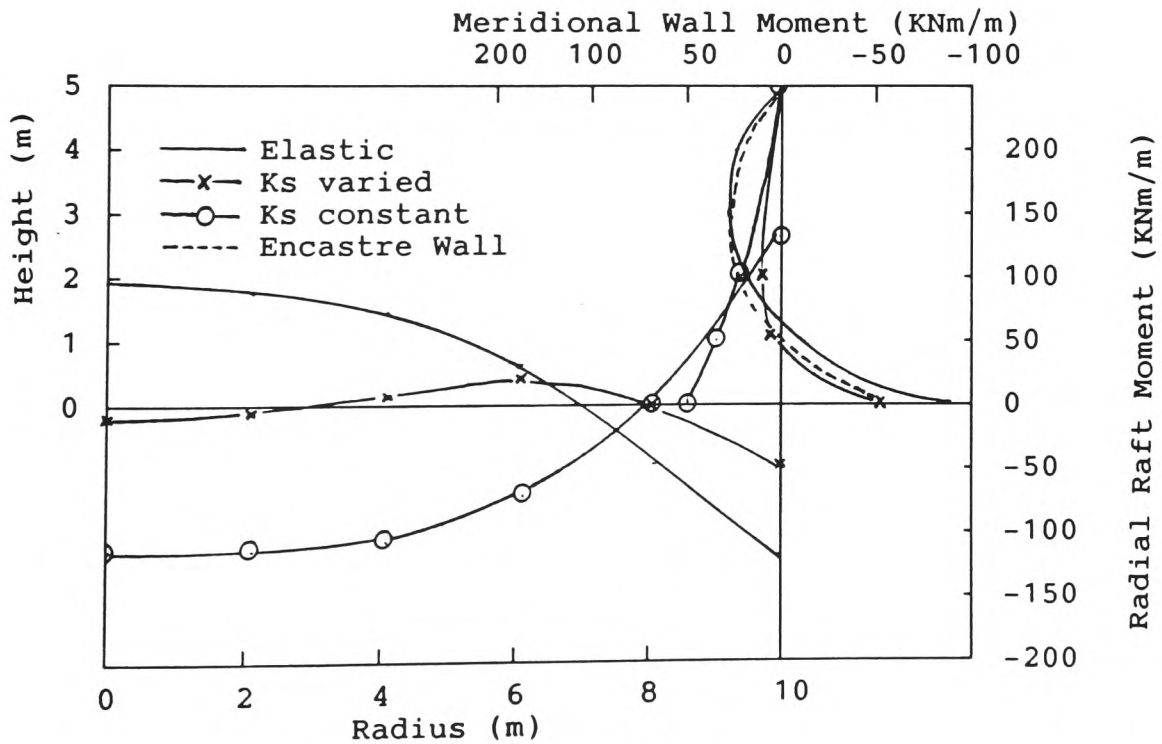


Plan of raft

Figure 7.11.: Idealized frame for S.S.R.T. analysis.

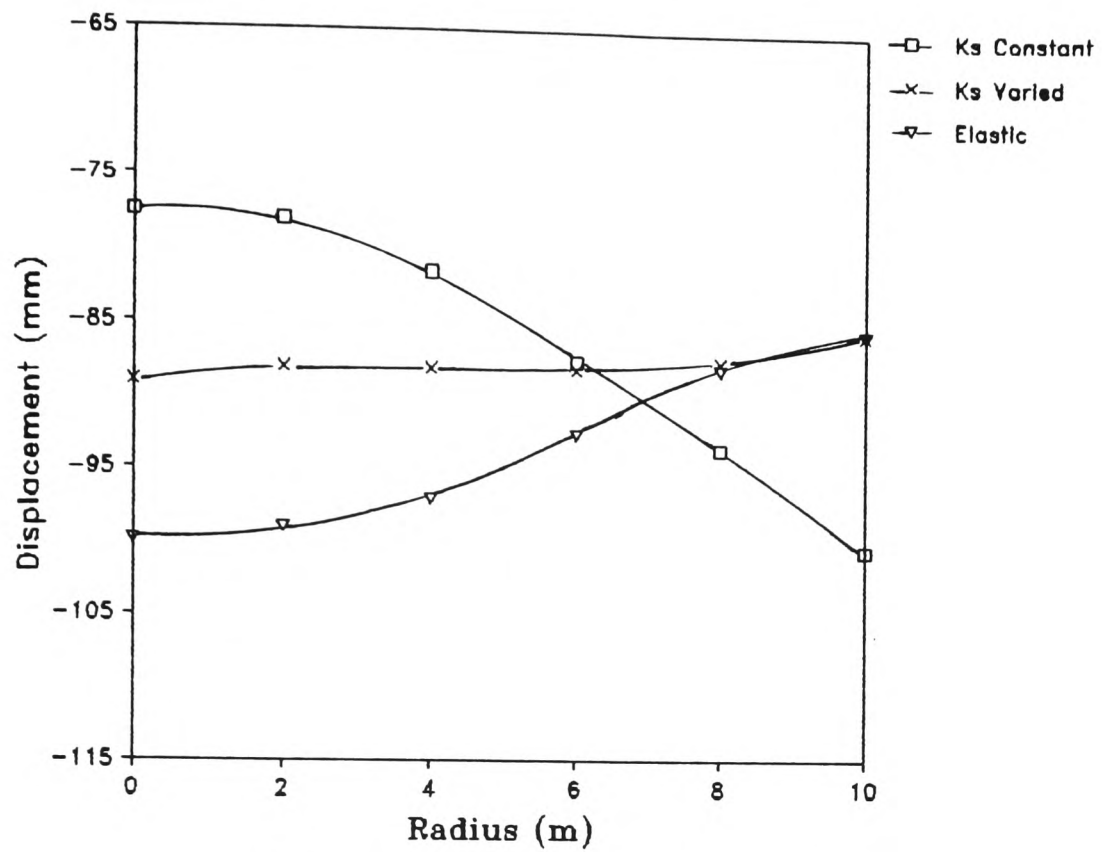


(a) Empty Tank

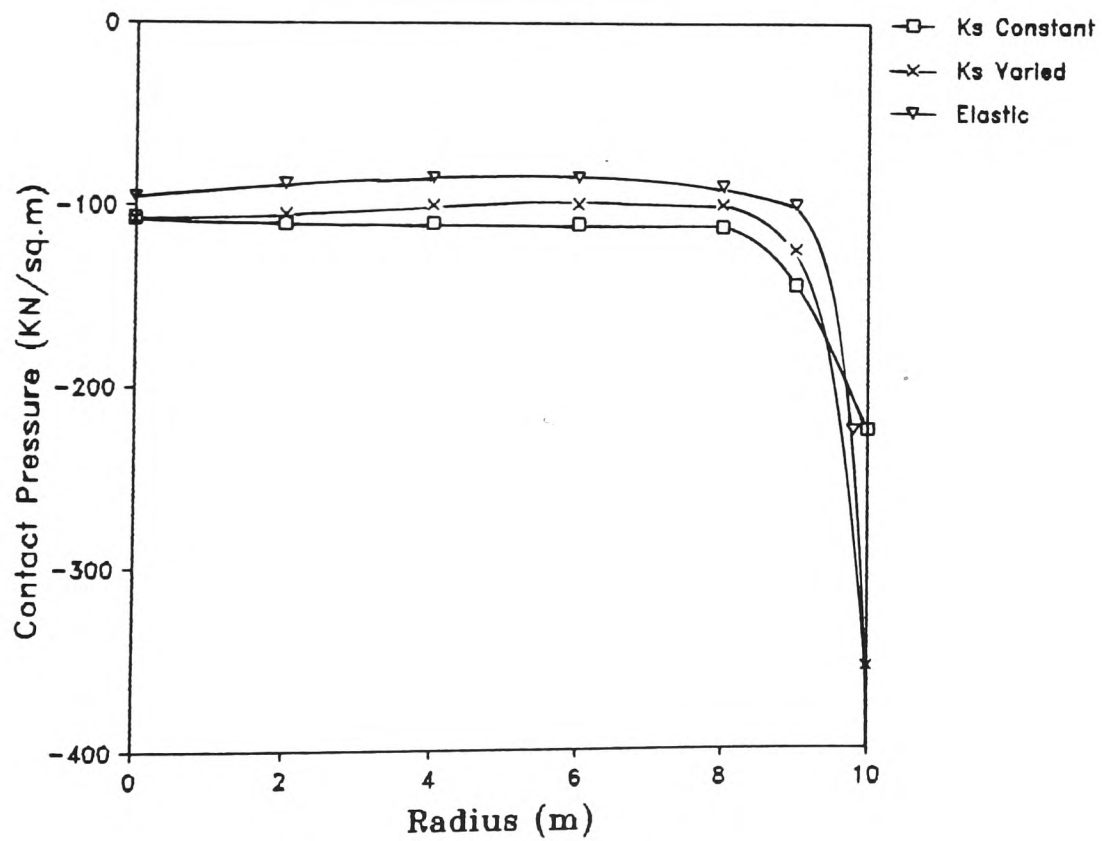


(b) Full Tank

Figure 7.12. Raft and Wall Moments In Storage Tank.

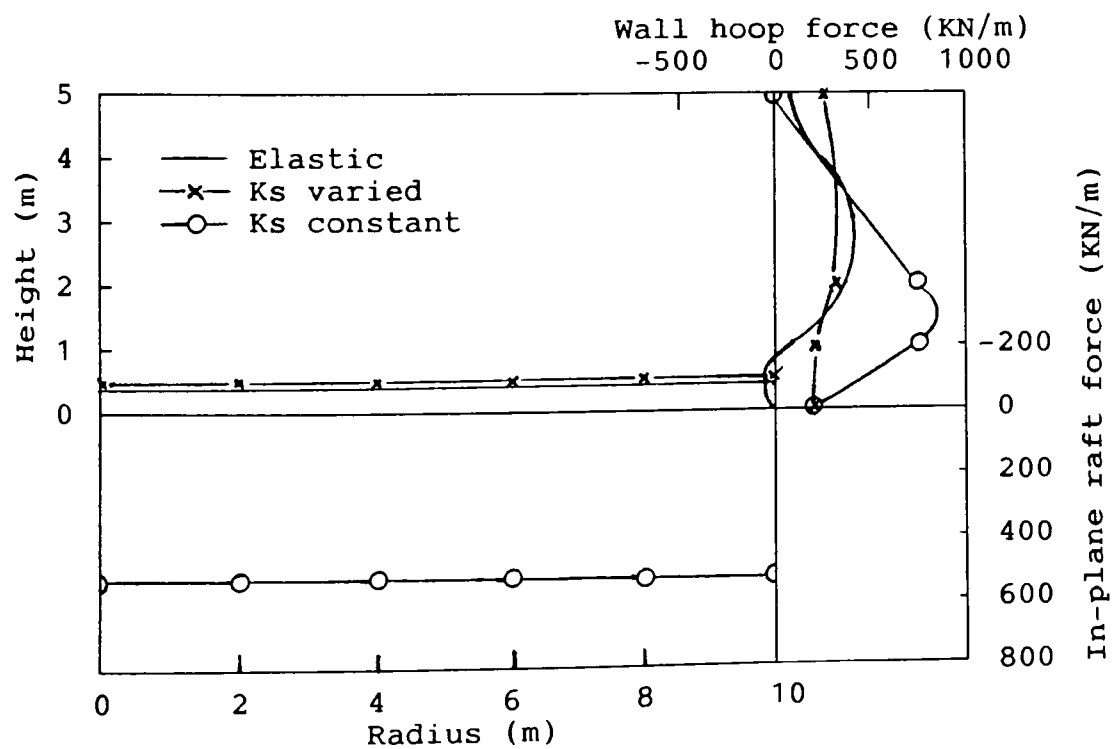


(a) Raft displacements.



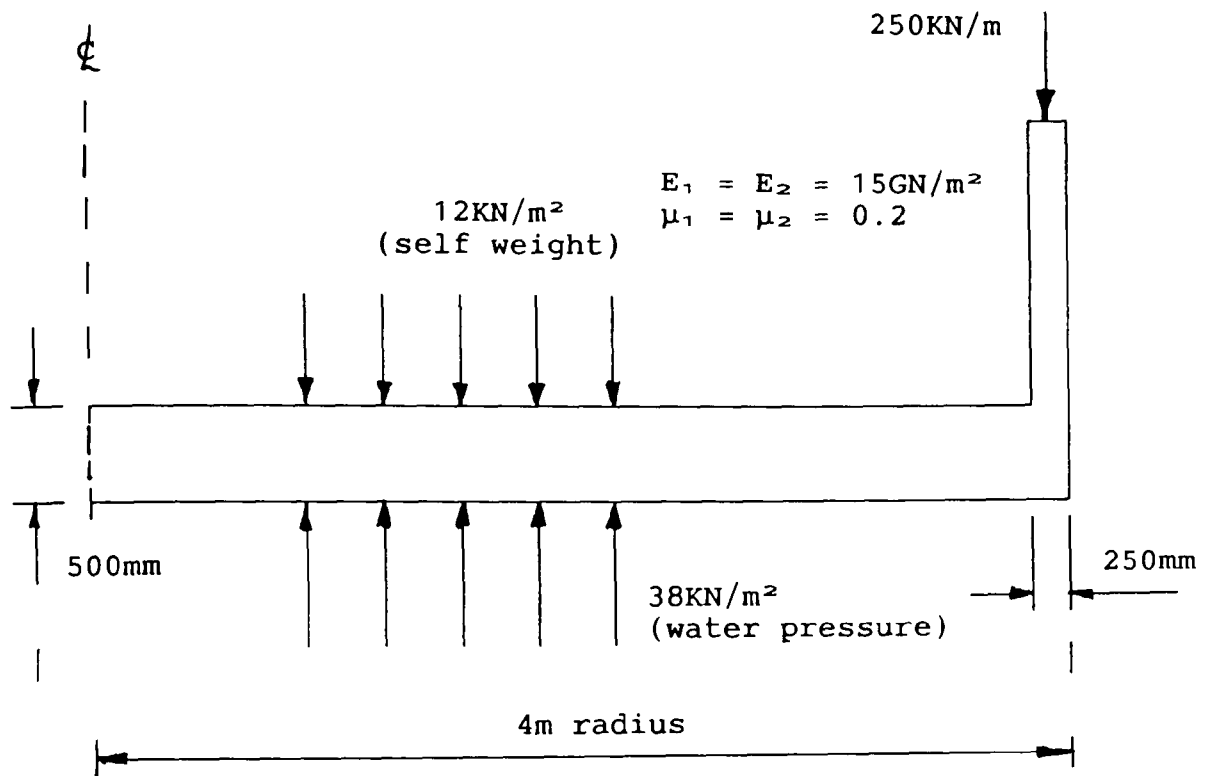
(b) Contact pressures.

Figure 7.13.: Further results for full storage tank.

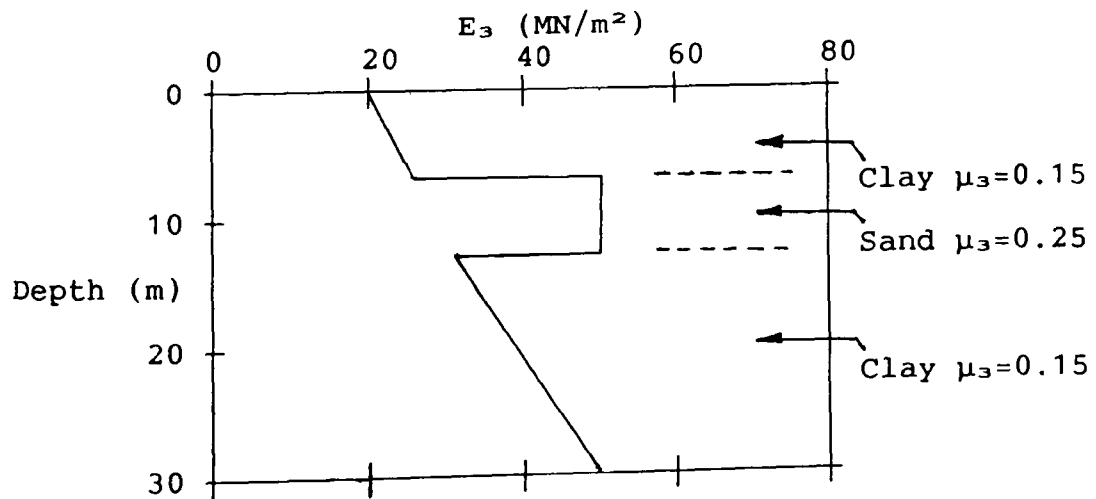


(c) In-plane raft and wall forces.

Figure 7.13.: Further results for full storage tank.

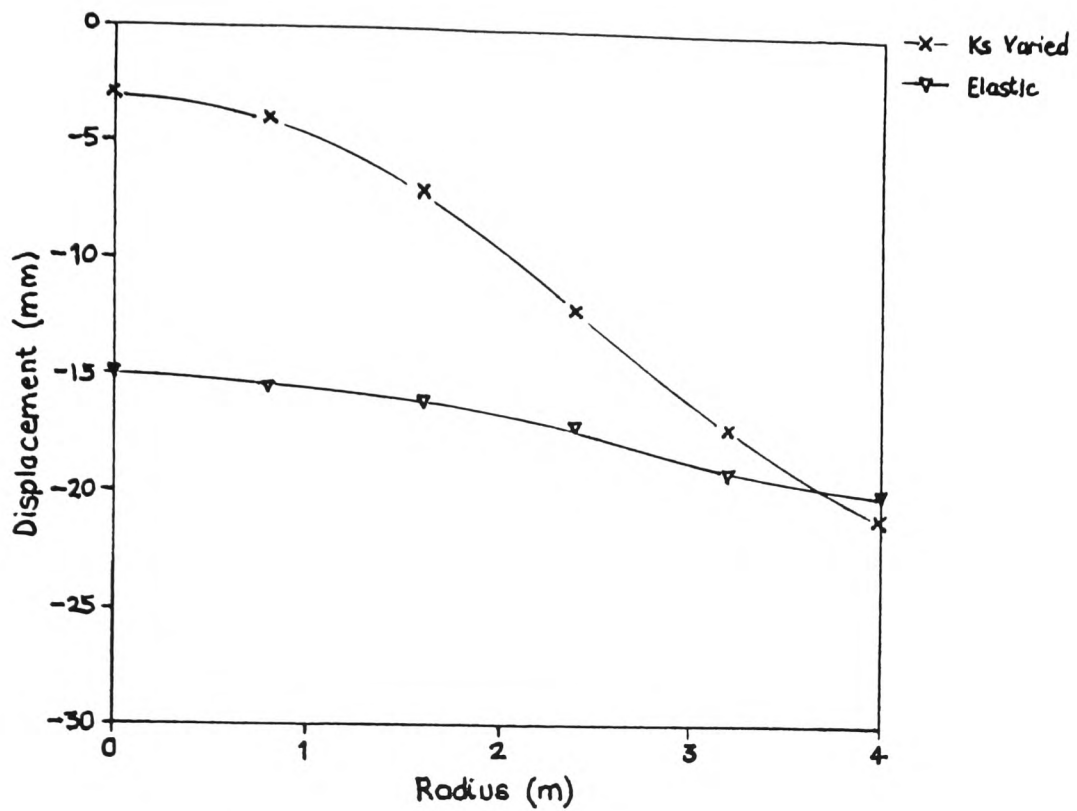


(a) Idealized building core.

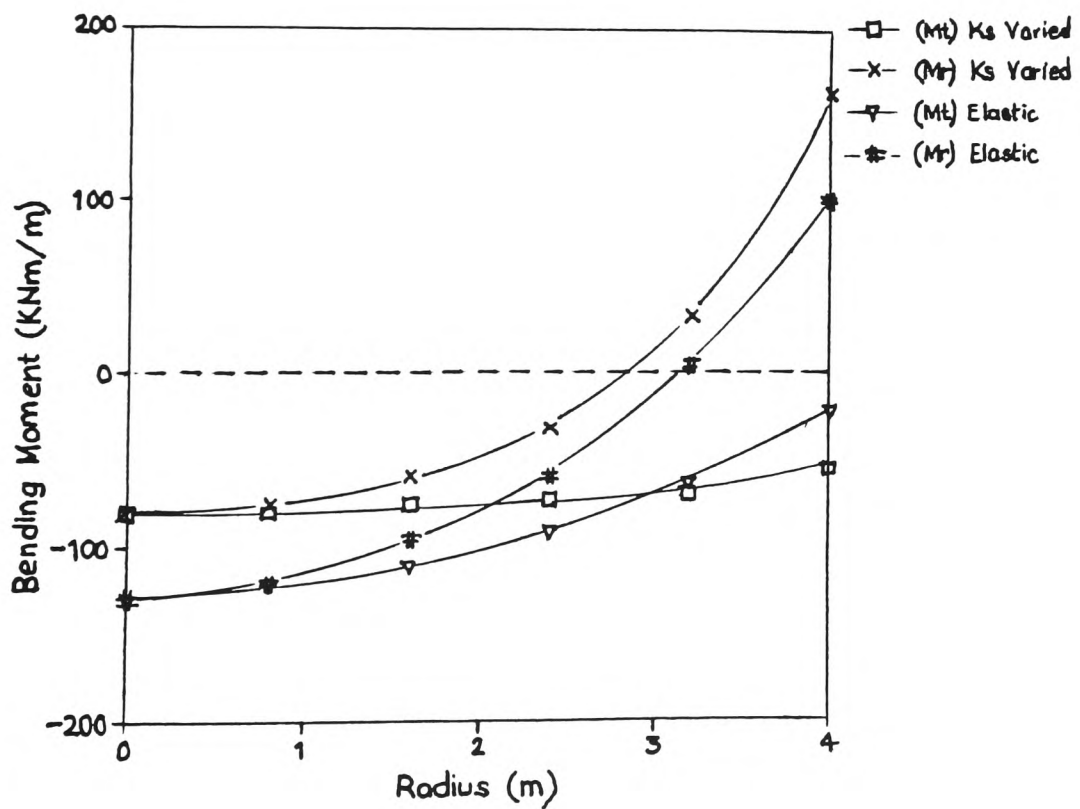


(b) Idealized soil properties.

Figure 7.14.: Data for core base analysis.



(a) Raft displacements.



(b) Bending moments.

Figure 7.15.: Results for core base analysis.

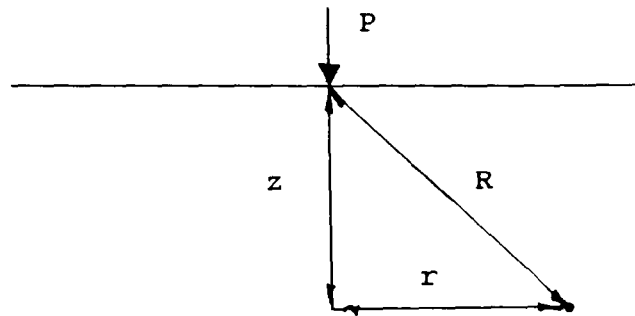


Figure 7.16.: Boussinesq's idealization.

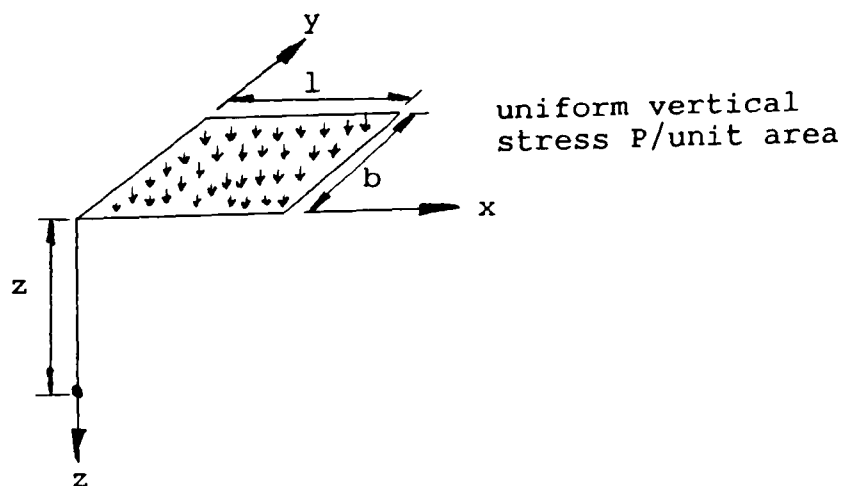
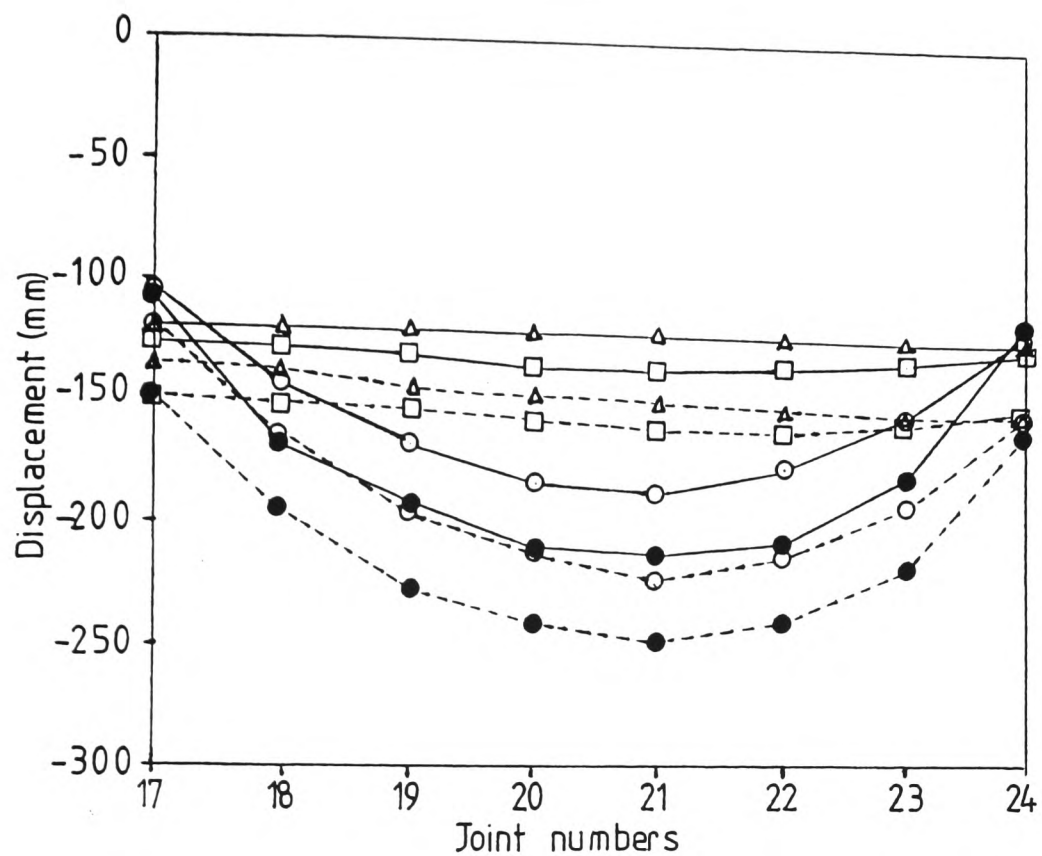


Figure 7.17.: Holl's Idealization.



Key

- No raft
- 0.91m raft (unrestrained)
- 0.91m raft (restrained)
- △ 5.60m raft (unrestrained)
- after Hooper and Wood.
- - - proposed method.

1	2	3	4	5	6	7	8	
θ_v	θ_v	θ_v	θ_v	θ_v	θ_v	θ_v	θ_v	θ_v
9	10	11	12	13	14	15	16	
θ_v	θ_v	θ_v	θ_v	θ_v	θ_v	θ_v	θ_v	θ_v
17	18	19	20	21	22	23	24	
θ_v	θ_v	θ_v	θ_v	θ_v	θ_v	θ_v	θ_v	θ_v
25	26	27	28	29	30	31	32	
θ_v	θ_v	θ_v	θ_v	θ_v	θ_v	θ_v	θ_v	θ_v
33	34	35	36	37	38	39	40	
θ_v	θ_v	θ_v	θ_v	θ_v	θ_v	θ_v	θ_v	θ_v
			41	42	43	44	45	
			θ_v	θ_v	θ_v	θ_v	θ_v	θ_v

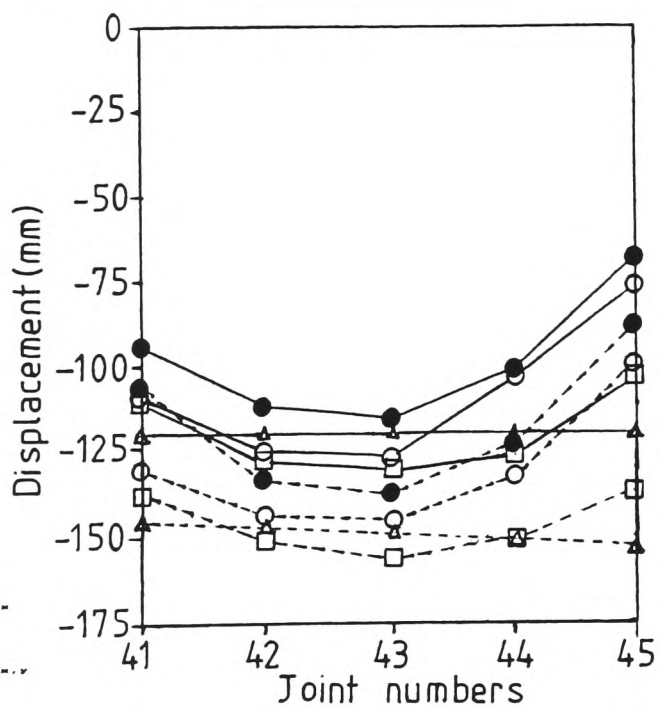


Figure 7.18: Drained raft settlements of Ebenezer House.

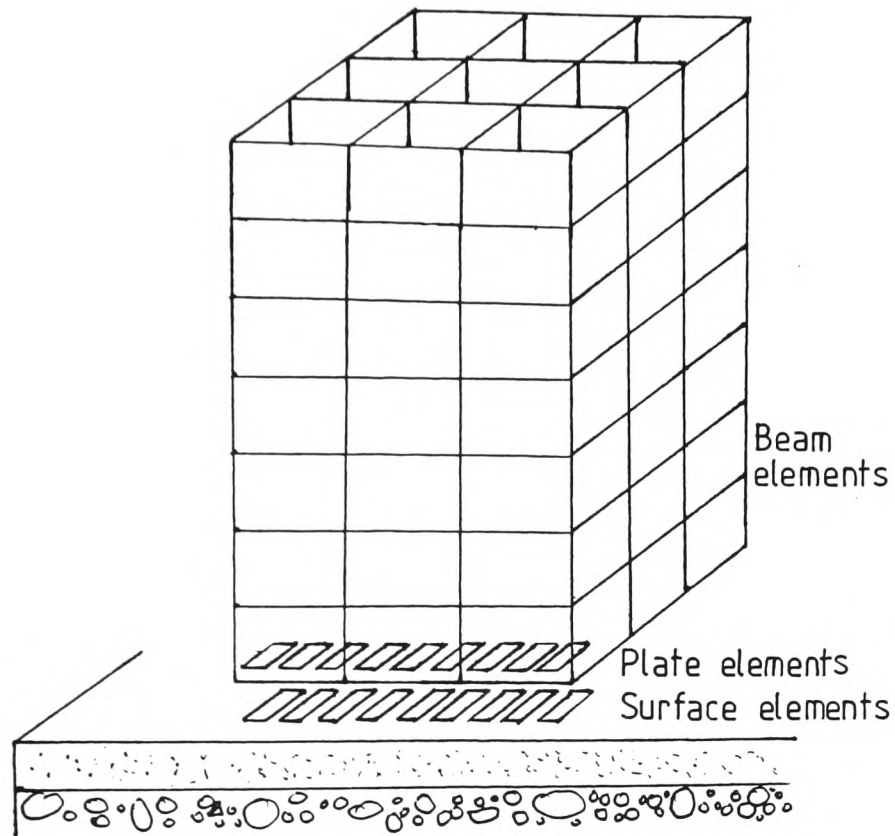


Figure 7.19.: Components of model.

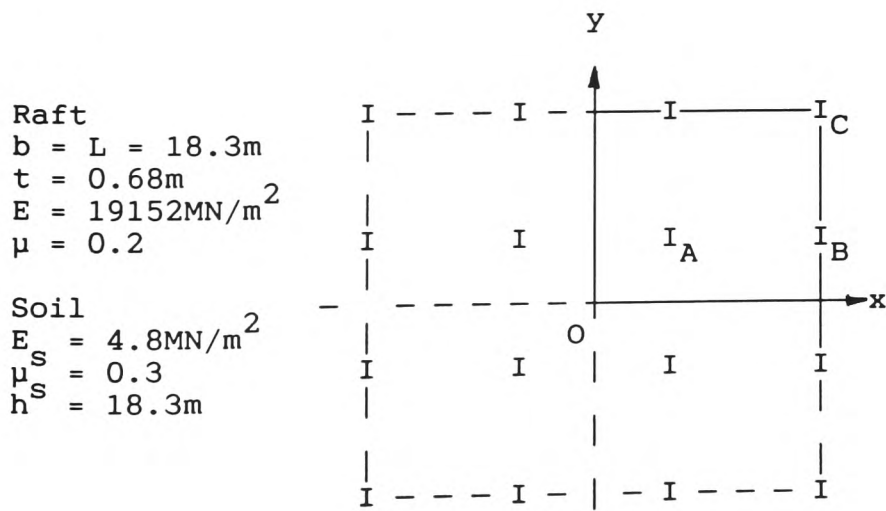
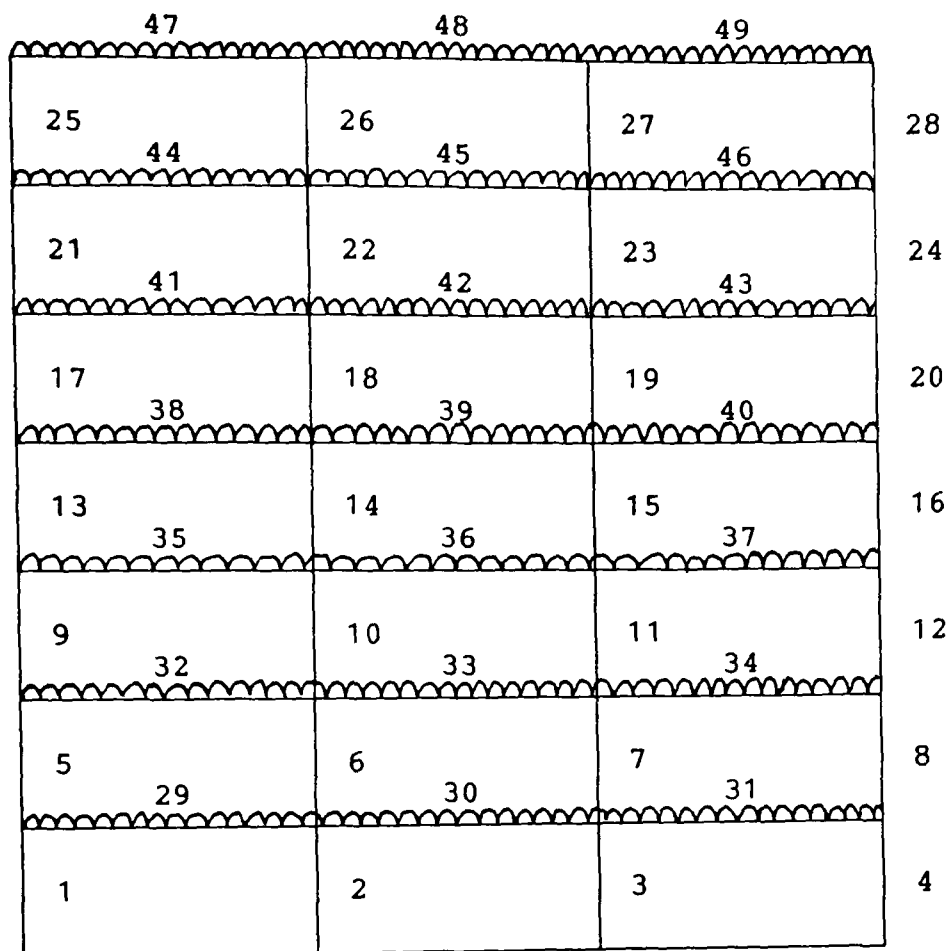


Figure 7.20: Details of model.



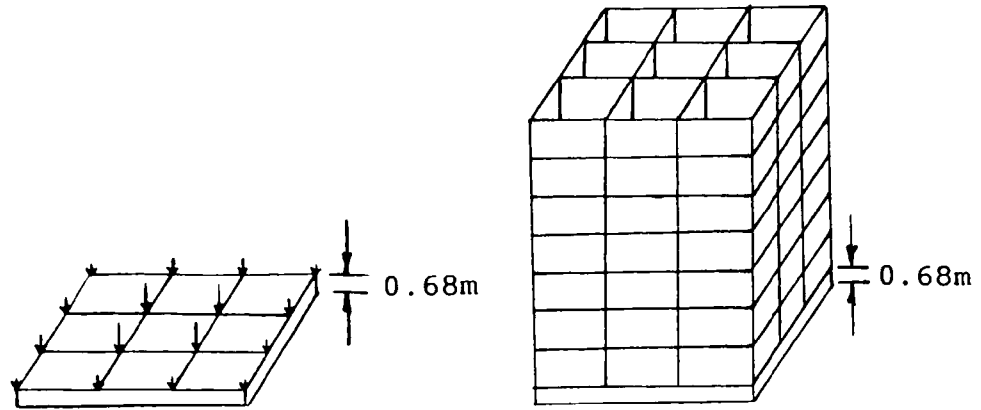
Member No.	I ($10^{-6}m^4$)	A ($10^{-3}m^2$)	l (m)
Beams 44-49	370	10.4	6.096
38-43	410	11.4	6.096
29-37	456	12.5	6.096
Cols. 17-28	143	11.4	3.658
5-16	226	16.9	3.658
1-4	387	20.1	4.572

Exterior beam load 14.6KN/m

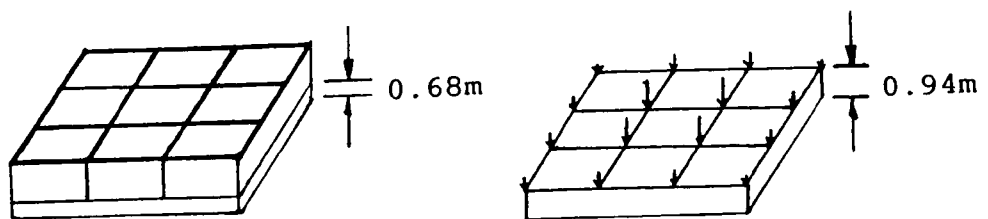
Interior beam load 29.2KN/m

No wind load

Figure 7.21.: Details of superstructure.



Case 1: No superstructure. Case 2: Full superstructure.



Case 3: Equivalent single storey. Case 4: Equivalent raft.

Figure 7.22.: Superstructure idealizations.

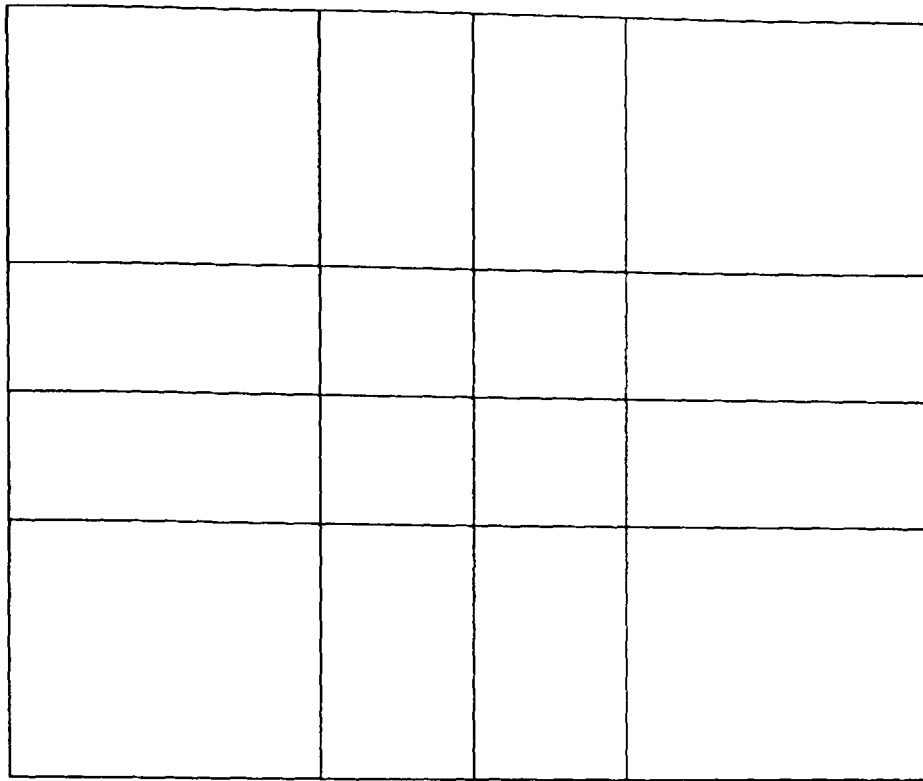


Figure 7.23: Coarse grillage.

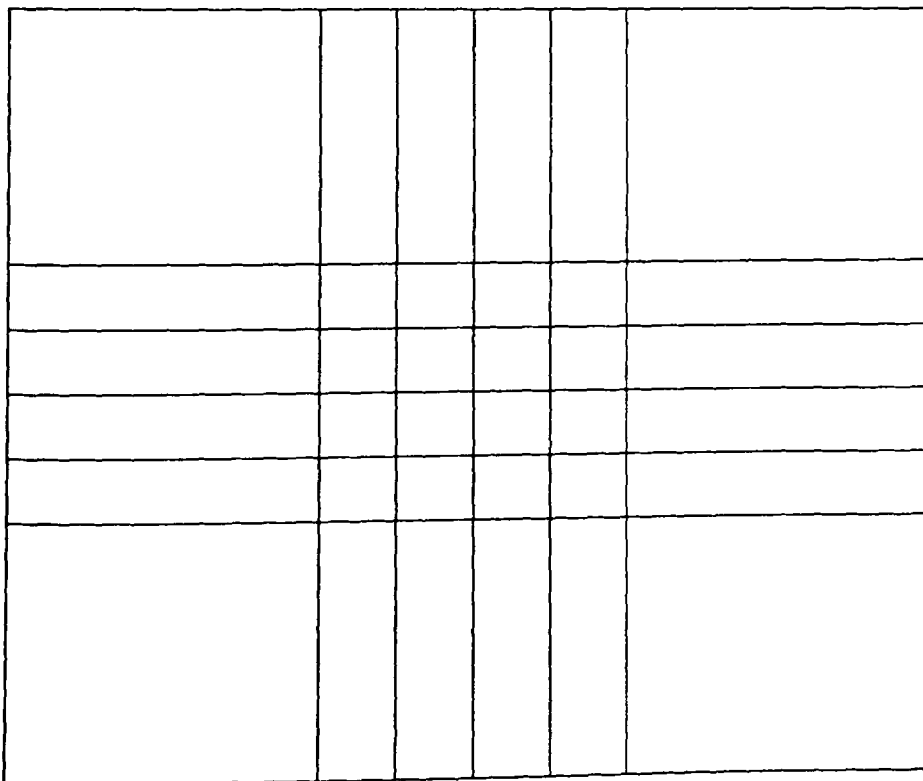


Figure 7.24.: Refined grillage.

CHAPTER 8.

NON-LINEAR PILE-SOIL BEHAVIOUR.

8.1. GENERAL.

The non-linear soil behaviour of a heavily loaded pile is complex. It is difficult to model this behaviour, especially when the pile is embedded in a layered soil. For these reasons, t-z and p-y methods of analysis are probably the most widely adopted approaches to the problem. For static analyses these methods enable load-displacement curves to be determined for the pile up to failure of the soil. They also represent the most practical method of modelling the dynamic behaviour of piles as the soil degrades.

It is proposed to develop the S.S.R.T. approach to accommodate non-linear pile-soil behaviour. The procedure involves replacing the soil surrounding the pile by a series of discrete springs. Stiffness values are assigned to the springs by comparison with established non-linear empirical t-z and p-y curves. Traditionally the pile-soil system is then solved iteratively for each load increment or by using finite difference techniques. It is proposed to use a finite element representation of the pile as this enables a closed form solution to be obtained for each load increment. The analysis can then be carried out using a standard structural program. Both the validity and applicability of the proposed method are demonstrated.

8.2. COMPARISON WITH O'NEILL ET AL.

8.2.1. The Method Of O'Neill et al.

O'Neill et al (1982a) presented results of the measured axial load transfer in a full-sized group of nine 10.75in. diameter steel pipe piles. The piles were driven with closed ends to a depth of 43ft. in a layered overconsolidated clay. They also presented the load transfer behaviour of two identical reference piles, driven and tested separately near the group. The wall thickness of all piles was 0.365ins.. The piles in the group were installed in a 3x3 square array with a nominal spacing of 3 diameters. Pilot holes 10ft. deep and 8ins. in diameter were drilled prior to driving the piles. The soil strata encountered is described in Table 8.1.

All piles were instrumented with electronic strain gauges to measure load transfer during driving and loading. The soil was instrumented with mechanical vertical-displacement sensors and piezometers. Lateral total stress and pore pressure sensors were placed on some piles.

Residual stresses were developed during installation. The pore water pressure dissipation rate was rapid and the authors estimated that the maximum side shear capacities were reached approximately four days after driving.

The average measured load-settlement curves of the two reference piles for three load tests are presented in Figure 8.1.. The measured load and stress distribution along the reference piles is shown in Figure 8.2. These distributions were determined by assuming the piles to be unstressed before loading. The authors also constructed f_z and q_z curves of side shear and end bearing against

displacement respectively by transforming the collected data. This enabled load-settlement curves to be created using a computer program based on the method of Coyle and Reese (1966) as described in Section 8.3.1..

The authors analytically formulated f-z and q-z unit load transfer curves as follows.

$$\frac{f}{f_{\max}} = \sin\left(\frac{\pi z}{2 z_c}\right) - 0.025 \sin\left(\frac{2 \pi z}{z_c}\right); \quad z \leq z_c \quad \dots\dots 8.1.$$

$$\frac{q}{q_{\max}} = \left[\frac{z}{z_c} \right]^{0.40}; \quad z \leq z_c \quad \dots\dots\dots 8.2.$$

Where f_{\max} = maximum unit load transfer at a given depth; q_{\max} = maximum tip stress; and z_c = pile displacement corresponding to the respective maximum stresses. Equation 8.1. is a Fourier approximation which the authors claimed fitted observations more accurately in the low stress range than did curves proposed by others; such as Vijayvergiya (1977). The equations only consider residual stresses implicitly ie. they are formulated for the usual analysis which assumes the pile to be unstressed before loading.

The z_c parameter for the f-z curve was evaluated as:

$$z_c = \frac{f_{\max} r_p}{G_{(y)}} \left[0.67 + \ln\left(\frac{2 p L (1 - \mu_s)}{r_p}\right) \right] \quad \dots\dots\dots 8.3.$$

Where r_p = pile radius; $G_{(y)}$ = shear modulus of the undisturbed soil at the depth for which the curve is being generated; μ_s = Poisson's ratio of the soil; L = pile length; and $p = G_{(y=L/2)}/G_{(y=L)}$.

The parameter z_c for the q-z curve is approximately 3% of the tip diameter.

The authors used these formulations to model the pile group behaviour. This was achieved by stretching the f-z and q-z curves to accommodate increased settlement due to interaction. The computed group load-settlement results were encouraging, although these slightly exceeded the measured values.

8.2.2. The Proposed Method.

Due to the added complexity of pile group behaviour, only the average results for the two single reference piles have been considered.

The pile was subdivided into 8 elements with 9 nodes. Each element was assigned a Young's modulus of 4.176×10^9 psf and a cross sectional area of $82.7 \times 10^{-3} \text{ ft}^2$. Load and stress distributions along the pile are presented in Figure 8.2. for two loads of 62Kips and 150Kips representing a working and failure load respectively. The idealized pile is presented in Figure 8.3.

As a first estimate for the spring stiffness values to be used for the idealization of the soil, the initial tangent of the f-z and q-z curves presented by O'Neill et al (1982a) for the measured performance were used. The initial stiffness values used to model skin friction were 142857, 705882, 857143 and 2571429 lbs/ft^3 in layers A, B, C and D respectively. These were multiplied by the relevant shaft-soil contact areas to determine initial spring stiffness values. A load increment of 10 Kips was applied to the idealized pile. The initial load and

displacement profiles were then determined by solution of the stiffness matrix for the pile-soil configuration.

Having determined a first estimate of load and displacement, Equations 8.1 and 8.2 were used to model the non-linear behaviour of the soil. Because the shear strength of each soil layer was not given, f_{\max} and z_c were scaled from the f - z curves for the measured performance and are given in Table 8.2.

Similarly, q_{\max} was scaled from the q - z curve as 58×10^3 psf. The corresponding z_c value for end bearing was 0.225ins..

These values were then used in Equations 8.1. and 8.2. to calculate new values of f , z and hence soil stiffness values for each load increment. As this work was laborious, a supplementary computer program was written to compute the new soil stiffness for each load increment. For load increments of 10Kips, incremental displacements δz and load δf were determined at each node. These were summed up to give the overall load-settlement curve. At each increment, the load in every spring was calculated; and hence the soil stress. When the stress in the soil, f , reached f_{\max} the corresponding spring was removed.

The load and stress distributions in the soil are presented in Figure 8.2.. The computed results were very encouraging and agreed well with the measured performance. The computed load distributed down the pile shaft slightly underestimated the measured values. This was reflected in the computed distribution of soil stress, f , with depth being slightly higher than the measured values over the upper region of the pile. Apart from a difference between

results near the pile tip, the agreement between computed and measured soil stress profiles was very good. This demonstrated that the proposed method successfully modelled the important feature of load transfer of a pile within a multi-layered soil. The discrepancy at the tip is considered to be due to the influence of the considerable spring stiffness representing end bearing resistance. This could possibly be overcome using a finer element length near the pile tip or using a lower end bearing stiffness.

The load-settlement curve, presented in Figure 8.1. was also determined. The displacement at the peak load agreed well with that for Test 1 (after 18 days) and the maximum load carrying capacity agreed well with that of Test 3 (after 108 days). Although the computed load-settlement curve was non-linear, on reaching the peak load the pile failed with increasing settlement under a constant load. The method did not compute failure of the pile at a lower residual strength because of the incremental procedure adopted. Results for the simplified proposed method were generally encouraging. This demonstrated the applicability of a modified S.S.R.T. approach to analyse pile behaviour in a non-linear heterogeneous soil.

8.3. COMPARISON WITH COYLE AND REESE.

8.3.1. The Method Of Coyle And Reese.

Reese (1964) developed an analytical method to compute load-displacement curves for axially loaded piles. The procedure involved dividing the pile into a number of elements. Beginning at the pile tip, a small tip displacement was assumed. Based on a single curve of the

ratio of load transfer to soil shear strength against pile displacement, the force and displacement of each element was calculated by working up the pile. Finally, the load at the top of the pile, Q_0 , and the corresponding displacement, δ , were determined for different assumed tip displacements. This enabled a load-displacement curve to be plotted for the pile head. The method was cumbersome and an iterative process was used to calculate each point on the load-displacement curve. By implication from the procedure used, convergence of results may depend on the arbitrary initial tip displacement assumed.

Coyle and Reese (1966) considered that the method was useful for predicting the behaviour of an axially loaded pile in clay. However, they noted that a single curve of the ratio of load transfer to soil shear strength against pile displacement was inadequate to accurately represent the behaviour. Consequently, they recommended that it was necessary to replace the single curve with a family of curves to represent the pile-soil behaviour at different depths.

Clays experience a change in strength after pile driving, with soft clays increasing in strength and stiff clays decreasing in strength. Consequently, Coyle and Reese also presented a graph, after Woodward et al (1961), to develop coefficients relating the maximum load transfer that could be developed along a steel pipe pile for a given shear strength. This graph is reproduced in Figure 8.4.

They compared results computed using this method with actual load-displacement curves for some typical field tests. The data used to compute one load-displacement

curve was taken from Plate 308 of Peck (1961). The steel pipe pile had a 10.75in. external diameter with a wall thickness of 0.312in.. A 0.75in. thick, 11.5in. diameter steel plate was fixed to the base of the pipe, and the embedded length of the pile was 111ft.. The soil strata and average soil shear strength values are presented in Table 8.3.

The soil shear strength for this test was reduced using factors determined from Figure 8.4. for a stiff clay. They considered that their computed load-displacement curve for this test, presented in Figure 8.5. was conservative in relation to the actual curve. They computed the load carrying capacity as 315Kips and reported that the actual load carrying capacity was 415Kips. However, by examination of the original pile test data the load at 1in. pile displacement was 415Kips. There were no more readings reported above this load. It is therefore possible that the failure criteria for this pile was taken as the load to produce a 1in. displacement or a displacement equivalent to 10% of pile diameter.

8.3.2. The Proposed Method.

The pile test reported in Plate 308 by Peck (1961) presented by Coyle and Reese (1966) was analysed using the proposed S.S.R.T. iterative analysis.

The pile was subdivided into 8 elements as presented in Figure 8.6.. The cross sectional area of the pile was taken as $36.06 \times 10^{-3} \text{ ft}^2$ and Young's modulus was assumed to be $4.176 \times 10^9 \text{ psf}$. The average soil shear strength of each layer was adjusted using reduction factors reproduced in

Figure 8.4.. In each case the reduction coefficient was taken as 0.29. This gave maximum shear strengths of 2287, 2123, 2940 and 3920 lbs/ft² in layers 1, 2, 3 and 4 respectively. The maximum tip load was estimated as shown below.

$$\begin{aligned}\text{Tip load} &= \text{bearing area} \times 9 \times \text{soil shear strength at tip} \\ &= 0.721 \times 9 \times 3920 \\ &= 25.5 \times 10^3 \text{ lbs} = 25.5 \text{ Kips.}\end{aligned}$$

This value agreed with that computed by Coyle and Reese. To calculate the maximum load transfer, f_{\max} , which could be developed at the pile-soil interface, the adjusted field curves presented by Coyle and Reese were used. These are reproduced in Figure 8.7. The relevant data extrapolated from these curves is presented in Table 8.4., where y_c is the settlement required to produce f_{\max} .

The extrapolated initial gradient K_0 of each curve and the maximum load transfer that could develop at each node are also presented. A check was made to determine the load carrying capacity of the pile by adding the skin friction and end bearing resistance. The skin friction was calculated as $\Sigma (f_{\max} \times \text{circumference} \times \text{element length})$ giving a value of 708.2×10^3 lbf. Adding the end bearing resistance gave a load carrying capacity of 733.7×10^3 lbf; considerably greater than that obtained from Coyle and Reese's load-displacement curve. However, there was no reported basis on which to reduce the load carrying capacity.

To analyse the pile, initial soil spring stiffness values were determined for each node along the pile. The maximum end bearing stress q_{\max} was calculated as 35.4×10^3 lbf/ft². O'Neill et al (1982a) recommended that y_c for

q_{\max} be taken as 3% tip diameter; y_c was thus calculated as 0.345ins. An initial end bearing stiffness was approximated through multiplying q_{\max} by (base area/ y_c). The initial spring stiffness values were then input into the program to determine a first estimate of displacement. The load was increased in increments of 50 Kips and an incremental displacement calculated for each load increment. The spring stiffness for the next increment was determined using the program written to solve O'Neill's equations. The spring load was limited to the calculated maximum pile-soil transfer load; the spring being removed at points where this was reached.

The computed load-displacement curve at the pile head is superimposed on Figure 8.5.. Up to a load of 315 Kips the agreement between these results and those of Coyle and Reese is excellent. However, the maximum load the pile carried before every spring was removed was 794.7 Kips; which was slightly higher than the calculated pile capacity of 733.7 Kips. The small discrepancy is considered to be due to relatively large increments of load used. The maximum load carried by the pile was much greater than that of Coyle and Reese and the value presented from the load test. However, as previously explained, the failure criteria for the test pile may possibly have been a displacement of 10% of the pile diameter. If this is the case, the pile may not have reached its total load carrying capacity. Based on a 1in. displacement, the load carried by the pile from this method was 350 Kips which was in better agreement with the test load than that of Coyle and Reese.

To conclude, the proposed method satisfactorily modelled the pre-failure non-linear behaviour of an axially loaded pile embedded in a heterogeneous soil. The discrepancy between these results, those of Coyle and Reese and the measured performance was due to the defined different values for the ultimate load carrying capacity of the pile. The proposed S.S.R.T. was applied to analyse the non-linear behavior using a standard structural package. The approach is considered to be simpler than that of Coyle and Reese because an iterative process is not used to define each point on the load-displacement curve.

8.4. COMPARISON WITH MATLOCK.

8.4.1. The Method Of Matlock.

(a) General.

Matlock (1970) developed correlations for the design of laterally loaded piles in soft clay. These were largely empirical and based on a program of research on laterally loaded piles for offshore structures. The research included field tests on an instrumented pile and laboratory model testing. He considered both static and cyclic loading. However for simplification, only the static loading tests are considered here.

(b) Ultimate static resistance.

Matlock's proposed method involved a p-y approach. In order to construct p-y curves, the ultimate resistance of the pile per unit length, P_u , needs to be determined. He considered that if soft clay soil was confined so that plastic flow around a pile only occurred in horizontal

planes, then P_u could be expressed as:

$$P_u = N_p c d \dots\dots\dots 8.4.$$

where c = soil strength, d = pile diameter and N_p is a non-dimensional ultimate resistance coefficient. For soft clay soils flowing around a cylindrical pile at a considerable depth below the ground surface it was proposed that N_p should be taken as 9. Near ground surface, the soil in front of the pile failed by shearing forward and upward, the corresponding value of N_p reduced to a value between 2 and 4, depending on pile shape. For a cylindrical pile he considered a value of 3 to be appropriate. He thus proposed that the value of N_p varied from 3 at the surface to a maximum value of 9 at some depth x_r ; which was termed the depth of reduced resistance. Within the upper soil zone, the resistance to upward movement was provided by the overburden pressure σ_x from the soil weight and by resistance developed by deformation within the surrounding mass. This resistance increased with distance from the free soil surface. Matlock presented the following equation for the variation of N_p with depth, x :

$$N_p = 3 + \frac{\sigma_x}{c} + J \frac{x}{d} \dots\dots\dots 8.5.$$

The first term represents the resistance at the surface, the second term represents the increase with depth due to overburden pressure and the third term represents the geometrically related restraint that even a weightless soil around a pile provides against upward flow of soil. Matlock indicated that the coefficient J should be determined empirically. He proposed a value of 0.5 for use in connection with offshore clays in the Gulf of Mexico.

Where the soil strength c and effective unit weight g are constant with depth, the depth x_r is determined by equating N_p to 9 in Equation 8.5. and rearranging to give:

$$x_r = \frac{6 d}{(g d/c) + J} \dots\dots\dots 8.6.$$

Where soil properties vary considerably with depth, Matlock recommended that the soil should be considered as a system of thin layers, with x_r computed as a variable with depth according to the properties of each layer. However, at the time, [1970], this had not been physically tested.

(c) Matlock's proposed construction of p-y curves.

Matlock presented a general p-y curve for short-time static loading. This curve is reproduced in Figure 8.8. Application of the curve at numerous depths along the pile produced a family of p-y curves. The curve is presented in non-dimensional form with the ordinates normalized according to the static ultimate resistance, P_u , determined for each depth as described above. The horizontal axis is the pile deflection, y , divided by the deflection, y_c at point c. Point c represents half the ultimate static resistance.

The pre-plastic curve up to point e is given by:

$$P/P_u = 0.5 (y/y_c)^{1/3} \dots\dots\dots 8.7.$$

This equation is based on semilogarithmic plots of experimental p-y curves. On the basis of Skempton's (1951) concepts, Matlock approximated the value of the pile deflection, y_c , at point c, as:

$$y_c = 2.5 \epsilon_c d \dots\dots\dots 8.8.$$

Where ϵ_c is the strain which occurs at one half of the maximum stress on a laboratory stress-strain curve. Matlock proposed that ϵ_c may also be determined by dividing the shear strength, c , by an estimated secant modulus of elasticity, E_c . He contended that on the basis of Skempton's recognition that the ratio E_c/c lay between the limits of 50 and 200 for most clays, a value of ϵ_c may be assumed between 0.005 and 0.020. It was considered that the lower value of ϵ_c was applicable to brittle or sensitive clays and the higher value to disturbed or remoulded soils or unconsolidated sediments. He suggested that an intermediate value of 0.010 was probably satisfactory for most purposes.

Having developed a p-y curve for each node along the pile, a lateral load-deflection curve for the overall pile was determined using a computer program developed by Matlock and Haliburton (1964). This also enabled the pile bending moment distribution to be determined. The solution process was elaborate and similar to that for the non-linear behaviour of axially loaded piles described previously. It involved making repeated trial and error adjustments until complete compatibility was obtained between pile deflections and reactions with those prescribed by a family of p-y curves.

(d) Matlock's correlation with static test results.

Matlock correlated his results with those determined from a series of laterally loaded experimental tests at Sabine. The steel test pile was 12.75ins. in diameter with a 42ft. embedded length. 35 pairs of electric

resistance strain gauges were installed along the shaft. Gauge spacings varied from 6 ins. near the top to 4ft. in the lowest section. Free head tests were carried out with only lateral loading applied at the mudline. From laboratory stress-strain data, Matlock selected a value of 0.007 for the strain ϵ_c at the half stress point. The corresponding value of y_c was 0.223ins.

A family of p-y curves for short term static loading were constructed according to the data and conditions of the Sabine tests. P-y curves at six depths along the pile are reproduced in Figure 8.9. The ultimate resistance, P_u , for the 432in. depth was based on a value of 9 for N_p . All depths greater than 120 inches were found to have x_r values less than the depth considered. The ultimate resistance values for all shallower depths were determined using Equation 8.5. For locations along the pile between depths of the constructed p-y curves linear interpolations were made with respect to depth.

Matlock used the p-y curves reproduced in Figure 8.9. as input data for computer simulation of the Sabine pile-soil system under consideration. Representative loadings from each series of static field tests were selected for comparison with the computed results. The bending moment distributions determined from Matlock's method and typical field moments for the free headed pile are presented in Figure 8.10.(a). The agreement between Matlock's computed results and the test results was good over a wide range of loadings. The satisfactorily established correlation for short term static loadings qualified his method for construction of p-y curves.

8.4.2. The Proposed Method.

The free head laterally loaded Sabine pile test was also analysed using the S.S.R.T. iterative analysis. The approach used to construct the p-y curves was identical to that of Matlock. However, the proposed solution process is simpler in that repeated trial-and-error adjustments are not made to determine each point on the load-displacement curve. Because Matlock did not report the number and spacing of pile elements for his analysis it was unlikely that the same discretisation was used by the proposed method.

The idealized pile comprised 37 elements with a constant spacing of 12ins. Each element was assigned a Young's Modulus, E_p , of 29×10^6 lbf/in² and a second moment of area of 191.82in⁴.

A value of ϵ_c of 0.007 was taken for the soil. The resulting deflection y_c was 0.223ins. Thus the deflection, $8y_c$, where the soil was fully plastic and offered no further resistance, was 1.784ins. The ultimate resistance P_u at various depths were taken from Figure 8.9. Values of the initial lateral spring stiffness along the pile were also determined from Figure 8.9. These were computed from the initial tangent to the p-y curve at a deflection, y , of 0.03ins. to determine an initial P value. The soil stiffness was then given by $P/0.03$ lbf/in². To obtain spring stiffness values, K_h , the soil stiffness in lbf/in² was multiplied by the relevant element lengths. The data extrapolated from Figure 8.9. is presented in Table 8.5.

A stiffness matrix was constructed to represent the initial pile-soil system using the initial soil stiffness values. A lateral load of 1Kip was applied to the pile and the resulting deflections obtained. The calculated deflections, y , at each node were input into Equation 8.7. to calculate a more accurate value of the initial spring stiffness. The new spring stiffness values were then applied to the pile which was analysed under increasing load increments. The loads used were 1, 2, 4, 6, 8, 10, 12, 14, 16 and 18Kips. Where a nodal deflection reached a limiting value of $8y_c$, equal to 1.784ins., the spring stiffness at the node was removed. The solution at each load increment was of a closed-form.

The resulting bending moment distributions are shown in Figure 8.10.(a). The bending moment distributions from the proposed method agreed reasonably well with those of Matlock and the experimental results. Matlock's theoretical results and the measured values indicated that the bending moments were amplified by consideration of the non-linear behaviour of the soil. Results from the proposed method also exhibit the same effect but to a lesser extent. The proposed method underestimated the maximum bending moment from Matlock's method by -17% to -25% over the range of loadings.

Matlock did not present deflections for the pile head under various loadings for comparison. The deflections from the S.S.R.T. analyses are presented in Figure 8.10.(b). Based on the initial stiffness values using linear elastic springs the deflection at 18Kips was 1.05ins. compared to 2.20ins. using a non-linear analysis.

The necessity of considering the non-linear nature of the soil for heavy lateral loading of a pile was demonstrated. Both bending moments and deflections were amplified by non-linear soil behaviour. It was shown that the proposed iterative S.S.R.T. analysis successfully modelled the non-linear behaviour. This approach is considered to be simpler than that of Matlock because iterations are not required to determine each point on the load-deflection curve. The solution process was again carried out using a standard structural program operating on a microcomputer.

8.5. DISCUSSION AND CONCLUSIONS.

The importance of modelling the non-linear behaviour of axially and laterally loaded piles was demonstrated. The interaction of a single pile with the soil was modelled using non-linear $t-z$ and $p-y$ curves for axial and lateral behaviour respectively. Various researchers have proposed different curves for specific ground and loading conditions. The reported solution procedures were similar in nature and the computed results correlated well with field tests. However, the numerical approach was cumbersome and elaborate as the determination of each point on the load-displacement curve was an iterative process.

The S.S.R.T. method was applied to the non-linear analysis by employing $t-z$ and $p-y$ curves proposed by various researchers for specific pile-soil problems. Once the non-linear curves were established, spring stiffness values were determined to represent the soil resistance at various loads. The stiffness of the springs was

incorporated into the pile stiffness matrix and a closed form solution obtained for each load increment. From the computed load and displacement at each node a new spring stiffness was calculated and used for the next load increment. When the plastic limit of the soil at a node was reached the spring was removed. This approach is considered to be more efficient than other reported methods because the number of iterations is considerably reduced. Moreover, these other methods rely on assuming initial arbitrary pile displacements which may affect the rate of convergence of results.

The results determined using the iterative S.S.R.T. analysis of an axially loaded pile embedded in multi-layered soil satisfactorily modelled the transfer of load from the pile to the soil. The pre-failure non-linear load-displacement curve was also satisfactorily modelled. However, for the comparison made with Coyle and Reese the ultimate load which could be carried by the pile was ambiguous which was reflected by the three different load-displacement curves. The proposed method was also applied to the analysis of the non-linear behaviour of a laterally loaded pile embedded in a soil which increased in stiffness with depth. The computed results satisfactorily modelled the amplified bending moment distribution along the pile shaft caused by non-linear soil behaviour. The maximum bending moment computed by the proposed method was about 25% less than that from Matlock's method and the experimental value.

The validity and versatility of the S.S.R.T. for the analysis of non-linear pile-soil behaviour was

demonstrated. Using a finite element representation of the pile enables a pile with varying cross section or material properties to be analysed. The plastic moment of resistance of the pile was not considered in these analyses. However, this could be accommodated by inserting a hinge in the pile at locations where the bending moment reached the ultimate value.

Layer	Depth (feet)	Description
A	0.0 - 8.5	very stiff CH
B	8.5 - 26	stiff to very stiff slicken sided CH
C	26 - 30	medium stiff, silty CH
D	30 - 47	stiff to very stiff sandy CL with sand partings

Table 8.1.: Soil Strata Described
By O'Neill et al (1982a)

LAYER	f_{\max} (psf)	z_c (ins.)
A	375	0.033
B	1350	0.038
C	1225	0.043
D	1750	0.021

Table 8.2.: f_{\max} And z_c Values Used For
S.S.R.T. Analysis.

LAYER	DEPTH (ft)	AVERAGE Q_u (lbs/ft ²)
1	0 - 35	7,840
2	35 - 70	7,280
3	70 - 100	10,080
4	100 - 111	13,440

Table 8.3.: Soil Strata And Average Shear Strengths
From Plate 308 Peck (1961).

Depth (ft)	Curve	$(f/Q)_{\max}$	y_c (in)	Initial gradient K_o (lbf/ft ³)
0 - 10	A	0.50	0.200	48 Q
10 - 20	B	0.85	0.200	83 Q
> 20	C	1.00	0.075	240 Q

Table 8.4.: Relevant Data Extrapolated From Figure 8.7.

Depth (in)	P_u (lbf/in)	Initial P (at $y=0.03$) (lbf/in)	Initial stiffness (lbf/in ²)
24	103	26	867
48	120	31	1033
72	163	42	1392
96	223	57	1904
120	238	61	2033
432	246	114	3809

Table 8.5.: Relevant Data Extrapolated From Figure 8.9.

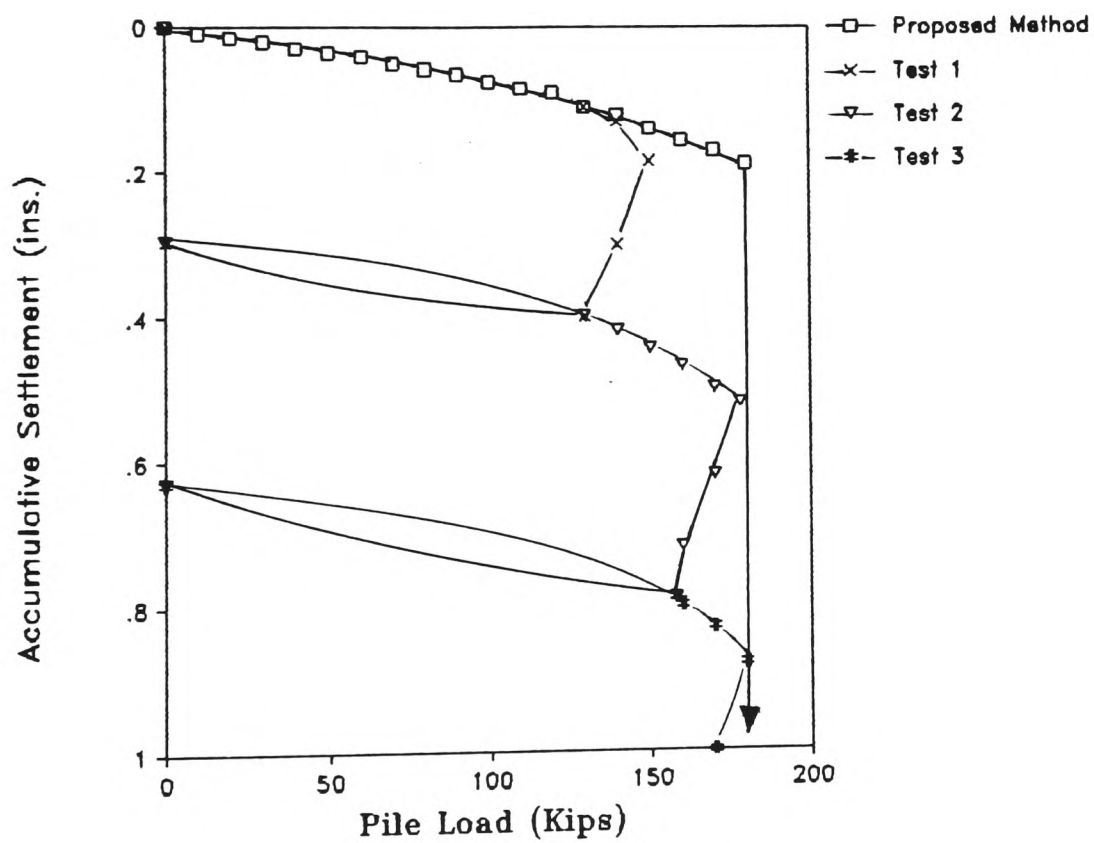
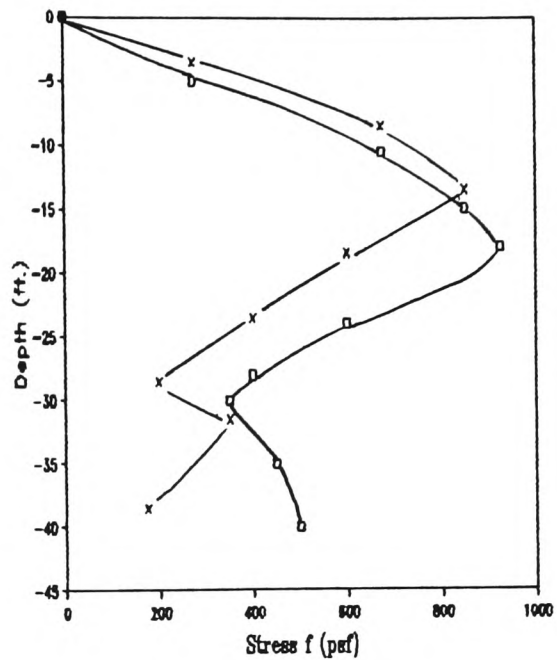
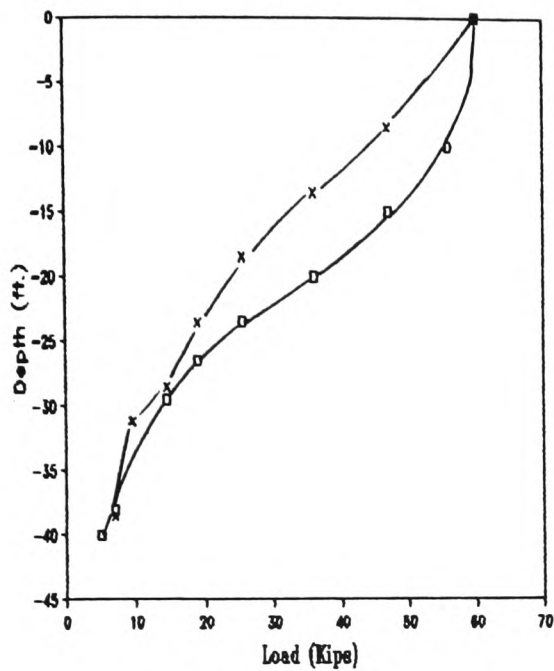
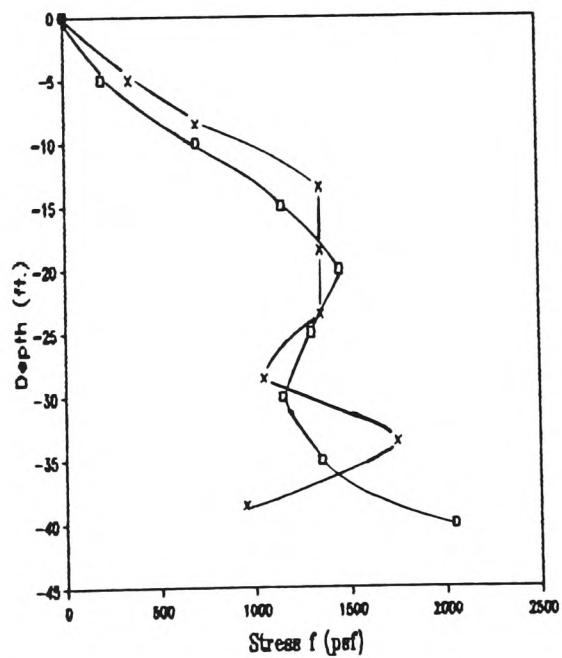
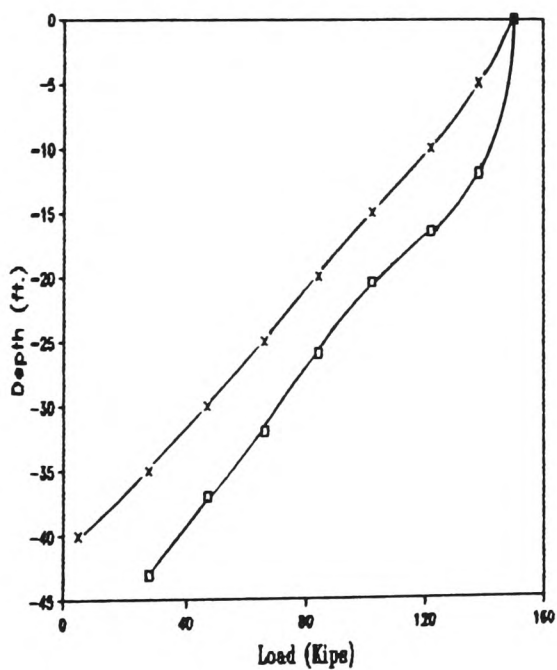


Figure 8.1.: Comparison with the load-settlement curves of O'Neill et al.



(a) Working load.



—x— Proposed method
—o— O'Neill et al

(b) Failure load.

Figure 8.2.: Comparison with pile load and soil stress distribution curves of O'Neill et al.

node	Depth (ft.)	
1	0	LAYER A
2	8.5	
3	13.5	LAYER B
4	18.5	
5	23.5	LAYER C
6	28.5	
7	33.5	LAYER D
8	38.5	
9	43.0	

Figure 8.3.: S.S.R.T. pile idealization for comparison with O'Neill et al.

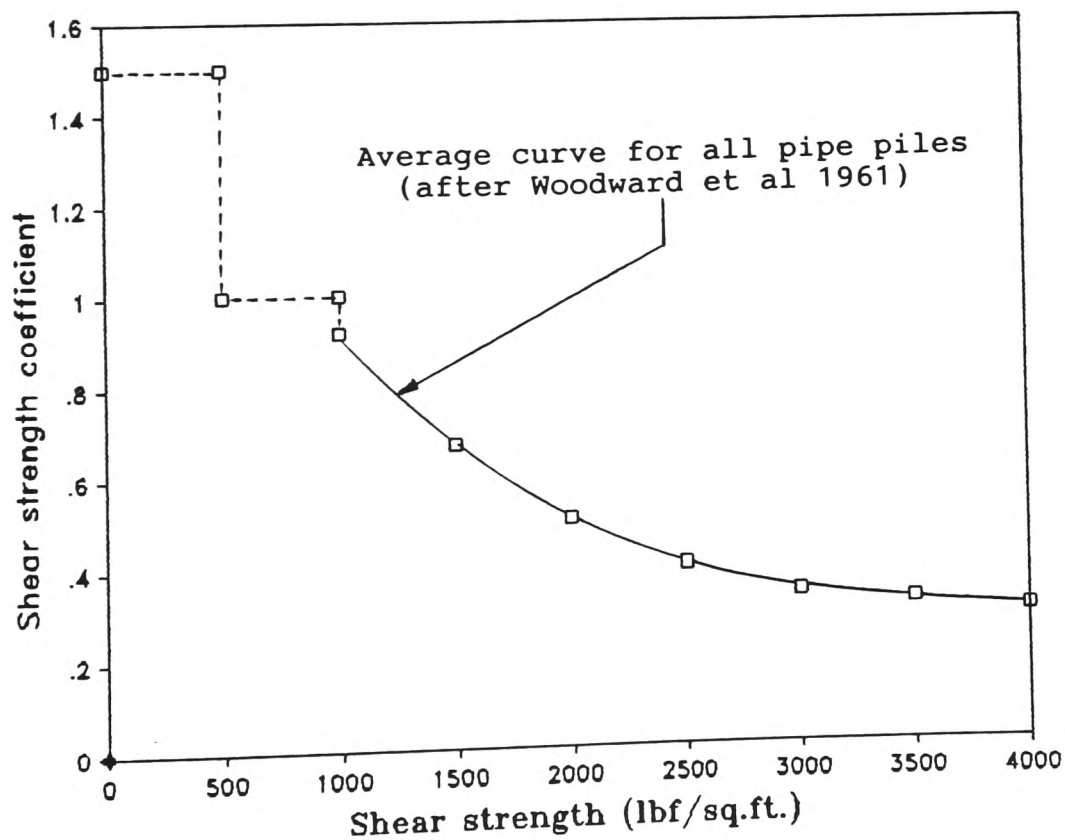


Figure 8.4.: Shear strength coefficients.

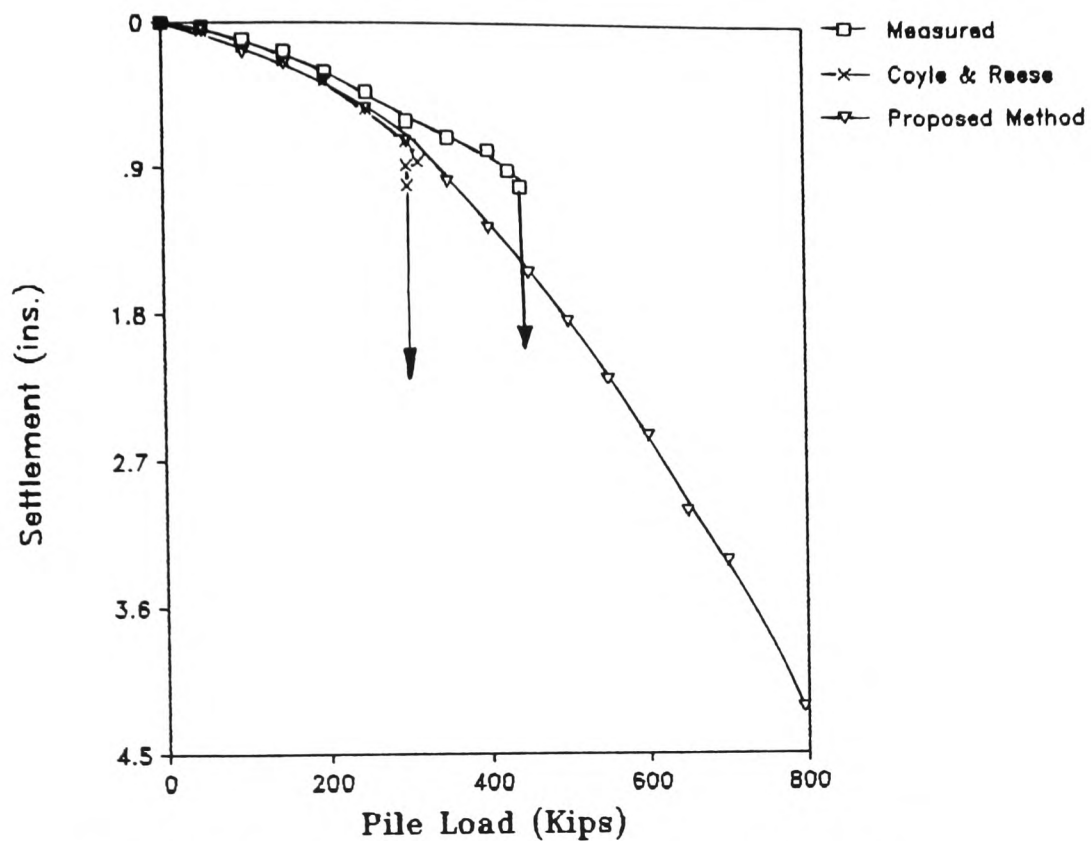


Figure 8.5. Comparison with load-settlement curves of Coyle and Reese.

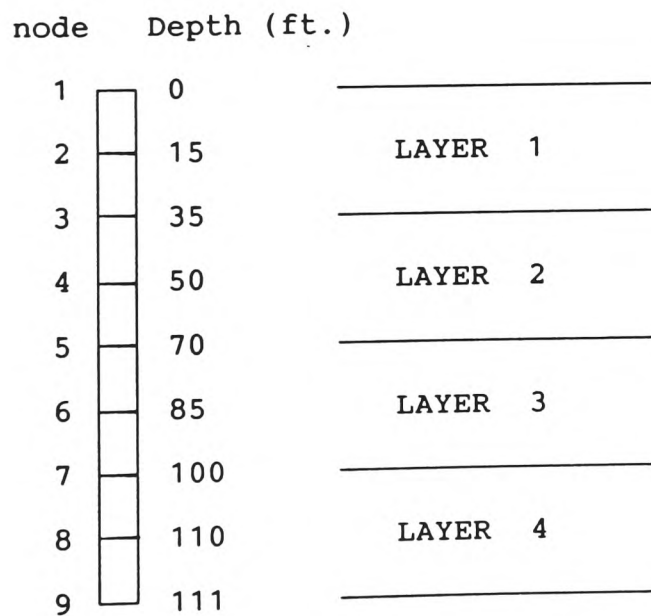


Figure 8.6.: S.S.R.T. Pile Idealization For Comparison With Coyle and Reese.

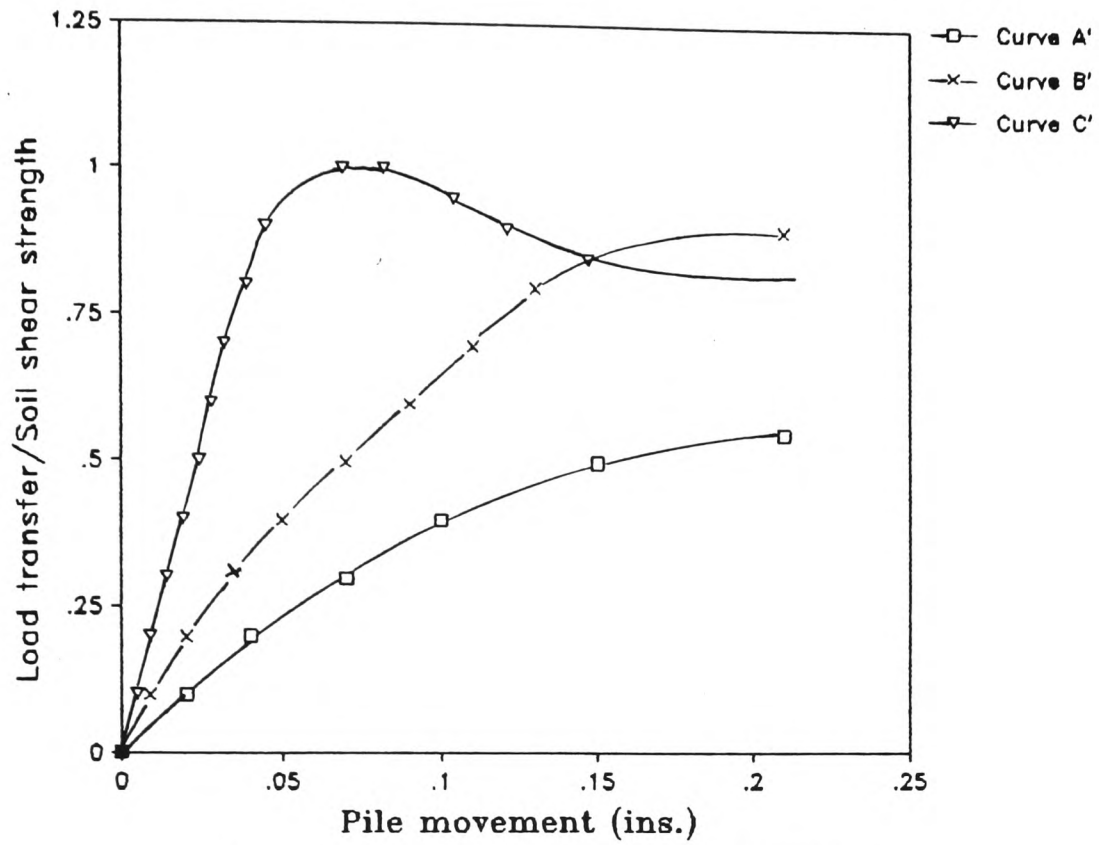


Figure 8.7. Adjusted field curves.
[after Coyle and Reese]

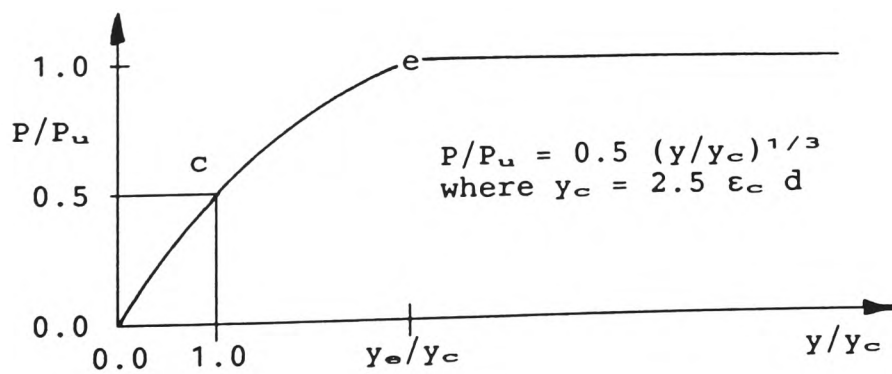


Figure 8.8.: p-y Curve For Short Term Static Loading.

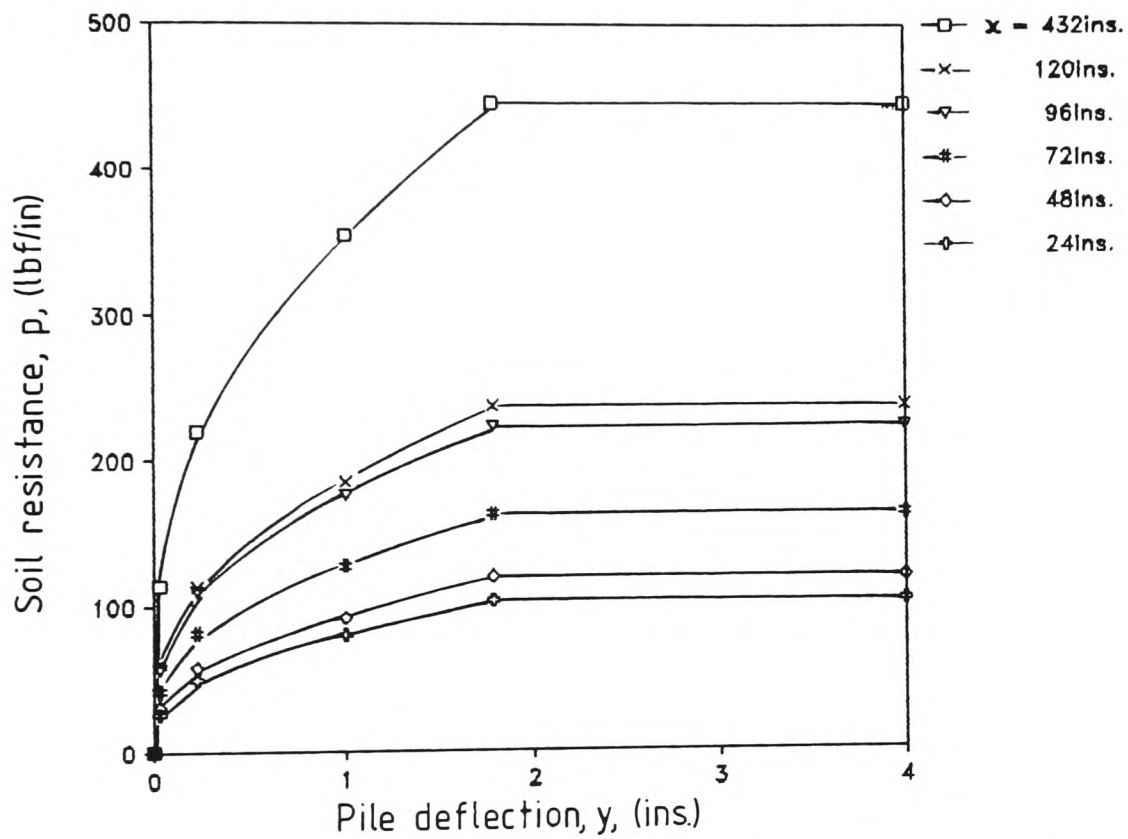
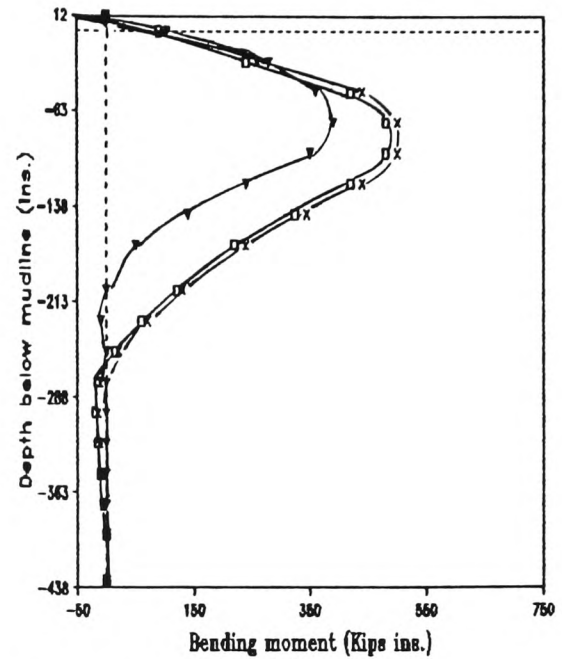
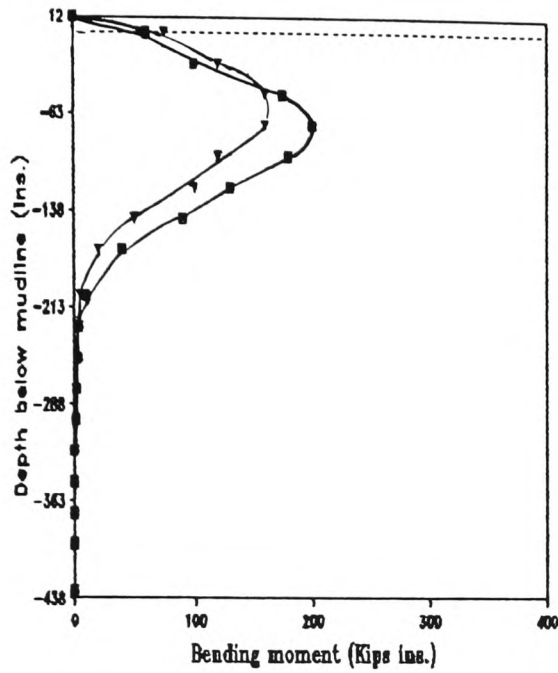
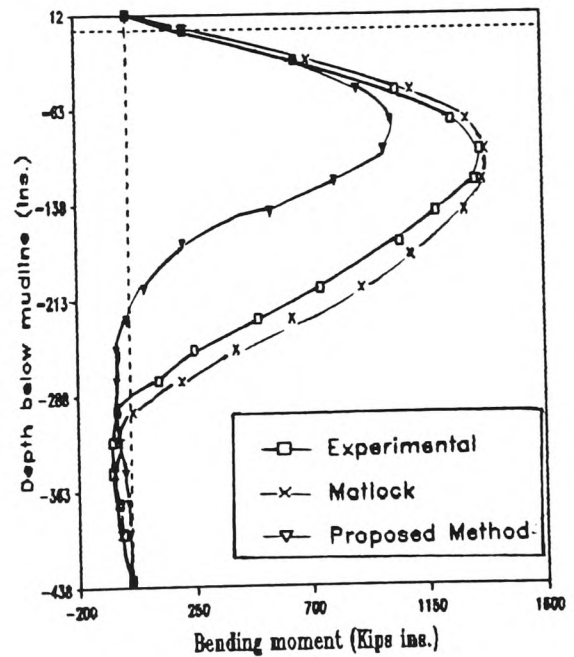
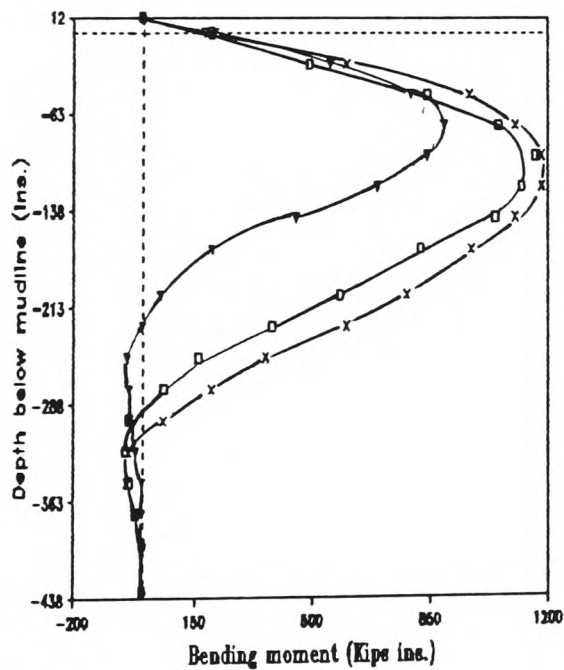


Figure 8.9.: Predicted family of p-y curves for Sabine clay for short term static loading.



(i) Lateral load = 4.0Kips (ii) Lateral load = 8.0Kips



(iii) Lateral load = 16.0Kips (iv) Lateral load = 18.0Kips

Figure 8.10.(a).: Comparison of bending moments for Sabine free head static loadings.

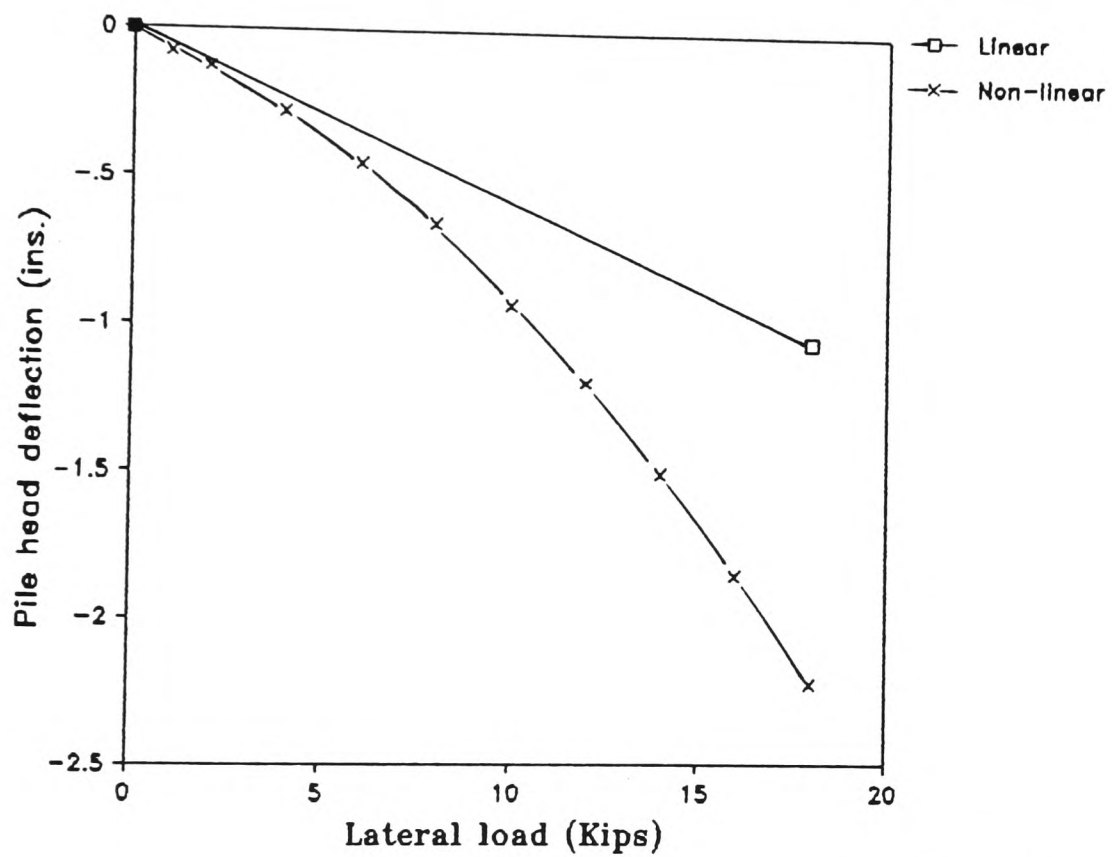


Figure 8.10.(b).: Load-deflection curves for Sabine free head static loadings using proposed method.

CHAPTER 9.

DISCUSSION AND CONCLUSIONS.

The soil-structure interaction of various substructures has been investigated. A skeletal frame on foundation was used throughout to model and generate the superstructure and substructure stiffness. This enabled standard structural engineering programs which operate on microcomputers to be used for the analysis of complex soil-structure interaction problems.

Initial studies indicated that a skeletal frame supported by springs could be used to model the behaviour of a raked pile group with a raft in contact with the ground. The stiffness method of analysis was used to determine the load-deformation response of the discretized substructure. It was concluded that more than three elements; preferably at least ten; were required to satisfactorily discretize each pile.

Relationships were derived to enable axial and lateral spring stiffness values, K_v and K_h , to be determined from the more common values of soil moduli, E_s , for a wide range of pile-soil configurations. These relationships enabled the S.S.R.T. method to be used for the analysis of a pile embedded in an isotropic elastic half-space.

The relationships developed between K_v , K_h and E_s were applied to the analysis of single piles and pile groups without pile-soil-pile interaction. The computed results were compared with those from several full scale tests on single piles, the measured performance of a piled bridge abutment and elastic solutions using the PGROUP

program. The computed displacements of laterally and axially loaded piles using the proposed S.S.R.T. method were within $\pm 20\%$ of the PGROUP and measured values. It was demonstrated that the analysis of laterally loaded piles required a relatively short element length, down to $L/75$ near the ground surface. This was necessary to accurately compute the bending moment distribution along the pile shaft. Axially loaded piles were not so sensitive to element refinement. Six elements were satisfactory to model the axial load distribution accurately along the shaft of a pile embedded in a homogeneous soil. There were too many unknown variables to enable accurate back-analysis of the pile loading tests of the bridge abutment. However, this work demonstrated the importance of modelling the different rates of load transfer along the shaft of a pile embedded in a multi-layered soil. The computed load distribution in the pile cap of the bridge abutment using the proposed S.S.R.T. method was more uniform than that computed by PGROUP and agreed more closely with the measured distribution.

The interaction of axially and laterally loaded pile groups and axially loaded piled rafts was also considered. The proposed method of analysis was developed using Poulos and Davis' interaction factors. A simplified treatment of interaction was proposed to compute the overall group displacement where piles carried approximately equal loads; which is common in the long term as the load is redistributed. However, a more rigorous approach was also presented where piles could carry substantially different proportions of loads which is the case for closely spaced

piles in the short term. The computed results were compared with those from laboratory tests, field measurements and PGROUP solutions. The proposed method computed the displacement and load distribution of pile groups and piled rafts satisfactorily under both axial and lateral loading. The total displacements from the proposed method were generally within 10% of the PGROUP values; although, in one instance the displacements differed by 20%. The more rigorous S.S.R.T. analysis computed load distributions in the pile cap similar to those from PGROUP. However, this approach overestimated the axial loads in some piles by up to 50%. Results from the proposed method were also compared to the measured performance of two existing piled raft foundations and other analytical solutions. There was a degree of uncertainty as to the assumptions made in the analysis of the piled raft foundation at Basildon. The agreement between the results from the proposed method with those from the reported analytical solution and measured values was generally poor. Hain and Lee's analysis of the piled raft foundation to Hyde Park Cavalry Barracks was well documented. The computed load distribution in the pile cap by the proposed method agreed to within 20% of that determined by Hain and Lee and agreed more closely with the measured values. The S.S.R.T. computed drained settlements were within 10% of those from Hain and Lee, with both methods considerably overestimating the measured values.

Consistent soil matrices were presented to distribute the axial and lateral soil resistance over the length of the pile element. Sensitivity studies were carried out to

examine the convergence of results with the number of elements used. For the idealization of laterally loaded piles, results from both the S.S.R.T. and PGROUP were sensitive to the number of elements used to model the pile. Whereas convergence of results from the consistent matrix method (C.M.M.) was excellent; 2 elements being satisfactory to model the bending profile of a laterally loaded pile with a restrained head. All analytical techniques were relatively insensitive to the number of elements used for the analysis of an axially loaded pile. Use of the C.M.M. in a large pile configuration would clearly be beneficial as this would result in a significant reduction in the size of the matrices for the complete system.

The limitations of the S.S.R.T. combined with a grillage to model raft-soil behaviour were investigated. Comparisons were made with solutions from elastic half-space ground models. It was concluded that the use of the S.S.R.T. to predict the settlement and bending moment distributions of general plain raft foundations could not be recommended. A more suitable method of analysis was therefore required.

An alternative method of analysis for plain raft foundations was developed based on the surface element method (S.E.M.). The soil was approximated as a heterogeneous anisotropic elastic continuum. The raft and superstructure were again modelled using a skeletal frame. A computer program was written for the analysis of both plain rafts and three dimensional structures supported by rafts. The program is capable of solving relatively large

practical problems on a microcomputer limited to a memory capacity of 640Kb. The computed results were compared with the measured performance of an existing building founded on a raft and other analytical solutions. The total settlements computed by the proposed method were 16% to 23% greater than those of Hooper and Wood and about 25% greater than the measured values. It was demonstrated that a grillage idealization satisfactorily modelled raft performance.

The developed S.E.M. program was also applied to the analysis of a worked example presented by Wardle and Fraser to investigate the contribution of the stiffness of the superstructure in resisting differential settlements. The computed total settlements from the proposed method were generally 25% lower than those of Wardle and Fraser. Differential settlements from the proposed method were approximately double that of Wardle and Fraser's values. The difference in results is attributed to different modelling procedures being used for the soil. It was shown that in order to compute raft bending moment and column loads satisfactorily at least a one storey collapsed structure needed to be idealized. This was in agreement with Wardle and Fraser's observations. Collapsing the superstructure completely into a plain raft resulted in the raft bending moments being overestimated; thus invalidating a two dimensional analysis. Also, two dimensional models were found to be incapable of predicting the redistribution of column loads caused by soil-structure interaction.

The application of the S.S.R.T. to modelling the non-linear behaviour of axially and laterally heavily loaded

piles was demonstrated. The method was applied to the non-linear analysis by employing t-z and p-y curves proposed by various researchers. Soil spring stiffness values were determined on a load increment basis from these curves. The procedure enabled a closed-form solution to be obtained for each load increment. This approach is considered to be more efficient than the alternative numerical techniques which require a trial and error solution to determine each point on the load-displacement curve. The computed load-displacement curves for axially loaded piles agreed well with measured values and those from other analytical procedures.

The comparison made with Coyle and Reese showed a discrepancy between results due to different values being taken for the ultimate load carrying capacity of the pile. The importance of modelling the axial load transfer of a pile embedded in a multi-layered soil was demonstrated. In this instance, the computed load-distribution along the pile shaft using the proposed method slightly underestimated the measured values; the agreement between the soil stress profiles being most satisfactory. The analysis of a laterally loaded pile demonstrated that the bending moment distribution was amplified due to the non-linear behaviour of the soil. The computed maximum bending moments by the proposed method underestimated the measured and other analytical values by -17% to -25%. It was concluded that the proposed S.S.R.T. method satisfactorily represented the non-linear behaviour of single piles. Also, the use of beam-column elements enabled a pile with

varying cross section or heterogeneous material properties to be analysed.

To summarize, a skeletal frame was used throughout to discretize both the superstructure and substructure. For pile foundations, it was demonstrated that spring analogies modelled the soil response satisfactorily. This in turn enabled solutions to be determined for piles embedded in an elastic continuum or soil-pile systems which exhibited non-linear behaviour. It is considered that the proposed simplified and rigorous procedures for the analysis of pile-soil-pile interaction will enable the determination of both the short and long term load distributions. As the loads are redistributed with time, both of these cases need to be considered in order to determine the maximum carrying capacity of different piles within the group. For raft foundations, the spring analogy was not generally satisfactory and a method of analysis was developed based on the S.E.M.. A computer program was written in order to analyse general plain raft foundations using the proposed method. The program also considered the geometry of three dimensional superstructures supported by a raft foundation.

The manual effort involved in analysing foundations comprising a large number of piles was found to be considerable. It is therefore recommended that a program for piled foundation analysis should be developed by directly employing Mindlin's equations to model the interaction. The success of the proposed modelling procedure using a spring analogy indicated that an integral transform analysis is not generally necessary. It is considered that the process of analysis using a simplified

method as in the proposed S.E.M. for raft foundations was both valid and helpful. The use of consistent soil matrices in such a program would enable the number of discretized pile elements to be reduced considerably with a corresponding reduction in both the time and cost of analysis.

It was demonstrated that the proposed S.S.R.T. method could satisfactorily be extended to model non-linear pile-soil behaviour. Now that the algorithm has been demonstrated to be correct, it is proposed that the manual effort involved in the solution process could be replaced by developing a suitable program to carry out an iterative analysis.

REFERENCES

- ABDRABBO, F.M. (1976)
A model scale study of single piles and pile groups under general planar loads.
PhD Thesis, University of Southampton.
- ALIZADEH, M. (1969)
Lateral load tests on instrumented timber piles.
American Society for Testing and Materials, STP444, pp.379 to 394.
- ALIZADEH, M. & DAVISSON, M.T. (1970)
Lateral load tests on piles - Arkansas River Project.
Proc. Am. Soc. Civ. Engrs., Jnl. Soil Mech. Found. Div., Vol.96, No. SM5, pp.1583 to 1604.
- AMERICAN PETROLEUM INSTITUTE (1986, 1987)
Recommended practice for planning, designing and constructing fixed offshore platforms.
16th and 17th edn.
- ANDERSON, P. (1956)
Substructure analysis and design.
2nd ed., The Ronald Press Company, New York, p.170.
- ASCHENBRENNER, R. (1967)
Three dimensional analysis of pile foundations.
Proc. Am. Soc. Civ. Engrs., Jnl. Structural Div., vol. ST1-93, Feb., pp.201 to 219.
- BAGUELIN, F., BUSTAMANTE, M., FRANK, R. & JEZEQUEL, J.F. (1975)
La capacite portante des pieux.
Annales de l'Institut du Batiment et des Travaux Publics.
Suppl. 330, Serie SF/116, 1-22.
- BANERJEE, P.K. (1971)
Foundations within a finite elastic layer.
Civ. Engng. Publ. Wks. Rev. 66(784), pp.1197 to 1202.
- BANERJEE, P.K. (1976a)
Integral equation methods for analysis of piece-wise non-homogeneous, three-dimensional elastic solids of arbitrary shape.
Int. Jnl. Mech. Sci., 18, pp.293 to 303.
- BANERJEE, P.K. (1976b)
Analysis of vertical pile groups embedded in non-homogeneous soil.
Proc. 6th European Conf. Soil Mech. Found. Engng, Vienna, 1976, pp.345 to 350.
- BANERJEE, P.K. & DRISCOLL, R.M. (1976)
Three dimensional analysis of raked pile groups.
Proc. Instn Civ. Engrs, Part 2 61, pp.653 to 671.
- BANERJEE, P.K. & BUTTERFIELD, R. (1977)
"Boundary element methods in geomechanics".
Finite Element Methods in Geomechanics, Gudehus, G. (Ed.), John Wiley & Sons, New York, pp.529 to 570.

- BANERJEE, P.K. & DAVIES, T.G. (1977)
Analysis of pile groups embedded in Gibson soil.
Proc. 9th Int. Conf. Soil Mech. Found. Engrng, Tokyo.
- BANERJEE, P.K. (1978)
Analysis of axially and laterally loaded pile groups.
Developments in Soil Mechanics -1. Applied Science
Publications, pp.317 to 345.
- BANERJEE, P.K. & DAVIES, T.G. (1979)
Analysis of some reported case histories of laterally
loaded pile groups.
Conf. Num. Methods in Offshore Piling, Instn. Civ. Engrs.,
London.
- BANERJEE, P.K. & DAVIES, T.G. (1980)
Analysis of some reported case histories of laterally
loaded pile groups.
Numerical methods in offshore piling, pp.101 to 108.
London: Institution of Civil Engineers.
- BANERJEE, P.K., DRISCOLL, R.M. & DAVIS, T. (1981)
Program for the analysis of pile groups of any geometry
subjected to horizontal and vertical loads and moments,
PGROUP. HECB/B/7 Department of Transport, HECB, London.
- BANERJEE, P.K., DAVIES, T.G. & FATHALLAH, R.C. (1983)
Behaviour of axially loaded driven piles in saturated clay
from model studies.
Developments in soil mechanics and foundation engineering-
1. Applied Science Publishers.
- BARKAN, D.D. (1962)
Dynamics of bases and foundations.
McGraw Hill.
- BEREZANTZEV, V.G., KRISTFOROV & GOLUBLOV (1961)
Load bearing capacity and deformation of pile foundations.
Proc. 5th. Int. Conf., Soil Mech. Found. Engrng., 2, p.11.
- BOLTON, M. (1979)
A guide to soil mechanics.
Macmillan.
- BOUSSINESQ, J. (1885)
Application des potentiels a l'etude de l'equilibre et du
mouvement des solides elastiques.
Gauthier-Villars, Paris.
- BOWLES, J.E. (1968)
Foundation analysis and design.
McGraw-Hill, United States.
- BROMS, B.B. (1964a)
Lateral resistance of piles in cohesive soils.
Proc. Am. Soc. Civ. Engrs., Jnl. Soil Mech. Found. Div.
Mar 1964 90(SM2), pp.27 to 63.

BROMS, B.B. (1964b)

Lateral resistance of piles in cohesionless soils.
Proc. Am. Soc. Civ. Engrs., Jnl. Soil Mech. Found.
Div., Vol. 90, No. SM3, pp.123 to 156.

BROMS, B.B. (1965)

Design of laterally loaded piles.
Proc. Am. Soc. Civ. Engrs., Jnl. Soil Mech. Found. Div.,
SM3, May 1965.

BROWN, P.T. (1969a)

Numerical analyses of uniformly loaded circular rafts on
elastic layers of finite depth.
Geotechnique, Vol. 19, pp.301 to 306.

BROWN, P.T. (1969b)

Numerical analyses of uniformly loaded circular rafts on
deep elastic foundations.
Geotechnique, Vol. 19, pp.399 to 404.

BURLAND, J.B., BUTLER, F.G. & DUNICAN, P. (1966)

The behaviour and design of large bored piles in stiff
clay.
Proc. of the Symp. Large Bored Piles, Instn. of Civ. Engrs,
Feb., pp.51 to 71.

BURLAND, J.B. (1973)

Shaft friction of piles in clay - a simple fundamental
approach.
Ground Engineering, 6(3), pp.30 to 42.

BURLAND, J.B. & KARLA, J.C. (1986)

Queen Elizabeth II Conference Centre:- geotechnical aspects
Proc. Instn. Civ. Engrs., Vol 80, Part 1, pp.1479 to 1503.

BURMISTER, D.M. (1940)

Stress distribution for pile foundations.
Proc. Conf. Soil Mech. & its applications, Purdue Univ., p.339

BURMISTER, D.M. (1943)

The theory of stresses and displacements in layered systems
and applications to the design of airport runways.
Proc. Highway Res. Board, Vol.23, pp.127 to 148.

BURMISTER, D.M. (1945)

The general theory of stresses and displacements in layered
soil systems.
Jnl. Appl. Phys., Vol.16, No.2, pp.89 to 96, No.3, pp.126
to 127, No.5, pp.296 to 302.

BUTTERFIELD, R. & BANERJEE, P.K. (1970)

A note on the problem of a pile-reinforced half space.
Geotechnique, Vol. 20, part 1, pp.100 to 103.

BUTTERFIELD, R. & BANERJEE, P.K. (1971a)

A rigid disc embedded in an elastic half space.
Geotech. Engng. 2(1), pp.35 to 52.

BUTTERFIELD, R. & BANERJEE, P.K. (1971b)

The elastic analysis of compressible piles and pile groups.
Geotechnique, Vol 21, part 1, pp.43 to 60.

- BUTTERFIELD, R. & BANERJEE, P.K. (1971c)
The problem of pile group - pile cap interaction.
Geotechnique, Vol 21, part 2, pp.135 to 142.
- BUTTERFIELD, R. & BANERJEE, P.K. (1977)
"Boundary element methods in geomechanics"
Finite Elements in Geomechanics. John Wiley & Sons,
pp.529 to 570.
- BUTTERFIELD, R. & DOUGLAS, R.A. (1981)
Flexibility coefficients for design of piles and pile groups.
CIRIA Technical Note 108.
- CHEUNG, Y.K. & ZIENKIEWICZ, O.C. (1965)
"Plates and tanks on elastic foundations - an application
of finite element method"
Int. Jnl. Solids Struct., Vol 1, pp.451 to 461.
- CHOW, Y.K. (1986a)
Analysis of vertically loaded pile groups.
Int. Jnl. Numer. Analyt. Meth. Geomech. 10, No.1, pp.59 to
72.
- CHOW, Y.K. (1986b)
Discrete element analysis of settlement of pile groups.
Computers Structs 24, No.1, pp.157 to 166.
- CHOW, Y.K. (1987)
Iterative analysis of pile-soil-pile interaction.
Geotechnique, 37, No. 3
- CHOW, Y.K. & SMITH, I.M. (1982)
Static/dynamic analysis of an axially loaded pile.
Proc. 4th Conf. Numerical Methods in Geomechanics,
Edmonton, Canada. pp.819 to 824.
- COATES, R.C., COUTIE, M.G. & KONG, F.K. (1988)
Structural Analysis.
3rd Edition, Van Nostrand Reinhold UK.
- COOKE, R.W. (1974)
The settlement of friction pile foundations.
Proc. Conf. on Tall Buildings, Kuala Lumpur.
- COOKE, R.W., PRICE, G. & TARR, K. (1979)
Jacked piles in London Clay: a study of load transfer and
settlement under working conditions.
Geotechnique 29, No. 2, pp.113 to 147.
- COOKE, R.W. (1981)
Some observations of the foundation loading and settlement
of a multi storey building on a piled raft foundation.
Proc. Instn. Civ. Engrs., Vol 70, part 1, pp.433 to 460.
- COOKE, R.W. (1986)
Piled raft foundations on stiff clays - a contribution to
Design Philosophy.
Geotechnique 36, No.2, pp.169 to 205.

- COYLE, H.M. & REESE, L.C. (1966)
Load transfer for axially loaded piles in clay.
Proc. Am. Soc. Civ. Engrs., Jnl. Soil Mech. Found. Div.,
vol.92, SM2, pp.1 to 26.
- DAVIS, E.H. & POULOS, H.G. (1972)
The analysis of pile raft systems
Australian Geomech. Jnl. G2(1), pp.21 to 27.
- DAVISSON, M.T. & GILL, H.L. (1963)
Laterally loaded piles in a layered soil system.
Proc. Am. Soc. Civ. Engrs., Jnl. Soil Mechs. Found. Div.,
Vol.89, No. SM3, May, 1963, pp.63 to 84.
- DAVISSON, M.T. & SALLEY, J.R. (1970)
Model study of laterally loaded piles.
Proc. Am. Soc. Civ. Engrs., Jnl. Soil Mechs. Found. Div.,
SM, Sept.
- DELPACK, R. & PESHKAM, V. (1984)
Use of linear parametric element in analysing space
structures.
3rd Int. Conf. on Space Structures, Elsevier Applied
Science Publications, University of Surrey, Guildford, 11-
14 Sept 1984, pp.343 to 348.
- DIXON, H.H. & BERRY, D.W. (1970)
Extensions to the Chania-Sasumua water supply scheme for
Nairobi.
Proc. Instn. Civ. Engrs., Vol 45, pp.35 to 64.
- DORR, H. (1922)
"Die Tragfähigkeit der Pfähle"
Verlang W.Ernst & Sohn, Berlin.
- DOUGLAS, D.J. & DAVIS, E.H. (1964)
The movement of buried footings due to moment and
horizontal load and the movement of anchor plates.
Geotechnique, 14, p.115-
- ELLISON, R.D. (1968)
An analytical study of the mechanics of single pile
foundations.
Thesis presented to Carnegie-Mellon University, Pittsburgh,
Pennsylvania, p.230.
- ELSON, W.K. (1984)
Design of laterally loaded piles.
CIRIA Report 103.
- FEAGIN, B. (1953)
Lateral load tests on groups of vertical and battered piles
Symp. on Lateral Load Tests On Piles, Am. Soc. Civ. Engrs.,
New York, pp.12 to 20.
- FOCHT, J.A. & KOCH, K.J. (1973)
Rational analysis of lateral performance of offshore pile
groups.
Proc. 5th Offshore Technology Conf., Houston 2, pp.701 to
708.

- FOPPL,A. (1934)
O.K.Frohlich.
Druckverteilung im Baugrunde, Vienna.
- FOX,E.N. (1948)
The mean elastic settlement of a uniformly loaded area at a depth below the ground surface.
Proc. 2nd Int. Conf. on Soil Mechanics and Foundation Engineering (Rotterdam), 1948, Vol. 1, pp.129 to 132.
- FRANCIS,A.J. (1964a)
Analysis of pile groups with flexural resistance.
Proc. Am. Soc. Civ. Engrs., Jnl. Soil Mech. Found. Div., vol. SM3-90, May, pp.1 to 32.
(See also July, 1965, for errata and closure.)
- FRANCIS,A.J. (1964b)
Analysis of pile groups with flexural resistance:
Discussion by Gray, Barmby and Priddle.
Proc. Am. Soc. Civ. Engrs., Jnl. Soil Mech. Found. Div., vol. SM6-90, Nov., pp.227 to 237.
- FRANK,R. (1974)
Etude theorique du comportement des pieux sous charge verticale, introduction de la dilatante.
Dr-Eng. thesis, University Paris VI (Pierre et Marie Curie University).
- FRASER,R.A. & WARDLE,L.J. (1976)
Numerical analysis of rectangular rafts on layered foundations.
Geotechnique 26(4), pp.613 to 630.
- GHABOUSSI,J., WILSON,E.L. & ISENBERG,J. (1973)
Finite element for rock joints and interfaces.
Proc. Soil Mech. Found. Engrng., Jnl. Soil Mech. and Found. Div., Vol.99. SM10, Oct.
- GHOSH,N. (1975)
A model scale investigation of the working load stiffness of single piles and groups of piles in clay under centric and eccentric vertical loads.
PhD Thesis - University of Southampton.
- GIBSON,R.E. (1974)
The analytical method in soil mechanics.
Geotechnique, 24, pp.113 to 140.
- GIROUD,J.P. (1970)
Stresses under linearly loaded rectangular area.
Proc. Am. Soc. Civ. Engrs., Jnl. Soil Mechs. Found. Div., Vol. 96, No. SM1, pp.263-268.
- GOODMAN,R.E., TAYLOR,R.L. & BREKKE, T.L. (1968)
A model for the mechanics of jointed rock.
Proc. Am. Soc. Civ. Engrs., Jnl. Soil Mech. and Found. Div., Vol.94. SM3.

- GRAY, BARMBY & PRIDDLE (1964)
 Discussion: Francis, A.J. "Analysis of pile groups with flexural resistance."
 Proc. Am. Soc. Civ. Engrs., Jnl. Soil Mech. Found. Div., vol. SM6-90, Nov., pp.227 to 237.
- HAIN, S.J. (1977)
 A rational analysis for raft and raft-pile foundations.
 PhD Thesis, University of New South Wales.
- HAIN, S.J. & LEE, I.K (1974)
 Rational analysis of raft foundation.
 Proc. Am. Soc. Civ. Engrs., Jnl. Geotech. Engng. Div., 100, No. GT7, Proc. Paper 10683, July, pp.843 to 860.
- HAIN, S.J. & LEE, I.K (1978)
 The analysis of flexible raft pile systems.
 Geotechnique 28, No.1, pp.65 to 83.
- HEMSLEY, J.A. (1987a)
 Elastic solutions for axisymmetrically loaded circular raft with free or clamped edges on Winkler springs or a half space.
 Proc. Instn. Civ. Engrs., Part 2, 83, Mar., pp.61 to 90.
- HEMSLEY, J.A. (1987b)
 Influence of wall superstructure on the foundation interaction analysis of a circular raft.
 Proc. Instn. Civ. Engrs., Part 2, 83, Mar., pp.115 to 142.
- HETENYI, M. (1946)
 Beams on elastic foundations.
 Ann Arbor, Mich., Univ. of Mich. Press
- HIGHT, D.W. & GREEN, P.A. (1976)
 The performance of a piled-raft foundation for a tall building in London.
 Proc. 6th European Conf. on Soil Mechanics and Foundation Engineering (Vienna), Vol. 1.2, pp.467 to 472.
- HOLL, D.L. (1940)
 Stress transmission in earths.
 Proc. High. Res. Brd., Vol. 20. pp.709-721.
- HONGLADAROMP, T. CHEN, N.J. & LEE, S.L. (1973)
 Load distribution in rectangular footings on piles.
 Geotech. Engng., 4(2), pp.77 to 90.
- HOOKE, R. (1675)
 A description of helioscopes, and some other instruments.
 (London).
- HOOPER, J.A. (1973)
 Observations on the behaviour of a piled-raft foundation on London Clay.
 Proc. Instn. Civ. Engrs., 55(2), pp.855 to 877.
 (Discussion 1974 57(2) pp.547 to 552.)

- HOOPER, J.A. & WOOD, L.A. (1976)
Foundation analysis of a cross wall structure.
Proc. Int. Conf. Performance Bldg Struct., Glasgow, 1,
pp.229 to 248.
- HOOPER, J.A. & WOOD, L.A. (1977)
Comparitive behaviour of raft and piled foundations.
9th, Int. Conf. Soil Mech. and Found. Engng., Vol 1, Tokyo.
- HOOPER, J.A. (1978)
"Foundation interaction analysis"
in Developments in Soil Mechanics. Applied Science
Publication, Chap 5, pp.149 to 211.
- HOOPER, J.A. (1979)
Review of behaviour of piled raft foundations.
CIRIA Report 83.
- HOOPER, J.A. (1983)
Interactive analysis of foundations on horizontally
variable strata.
Proc. Instn Civ. Engrs, Part 2, 75, pp.491 to 524.
- HOOPER, J.A. & WEST, D.J. (1983)
Structural analysis of a circular raft on yielding soil.
Proc. Instn Civ. Engrs, Part 2, 75, pp.205 to 242.
- HOOPER, J.A. (1984)
Raft analysis and design-some practical examples.
The Structural Engineer, 62A(8).
- HOOPER, J.A. & PHILIASTIDES, A. (1986)
Design of a flexible raft foundation of irregular shape.
Proc. Instn Civ. Engrs, Part 1, 80, pp.1013 to 1038.
- HRENNIKOFF, A. (1950)
Analysis of pile foundations with batter piles.
Trans. Am. Soc. Civ. Engrs., vol. 115, pp. 351 to 381.
- INSTITUTION OF STRUCTURAL ENGINEERS (1977)
Structure-soil interaction: A state of the art report.
The Institution Of Structural Engineers.
- INSTITUTION OF STRUCTURAL ENGINEERS, INSTITUTION OF CIVIL
ENGINEERS AND INTERNATIONAL ASSOCIATION FOR BRIDGE AND
STRUCTURAL ENGINEERING (1989)
Soil-structure interaction: The real behaviour of
structures.
The Institution Of Structural Engineers.
- IRELAND, H.O. (1964)
Settlement of a friction pile foundation.
Proceedings, Conference on Deep Foundations, Mexico City,
Vol. 1, p. 373.
- KAY, S., KOLK, H.J. & VAN HOOYDONK, W.R. (1983)
Site specific design of laterally loaded piles.
Proc. Conf., Geotechnical Practice in Offshore Engineering,
Austin, pp. 557 to 580.

- KING, G.J.W. & CHANDRASEKARAN, V.S. (1974)
An assessment of the effects of inter-action between a structure and its foundation.
Proc. Conf. Settlement Of Structures, Cambridge Pentech Press, London.
- KRAFT, L.M., RAY, R.P. & KAGAWA, T. (1981a)
Theoretical t-z curves.
Proc. Am. Soc. Civ. Engrs, Jnl. Geotech. Engng Div., Vol. 107, No. SM3, pp.1543 to 1561.
- KRAFT, L.M., FOCHT, J.A. & AMERASINGHE, S.F. (1981b)
Friction capacity of piles driven into clay.
Proc. Am. Soc. Civ. Engrs., Jnl. Soil Mech. & Found. Engng. Nov., pp.1521 to 1541.
- KRAFT, L.M. (1991)
Performance of axially loaded pipe piles in sand.
Proc. Am. Soc. Civ. Engrs, Jnl. Geotech. Engng Div., Vol. 117, No. 2, pp.272 to 296.
- KOCSIS, P. (1968)
Lateral loads on piles.
Chicago: Bureau of Eng.
- LAMBE, T.W. & WHITMAN, R.U. (1969)
Soil mechanics.
John Wiley.
- LARNACH, W.J. (1970)
Computation of settlements in building frames.
Civ. Eng. & Pub. Wks. Rev., 65, p. 1040.
- LEE, I.K. (1968)
Selected topics in soil mechanics.
Butterworth. p.568-
- LEUNG, C.F. & CHOW, Y.K. (1987)
Response of pile groups subjected to lateral loads.
Int. J. Numer. Analyt. Meth. Geomech. 11, No.3, pp.307 to 314.
- LOHMEYER, E. (1930)
Die berechnungverankerter bohlwerke.
Bautechnik, 8.
- MAJIID, K.I & CUNNELL, M.D. (1976)
A theoretical and experimental investigation into soil-structure interaction.
Geotechnique 26, No. 2, pp.331 to 350.
- MANSUR, C.I. & HUNTER, A.H. (1970)
Pile tests - Arkansas River Project.
Proc. Am. Soc. Civ. Engrs., Jnl Soil Mechs. Found. Div., (96) SM5, pp.1545 to 1582.
- MATLOCK, H. & REESE, L.C. (1960)
Generalized solutions for laterally loaded piles.
Proc. Am. Soc. Civ. Engrs., Jnl. Soil Mech. Found. Div., vol 86, SM5: pp.63 to 91.

- MATLOCK, H. & REESE, L.C. (1961)
Foundation analysis of offshore pile supported structures.
Proc. 5th Int. Conf. Soil Mech. Found. Engng., vol 2, pp.91 to 97.
- MATLOCK, H. & HALIBURTON, T.A. (1964)
"A program for Finite-Element Solution of Beam-Columns on Nonlinear Supports", a report to The California Company, Shell Development Company and Humble Oil and Refining Company, June 1964, 171 pp.
- MATLOCK, H. (1970)
Correlations for design of laterally loaded piles in soft clay.
Proc. 2nd Offshore Tech. Conf., Houston, Texas, 1970, Vol.1, pp.577 to 594.
- MATTES, N.S. (1969)
The influence of radial displacement compatibility on pile settlements.
Geotechnique, vol. 19, pp.157 to 159.
- MATTES, N.S. & POULOS, H.G. (1969)
Settlement of a single compressible pile.
Proc. Am. Soc. Civ. Engrs., Jnl. Soil Mech. Found. Div., Vol.95, No.SM1, pp.189 to 207.
- MAWDITT, J.M. (1982)
The influence of discrete and continuum soil models on the structural design of raft foundations.
MSc. dissertation, University of Surrey, UK.
- MCCLELLAND, B. & FOCHT, J.A. (1956)
Soil modulus for laterally loaded piles.
Jnl. Am. Soc. Civ. Engrs., SM4, Oct.
- MCCLELLAND, B. (1972)
Design and performance of deep foundations in clay.
General Report. Am. Soc. Civil Engineers Speciality Conf. Performance of Earth and Earth Support Structures, Vol.2, pp.111 to 114.
- MEYER, P.L., HOLMQUIST, D.V. & MATLOCK, H. (1975)
Computer predictions for axially-loaded piles with non-linear supports.
Proceedings of the 7th Offshore Technology Conference, Paper No. 2186, Houston, Texas.
- MEYERHOF, G.G. (1947)
The settlement analysis of building frames.
Structural Engineer, Vol 25, part 9, p.369
- MEYERHOF, G.G. (1953)
Some recent foundation research and its application to design.
Structural Engineer., 31, pp.151 to 167.
- MEYERHOF, G.G. (1976a)
Compaction of sands and bearing capacity of piles.
Proc. Am. Soc. Civ. Engrs., Jnl. Soil Mech. Found. Div., Vol. 85, SM6, Part 1, p. 1.

MEYERHOF, G.G. (1976b)
 Bearing capacity and settlement of pile foundations.
 11th Terzaghi Lecture, Proc. Am. Soc. Civ. Engrs., Jnl.
 Geotech. Engrg Div, 102(GT3), pp.195 to 228.

MINDLIN, R.D. (1936)
 Force at a point in the interior of a semi-infinite solid.
 Physics 7, pp.195-202.

MINIPOINT
 Department of Transport, Highways Computing Division. UK.

MOORE, J.F.A. & JONES, C.W. (1975)
 In situ deformation in Bunter Sandstone.
 Proceedings of Conference on Settlement of Structures,
 Cambridge, Pentech Press, pp.311 to 319.

NAIR, K., GRAY, H. & DONOVAN, N. (1969)
 Analysis of pile group behaviour.
 Am. Soc. Test. Mats., STP 444, pp.229 to 261.

NAVFAC DM7 (1971)
 Design manual: soil mechanics, foundation and earth
 structures.
 US Navy.

NEWMARK, N.M. (1942)
 Influence charts for computation of stresses in elastic
 soils.
 Univ. of Ill., Eng. Expt. Stn., Bull. No. 338.

NISHIDA, Y. (1966)
 Vertical stress and vertical deformations of ground under a
 deep circular uniform pressure in the semi-infinite.
 Proc. 1st Congress International Society for Rock Mechanics
 (Lisbon), 1966, Vol. 2, pp.493 to 497.

O'NEILL, M.W. & REESE, L.C. (1972)
 Behaviour of bored piles in Beaumont Clay.
 Proc. Am. Soc. Civ. Engrs., Jnl. Soil Mechs. Found. Div.,
 No.SM2, Feb., pp.195 to 213.

O'NEILL, M.W. GHAZZALY, O.I. & HA, H.B. (1977)
 Analysis of three-dimensional pile groups with non-linear
 soil response and pile-soil-pile interaction.
 Proc. 9th Offshore Technology Conf., Houston 2, pp.245 to
 256.

O'NEILL, M.W., HAWKINS, R.A. & MAHAR, L.J. (1982a)
 Loaded transfer mechanisms in piles and pile groups.
 Proc. Am. Soc. Civ. Engrs, Jnl. Geotech. Engng Div.,
 108, GT12, pp.1605 to 1623.

O'NEILL, M.W., HAWKINS, R.A. & AUDIBERT, J.M.E. (1982b)
 Installation of pile group in overconsolidated clay.
 Proc. Am. Soc. Civ. Engrs, Jnl. Geotech. Engng Div.,
 Vol. 108, No. GT11, Nov., 1982, pp.1369 to 1386.

- O'NEILL, M.W. & MURCHINSON, J.M. (1983)
An evaluation of p-y relationships in sands.
A report to the American Petroleum Institute, May.
- OTTAVIANI, M. (1975)
Three-dimensional finite element analysis of vertically loaded pile groups.
Geotechnique 25(2), pp.159 to 174.
(Discussion 1976 26(1), pp.238 to 240)
- PADFIELD, C.J. & SHARROCK, M.J. (1983)
Settlement of structures on clay soils.
CIRIA/PSA Publication
- PARRY, R.G.H. (1976)
Piles and piled foundations.
Offshore Soil Mechanics, Lloyds Register, Cambridge
University Engineering Department, 1976, pp.178 to 223.
- PECK, R.B. (1961)
"Records of Load Tests on Friction Piles".
Special Report No. 67, Highway Research Bd., Natl. Research
Council, Washington, D.C.
- PGROUP User Manual (1977, 1981)
Program for the analysis of pile groups of any geometry
subjected to horizontal and vertical loads and moments.
HECB/B/7 Department of Transport, HECB, London.
- POULOS, H.G. (1968a)
Analysis of the settlement of pile groups.
Geotechnique 18, No. 4, pp.449 to 471.
- POULOS, H.G. (1968b)
The influence of a rigid pile cap on the settlement
behaviour of an axially-loaded pile.
Civ. Eng. Trans., Inst. Engrs. Aust., vol. CE10, no. 2:
pp.206 to 208.
- POULOS, H.G. & DAVIS, E.H. (1968)
The settlement behaviour of single axially loaded
incompressible piles and piers.
Geotechnique, Vol.18, pp.351 to 371.
- POULOS, H.G. & MATTES, N.S. (1969)
The behaviour of axially-loaded end-bearing piles.
Geotechnique, Vol.19, pp.285 to 300.
- POULOS, H.G. (1971a)
Behaviour of laterally loaded piles: I-single piles.
Proc. Am. Soc. Civ. Engrs., Jnl. Soil Mech. Found. Div.,
Vol.97, No. SM5, pp.711 to 731.
- POULOS, H.G. (1971b)
Behaviour of laterally loaded piles: II-pile groups.
Proc. Am. Soc. Civ. Engrs., Jnl. Soil Mech. Found. Div.,
Vol.97, No. SM5, pp.733 to 751.

- POULOS, H.G. & MADHAV, M.R. (1971)
Analysis of the movements of battered piles.
Proc. 1st Australia-New Zealand Conf. on Geomechanics
(Melbourne), Vol. 1, pp.268 to 275.
- POULOS, H.G. & MATTES, N.S. (1971a)
Settlement and load distribution analysis of pile groups.
Australian Geomech. Jnl. G1(1), pp.18 to 28.
- POULOS, H.G. & MATTES, N.S. (1971b)
Displacements in a soil mass due to pile groups.
Australian Geomech. Jnl. G1(1), pp.29 to 35.
- POULOS, H.G. (1974)
Analysis of pile groups subjected to vertical and
horizontal loads.
Australian Geomech. Jnl. G4(1), pp.26 to 32.
- POULOS, H.G. & MATTES, N.S. (1974)
Settlement of pile groups bearing on stiffer strata.
Proc. Am. Soc. Civ. Engrs., Jnl. Geotech. Engng. Div.,
100(GT2), pp.185 to 190.
- POULOS, H.G. (1975a)
Design of pile foundations.
Research Report 271, University of Sydney, School of
Engineering.
- POULOS, H.G. (1975b)
Lateral load deflection prediction for pile groups.
Proc. Am. Soc. Civ. Engrs., Jnl. Geotech. Engng. Div.,
Jan., 101(GT1), pp.19 to 33.
- POULOS, H.G. (1980)
An approach for the analysis of offshore pile groups.
Numerical methods in offshore piling, pp.119 to 126.
London: Institution of Civil Engineers.
- POULOS, H.G. & DAVIS, E.H. (1974)
Elastic solutions for soil and rock mechanics.
John Wiley.
- POULOS, H.G. (1979)
Settlement of Single Piles in Nonhomogeneous Soil.
Proc. Am. Soc. Civ. Engrs., Jnl. Geotech. Engng. Div., May,
105(GT5), pp.627 to 641.
- POULOS, H.G. & DAVIS, E.H. (1980)
Pile foundation analysis and design.
John Wiley.
- PRAKASH, S.L. (1961)
Behaviour of pile groups subjected to lateral loads.
Thesis for a Doctor of Philosophy Degree submitted to the
Department of Civil Engineering, University of Illinois,
Dec.
- PRAKASH, S.L. & SARAN, D. (1967)
Behaviour of laterally-loaded piles in cohesive soil.
Proc. 3rd Asian Conf. on Soil Mechanics, Halsa, pp.235 to
238.

- PRICE, G. & WARDLE, I.F. (1986)
Queen Elizabeth II Conference Centre:- monitoring of load sharing between piles and raft.
Proc. Instn. Civ. Engrs., Vol 80, Part 1, pp.1505 to 1518.
- RANDOLPH, M.F. & WROTH, C.P. (1978)
Analysis of deformation of vertically loaded piles.
Journal of the Geotechnical Engineering Division, ASCE, Vol.104, No.GT12, Dec., pp.1465 to 1488.
- RANDOLPH, M.F. & WROTH, C.P. (1979)
An analysis of the vertical deformation of pile groups.
Geotechnique 29, No.4, pp.423 to 439.
- RANDOLPH, M.F. (1980)
PIGLET-a computer program for the analysis and design of laterally loaded piles under general loading conditions.
Cambridge University Research Report CUED/D-Soils TR 91.
- RANDOLPH, M.F. (1981)
The response of flexible piles to lateral loading.
Geotechnique, June, 31(2), pp.247 to 259.
- REDDAWAY, A.L. & ELSON, W.K. (1982)
The performance of Newhaven Bridge.
CIRIA Technical Note 109.
- REESE, L.C. & MATLOCK, H. (1956)
Non-dimensional solutions for laterally loaded piles with soil modulus assumed proportional to depth.
Proceedings of the 8th Texas Conference on Soil Mechanics and Foundation Engineering, Austin, Texas, pp.1 to 41.
- REESE, L.C. (1964)
Load versus settlement for an axially loaded pile.
Proceedings of the Symposium on Bearing Capacity of Piles, Part 2, held at the Central Bldg. Research Inst., Roorkee, India, February, 1964, Cement and Concrete, New Delhi, India, pp.18 to 38.
- REESE, L.C. & COX, W.R. (1969)
Soil behaviour from the analysis of tests of uninstrumented piles under lateral loading.
American Society for Testing Materials, Special Technical Publication (ASTM. STP) 444, 1969, pp.160 to 176.
- REESE, L.C., O'NEILL, M.W. & SMITH, R.E. (1970)
Generalized analysis of pile foundations.
Proc. Am. Soc. Civ. Engrs., Jnl. Soil Mech. Fndn. Div., vol. 96, SM1, 235.
- REESE, L.C., COX, W.R. & KOOP, F.B. (1974)
Analysis of laterally loaded piles in sand.
Proceedings of the 6th Offshore Technology Conference, Houston, Texas, paper No. OTC 2080, pp.473 to 483.

- REESE, L.C., COX, W.R. & KOOP, F.B. (1975)
Field testing and analysis of laterally-loaded piles in stiff clay.
Proc. 7th Offshore Tech. Conf. Houston, Texas, Vol. 12, pp.671 to 690.
- REESE, L.C. (1977)
Laterally loaded piles: program documentation.
Proc. Am. Soc. Civ. Engrs., Jnl. Geotech. Engng. Div., April, 103(GT4), pp.287 to 305.
- REISSNER, E. (1958)
A note on deflections of plates on a visco-elastic foundation.
Jnl. of Applied Mechanics, Vol. 80., pp.144 to 145.
- RICKARD, C.E., MANIE, B., PRICE, G., SIMONS, N.E., WARDLE, I. & CLAYTON, C.R.I. (1985)
Interaction of a piled raft foundation at Basildon, UK.
Proc. 11th Int. Conf. Soil Mech. and Found. Engng, Vol. 4, San Francisco.
- SAUL, W.E. (1968)
Static and dynamic analysis of pile foundations.
Proc. Am. Soc. Civ. Engrs., Jnl. Struct. Div., vol. 94, ST5, pp.1077 to 1100.
- SAWKO, F. (1968)
A simplified approach to the analysis of piling systems.
Struct. Eng., vol. 46, no. 3, pp.83 to 86.
- SCOTT, C.R. (1974)
An introduction to soil mechanics and foundations.
Applied Science Publishers (Barking).
- SEED, H.B. & REESE, L.C. (1957)
The action of soft clay along friction piles.
Transactions, Am. Soc. Civ. Engrs., Vol. 122, pp.731 to 754.
- de SIMONE, S.V. (1966)
Suggested design procedures for combined footings and mats.
Jnl. Am. Conc. Inst., Oct., p. 1041.
- SKEMPTON, A.W. (1951)
"The Bearing Capacity of Clays"
Building Research Congress, Division 1, Part 3, London, pp.180 to 189.
- SKEMPTON, A.W. (1953)
Discussion, Session 5-"Piles and pile foundations, settlements of pile foundations"
Proceedings, 3rd Internatl. Conf. on Soil Mechanics and Foundation Engng., Switzerland, Vol. III, p.172.
- SMITH, G.N. & POLE, E.L. (1980)
Elements of Foundation Design.
Granada Publishing Limited.

SMITH, I.N. (1982)
 Programming the Finite Element Method with application to
 Geomechanics.
 Chichester: Wiley

SOWERS, G.F. et al (1961)
 The bearing capacity of friction pile groups in homogeneous
 clay from model studies.
 Proc. 5th Int. Conf. Soil Mech. Found. Engrng, 2, p.155

SOWERS, G.B. & SOWERS, G.F. (1970)
 Introductory soil mechanics and foundations.
 MacMillan Co., New York.

SPILLERS, W.R. & STOLL, R.D. (1964)
 Lateral response of piles.
 Proc. Am. Soc. Civ. Engrs., 90, SM6, 1.

STEINBRENNER, W. (1934)
 Tafeln zur setzungberechnung.
 Die strasse, Vol. 1, p.121.

STRAPP II
 Strapp II program from the IBM package of structural
 programs.

SW PILE
 Midland Road Construction Unit, Warwickshire County
 Council. Available from Ove Arup and Partners, Warwick.

TAMAKI, O., MITSUHASHI, K. & IMAI, T. (1971)
 Horizontal resistance of a pile group subjected to lateral
 load.
Proc. 4th Asian Regional Conference on Soil Mechanics and
Foundation Engineering, Vol 1, pp.311 to 315.

TAYLOR, D.W. (1974)
 Fundamentals of soil mechanics.
 John Wiley.

TERZAGHI, K. (1943)
 Theoretical soil mechanics.
 Chichester. John Wiley & Sons Inc.

TERZAGHI, K. (1955)
 Evaluation of Coefficients of Subgrade Reaction.
 Geotechnique, Vol. V, No. 4

TERZAGHI, K. & PECK, R.B. (1967)
 Soil mechanics in engineering practice.
 John Wiley & Sons, New York.

THOMSON, W. (1848)
 Cambridge and Dublin Math.J.

THURMAN, A.G. & D'APPOLONIA, E. (1964)
 Prediction of Pile Action by a Computer Method.
Proceedings, Conf. on Deep Foundations, Mexico City,
 Mexico, December.

- THURMAN, A.G. & D'APPOLONIA, E. (1965)
 Computed movement of friction and end-bearing piles
 embedded in uniform and stratified soils.
 Proc. 6th Int. Conf. Soil Mech. Found. Engng., Vol.2,
 pp.323 to 327.
- TOMLINSON, M.J. (1977)
 Pile design and construction practice.
 A Viewpoint Publication.
- TOMLINSON, M.J. (1980, 1986)
 Foundation design and construction.
 4th Edition. Pitman Press.
 Fifth Edition. Longman Scientific & Technical.
- TOOLAN, F.E. & HORSNELL, M.R. (1979)
 Analysis of load-deflexion behaviour of offshore piles and
 pile groups.
 Numerical methods in offshore piling, pp.147 to 155.
 London: Institution of Civil Engineers.
- TROCHANIS, A.M., BIELAK, J. & CHRISTIANO, P. (1991a)
 Three-dimensional nonlinear study of piles.
 Proc. Am. Soc. Engrs., Jnl of Geotech. Engng, Vol. 117, No.
 3, March, pp.429 to 447.
- TROCHANIS, A.M., BIELAK, J. & CHRISTIANO, P. (1991b)
 Simplified model for analysis of one or two piles.
 Proc. Am. Soc. Engrs., Jnl of Geotech. Engng, Vol. 117, No.
 3, March, pp.448 to 466.
- TURZYNSKI, L.D. (1960)
 Groups of piles under mono-planar forces.
 Structural Engineer, Sept., 38(9), pp.286 to 293.
- VESIC, A.S. (1961)
 Bending of beams resting on isotropic elastic solid.
 Proc. Am. Soc. Civ. Engrs., Jnl. Eng. Mechs. Div., Vol.
 87, No. EM2, pp.35 to 53.
- VESIC, A.S. (1969)
 Experiments with instrumented pile groups in sand.
 Performance of Deep Foundations, Am. Soc. Test. Mats., STP
 No. 444, p.177.
- VESIC, A.S. (1970a)
 Load transfer in pile-soil systems.
 Proceedings, Conference on Design and Installation of Pile
 Foundations and Cellular Structures, Lehigh Univ.
- VESIC, A.S. (1970b)
 Tests on instrumented pile, Ogeechee River site.
 Proc. Am. Soc. Civ. Engrs., Jnl. Soil Mech. Found. Div.,
 (96) SM2, pp.561 to 584.
- VIJAYVERGIYA, V.N. (1977)
 Load movement characteristics of piles.
 Ports 77 Conf., Long Beach, California.

- WARDLE, L.J. & FRASER, R.A. (1975)
Methods for raft foundation design including soil-structure interaction.
Proc. Symp. Raft Fdns., Perth, Australia, pp.1 to 11.
- WEBB, D.L. (1975)
Observed settlement and cracking of a reinforced concrete structure founded on clay.
Proc. Conf. on Settlement Struct., Cambridge, Pentech Press, London, p.443.
- WHITAKER, T. (1957)
Experiments with model piles in groups.
Geotechnique 7, p.147.
- WHITAKER, T. (1960)
Some experiments on model pile foundations.
Symp. Pile Fdn IABSE, Stockholm.
- WHITAKER, T. & COOKE, R.W. (1966)
An investigation of the shaft and base resistances of large bored piles in London Clay.
Proc. of Symp. Large Bored Piles, Instn of Civ. Engrs., London, Feb., pp.7 to 49.
- WHITAKER, T. (1976)
The design of piled foundations
Pergamon Press (Oxford), 2nd Edition, pp.169 to 170.
- WINKLER, E. (1867)
Die Lehre von der Elastizitat und Festigkeit.
(Prag.), p.182.
- WOOD, L.A. (1972)
Some aspects of soil-structure interaction.
PhD thesis, II, Bristol Univ.
- WOOD, L.A. & LARNACH, W.J. (1974)
The effects of soil-structure interaction on raft foundations.
Proc. Conf. Settlement Of Structures, Cambridge Pentech Press, London.
- WOOD, L.A. & LARNACH, W.J. (1975)
"The interactive behaviour of a soil-structure system and its effect on settlements."
Symp. Geot. Struct., Univ. N.S.W.
- WOOD, L.A. (1977)
The economic analysis of raft foundations.
International Journal for Numerical and Analytical Methods in Geomechanics, 1, 397.
- WOOD, L.A., LARNACH, W.J. & WOODMAN, N.J. (1977)
Observed and computed settlements of two buildings.
Proc. Symp. soil-structure Interaction, Roorkee, India.
pp.129 to 136.

WOOD, L.A. (1978)

RAFTS: A program for the analysis of soil-structure interaction.

Advances in Engineering Software, 1, 11.

WOOD, L.A. (1979)

LAWPILE - A program for the analysis of laterally loaded pile groups and propped sheetpile and diaphragm walls.

Proc. 1st Int. Conf. on Engineering Software, Vol. 1.4 pp.614 to 632.

WOOD, L.A. (1982)

Discussion of Majid and Rahman, Non-linear analysis of structure soil systems.

Proceedings of the Institution of Civil Engineers, London, 73(2), pp.527 to 528.

WOODWARD, R.J., LUNDGREN, R. & BOITANO, J.D., Jr. (1961)

Pile loading tests in stiff clays.

Proceedings, 5th Internatl. Conf. on Soil Mechanics and Foundation Engrg., Paris, France, July, Vol. II.

YU, T.M., SHU, W.Y. & TONG, Y.X. (1965)

Settlement analyses of pile foundations in Shanghai

Proceedings, 6th Internatl. Conf. on Soil Mechanics and Foundation Engrg., Montreal, Vol. II, p. 356.

ZIENKIEWICZ, O.C., BEST, B., DULLAGE, C. & STAGG, K.G. (1970)

Analysis of non-linear problems in rock mechanics with particular reference to jointed rock systems.

Proc. 2nd Congress Int. Soc. Rock Mech., Vol.3, Belgrade.

ZIENKIEWICZ, O.C. (1971)

The Finite Element Method in Engineering Science.

McGraw-Hill, London.

ZIENKIEWICZ, O.C. (1977)

The finite element method.

(3rd ed.) (Maidenhead: McGraw-Hill).

APPENDIX A
THE SURFACE ELEMENT METHOD
APPLIED TO RAFT FOUNDATION ANALYSIS

In the surface element method (S.E.M.), the Boussinesq Equation A.1. is used to determine the σ_z stress distribution beneath the raft.

$$\sigma_z = \frac{3 P}{2 \pi z^2} \left[\frac{1}{1 + (r/z)^2} \right]^{1/2} \dots\dots\dots A.1.$$

where P = concentrated vertical load
 z = vertical distance to point considered from the underside of the raft
 r = horizontal distance to point considered from the line of action of the load.

Knowing the stress distribution, the strains within the soil mass can be determined and hence the vertical displacement. This method is useful for the analysis of a layered soil mass. For a homogeneous elastic half-space the vertical displacement δ_z can be determined directly from Equation A.2.

$$\delta_z = \frac{P (1+\mu_s)}{2 \pi E_s R} \left[2(1-\mu_s) + \frac{z^2}{R^2} \right] \dots\dots\dots A.2.$$

where E_s = soil modulus
 μ_s = Poisson's ratio of the soil
 $R = (r^2 + z^2)^{1/2}$

This enables the vertical displacements at any point on the surface of a linear elastic half-space due to the application of a vertical force at any other node point to be determined. The equation can be written in the form:

$$\delta_j = P_i f_{ij} \dots\dots\dots A.3.$$

where δ_j = vertical displacement at j
 P_i = vertical force at point i

f_{ij} = flexibility term dependent on elastic properties of the ground and distance between i and j . This can be determined by using Equation A.1 or A.2.

This is repeated for each node i in turn for a total of n nodes and the cumulative displacement at j is given by:

$$\delta_j = \sum_{i=1}^n P_i f_{ij} \dots\dots\dots A.4.$$

The cumulative displacement in terms of P for each node in the group is then expressed by a set of linear simultaneous equations. This is given in matrix form as:

$$\{\delta\} = [Fs] \{P\} \dots\dots\dots A.5.$$

Where $\{\delta\}$ and $\{P\}$ are displacement and force vectors respectively and $[Fs]$ is the soil flexibility matrix. By rearranging the equation and inverting $[Fs]$ the soil stiffness matrix $[Ks]$ is determined to give:

$$\{P\} = [Ks] \{\delta\} \dots\dots\dots A.6.$$

For the raft plate bending elements, the relationship between the applied loads $\{Q\}$, raft-soil contact forces $\{P\}$ and the displacements $\{\delta\}$ is given by:

$$\{Q-P\} = [Kr] \{\delta\} \dots\dots\dots A.7.$$

where $[Kr]$ is the stiffness of the raft.

Substitution of Equation A.6. into A.7. gives:

$$\{Q\} = [Kr+Ks] \{\delta\} \dots\dots\dots A.8.$$

The applied load $\{Q\}$ and the stiffness of the system $[Kr+Ks]$ are known values, hence, the matrices can be solved to determine nodal point displacements $\{\delta\}$. By back substitution the contact pressure and bending moment distribution are obtained.

APPENDIX B

THE INTERACTION FACTOR METHOD.

B.1. ANALYSIS OF FREE STANDING PILE GROUPS.

B.1.1. Interaction Due To Vertical Loading.

(a) Two pile interaction.

Poulos (1968a) and Poulos and Mattes (1971a) considered the increase in vertical displacement of a pile due to an adjacent identical pile in terms of an interaction factor α . The relevant parameters are defined below.

α = ratio of increase in displacement due to adjacent pile to displacement of single pile only.
S = pile spacing
d = pile diameter
h = depth of soil layer
L = pile length
E_p = pile modulus
E_s = soil modulus
 μ_s = soil Poisson's ratio
and K = pile stiffness factor

$$\text{where } K = \frac{E_p R_A}{E_s} \quad \text{and } R_A = \frac{\text{Area of pile section}}{\pi d^2 / 4}$$

The variation of α with the S/d ratio is reproduced in Figure B.1 for two incompressible piles in a finite layer. For a L/d ratio of 25 the effect of Poisson's ratio μ_s on the interaction factor α is shown in Figure B.2. For S/d ratios greater than 2 the effect of the Poisson's ratio on α is minimal. Poulos and Davis (1974) presented graphs of α against the S/d ratio for two general compressible piles in a semi-infinite mass having a Poisson's ratio of 0.5. These graphs are reproduced in Figures B.3 (a) and (b) for three L/d ratios.

(b) Analysis of general pile groups.

This type of analysis applies to pile groups without a raft; or free standing piled rafts ie. with no cap contact. The two pile interaction factors in Figures B.1 and B.3 were used by Poulos and Davis to analyse the displacement and load distribution in any general pile group by employing the principle of superposition. They claimed that the principle of superposition had "been found to apply closely for pile groups". However, they also recognised that superposition could not hold rigorously as the presence of the piles in the elastic mass involved a change in the overall elastic system.

For any pile "i" in a group of "k" piles, the displacement is given by:

$$\delta_i = \delta_1 \left[\sum_{\substack{j=1 \\ j \neq i}}^k P_j \cdot \alpha_{ij} + P_i \right] \dots\dots\dots B.1.$$

where δ_1 = displacement of single pile under unit load
 α_{ij} = interaction factor for spacing between piles i and j
 P_j = load in pile j.

Equation B.1. is then written for all the piles in the group and use is made of the equilibrium equation:

$$P_G = \sum_{j=1}^k P_j \dots\dots\dots B.2.$$

where P_G = total group load.

In order to solve the equations one of two boundary conditions needs to be implemented.

(i) equal displacement of all piles. This corresponds to a rigid pile cap, and the distribution of load at the pile heads and the uniform displacement of the group is computed.

(ii) equal load in all piles. This corresponds to a uniformly loaded flexible pile cap, and the distribution of pile head displacement in the group is computed.

Poulos (1968a) and Poulos and Mattes (1971a) presented typical solutions for the settlement and pile head load distribution for various pile groups.

B.2. Analysis Of Piled Rafts.

(a) General.

Davis and Poulos (1972) extended the above method to the analysis of pile raft systems. For piled rafts the basic unit is taken to be a single pile with an attached pile cap resting on the soil surface. This is in contrast to the basic unit of a single pile only for free standing groups. The work is confined to units consisting of a rigid pile attached to a rigid cap and situated in a semi-infinite mass, and for simplicity, the cap is assumed to be circular. It was subsequently shown that the behaviour of such a unit was identical with that of a unit having a square (or rectangular) cap of the same area.

The authors contended that the solutions given for rigid units in a semi-infinite mass could be adjusted to approximately accommodate the effects of finite pile compressibility and finite soil depth. This could be achieved by comparison with solutions previously obtained for free standing piles. They cited the following solutions as a basis of inferring the approximate corrections. The solutions obtained by Poulos and Mattes (1971) for groups of compressible friction piles showed that settlement interaction decreased as the relative

compressibility of the pile increased. Also, Poulos (1968a) showed for incompressible friction pile groups in a finite soil layer that the settlement interaction was "damped out" at larger spacings by the presence of a stiff underlying stratum. However, the authors stated:

"If the compressibility of the pile were to be considered, the pile displacements could be determined as described by Mattes and Poulos (1969), while the flexibility of the pile cap could be taken into account by the method described by Brown (1969)."

Also of interest is the authors' following statement:

"No ready information appears to be available for assessing the influence of finite flexibility of the pile cap on the interaction between units, but it would appear unlikely that cap flexibility would seriously affect interaction."

(b) Analysis of two unit systems.

The graph of the ratio F_R of settlement of the pile cap unit to that of a single pile, with the relative diameter of the pile cap is reproduced in Figure B.4. The interaction between two such pile cap units is a combination of the analyses described by Poulos (1968b) for a single unit and by Poulos (1968a) for two free standing piles. The settlement results of the analysis for the two unit system are evaluated for various cap diameter, d_c , to pile diameter, d , (d_c/d) ratios and dimensionless centre-to-centre pile spacing S/d ratios. The results are expressed in terms of an interaction factor α_r , where:

$$\alpha_r = \frac{\text{additional settlement due to adjacent unit}}{\text{settlement of single unit}} \dots\dots B.3.$$

The results relating α_r to the S/d ratio are reproduced for various values of d_c/d in Figures B.5. to B.8. for three L/d ratios and a Poisson's ratio μ_s of 0.5.

The interaction increases as dc/d increases, but the effect of dc/d becomes less as the L/d ratio increases. In Figure B.9. the corresponding graph is reproduced for a Poisson's ratio of 0.0 and a L/d ratio of 25. By comparison of this graph with the corresponding graph for $\mu_s=0.5$, for a value of $dc/d < 10$ greater interaction occurs for $\mu_s=0$ than for $\mu_s=0.5$, but that for $dc/d > 10$, μ_s has little effect on interaction. In these figures the portions of the curves shown as dashed lines are for spacings and cap diameters where an overlap occurs.

(c) Analysis of general systems.

General pile raft systems are considered to comprise several pile cap units, each having an equivalent value of dc/d such that the area occupied by the unit is the same as that occupied by a typical portion of the cap in the group. For a square arrangement of piles in a group the equivalent dc/d ratio is simplified to:

$$\text{equivalent } dc/d = \frac{S}{d} \left[\frac{4}{\pi} \right]^{1/2} \dots\dots\dots B.4.$$

The appropriate interaction factor α_r is then selected for each S/d ratio from the graphs in Figures B.5. to B.8. The authors found that superposition could be applied to symmetrical arrangements of pile cap units in a similar manner to that described by Poulos (1968a) and Poulos and Mattes (1971a) for free standing piles, ie. the additional settlement of each unit in the system due to the other units is the sum of the increase in displacements due to each of the other units in turn.

In a system of "m" units, the settlement of a typical unit "i" is given by:

$$\delta_i = \delta_1 \cdot \left(\sum_{\substack{j=1 \\ j \neq i}}^m P_j \cdot \alpha_{rij} + P_i \right) \dots\dots\dots B.5.$$

where α_{rij} = the value of α_r , for the equivalent dc/d ratio of unit j, corresponding to the spacing between units i and j.

P_j = load in unit j

δ_1 = settlement of a single pile cap unit under unit load.

From Figure B.4., δ_1 can be expressed as:

$$\delta_1 = F_R \cdot \delta_1 \dots\dots\dots B.6.$$

where δ_1 = settlement of free standing pile under unit load
 F_R = ratio of settlement of pile cap unit to settlement of free standing pile.

As shown previously, "m" equations can be obtained from Equation B.5. for the "k" piles in the group, together with the equilibrium equation:

$$P_G = \sum_{j=1}^m P_j \dots\dots\dots B.7.$$

As before, the boundary conditions which need to be specified in order to solve the equations are: (i) Equal displacement of each unit (corresponding to a rigid raft) or (ii) Equal load in each unit.

The latter boundary condition corresponds to a perfectly flexible raft with a uniformly applied load. However, each pile cap unit displaces vertically as a rigid unit and the displacements of adjacent units are generally non-compatible ie. instead of varying continuously the displacement varies in "steps" from one unit to the next. The authors observed that "the idealization of equal load in each unit is at best an approximation".

In addition the authors stated:

"In principle, the above analysis could also be extended to consider approximately the case of a raft of finite flexibility. However, a more satisfactory analysis would require consideration of compatibility of both displacement and rotation between adjacent units having a cap of finite flexibility. Such analyses lie outside the scope of the present paper."

Their simplified method enables the number of piles to be determined which need to be added to a raft in order to reduce the settlement to a tolerable amount. It is concluded that provided the raft itself has an adequate factor of safety against undrained failure, considerable reduction in settlement may be achieved by the addition of relatively few long piles, even though these piles may have reached their ultimate load.

B.3. INTERACTION OF LATERALLY LOADED PILES.

B.3.1 General.

The interaction of laterally loaded piles was considered by Poulos (1971b). The idealization of the geometry and loading is as shown in Figure B.9. Where:

H = applied horizontal load
M = applied moment
L = pile length
d = diameter
 β = angle between line of piles and direction of loading
S = pile spacing.

As with axially loaded piles the increase in lateral displacement and rotation of the pile head displacement due to the presence of an identical adjacent pile can be expressed in terms of an interaction factor α where:

α = ratio of increase in displacement (or rotation) due to the adjacent pile displacement (or rotation) of a single pile.

Five interaction factors are considered for free head piles:

- α_{pH} = interaction factor for displacement due to horizontal load only.
- α_{pM} = interaction factor for displacement due to moment only.
- $\alpha_{\theta H}$ = interaction factor for rotation due to horizontal load only ($\alpha_{\theta H} = \alpha_{pM}$).
- $\alpha_{\theta M}$ = interaction factor for rotation due to moment only

For a fixed head pile the following interaction factor applies:

- α_{pF} = interaction factor for displacement of fixed head pile.

The interaction factors α_{pH} , α_{pM} , $\alpha_{\theta M}$ and α_{pF} are reproduced against the dimensionless pile spacing S/d ratio in Figures B.10 to B.25 for various values of the pile flexibility factor K_R . Where:

$$K_R = \frac{E_p \cdot I_p}{E_s \cdot L^4} \dots\dots\dots B.8.$$

Where: E_p = pile modulus
 E_s = soil modulus
 L = pile length
 I_p = second moment of area of pile.

The interaction factors are plotted for values of β of 0° and 90° . For other values of β Poulos recommends that it is sufficiently accurate to interpolate linearly between the curves for 0° and 90° .

B.3.2. Analysis Of General Pile Groups.

As with axially loaded friction pile groups, the principle of superposition can be used together with the two pile interaction factors to compute the loads and displacements within the group for the case of equal displacement of all piles, or equal loads in all piles.

For fixed head piles, the horizontal displacement of a pile "i" in a group of "k" piles is given by:

$$\delta_i = \bar{\delta}_H \left(\sum_{\substack{j=1 \\ j \neq i}}^k H_j \cdot \alpha_{pHij} + H_i \right) + \bar{\delta}_M \left(\sum_{\substack{j=1 \\ j \neq i}}^k M_j \cdot \alpha_{pMij} + M_i \right) \dots B.9.$$

where:

- H_j = horizontal load in pile j
- α_{pHij} = value of α_{pH} for spacing and value of β between piles i and j
- $\bar{\delta}_H$ = horizontal movement of single pile due to unit applied horizontal load
- M_j = moment in pile j
- α_{pMij} = values of α_{pM} for spacing and values of β between piles i and j
- $\bar{\delta}_M$ = horizontal movement of single pile due to unit applied moment.

A similar expression can be determined for the rotation of pile "i", or for the displacement of pile "i" for a group of fixed head piles.

Application of Equation B.9. to all piles in the group, together with the equilibrium equations enables solutions to be determined for the load and moment distributions and the pile head displacement and rotation of the group. However, again the two limiting boundary conditions are either equal loads and moments in all piles or equal displacement and rotation of all piles.

For moment loading Poulos stated that "the effect of the axial pile loads must be considered". However, he did not indicate how this effect should be considered. Also, for the case of horizontal loading only, the rotation of the pile cap induces axial loads in the piles. By not accommodating this effect the displacement is overestimated. Poulos did not suggest a procedure to overcome this problem.

Typical solutions for the displacement of a fixed head group of piles for the equal displacement case are

given by Poulos (1971b). However, for most practical pile groups, even with a perfectly rigid pile cap, the horizontal loading induces rotation of the cap and hence the pile head is not strictly fixed against rotation.

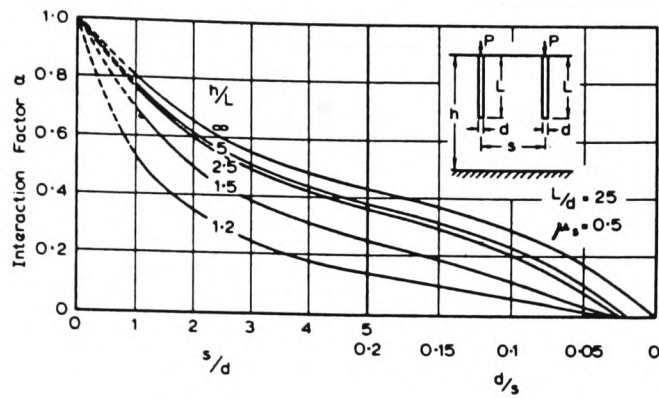


Figure B.1. Interaction factors for two incompressible piles in a finite layer [after Poulos and Davis (1974)].

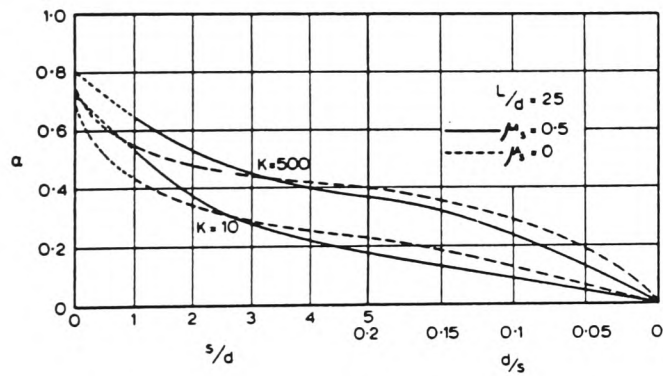
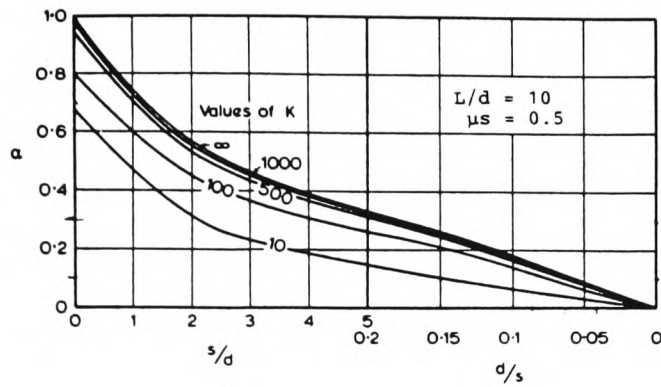
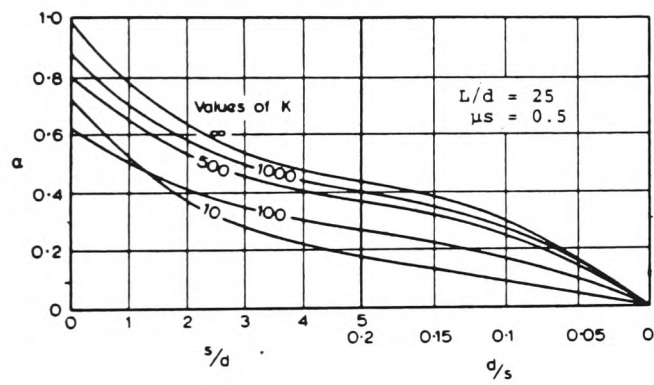


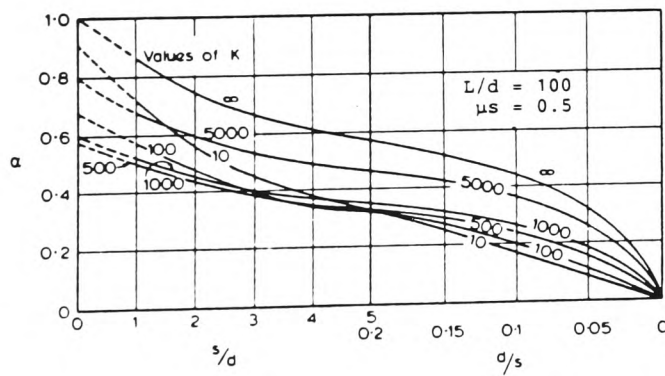
Figure B.2. Effect of μ_s on interaction factors for two floating piles in a semi-infinite mass [after Poulos and Davis (1974)].



(a) $L/d = 10$



(b) $L/d = 25$



(c) $L/d = 100$

Figure B.3. Interaction factors for two floating piles in a semi-infinite mass [after Poulos and Davis (1974)].

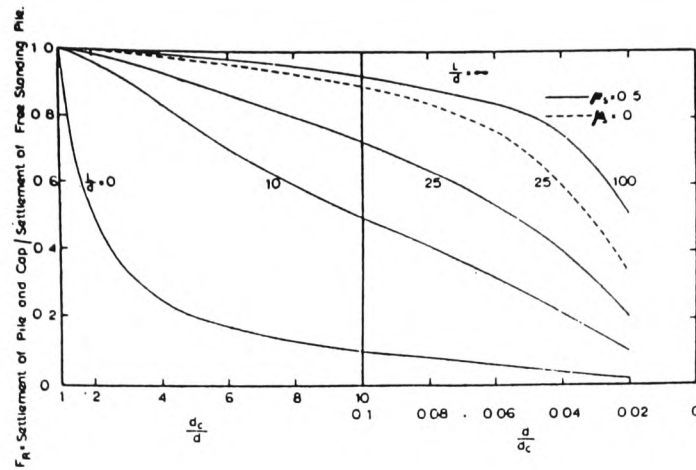


Figure B.4. Influence of a pile cap on the settlement of a single pile [after Davis and Poulos (1972)]

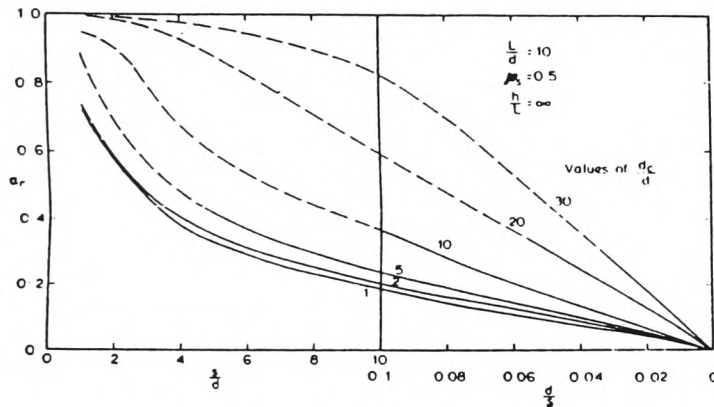


Figure B.5. Interaction factors for pile-raft units, $L/d = 10$. [after Davis and Poulos (1972)].

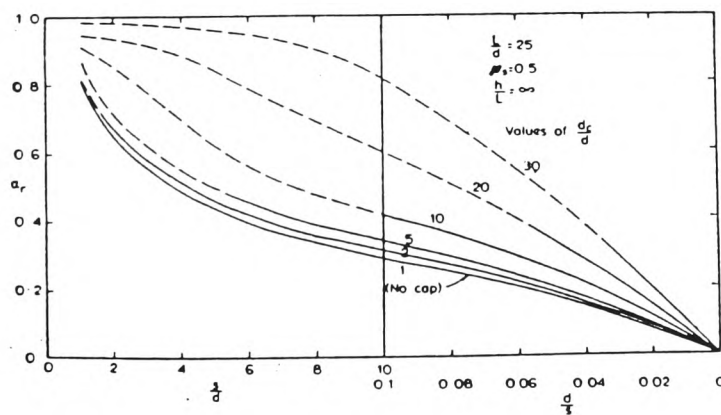


Figure B.6. Interaction factors for pile-raft units, $L/d = 25$. [after Davis and Poulos (1972)].

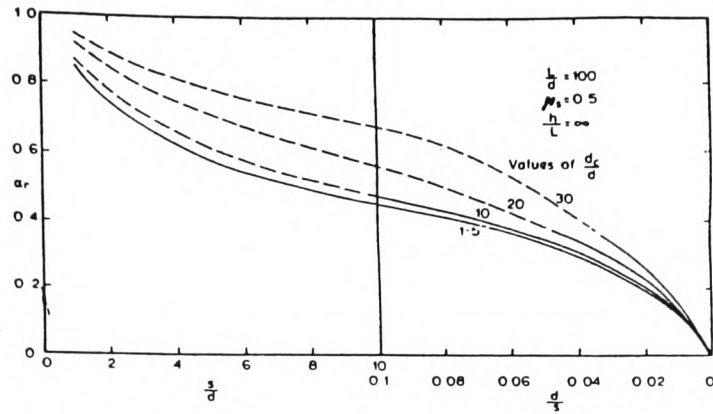


Figure B.7. Interaction factors for pile-raft units,
 $L/d = 100$. [after Davis and Poulos (1972)].

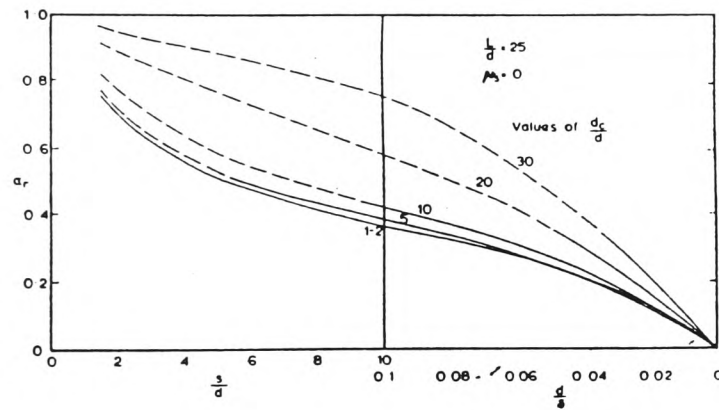


Figure B.8. Interaction factors for pile-raft units,
 $L/d = 25$, $\mu_s = 0$. [after Davis and Poulos (1972)].

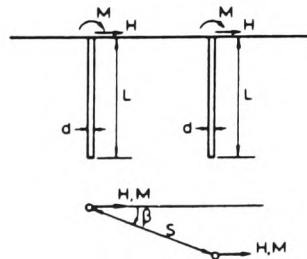


Figure B.9. Interaction between two identical piles
 [after Poulos and Davis (1974)].

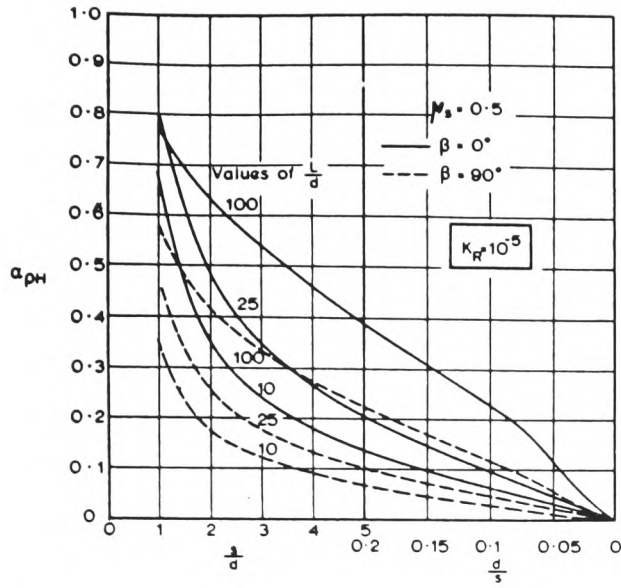


Figure B.10. Interaction factor $\alpha_{\rho H}$, $K_R = 10^{-5}$, [after Poulos and Davis (1974)].

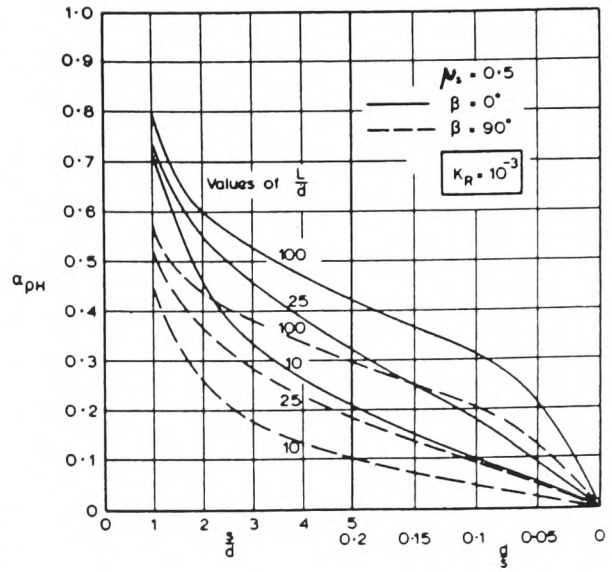


Figure B.11. Interaction factor $\alpha_{\rho H}$, $K_R = 10^{-3}$, [after Poulos and Davis (1974)].

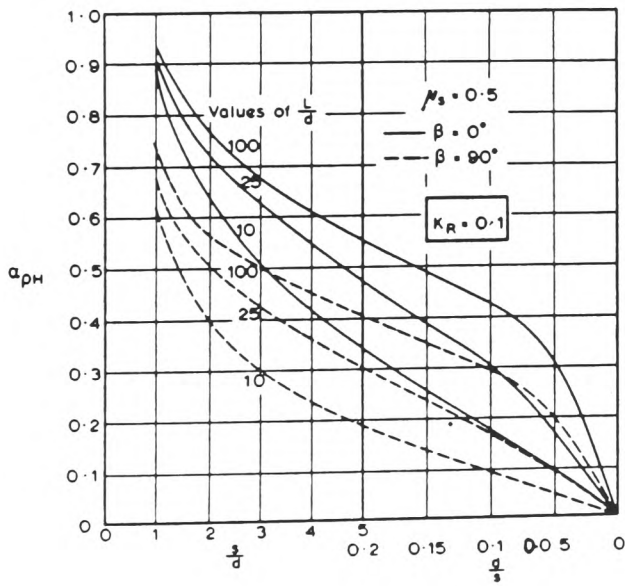


Figure B.12. Interaction factor $\alpha_{\rho H}$, $K_R = 0.1$, [after Poulos and Davis (1974)].

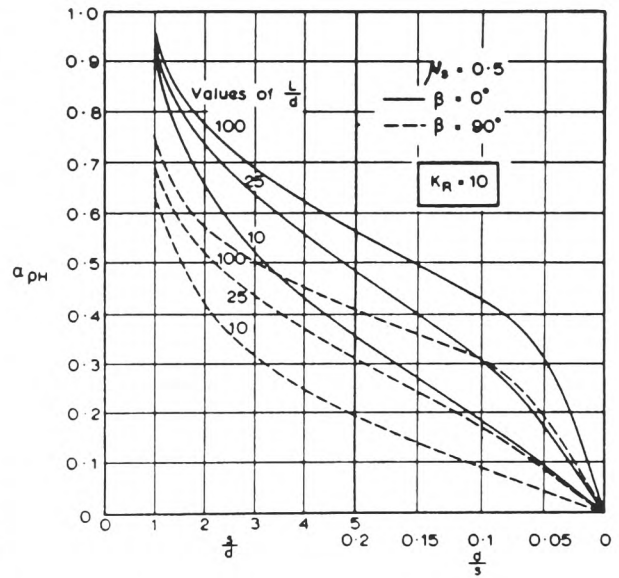


Figure B.13. Interaction factor $\alpha_{\rho H}$, $K_R = 10.$, [after Poulos and Davis (1974)].

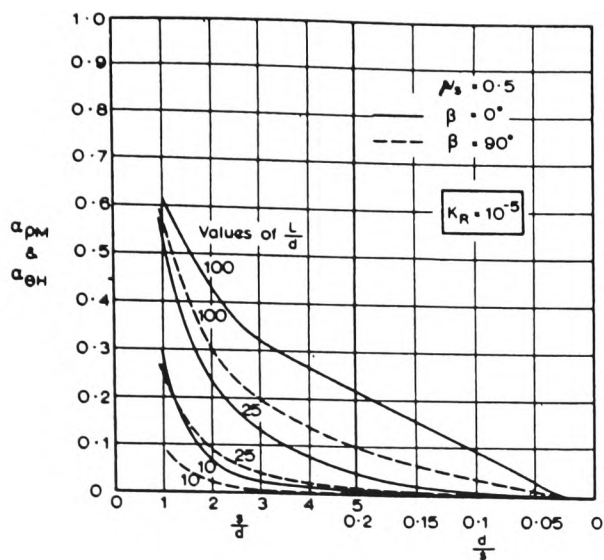


Figure B.14. Interaction factors $\alpha_{\rho H}$ and $\alpha_{\theta H}$, $K_R = 10^{-5}$, [after Poulos and Davis (1974)].

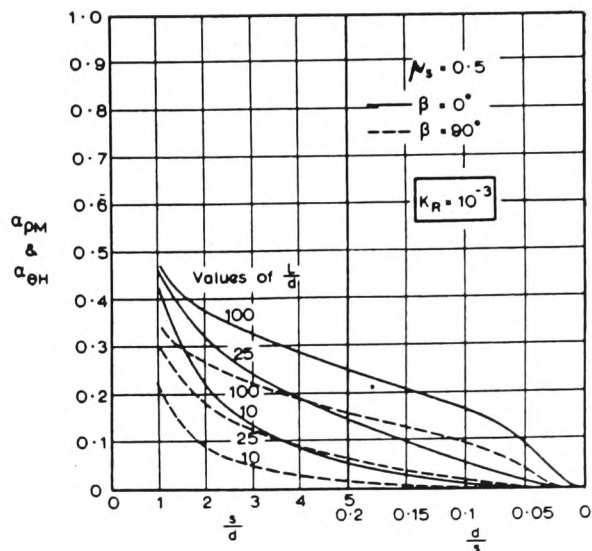


Figure B.15. Interaction factors $\alpha_{\rho H}$ and $\alpha_{\theta H}$, $K_R = 10^{-3}$, [after Poulos and Davis (1974)].

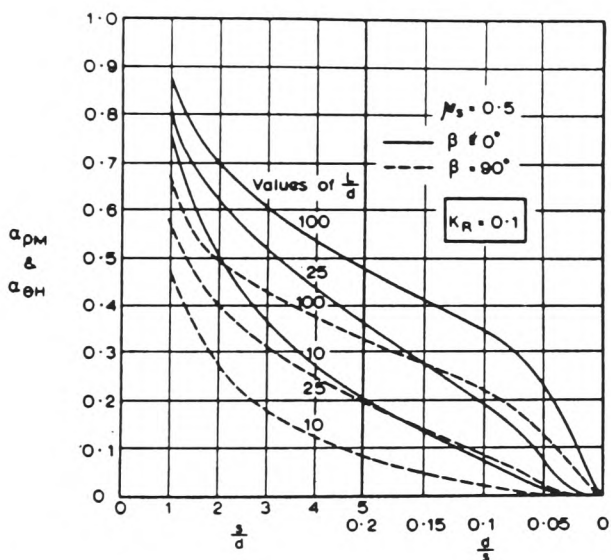


Figure B.16. Interaction factors $\alpha_{\rho H}$ and $\alpha_{\theta H}$, $K_R = 0.10$, [after Poulos and Davis (1974)].

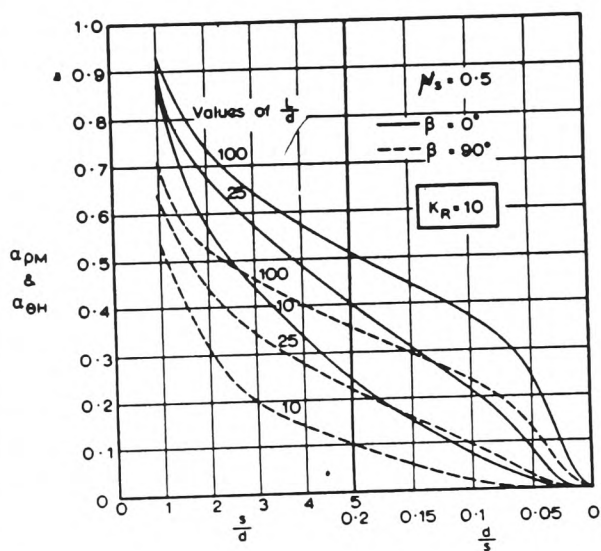


Figure B.17. Interaction factors $\alpha_{\rho H}$ and $\alpha_{\theta H}$, $K_R = 10$, [after Poulos and Davis (1974)].

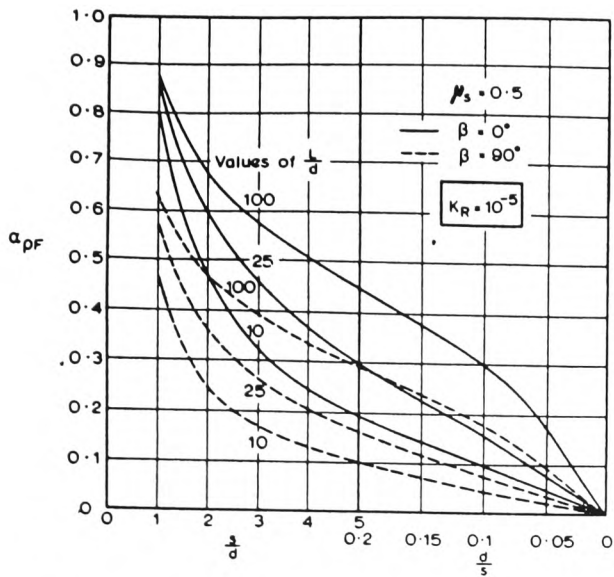


Figure B.18. Interaction factor α_{PF} , $K_R = 10^{-5}$, [after Poulos and Davis (1974)].

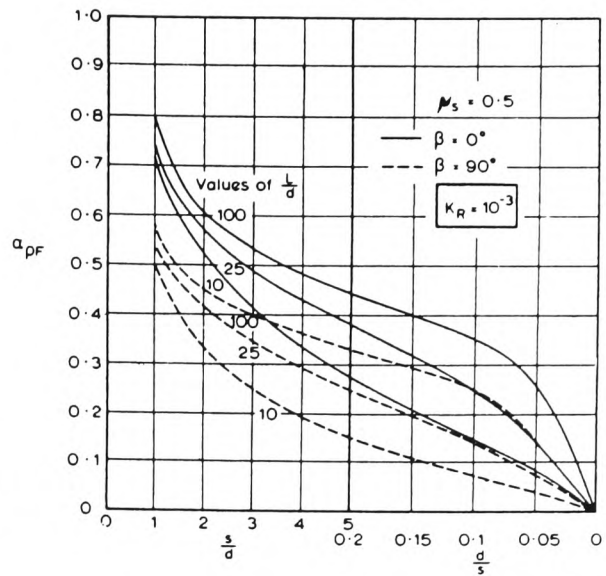


Figure B.19. Interaction factor α_{PF} , $K_R = 10^{-3}$, [after Poulos and Davis (1974)].

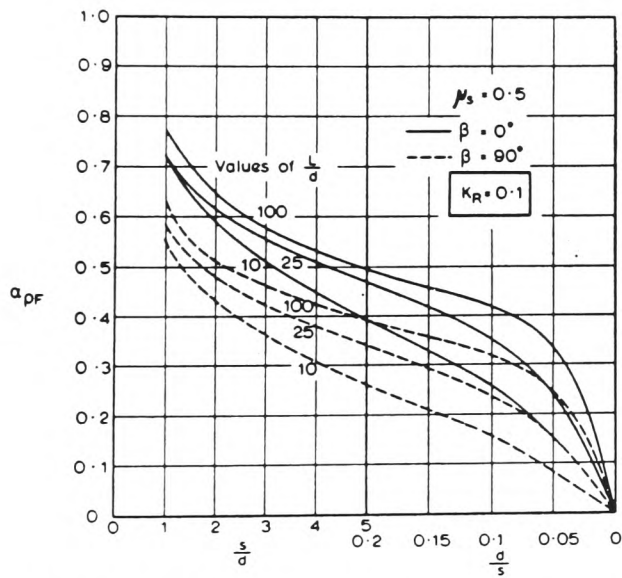


Figure B.20. Interaction factor α_{PF} , $K_R = 0.1$, [after Poulos and Davis (1974)].

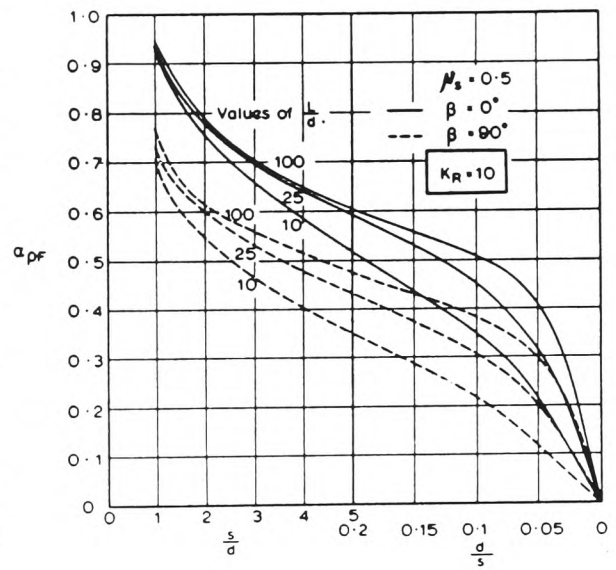


Figure B.21. Interaction factor α_{PF} , $K_R = 10$, [after Poulos and Davis (1974)].

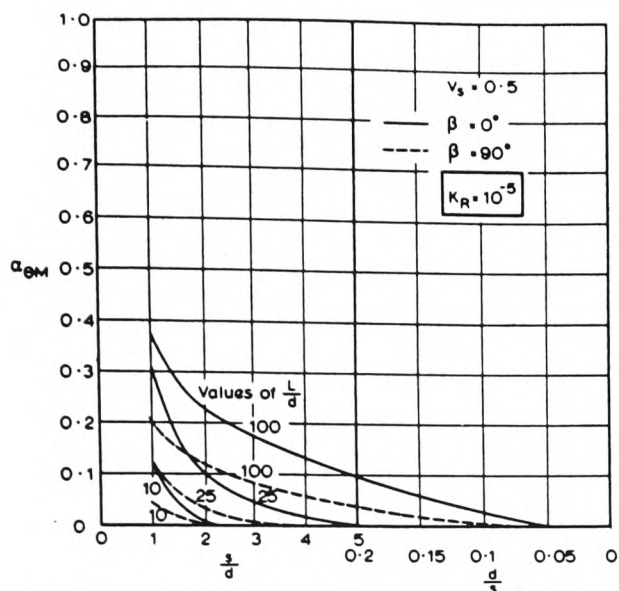


Figure B.22. Interaction factor $\alpha_{\Theta M}$, $K_R = 10^{-5}$, [after Poulos and Davis (1974)].

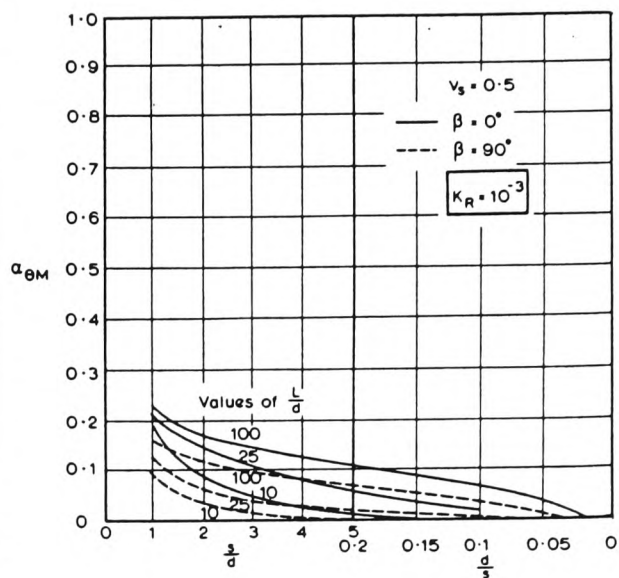


Figure B.23. Interaction factor $\alpha_{\Theta M}$, $K_R = 10^{-3}$, [after Poulos and Davis (1974)].

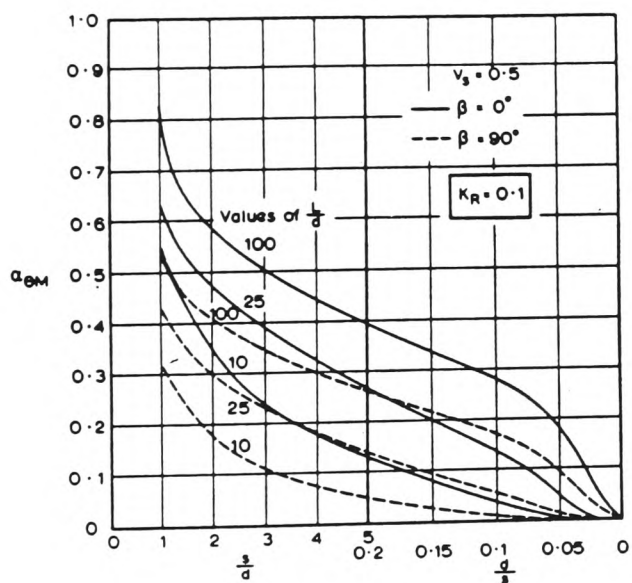


Figure B.24. Interaction factor $\alpha_{\Theta M}$, $K_R = 0.1$, [after Poulos and Davis (1974)].

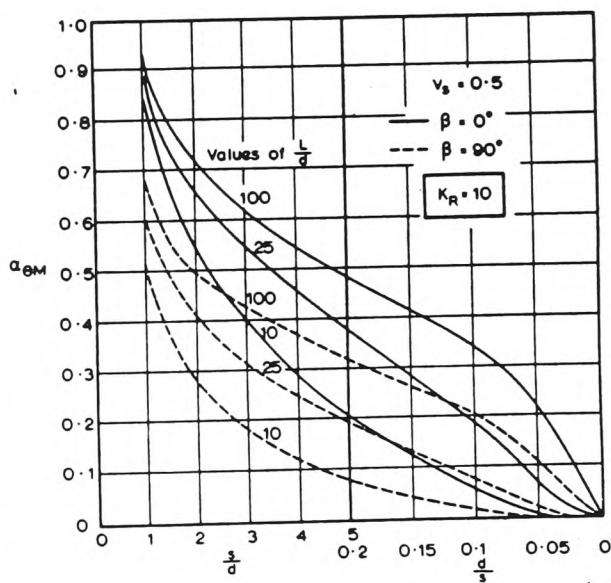


Figure B.25. Interaction factor $\alpha_{\Theta M}$, $K_R = 10$, [after Poulos and Davis (1974)].

APPENDIX C

DERIVATION OF THE STIFFNESS MATRIX FOR A ROD SUPPORTED BY AN ELASTIC SUBGRADE.

If an axially loaded pile is represented as a rod supported by an infinite number of springs of stiffness K_v' , as shown in Figure C.1.(a), then the force on any element of length dx can be depicted as shown in Figure C.1.(b). Let the vertical displacement at any arbitrary point be u .

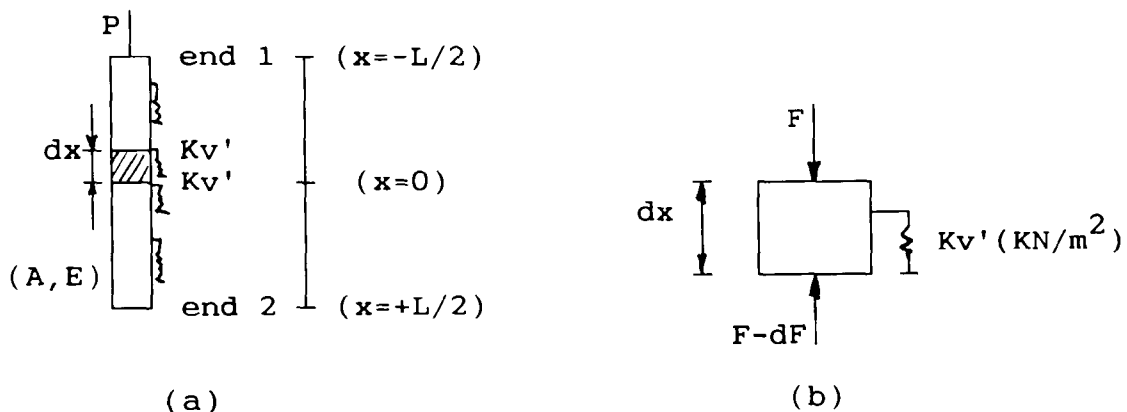


Figure C.1.: Representation of elastic subgrade to resistance of pile axial loading

From Figure C.1.(b), by equilibrium of forces:

$$dF = -[K_v' dx] u \dots\dots\dots C.1.$$

Now,

$$\text{Force } F = A E \frac{du}{dx}$$

and

$$dF = \frac{\delta F}{\delta x} dx$$

Therefore,

$$dF = A E \frac{\delta^2 u}{\delta x^2} dx \dots\dots\dots C.2.$$

By substitution of C.2. in C.1.

$$A E \frac{\delta^2 u}{\delta x^2} dx = -K_v' u dx$$

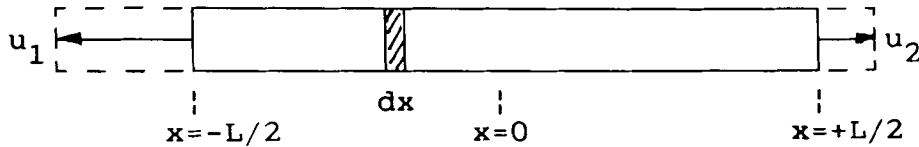
Rearranging

$$A E \frac{\delta^2 u}{\delta x^2} + K v' u = 0$$

Or,

$$A E \ddot{u} + K v' u = 0 \dots\dots\dots C.3.$$

If the bar has the below properties:



the displacement function for the bar will be given by:

$$u = u_1 (0.5 - x/L) + u_2 (0.5 + x/L) \dots\dots\dots C.4.$$

ie. when $x = -L/2$, $u = u_1$
 $x = +L/2$, $u = u_2$
 $x = 0$, $u = (u_1 + u_2)/2$

Let $\phi_1 = (0.5 - x/L)$ and $\phi_2 = (0.5 + x/L)$

Then C.4. can be rewritten as:

$$u = \phi_1 u_1 + \phi_2 u_2 \dots\dots\dots C.5.$$

By substitution in the governing equation

$$E A \frac{\delta^2 (\phi_1, \phi_2)}{\delta x^2} \begin{Bmatrix} u_1 \\ u_2 \end{Bmatrix} + K v' (\phi_1, \phi_2) \begin{Bmatrix} u_1 \\ u_2 \end{Bmatrix} = 0 \dots\dots C.6.$$

The following procedure is used to determine values for u_1 and u_2 . The components of Equation C.6. are multiplied by the displacement function and integrated over the length of the element. Since a double differentiation of the displacement function results in a zero function, it is necessary to integrate by parts.

ie.

$$(\phi_1) \frac{\delta(\phi_2)}{\delta x^2} dx = - \frac{\delta(\phi_1)}{\delta x} \frac{\delta(\phi_2)}{\delta x} dx$$

Integrating C.6. gives:

$$\begin{aligned}
 & -L/2 \int^{L/2} \begin{Bmatrix} \phi_1 \\ \phi_2 \end{Bmatrix} E A \frac{\delta(\phi_1, \phi_2)}{\delta x^2} \begin{Bmatrix} u_1 \\ u_2 \end{Bmatrix} dx \\
 & + \int_{-L/2}^{L/2} \begin{Bmatrix} \phi_1 \\ \phi_2 \end{Bmatrix} K v' (\phi_1, \phi_2) \begin{Bmatrix} u_1 \\ u_2 \end{Bmatrix} dx = 0 \dots\dots\dots C.7.
 \end{aligned}$$

Which resolves to:

$$\begin{aligned}
 & A E \int_{-L/2}^{+L/2} \begin{bmatrix} \frac{\delta\phi_1}{\delta x} \cdot \frac{\delta\phi_1}{\delta x} & \frac{\delta\phi_1}{\delta x} \cdot \frac{\delta\phi_2}{\delta x} \\ \frac{\delta\phi_2}{\delta x} \cdot \frac{\delta\phi_1}{\delta x} & \frac{\delta\phi_2}{\delta x} \cdot \frac{\delta\phi_2}{\delta x} \end{bmatrix} \begin{Bmatrix} u_1 \\ u_2 \end{Bmatrix} dx \\
 & + K v' \int_{-L/2}^{+L/2} \begin{bmatrix} \phi_1 \cdot \phi_1 & \phi_1 \cdot \phi_2 \\ \phi_2 \cdot \phi_1 & \phi_2 \cdot \phi_2 \end{bmatrix} \begin{Bmatrix} u_1 \\ u_2 \end{Bmatrix} dx = 0 \dots\dots\dots C.8.
 \end{aligned}$$

The components are now evaluated

$$\text{Now} \quad \phi_1 = 0.5 - x/L \quad \phi_2 = 0.5 + x/L$$

$$\text{And} \quad \frac{\delta\phi_1}{\delta x} = -\frac{1}{L} \quad \frac{\delta\phi_2}{\delta x} = +\frac{1}{L}$$

$$\phi_1 \cdot \phi_1 = 0.25 - \frac{x}{L} + \frac{x^2}{L^2} \quad \phi_1 \cdot \phi_2 = 0.25 - \frac{x^2}{L^2}$$

$$\phi_2 \cdot \phi_2 = 0.25 + \frac{x}{L} + \frac{x^2}{L^2} \quad \phi_2 \cdot \phi_1 = 0.25 - \frac{x^2}{L^2}$$

Integrating the components from -L/2 to +L/2

$$\begin{aligned}
 & \int_{-L/2}^{+L/2} \frac{\delta\phi_1}{\delta x} \cdot \frac{\delta\phi_1}{\delta x} dx = \int_{-L/2}^{+L/2} \frac{-1}{L} \cdot \frac{-1}{L} dx = \int_{-L/2}^{+L/2} \frac{1}{L^2} dx = \left[\frac{x}{L^2} \right]_{-L/2}^{+L/2} \\
 & = \frac{L}{2L^2} - \frac{(-L)}{(2L^2)} = \frac{1}{L}
 \end{aligned}$$

$$\int_{-L/2}^{+L/2} \frac{\delta\phi_1}{\delta x} \cdot \frac{\delta\phi_2}{\delta x} dx = \int_{-L/2}^{+L/2} \frac{-1}{L} \cdot \frac{+1}{L} dx = \left[\frac{-x}{L^2} \right]_{-L/2}^{+L/2} = \frac{-1}{L}$$

Similarly,

$$\int_{-L/2}^{+L/2} \frac{\delta\phi_2}{\delta x} \cdot \frac{\delta\phi_1}{\delta x} dx = \frac{-1}{L} \quad \text{and} \quad \int_{-L/2}^{+L/2} \frac{\delta\phi_2}{\delta x} \cdot \frac{\delta\phi_2}{\delta x} dx = \frac{+1}{L}$$

Now,

$$\int_{-L/2}^{+L/2} \phi_1 \cdot \phi_1 dx = \int_{-L/2}^{+L/2} 0.25 - \frac{x}{L} + \frac{x^2}{L^2} dx = \frac{L}{3}$$

And,

$$\int_{-L/2}^{+L/2} \phi_1 \cdot \phi_2 dx = \int_{-L/2}^{+L/2} 0.25 - \frac{x^2}{L^2} dx = \frac{L}{6}$$

Similarly,

$$\int_{-L/2}^{+L/2} \phi_2 \cdot \phi_1 dx = \frac{L}{6} \quad \text{and} \quad \int_{-L/2}^{+L/2} \phi_2 \cdot \phi_2 dx = \frac{L}{3}$$

Substitution into C.8. gives:

$$A E \begin{bmatrix} 1/L & -1/L \\ -1/L & 1/L \end{bmatrix} \begin{Bmatrix} u_1 \\ u_2 \end{Bmatrix} + K_v' L \begin{bmatrix} 1/3 & 1/6 \\ 1/6 & 1/3 \end{bmatrix} \begin{Bmatrix} u_1 \\ u_2 \end{Bmatrix} = 0$$

For a bar with concentrated end forces P_1 and P_2 this can be written as :

$$\frac{A E}{L} \begin{bmatrix} 1 & -1 \\ -1 & 1 \end{bmatrix} \begin{Bmatrix} u_1 \\ u_2 \end{Bmatrix} + K_v' L \begin{bmatrix} 1/3 & 1/6 \\ 1/6 & 1/3 \end{bmatrix} \begin{Bmatrix} u_1 \\ u_2 \end{Bmatrix} = \begin{Bmatrix} P_1 \\ P_2 \end{Bmatrix}$$

Where the first term in this equation is the stiffness matrix for a bar and the second term is the

additional stiffness due to a subgrade of stiffness K_v'
acting continuously along the element length.

APPENDIX D

SEM USER MANUAL

AND

PROGRAM DETAILS.

SEM User Manual

A computer program for the analysis of plain rafts and 3 dimensional structures supported by raft foundations resting on an anisotropic elastic multi-layered soil using the S.E.M.

D.1. INTRODUCTION.

The computer program can analyse plain rafts and three dimensional structures supported by raft foundations resting on an anisotropic elastic multi-layered soil. The structure which may be analysed is skeletal in form comprising straight uniform members connected at their ends to form joints ie. it is a standard stiffness method of analysis. Thus the program can also analyse any skeletal structure by using joint restraints and specifying the number of soil layers as zero.

D.2. OPERATION OF THE PROGRAM.

Firstly, the program should be installed on the hard disk of the computer. Before using the program you should ensure that there is adequate space on your hard disk and backup any temporary files with .TMP extensions.

To analyse a two dimensional problem a virtual disk (VDISK) needs to be set up. To install the VDISK device driver append a statement as shown below in the CONFIG.SYS file on the hard disk.

```
device = vdisk.sys 300 512 2
```

This statement will then allocate 300KB of memory for a virtual file.

The program reads the input data for analysis from a data file on the hard disk. To create a data file use a wordprocessor or the screen editor EDLIN in the disk

operating system (DOS). Type the data into a file and save the file under a name with the .DAT extension e.g. STRUCT.DAT.

Before running the program ensure the printer is switched on; otherwise the results will not be printed out. To run the program from DOS enter SEM

The program will then prompt whether a 2 or 3 dimensional analysis is required. Enter 2 or 3.

It will then prompt for the title of a file in which the data has been created. Enter the name of the data file. eg. STRUCT.DAT

D.3. CREATING DATA FILES.

D.3.1. General.

The raft or structure is idealized by joints connected by straight members. The location of each joint is specified by co-ordinates relative to the global axes denoted by X,Y and Z. The members are defined by a member number, a start joint, an end joint, a member property and Gama. Gama is only defined for 3 dimensional problems. It is the rotation of the member about the X-axis as described by Coates et al (1988). For 3 dimensional structures the raft joints and elements must be numbered before the superstructure joints and members.

Plain rafts created for a 2-D analysis are assumed to lie in the global X-Y plane. The positive vertical direction Z is upwards. Rafts created for a 3-D analysis are assumed to lie in the X-Z plane; the positive vertical direction Y is upwards.

D.3.2. Data as read by the program.

The highlighted variables below are as read by the program. Parameters followed by * should be omitted for 2-D files.

PROBLEM DEFINITION

A\$
NE, NJ, SU, MP, NR*, ER* A\$ = "Title of file, any details"
NE = Total number of elements
NJ = Total number of joints
SU = Number of supports
MP = Number of member properties
NR = Number of raft joints
ER = Number of raft elements

JOINT CO-ORDINATES

FOR I=1 TO NJ
I, X(I), Y(I), Z(I)* I = Joint number
NEXT I X(I), Y(I), Z(I) are the global
co-ordinates of the joint

ELEMENT CONNECTIVITY

FOR I=1 TO NE
I, N1(I), N2(I), NP(I), GAM(I)* I = Element number
NEXT I N1(I) = Start joint
N2(I) = End joint
GAM(I) = Rotation about x-axis

PROBLEM TYPE

KK\$, V KK\$ = Type of problem being solved
currently limited to BEM. Enter
BEM without ""
V = Poisson's ratio of structure

MEMBER PROPERTIES

For 3-D problems

FOR I=1 TO MP I = Member property no.
I, E(I), AX(I), IX(I), IY(I), IZ(I) E(I) = Young's modulus
NEXT I AX(I) = Cross sectional area
IX(I), IY(I), IZ(I) are the
second moments of area about
the x, y and z member axes.

For 2-D problems

FOR I=1 TO MP
I, E(I), IY(I), J(I) IY(I) = Second moment of area
about y axis
J(I) = Torsional constant

JOINT RESTRAINTS

FOR I=1 TO SU

NN,DX, DY, DZ, MX, MY, MZ*

NEXT I

NN = Restrained joint number
DX, DY, DZ are displacement restraints in X, Y, Z global axes
MX, MY, MZ are rotational restraints in X, Y, Z global axes
Enter 1 for restraint and 0 for free movement.

JOINT LOADS

NN,DF,PL

NN = Loaded joint number
DF = Load direction
PL = Load intensity
To end joint loads enter 99,99,99

Load directions:

3-D: dx=1, dy=2, dz=3

mx=4, my=5, mz=6

2-D: dz=1, mx=2, mz=3

MEMBER LOADS

uniformly distributed loads (UDL)

MN,WF, W

MN = Loaded member number
WF = Load direction
(assumed as dz for 2-D)
W = Load intensity/unit length
To end member UDL enter 99,99,99

point loads

MN,WF, PL, A

MN = Loaded member number
WF = Load direction
PL = Point load intensity
A = Distance of load from start joint
To end member point loads enter 99,99,99,99

SOIL DETAILS

overall definition

N, MHV, MHH, X

N = Number of soil layers
MHV = Vertical/horizontal Poisson's ratio
MHH = Horizontal/ " " "
X = Ratio of vertical to horizontal modulus

layer properties

FOR I=1 TO N

I, EV(I), T(I)

NEXT I

I = Soil layer number
EV(I) = Vertical soil modulus
T(I) = Layer thickness

D.3.3. Worked Examples.

D.3.3.1. 3-D Analysis.

Using the 3-D program, a simple plain raft is idealized. The data file is called RAN.DAT; see computer

printout. The raft and soil profile being analysed are shown in Figure D.1.(a) and (b) respectively.

There are 4 joints and 4 members which all lie in the X-Z plane. All members have been assigned the same properties; member property=1, $\gamma=0$, $\mu=0.25$, $E=210$, $A_X=10000$, $I_X=150$, $I_Y=10000$ and $I_Z=600$.

There is a UDL=120KN/m acting vertically downward on member 2 and a point load=500KN acting vertically downward on member 1 at 1.5m from the start joint.

The raft lies on a 2 layer soil. The vertical and horizontal Poisson's ratios are 0.50 and 0.25 respectively. The ratio λ of E_v/E_h is 2.3. The vertical soil modulus of layer 1 is 100MN/m^2 with a thickness of 2.83m. The vertical soil modulus of layer 2 is 200MN/m^2 with a thickness of 2.83 m.

Having run the program for the data file generated, the output obtained is as shown in the computer printout. The input data is printed out as read by the program. The joint and equivalent joint loads are also printed out as a check. The results for joint displacements, member forces and soil reactions are then presented.

D.3.3.2. 2-D Analysis.

The worked example for the 2-D analysis is for data file TEST.DAT; see computer printout.

There are 12 joints, 9 members, 0 supports and 2 member properties. The 10x10m raft being analysed is presented in Figure D.2.(a) and the soil profile is presented in Figure D.2.(b). The joints are assigned 2-D co-ordinates consecutively. The 12 members are then

defined consecutively by start joint, end joint and member property. The BEM statement is inserted and Poisson's ratio for the raft is 0.50.

The two member properties are defined. A downward vertical point load of 23000 KN is applied in the centre at joint 1. There are no other loads.

There are 8 soil layers. The two Poisson's ratios for each soil layer are both 0.50 and the ratio X of E_v/E_h is 1.0. The soil stratum has been graded; the layer thickness increasing with depth. The vertical soil modulus E_v of each layer being 112.5 KN/m^2 . The results file is presented. Because the member properties are only printed to 3 decimal places I and J are shown as zero here. However, in its compiled form the program operates to a minimum of 16 decimal places with double precision operations to 32 decimal places.

D.4. PROGRAM DETAILS.

The three dimensional programs TRAN*.EXE are described below. The two dimensional programs STEM*.EXE follow the same basic outline. However, these are simpler in form because the element matrices are constructed in their transformed form, as described by Coates et al (1988).

A data file is created on the hard disk, drive C:, as described in the User Manual using a word processor. The solution process described below is executed by entering SEM from DOS and following the printed screen instructions.

(A) TRAN1.EXE

- (A.1.) The data file is read.
- (A.2.) The element lengths are calculated.
- (A.3.) The element transformation matrices are calculated.
- (A.4.) The load vector for each element is calculated.
- (A.5.) The load vectors are transformed into global axes.
- (A.6.) Temporary files for created data are written to hard disc.
- (A.7.) Memory is cleared and TRAN1B.EXE executed.

(B) TRAN1B.EXE.

- (B.1.) Memory is cleared.
- (B.2.) Created data is read from disk.
- (B.3.) Zeros are written into stiffness matrix on hard disk.
- (B.4.) Stiffness matrix is created for each element as described by Coates et al (1988).
- (B.5.) Element stiffness matrices are transformed.
- (B.6.) Symmetrical half of stiffness matrix is created on hard disk using a random access file. This is achieved by reading values from relevant locations in matrix, adding new transformed element matrix onto read value and putting new stiffness value into matrix on hard disk.
- (B.7.) Memory is cleared and TRAN2.EXE is executed.

(C) TRAN2.EXE

- (C.1.) Memory is cleared.
- (C.2.) Creates other symmetrical half of stiffness matrix on hard disk.
- (C.3.) Memory is cleared and TRAN2B.EXE is executed.

(D) TRAN2B.EXE

- (D.1.) Memory is cleared.
- (D.2.) The length and breadth of each raft rectangle is calculated by examining the connectivity of nodes; any 4 nodes must form a rectangle.
- (D.3.) The off-diagonal terms of a symmetrical half of the soil flexibility matrix $[F_S]$ are calculated using Boussineq's equations. This is carried out by calculating z and R the depth of the centre of each layer and the distance from the centre of the layer to the point load respectively. These values are then input into Equations 7.2, 7.3, and 7.4 to give the various stresses.
- (D.4.) The strain in the layer ϵ_z and hence the displacements δ_z is determined in terms of the load P .
- (D.5.) The other symmetrical half of the $[F_S]$ matrix is produced.
- (D.6.) The leading diagonal of the $[F_S]$ matrix is constructed using Holl's Equations 7.9, 7.10, and 7.11. σ_z , σ_x and σ_y are calculated using the depth z , length l and breadth b of each rectangle calculated previously.
- (D.7.) The elastic strain of each layer ϵ_z is calculated using 7.12 and hence the displacement δ_z is determined in terms of the applied pressure.
- (D.8.) The leading diagonal is constructed.
- (D.9.) The soil flexibility matrix $[F_S]$ is written onto the hard disk.
- (D.10.) Memory is cleared and TRAN5.EXE executed.

(E) TRAN5.EXE

- (E.1.) Memory is cleared.
- (E.2.) The soil flexibility matrix $[F_S]$ is read from the hard disk.
- (E.3.) Row reduction is used to invert the $[F_S]$ matrix and create the soil stiffness matrix $[K_S]$.
- (E.4.) The $[K_S]$ matrix is written onto the hard disk.
- (E.5.) Memory is cleared and TRAN6.EXE.

(F) TRAN6.EXE

- (F.1.) Memory is cleared.
- (F.2.) The soil stiffness matrix $[K_S]$ is added to the global structure stiffness matrix $[SSS.TMP]$. This is achieved using a random access file for the stiffness matrix without reading the whole matrix into memory. The relevant $[K_S]$ values are added to the relevant $(12I_z/L^3)$ terms in the stiffness matrix on the hard disk.
- (F.3.) Memory is cleared and TRAN7.EXE is executed.

(G) TRAN7.EXE

- (G.1.) Memory is cleared.
- (G.2.) Joint restraints and the load vector are read into memory.
- (G.3.) Joint restraints are applied to the stiffness matrix on hard disk.
- (G.4.) Stiffness matrix on the hard disk is reduced using Gaussian elimination.
- (G.5.) Displacements are obtained by backsubstitution and written to the hard disk.
- (G.6.) Memory is cleared and TRAN8.EXE executed.

(H) TRAN8.EXE

- (H.1.) Memory is cleared.
- (H.2.) Temporary data files are read.
- (H.3.) The input data and displacements are arranged and printed out.
- (H.4.) Member forces are calculated using transformed element matrices and by transforming the load vector into local axes.
- (H.5.) Member forces are printed out.
- (H.6.) Memory is cleared and TRANK.EXE executed.

(I) TRANK.EXE

- (I.1.) Memory is cleared.
- (I.2.) The soil stiffness matrix $[K_S]$ and displacement vector $\{D_P\}$ are read into memory.
- (I.3.) Soil reactions beneath the raft are calculated by multiplying $\{D_P\}$ by $[K_S]$.
- (I.4.) Soil reactions are printed out.
- (I.5.) END.

TRAN.DAT Data file.

"TRAN.DAT"

4,4,0,1,4,4

1,0,0,0,2,0,0,4,3,3,0,0,4,3,0,4

1,1,3,1,0,2,1,2,1,0,3,2,4,1,0,4,3,4,1,0

BEM, .25,1,210,10000,150,10000,600

99,99,99

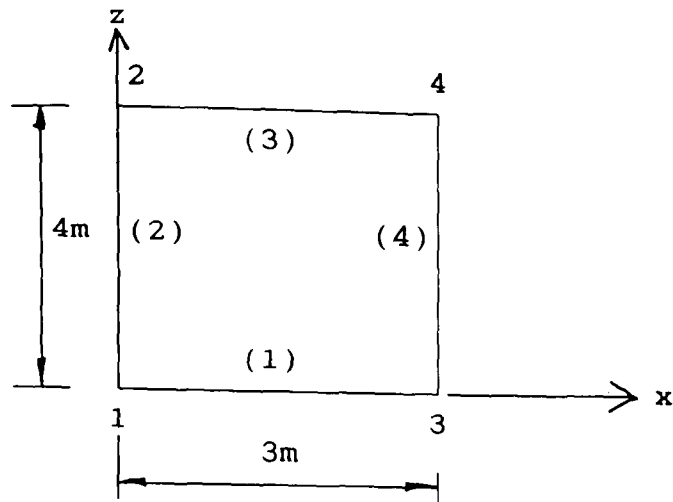
2,2,-120.,99,99,99,1,2,-500.,1.5,99,99,99,99

2,.5,.25,2.3

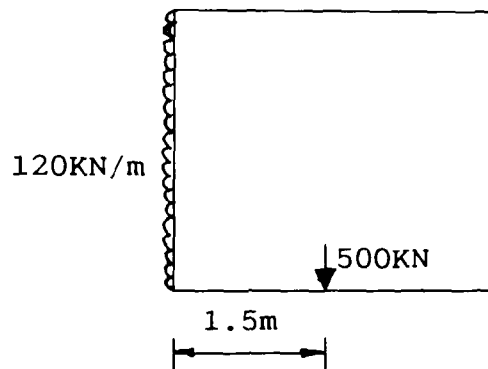
1,100E3,2.83

2,200E3,2.83

0,0,0,0,0,0,0,0

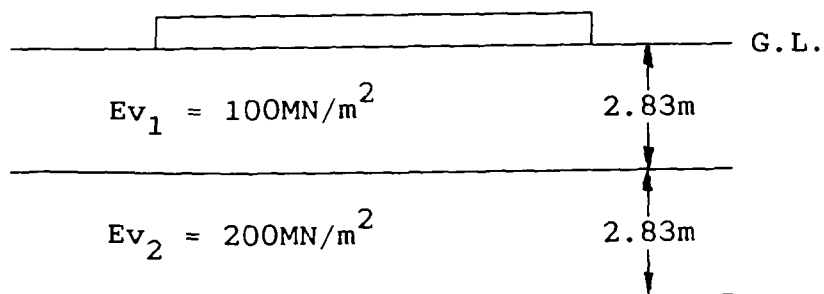


Node numbers, Element numbers (in brackets) and dimensions.



Applied vertical loading.

(a) Structural and loading details.



(b) Ground details.

Figure D.1.: Details of model idealized by TRAN.DAT.

Computer output results for TRAN.DAT.
 JOINT COORDINATES
 =====

JOINT NO.	X-COORD	Y-COORD	Z-COORD
=====	=====	=====	=====
1	0.000	0.000	0.000
2	0.000	0.000	4.000
3	3.000	0.000	0.000
4	3.000	0.000	4.000

ELEMENT CONNECTIVITY
 =====

ELEMENT NUMBER	START JOINT	END JOINT	MAT PROP NUMBER	GAMA
=====	=====	=====	=====	=====
1	1	3	1	0.00
2	1	2	1	0.00
3	2	4	1	0.00
4	3	4	1	0.00

MATERIAL PROPERTIES
 =====

POISSON'S RATIO= .25

PROP NO.	E	AX	IX	IY	IZ
=====	=====	=====	=====	=====	=====
1	210.000	10000.000			
			150.000	10000.000	600.000

JOINT AND EQUIVALENT JOINT LOADS

JOINT NO.	X	Y	Z
=====	=====	=====	=====
1 F	0.000	-490.000	0.000
1 M	160.000	0.000	-187.500
2 F	0.000	-240.000	0.000
2 M	-160.000	0.000	0.000
3 F	0.000	-250.000	0.000
3 M	0.000	0.000	187.500
4 F	0.000	0.000	0.000
4 M	0.000	0.000	0.000

JOINT DISPLACEMENTS

=====

JT NO.		X	Y	Z
=====		=====	=====	=====
1 D		0.000000	-0.000986	0.000000
1 R		0.002266	0.000000	-0.002011
2 D		0.000000	-0.000491	0.000000
2 R		-0.002514	0.000000	0.000066
3 D		0.000000	-0.000556	0.000000
3 R		0.000025	0.000000	0.002298
4 D		0.000000	-0.000060	0.000000
4 R		-0.000273	0.000000	0.000221

MEMBER FORCES

=====

MBR.	JT.	X	Y	Z
=====	=====	=====	=====	=====
1	1 F	0.000	250.000	0.000
1	1 M	9.412	0.000	6.541
1	3 F	0.000	250.000	0.000
1	3 M	-9.412	0.000	-6.541
2	1 F	0.000	240.000	0.000
2	1 M	-6.541	0.000	9.412
2	2 F	0.000	240.000	0.000
2	2 M	6.541	0.000	-9.412
3	2 F	0.000	0.000	0.000
3	2 M	-9.412	0.000	-6.541
3	4 F	0.000	-0.000	0.000
3	4 M	9.412	0.000	6.541
4	3 F	0.000	0.000	0.000
4	3 M	6.541	0.000	-9.412
4	4 F	0.000	-0.000	0.000
4	4 M	-6.541	0.000	9.412

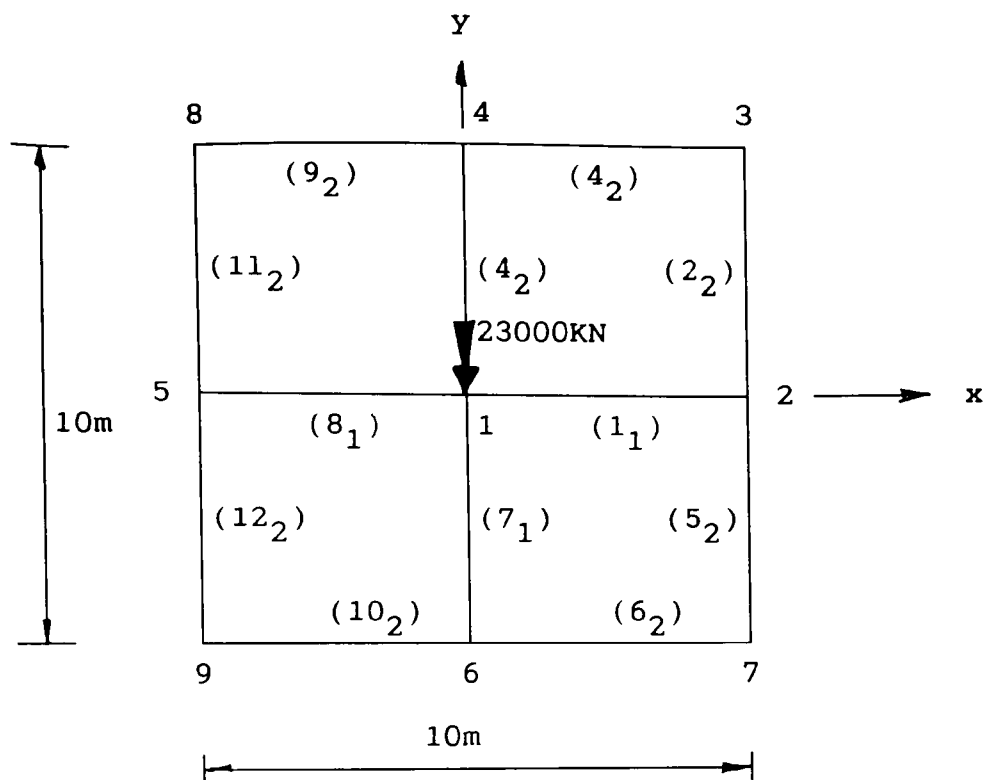
SOIL SUPPORT REACTIONS

JOINT	REACTION
1	-490.0000610351562
2	-239.9999847412109
3	-249.9999542236328
4	2.049855538643897E-006

TOTAL SOIL REACTION = -980

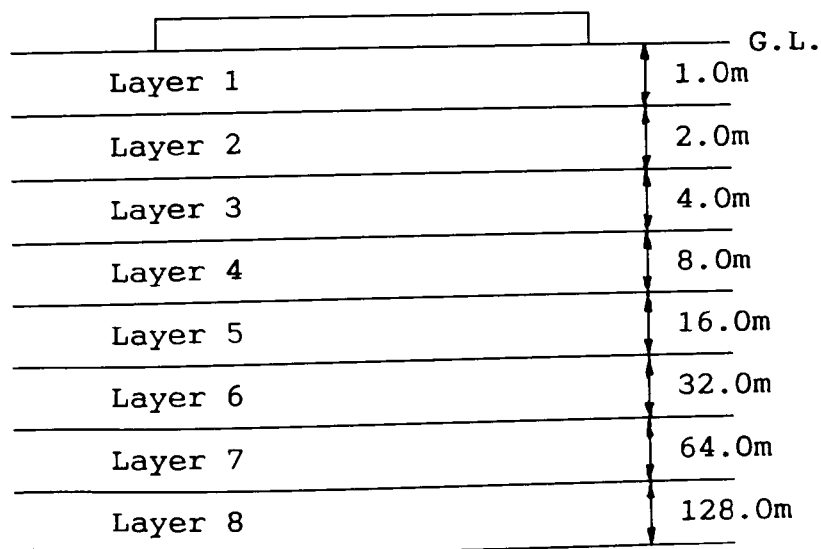
TEST.DAT data file.

```
"TEST.DAT"  
12,9,0,2  
1,0,0,2,5,0,3,5,5,4,0,5,5,-5,0  
6,0,-5,7,5,-5,8,-5,5,9,-5,-5  
1,1,2,1,2,2,3,2,3,1,4,1,4,3,4,2  
5,2,7,2,6,6,7,2,7,1,6,1,8,1,5,1  
9,4,8,2,10,6,9,2,11,5,8,2,12,5,9,2  
BEM, .5,1,15E6,5.20833E-6,10.41667E-6  
2,15E6,2.604167E-6,5.20833E-6  
1,1,-23000  
99,99,99  
99,99  
99,99,99  
8,.5,.5,1.0  
1,112.5,1.0  
2,112.5,2.0  
3,112.5,4.0  
4,112.5,8.0  
5,112.5,16.0  
6,112.5,32.0  
7,112.5,64.0  
8,112.5,128.0  
0,0,0,0,0,0,0
```



Node numbers, Element numbers (in brackets),
Element property numbers (in subscript),
dimensions and applied vertical loading.

(a) Structural and loading details.



$E_v = 112.5 \text{KN/m}^2$ for each layer.

(b) Ground details.

Figure D.2.: Details of model idealized by TEST.DAT.

Computer output results for TEST.DAT.

"TEST.DAT

"

JOINT COORDINATES

=====

JOINT NO.	X-COORD	Y-COORD
=====	=====	=====
1	0.000	0.000
2	5.000	0.000
3	5.000	5.000
4	0.000	5.000
5	-5.000	0.000
6	0.000	-5.000
7	5.000	-5.000
8	-5.000	5.000
9	-5.000	-5.000

ELEMENT CONNECTIVITY

=====

ELEMENT NUMBER	START JOINT	END JOINT	MAT PROP NUMBER
=====	=====	=====	=====
1	1	2	1
2	2	3	2
3	1	4	1
4	3	4	2
5	2	7	2
6	6	7	2
7	1	6	1
8	1	5	1
9	4	8	2
10	6	9	2
11	5	8	2
12	5	9	2

MATERIAL PROPERTIES

=====

POISSON'S RATIO= .5

PROP NO.	E	I	J
=====	=====	=====	=====
MP= 2			
1	%15000000	0.000	0.000
2	%15000000	0.000	0.000

JOINT AND EQUIVALENT JOINT LOADS

=====

JOINT NO.	PZ	MX	MY
1	-23000	0	0
2	0	0	0
3	0	0	0
4	0	0	0
5	0	0	0
6	0	0	0
7	0	0	0
8	0	0	0
9	0	0	0

JOINT DISPLACEMENTS

=====

JT NO.	Z-DISPL	X-ROTN	Y-ROTN
=====	=====	=====	=====
1	-43.073074	0.000000	0.000000
2	-12.255511	0.000000	-8.230417
3	-8.500671	2.141304	-2.141304
4	-12.255512	8.230418	0.000000
5	-12.255510	-0.000000	8.230416
6	-12.255514	-8.230418	0.000000
7	-8.500672	-2.141304	-2.141304
8	-8.500671	2.141304	2.141303
9	-8.500671	-2.141303	2.141304

MEMBER FORCES

=====

MBR. =====	JT. =====	PZ =====	MX =====	MY =====
1	1	-76.811	0.000	320.629
1	2	76.811	-0.000	63.428
2	2	5.994	-31.714	1.744
2	3	-5.994	31.714	-31.714
3	1	-76.811	0.000	320.628
3	4	76.811	-0.000	63.428
4	3	-5.994	31.714	31.714
4	4	5.994	-31.714	-1.744
5	2	5.994	31.714	1.744
5	7	-5.994	-31.714	-31.714
6	6	5.994	-31.714	1.744
6	7	-5.994	31.714	-31.714
7	1	-76.811	-0.000	320.629
7	6	76.811	0.000	63.428
8	1	-76.811	-0.000	320.629
8	5	76.811	0.000	63.428
9	4	5.994	-31.714	1.744
9	8	-5.994	31.714	-31.714
10	6	5.994	31.714	1.744
10	9	-5.994	-31.714	-31.714
11	5	5.994	31.714	1.744
11	8	-5.994	-31.714	-31.714
12	5	5.994	-31.714	1.744
12	9	-5.994	31.714	-31.714

SOIL SUPPORT REACTIONS

JOINT	REACTION
1	-22692.751953125
2	-88.79863739013672
3	11.98815536499023
4	-88.7994384765625
5	-88.79773712158203
6	-88.80128479003906
7	11.98716068267822
8	11.9871129989624
9	11.98824787139893

TOTAL SOIL REACTION =-22999.998046875